THE NATIONAL UNIVERSITY OF IRELAND MAYNOOTH

The Role of Bone Morphogenetic Protein Signalling in Adult Lung Health and Disease

Thérése Marion Lynn
B. Sc (Hons)

A thesis submitted to the
National University of Ireland Maynooth,
for the degree of

Doctor of Philosophy

in the
Department of Biology,
National University of Ireland Maynooth

Research Supervisor: Dr. Shirley O'Dea
Head of Department: Prof. Paul Moynagh

October 2015

Declaration of Authorship

I, Thérése Lynn declare that this thesis titled, 'Bone Morphogenetic Proteins in adult lung health and disease' and the work presented in it are my own.

I confirm that:

- Where any part of this thesis has previously been submitted for a degree or any other qualification at this University or any other institution, this has been clearly stated.
- Where I have consulted the published work of others, this is always clearly attributed.
- Where I have quoted from the work of others, the source is always given.
- I have acknowledged all main sources of help.
- Where the thesis is based on work done by myself jointly with others, I have made clear exactly what was done by others and what I have contributed myself.

_____

Thérése Lynn, B Sc.

Contents

Chapter 4

Chapter 5

Abstract

Bone morphogenetic protein (BMP) signalling is essential for correct lung morphogenesis. The pathway controls branching morphogenesis in the nascent lung and is also involved in the establishment of correct epithelial cell distribution throughout the airways. In the adult lung, BMP signalling is reactivated during airway injury and inflammation and there is evidence of aberrant signalling in lung cancer and in chronic lung diseases such as asthma and fibrosis. However, little is known about the role of BMP signalling in healthy adult airways. Furthermore the effect of incorrect BMP pathway expression during epithelial repair and inflammatory and malignant lung diseases remains elusive. The aims of this project were to characterise BMP pathway expression in the descending airways of large animal models and to investigate the role of BMP signalling during adult airway homeostasis, recovery and disease.

To investigate the role of BMP signalling in malignant lung disease we used a heterogeneous lung cancer cell line DLKP. We explored the effect of the BMP pathway on epithelial-to-mesenchymal (EMT) progression and phenotypic plasticity between the tumour subpopulations. BMP-4 treatment induced mesenchymal-like projections in the DLKP-SQ clones and significant morphological changes in the DLKP-M clones towards the stem-cell like colonies of DLKP-I populations. Elevated N-cadherin and Vimentin protein expression was also evident in the clones following BMP-4 treatment. By stably transfecting an E-cadherin gene in these E-cadherin-null cells we demonstrated the distinct phenotypic differences between these tumour subpopulations.

Healthy porcine and rhesus macaque lungs were used to characterise BMP pathway expression throughout the airways. Active BMP signalling was present in the descending airway epithelium and a gradient in pathway activation along the proximal-distal axis of the lungs was observed [1]. Using a primary porcine tracheal *in vitro* explant model the BMP signalling gradient was investigated further and it was found that by modulating BMP signalling, using exogenous BMP-4 stimulation, the epithelial phenotype of the porcine tracheal cells was altered.

Finally, to assess the role of BMP signalling during airway inflammation and repair an established non-human primate model of allergic airway disease was used. A reduction in pSMAD1/5/8 expression was present in the epithelium of asthmatic monkeys compared to healthy controls. In addition, following a period of six months in filtered air to facilitate airway repair, there was a significant increase in Proliferating Cell Nuclear Antigen (PCNA), BMP Receptor 1a (BMPRIa) and pSMAD1/5/8 throughout the asthmatic airways. Taken together, these data suggest that not only is the developmental pathway re-activated during inflammatory airway disease but that basal BMP pathway expression is important for maintaining healthy airways.

Overall these data highlight the presence and importance of BMP signalling gradients in healthy adult airways and further implicate BMP signalling in the pathogenesis of inflammatory and malignant airway diseases.

[1] T.M Lynn, E.L Molloy, J.C Masterson, S.F. Glynn, R.W. Costello, M.V. Avdalovic, E.S Schelegle, L.A. Miller, D.M Hyde, S O'Dea. 'SMAD signalling in descending airways of healthy versus asthmatic rhesus macaques highlights a relationship between inflammation and BMPs'. AJRCMB, In Press.

Acknowledgements

I would like to offer my sincere gratitude to my PhD supervisor Dr. Shirley O'Dea. I have been very lucky to carry out my post-graduate research under her stewardship and I would like to say thank you for the never-ending support, advice, understanding and encouragement over the past three years.

Thanks to all the guys and gals in the Epithelial lab and Avectas. Working alongside you all has been such a pleasure and I've appreciated all the chats and laughs that we've shared more than you know. It wouldn't have been the same without ye.

To everyone I met and worked with while studying in UC Davis, thank you for all the help and encouragement. From rebuilding microscopes to eating crepes all weekend I was lucky to have met you all and I will never forget my Californian adventure.

To all my fellow PhDers - you've made these three years unforgettable. Through all the ups and downs, I knew I could get to the finish line surrounded by you lot. Thanks for everything. Long live the chocolate breaks and the chats around the clock ☺

To my dear friends and housemates, thank you for always being there for me. Thank you for your thoughtfulness, understanding and patience - and for keeping me smiling.

Finally, to my parents Liam and Marion, to my brother Shane and my sister Helena - I want to say thank you from the very bottom of my heart. Knowing you believed in me and always having you by my side carried me through the tough times. Thank you for the unwavering love, help, support, patience and encouragement over these past few years, and always.

I dedicate this thesis to my loving family.

Abbreviations

α-SMA	Alpha smooth muscle actin
μM	micrometer
μl	microlitre
100 bp	100 base pair
1kb	1 kilobase
AB	antibody
AEC	Airway epithelial cell
ALK	Activin-receptor-like kinase
AQP5	Aquaporin-5
AR	Allergic rhinitis
ATCC	American type culture collection
BADJ	Bronchoalveolar duct junction
BAMBI	BMP associated membrane bound inhibitor
BASC	Bronchoalveolar stem cells
BEAS	Bronchial epithelial airway cells
BME	β -mercaptoethanol
BMP	Bone morphogenetic protein
BMPR	Bone morphogenetic protein receptor
BSA	Bovine serum albumin
BRE	BMP responsive element
CC10	Club cell 10
CCSP	Club cells secretory protein

CDK	Cyclin dependent kinase
COPD	Chronic obstructive pulmonary disease
CO_2	Carbon dioxide
CRMP	Collapsin response mediator protein
cDNA	Complementary DNA
CT	Cycle threshold
DAPI	4’6’-diamidino-2-phenylindole
DEPC	Diethylene pyrocarbonate
Der f	*Dermatophagoides farinae*
dH_20	distilled water
DLKP	Human lung cancer cell line
DMEM	Dulbecco’s modified eagle medium
DMSO	Dimethyl sulphoxide
DNA	deoxyribonucleic acid
dNTP	deoxyribonucleoside triphosphate
Dpp	Decapentapelagic
DSFM	Define serum free medium
E	embryonic day
ECL	Enhanced chemilumenescence
ECP	Eosinophil cationic protein
ECM	Extracellular matrix
ED50	Effective dose
EDTA	Ethylene diamine tetraacetic acid
EGFR	Epidermal growth factor receptor

EMP	Epithelial mesenchymal plasticity
EMT	Epithelial-to-mesenchymal transition
EpCAM	Epithelial cell adhesion molecule
EPO	Eosinophil perioxidase
ER	Endoplasmic reticulum
ERK	Extracellular signal related kinase
FA	Filtered Air
FACS	Fluorescence-activated cell sorting
FBS	Foetal bovine serum
FDA	U.S. Food and Drugs Administration
FFPE	Formalin fixed paraffin embedded
FGF	Fibroblast growth factor
FITC	Fluorescein isothiocyanate
FOX-A1	Forkhead box alpha 1
g	grams
GAPDH	Glyveradehyde 3-phosphate dehydrogenase
GATA	GATA-binding transcription factor
GDF	Growth differentiation factor
GFP	Green fluorescent protein
HCl	Hydrochloric acid
HLH	Helix loop helix
HDAC	Histone deacteylase
HDMA	House dust mite allergen
HMG	high mobility group chromosomal proteins

HRP	Horse radish peroxidase
ICAM	Intracellular cell adhesive molecule
ID	Inhibitor of DNA binding
IL	Interleukin
IFN- γ	Interferon gamma
IPF	Idiopathic pulmonary fibrosis
ITGA6	Integrin Alpha-6
IgG	Immunoglobin G
iSMAD	Inhibitory SMAD proteins
JNK	Jun N-terminal kinase
kDA	kilodalton
LEF1/Tcf	Lymphoid enhancer factor-1
l	litre
L-Glut	L-Glutamine
LPS	Lipopolysaccharide
MAD	Mother against decapentaplegic
MAEC	Murine airway epithelial cells
MAPK	Mitogen activated protein kinase
MBP	Major Basic Protein
MET	Mesenchymal-to-Epithelial transition
MFI	Mean Fluorescence intensity
mg	milligram
$MgCl_2$	Magnesium chloride
MH1	Mad homology domain 1

MH2	Mad homology domain 2
ml	millilitre
mM	millimolar
MMP	Matrix metalloprotease
NaCl	Sodium Chloride
NEB	Neuroendocrine body
NES	Nuclear export signal
ng/ml	nanograms per millilitre
NGF	neuronal growth factor
NLS	nuclear localisation sequence
nm	nanometre
NN	Nitronaphthelene
NSCLC	Non small cell lung cancer
o/n	overnight
OD	Optical density
PCNA	Proliferating cell nuclear antigen
PBS	Phosphate buffered saline
OP1	Osteogeneic protein 1
OVA	Ovalbumin
P	post natal day
PAH	pulmonary arterial hypertension
PCR	Polymerase chain reaction
P-D axis	Proximal distal axis
PDGF	Platelet derived growth factor

pH	$-\log_{10}[H+]$
PH	Pulmonary hypertension
PNEC	Pulmonary neuroendocrine cells
p/s	Penicillin streptomycin
pSMAD	phosphorylated SMAD
qPCR	Quantitative polymerase chain reaction
Rb	retinoblastoma
RIPA	radioimmunoprecipitation buffer
RPMI	Roswell Park Memorial Park Institute medium
RNA	ribonucleic acid
Rpm	revolutions per minute
R-SMAD	Receptor SMAD
Rt-PCR	Semi quantitative reverse transcriptase polymerase chain reaction
RTK	Receptor tyrosine kinase
SCC	Small cell carcinoma
c-SCC	Combined small cell carcinoma
SCLC	Small cell lung cancer
SCM	Serum containing medium
SFM	Serum free medium
SDS	Sodium dodecyl sulphate
SBE	SMAD binding element
SFTPC	Surfactant protein C
SIP1	SMAD interacting protein 1

SMAD	Mother against decapentaplegic homolog
SMG	Submucosal gland
Smurf-1	SMAD ubiquitin factor 1
SNAI1	Snail1
SNIP	Small nuclear interacting factor
SO2	Sodium hydoxide
SOX	SRY related HMG box- binding transcription factors
STAT	Signal transducers and activators of transcription
TAE	Tris acetate EDTA
TBS	Tris buffered saline
TGF- β	Transforming growth factor β
TGF- βR	Transforming growth factor β receptor
TNF- α	Tumour necrosis factor α
TJ	Tight junctions
UV	Ultraviolet
VCAM	Vascular cell adhesion molecule
YFP	Yellow fluorescent protein
ZEB	Zinc fingers binding homeobox
ZO	Zonula occuldens

1 Chapter 1

Introduction

1.1 The respiratory system: development, health and disease

The lungs are responsible for oxygenation of the blood and the removal of respiratory waste products from the body. On average, an adult human breathes 4,000 litres of air per day (Naclerio 2012). Air is inhaled through the nasal and mouth cavities where it is warmed and filtered before reaching the trachea and descending bronchi. Two main stem bronchi descend into the right and left lobes where the airways become progressively narrower and terminate in alveolar structures surrounded by a dense network of capillaries. Here, the oxygen in the air traverses the alveolar wall and is taken up by the red blood cells for transport around the body. Conversely, carbon dioxide and water vapour leave the blood and are exhaled out of the lungs. As a result of this, the lungs are constantly exposed to inhaled pathogens and disease-causing agents that exist in our atmosphere. The airway epithelium lining the lungs is a primary point of contact for these infectious agents and thus the lung plays an important barrier function for protection against infection and disease. The formation of this complex organ during embyonic development occurs in a specific pattern which is tightly controlled by growth factors, morphogens and signalling molecules (Warburton et al. 2000).

1.1.1 Lung morphogenesis

Originating from the endoderm, the primary lung buds develop as they invaginate from the laryngo-tracheal groove into the splanchnic mesenchyme (Spooner and Wessells 1970). The four stages of lung development are known as the pseudoglandular, canalicular, saccular and alveolar stages (Figure 1.0.1). Pseudoglandular development begins at embryonic day 9.5 (E9.5) in the mouse and week 7-17 in humans (Ten Have-Opbroek 1991). This stage

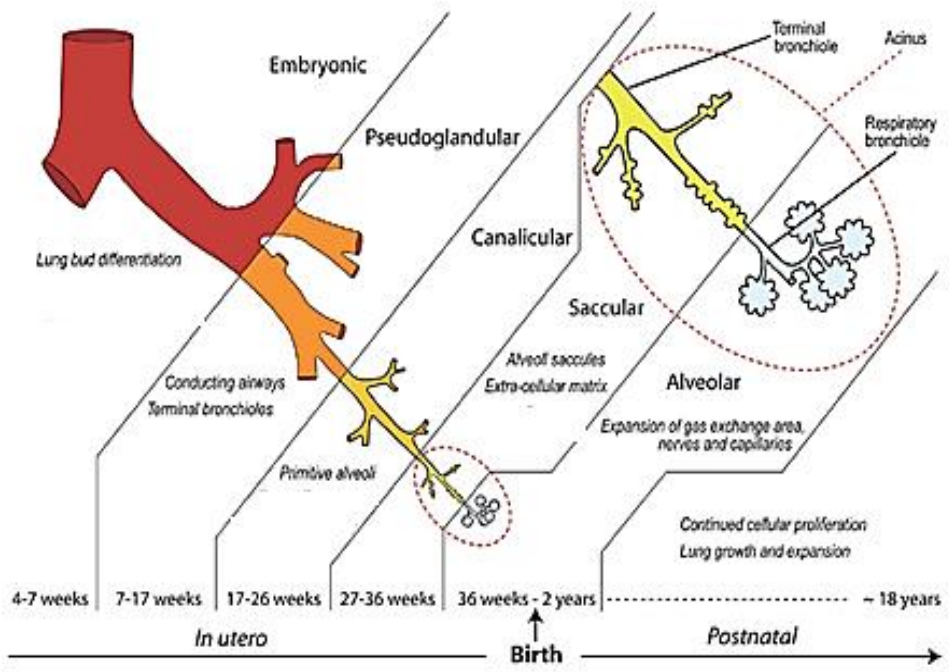

Figure 1.0.1 Lung bud development and morphogenesis

The development of the lung buds occurs in four main stages, beginning at embryonic week 4. Modified from (Kajekar 2007).

involves multiple branchings of the buds coupled with elongation and subdivision of the cells lining the buds. This allows the fundamental broncho-pulmonary tree to be formed. The canalicular phase follows from E16.5-17.5 in mice, week 17-26 in humans and involves extension of the broncho-pulmonary tree. The saccular stage occurs from E17.5 to postnatal in mice and week 27-36 in humans. During this stage, terminal sacs form on the bronchioles and the capillary network develops. The final stage of development is called the alveolar stage where the gas exchange function of the lungs is established. This occurs from post-natal day 4-28 in mice and from week 36 of foetal development to 36 months post-natal in humans (Alejandre-Alcázar et al. 2007; Hogan 1996; Sun et al. 2008).

1.1.2 Proximal-distal axis

The homeobox sequence NKX2.1 is expressed in the foregut endoderm-derived epithelial cells and is an early instructor of lung epithelial cell fate (Minoo et al. 1999; Morrisey et al. 2013). Subsequent lineage differentiation is tightly controlled by transcription factors, growth factors and signalling molecules. Proximal epithelial cells are under the control of the transcription factor SOX-2 whereas distal epithelial cells are instructed by SOX-9, GATA-6, ID-2 (Gontan et al. 2008; Que et al. 2009; Rawlins et al. 2009; Yang et al. 2002, 2014).

Growth factors originating from the endoderm or the underlying mesoderm are involved in complex signalling cascades to control epithelial cell differentiation along the proximal-distal axis and direct extension of the developing lung buds into the surrounding mesoderm (Morrisey et al. 2013). A broad range of signalling molecule families are involved in this process including Wnt- β-catenin, BMP, FGF, Notch, EGF and others (Cardoso 2001; Morrisey, E., Hogan 2010). The

complex communication between these growth factor families ultimately leads to the formation of the Epithelial-Mesenchymal-Trophic Unit (EMTU) (Figure 1.0.2). The EMTU is made up of opposing layers of epithelial and mesenchymal cells encompassing a network of basement membrane, fibroblasts, nerves and endothelial cells (Evans et al. 1999). The role of various growth factors and morphogens in lung development is explored further in section 1.2.3.

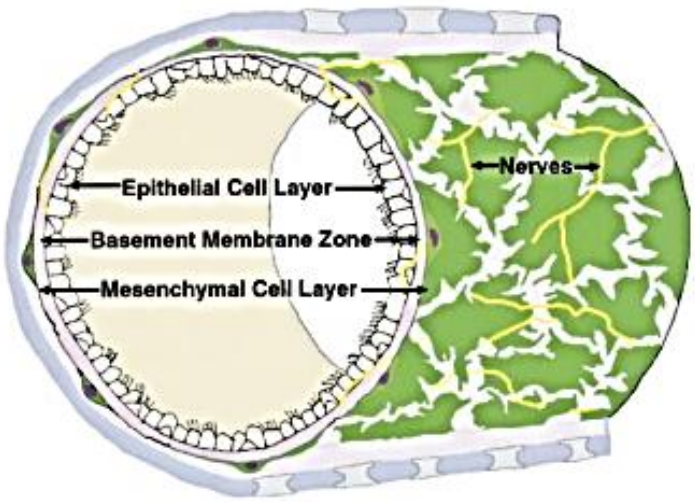

Figure 1.0.2 The Epithelial-Mesenchymal trophic unit (EMTU)

The fibroblast sheath consists of an epithelial cell layer and an mesenchymal cell layer with the basement membrane existing in the middle and joining the two (Evans et al. 1999)

1.1.3 Phenotypes of the epithelial cells lining the proximal-distal axis

Epithelial cells along the proximal-distal axis have different functions. The trachea and bronchi are lined with ciliated and secretory cells in the form of a pseudostratified epithelium to facilitate the mucociliary escalator and the clearance of inhaled pathogens. The tall columnar cells possess cilia to trap invading pathogens. Secretory cells such as goblet cells are interspersed with the ciliated cells (Figure 1.0.3). Goblet cells produce high molecular weight glycoproteins that facilitate pathogen trapping by the fluid on the surface of the epithelium (Chang, Shih, and Wu 2008). In human lungs goblet cells are present in the tracheobronchial airways and become less frequent in the smaller, distal airways where non-ciliated secretory club cells prevail. This is very different to mouse and small rodent airways, where club cells are the only secretory cell present in the airways (Chang et al. 2008; Plopper et al. 1983).

Basal cells facilitate attachment of ciliated and non-ciliated columnar cells to the basement membrane. They possess hemidesmosomes that anchor them to the basement membrane (Breeze and Wheeldon 1977). Basal cells are found at a higher frequency in the upper airways. In addition to their anchorage function, lineage-tracing experiments have demonstrated that basal cells can self-renew and transdifferentiate to give rise to ciliated, goblet and club cells following injury (Boers, Ambergen, and Thunnissen 1998; Hong et al. 2004; Rock et al. 2009).

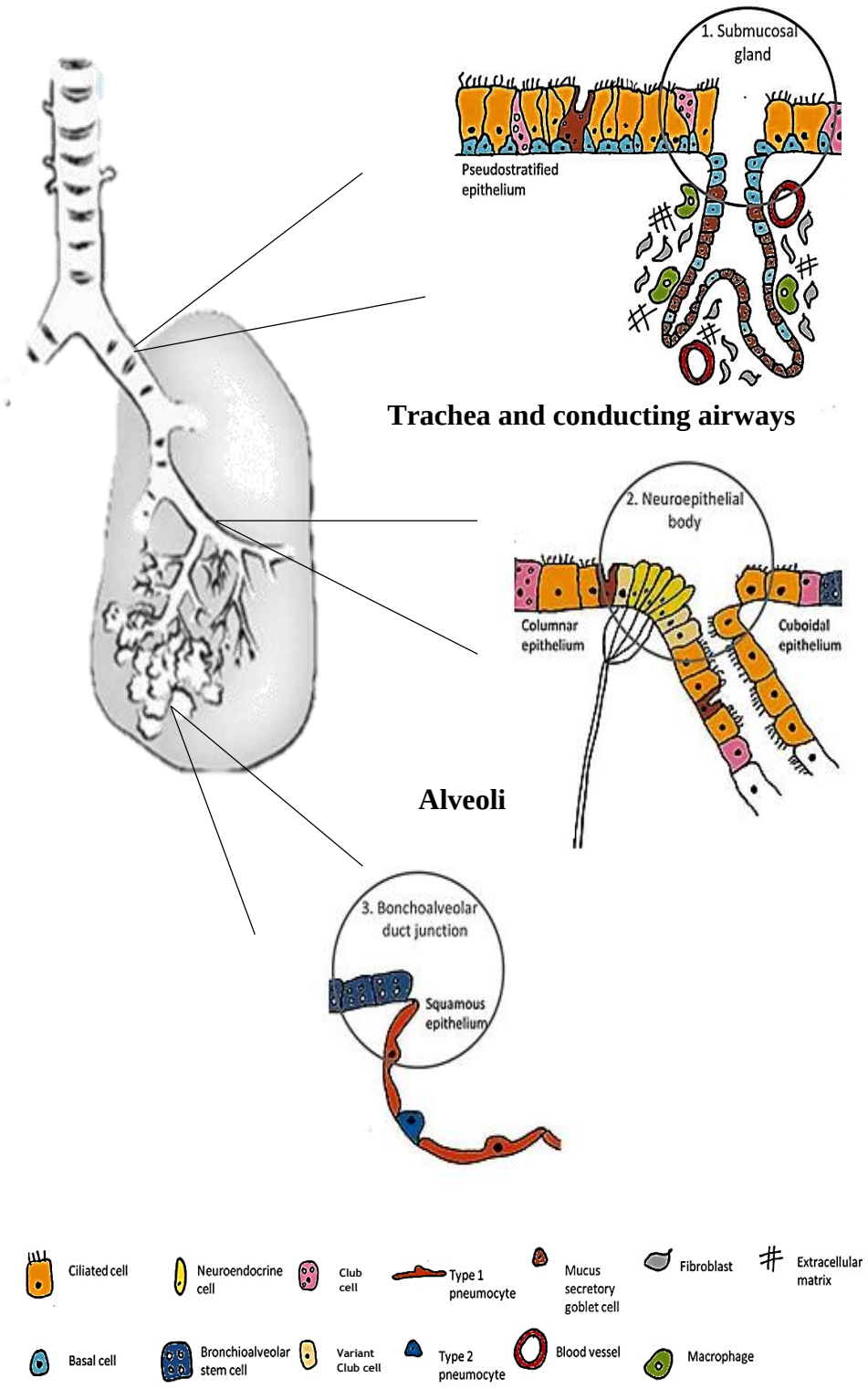

Figure 1.0.3 Epithelial cell types that exist along the proximal distal axis

Descending epithelial cell types along the trachea, bronchi and alveolar regions of the lung. Stem cell niches are circles and numbers 1-3. Diagram adapted from both (Chang et al. 2008; Kajekar 2007)

In the conducting airways and descending into the distal bronchioles, goblet cells and club cells function largely to protect the epithelium from invading pathogens. Club cells produce cytochrome p450 enzymes to detoxifying any harmful substances present in the lungs and they are also an established population of ciliated cell progenitors in the airways (Baron et al. 1988; Plopper et al. 1992).

At the terminal end of the bronchioles, a single layer of airway epithelial cells (AEC) type I and II line the alveolar sacs. These cells facilitate the bi-directional movement of gases between the airways and the blood (Chang et al. 2008). AEC I and II express low levels of EpCAM and AEC II are capable of self-renewal and differentiation to type I cells and express SFTPC (Barkauskas et al. 2013; Krieken and Litvinov 2003).

As well as the differentiated epithelial cells capable of self-renewal and transdifferentiation that exist in the respiratory tract, different regions along the airways contain progenitor cells capable of differentiation to restore epithelial integrity following injury. These regions are circle in black in Figure 1.0.3. In the submucosal gland, bromodeoxyuridine (BrdU) label-retaining cells remained in the subepithelial layer following weekly intratracheal detergent or SO_2 inhalation (Borthwick et al. 2001). By denuding tracheal airways of surface epithelial cells and carrying out xenograft transplantation, it was found that the stem cells residing in these SMGs had the ability to migrate and regenerate the surface airway epithelium. Pulmonary neuroendocrine cells (PNECs) and neuroepithelial bodies (NEBs) have also been shown as a reservoir for progenitor cells in the lung. NEBs are associated with club cell accumulation following epithelial injury (Hong et al. 2001; Reynolds et al. 2000). In the bronchoalveolar duct junction (BADJ), a progenitor population known as the bronchioalveloar stem cell (BASC) reside.

These cells can self-renew and are multipotent, maintaining club and AEC populations and mutations in these BASC result in adenocarcinoma formation (Kim et al. 2005). Finally, in the alveolar region a SFTPC- progenitor exists which is capable of differentiating into both SFTPC+ AEC I and AECII following bleomycin airway injury (Chapman et al. 2011).

1.1.4 The Lung epithelium

Airway epithelial cells are dependent on correct cell-cell contact between adjacent cell populations and anchorage to the basement membrane zone (BMZ) at the EMTU. The characteristics that define an epithelial cell include the ability of cells to grow as a continuous sheet, the polarised nature of the cells displaying distinctions between apical, lateral and basal regions and the immobile nature of the cells in the structure (Savagner 2007). Actin is responsible for establishing epithelial cell polarity (Angst et al, 2001). Various types of cell junctions exist between neighbouring epithelial cells (Figure 1.0.4). Tight junctions or zona occludens (ZO) exist in the apical region of epithelial cells and consist of at least three transmembrane proteins including occuldin, claudin, cytoplasmic adaptors and junctional adhesion molecules (Matter and Balda 2003). Claudin-1 is an example of a transmembrane protein which interacts in a homodimeric fashion to form the tight junction. The interaction of these proteins results in a tight seal forming between adjacent epithelial cells and the generation of a selectively permeable junction (Balda and Matter 2000; Jefferson, Leung, and Liem 2004). TJs interact with the actin cytoskeleton using adaptor molecules (Fanning et al. 1998). ZO-1, also known as Tight-junction-1, and afadin are an examples of such adaptor protein molecules that link intercellular homodimers to the cytoskeleton. CD2AP

is an intracellular scaffolding protein also believed to link tight junctions to the cytoskeleton (Matter and Balda 2003).

The second type of interepithelial junction is the cell adherens junction (ADJ). Cadherin homodimers form between adjacent epithelial cells in a calcium dependent interaction. Epithelial (E-), Neuronal (N-), Placental (P-) and Cadherin-12 are the four classic cadherin proteins involved in ADJ formation. These cadherin complexes are linked to the internal actin cytoskeleton by adaptor molecules such as γ-, β-,α-catenin, vinculin and p120 (Angst et al. 2001). β-catenin is involved in both regulation of the cell cycle via the Wnt signaling pathway and cell adhesion. When localised at the membrane, β-catenin protein interacts with the cadherin proteins and helps to stabilise the complex (Figure 1.0.5) (Angst et al. 2001) Thirdly, desmosomal junctions are formed by interactions with desmocollins and desmogleins and the intermediate cell filaments. Desmocollin and desmoglein are cadherin proteins. Following homodimer formation the complex interacts with intermediate filaments in the cytoplasm via desmoplakin plakoglobin or plakophilin. This complex is depicted in Figure 1.0.5.

Gap junctions are the fourth type of epithelial junction. These junctions connect the cytoplasm of adjacent epithelial cells through a hydrophilic channel made up of connexons. Gap junctions facilitate the movement of small molecules and ions from one cell to the next and they can exist as homotypic, heterotypic or heteromeric complexes (Goodenough and Paul 2009).

Finally, hemidesmosomes are the junctions responsible for cell-matrix interactions and the anchorage of epithelial cells to the BMZ. As previously mentioned, basal cells possess hemidesmosome junctions. Keratins, the intermediate filaments in the

epithelial cells are linked to laminins in the ECM via α_6 β_4-integrins interacting with cellular plectin, bulbous pemphigoid (BP) BP180 and possibly BP230 (Borradori and Sonnenberg 1999). Although not depicted in figure 1.0.4, focal adhesions exist on the basal surface of epithelial cells to anchor the cell to the BMZ. These junctions link the actin cytoskeleton to the ECM via interactions with integrin and docking adaptor molecules such as talin, paxillin and filamin (Van Tam et al. 2012; Wozniak et al. 2004).

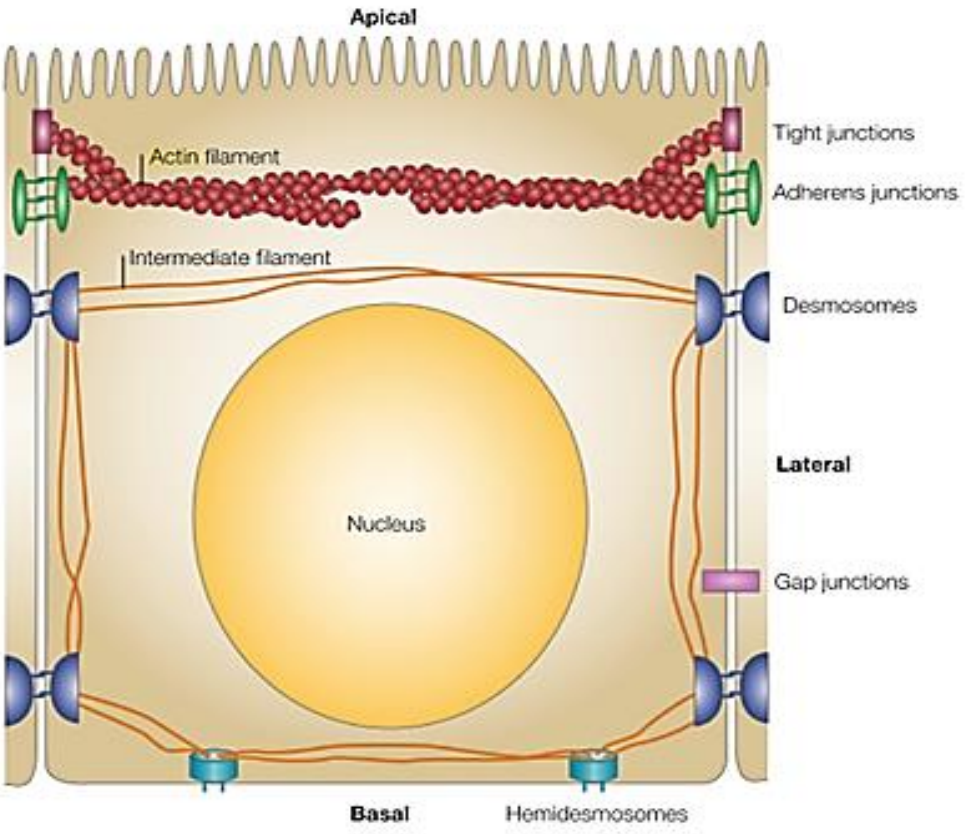

Figure 1.0.4 The epithelial cell junctions

Representative image of the interepithelial junctions. Tight junctions and adherens junctions are connected to the actin cytoskeleton. Desmosomes are linked to the intermediate filaments via desmoplakin. Adapted from (Matter and Balda 2003)

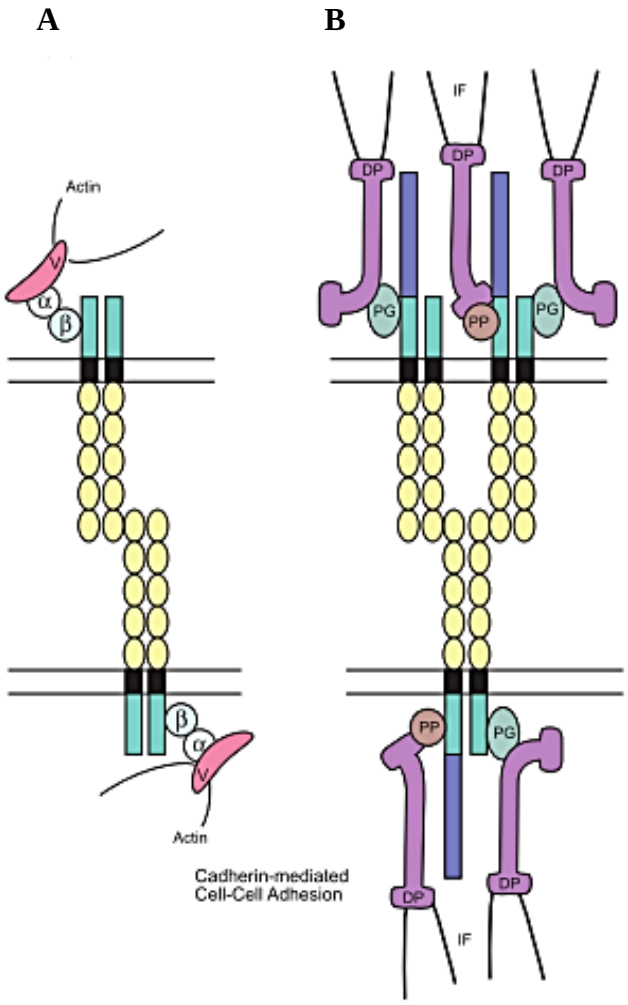

Figure 1.0.5 Adherens junctions and desmosomal junction

Classical cadherin mediated cell adhesion between cadherins possess five repeated extracellular domains. (A) Homodimeric cadherin junctions, in yellow, form in the interepithelial space linking the internal actin cytoplasmic networks between adjacent epithelial cells. This occurs via interactions with β-catenin (β),α-catenin (α) and vinculin (V). Neural (N-), Epithelial (E-), Placental (P-) are the three main types of classical cadherin proteins. (B) Desmosomal junctions use the desmosomal cadherins desmoglein and desmocollin in yellow. Interactions with the intermediate filaments (IF) occur via desmosomal plaques plakoglobin (PG), plakophilin (PP) and desmoplakin (DP). Adapted from (Angst et al. 2001)

1.1.5 Lung injury and repair

Due to the respiratory function of the lungs, the airway epithelium is constantly exposed to smoke, allergens, bacteria, viruses, noxious gases and infectious agents that exist in our atmosphere. However, the fact that the lungs usually maintain their function under these conditions is a testament to the highly effective barrier activities and immune response of the lung epithelium. A principle function of the epithelium is the formation of a mucociliary layer which provides a physical barrier against invading pathogens. This tightly-knit seal is formed by the various cell junctions and adherens junctions which exist between the epithelial cells, as explained in section 1.3. The epithelium produces a diverse range of secretory products which contribute to the mucociliary escalator of the lungs. In addition, the production of nitric oxide and arachidonic acid further help to fight infection and maintain airway homeostasis (Crosby and Waters 2010; Knight and Holgate 2003).

However, damage to the epithelium can arise following severe or prolonged exposure to harmful agents. Multicellular damage to the epithelium causes a cascade of events which, in the case of normal repair processes, will lead to the physical restitution of the denuded BMZ and the recruitment of immune cells to eradicate the invading pathogen responsible for the damage (Erjefalt et al. 1997a). The repair of the epithelium is the primary goal of the damage response as any breech in this protective layer can result in widespread infection and detrimental effects to the respiratory system and indeed, the organism.

Physical damage to the epithelium has been shown to induce a mechanical response in the cells. As the epithelium is a relatively immobile structure, loss of surface tension in the injured region triggers a stress response (Bilek, Dee, and Gaver 2003;

Ghadiali and Gaver 2008). The cells at the edge of the wound lose contact inhibition of locomotion and become leaky resulting in the passive movement of small extracellular molecules in these cells (Jacinto, Martinez-Arias, and Martin 2001). These events may trigger the downstream signalling cascades involved in epithelial repair. Extensive actin cytoskeleton rearrangements occurs following physical stress of an intact epithelium. This was shown by pulling an intact epithelium *in vitro* (Martin and Lewis 1992). The sequence of events involved in repairing the damaged epithelium are outlined in Figure 1.0.6 A.

Exposure of the BMZ following an injury activates residing macrophages which in turn recruit additional immune cells to the damaged site. The secretion of inflammatory cytokines, matrix metalloproteases and growth factors such as FGF, EGF, BMP and TGF from both immune cells and cells of the activated EMTU promotes the sealing of the epithelial layer and the eradication of pathogens (Crosby and Waters 2010). Fibronectin and collagen are produced by the underlying fibroblasts in response to the influx of growth factors such as TGF- β to repair the epithelial basement layer. Many *in vivo* epithelial restitution experiments have demonstrated that cell migration. rather than cell proliferation, is the primary event which occurs during restoration of the damaged epithelial region (Erjefalt et al. 1997b; Joanne C. Masterson et al. 2011; Zahm et al. 1997). As outlined in Figure 1.0.6 B, cells bordering the wounded region downregulate epithelial cell markers to assume a migratory phenotype and migrate onto the exposed BMZ. Resident lung progenitors undergo squamous cell metaplasia followed by migration and proliferation to restore epithelial integrity.

A

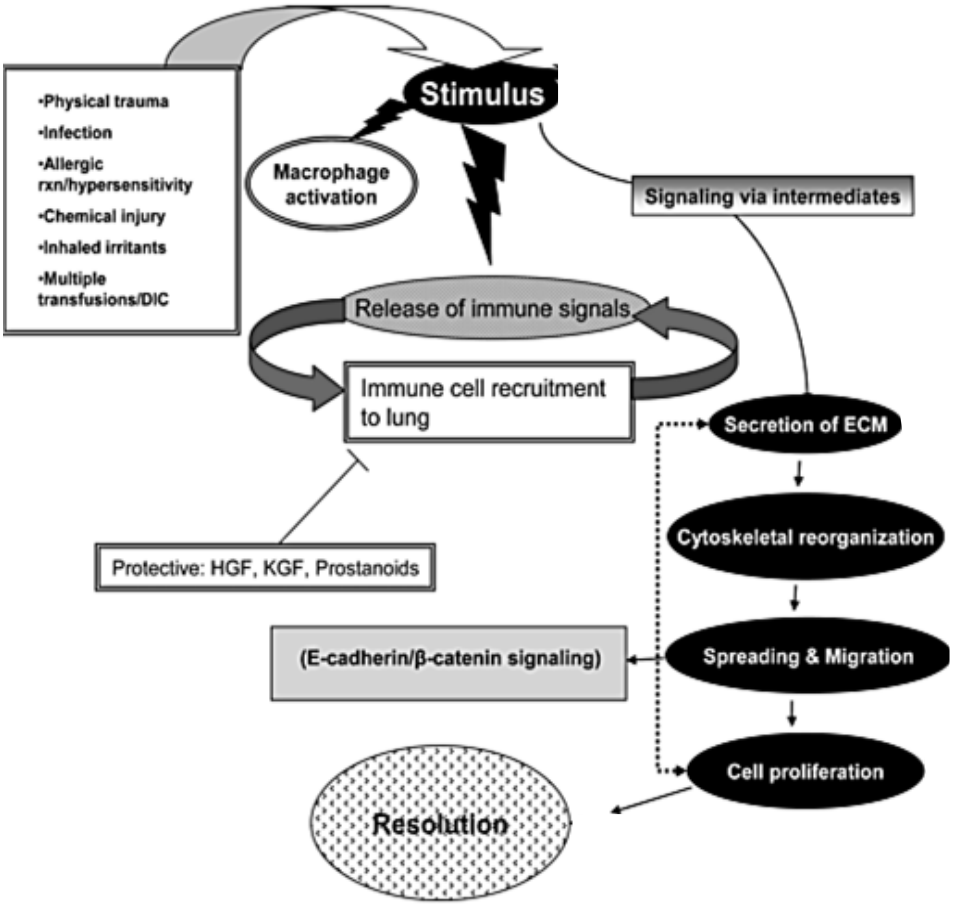
•Physical trauma
•Infection
•Allergic rxn/hypersensitivity
•Chemical injury
•Inhaled irritants
•Multiple transfusions/DIC
Stimulus
Macrophage activation
Signaling via intermediates
Release of immune signals
Immune cell recruitment to lung
Secretion of ECM
Cytoskeletal reorganization
Protective: HGF, KGF, Prostanoids
(E-cadherin/β-catenin signaling)
Spreading & Migration
Cell proliferation
Resolution

B

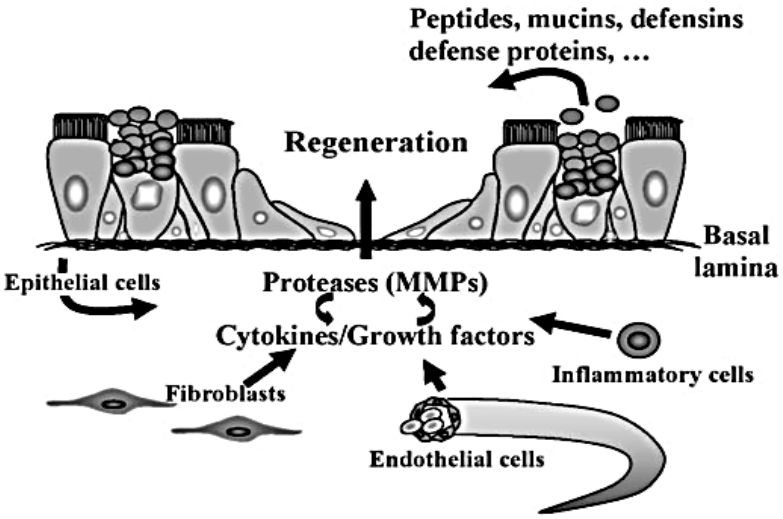

Figure 1.0.6 The sequence of events and signalling molecules involved in epithelial restitution

(A) Following epithelial damage, immune cells are recruited to the site and cause increased immune cell recruitment and the secretion of growth factors. ECM is deposited on the exposed BMZ and epithelial cell spreading, migration, proliferation and differentiation occur to restore the damaged region.

(B) Secretory molecules including peptides, mucins, proteases, cytokines and growth factors are secreted by epithelial, endothelial and fibroblast cells as well as infiltrating immune cells to induce and control the restoration events. Modified from (Crosby and Waters 2010; Puchelle et al. 2006)

Tightly controlled differentiation events occur following proliferation to reinstate epithelial function (Crosby and Waters 2010; Puchelle 2000; Puchelle et al. 2006; Warburton et al. 2008; Woolley and Martin 2000; Zahm, Chevillard, and Puchelle 1991). Experiments using adult human nasal epithelial xenografts on denuded tracheae in nude mice showed that while exposed BMZ were partially covered by a poorly differented epithelial layer after only three days post-implantation, it took up to five weeks for the establishment of a fully functional differentiated, pseudostratified epithelial barrier (Dupuit et al. 2000). This highlights the level of control and regulation required for correct epithelial cell repair.

The regulation and subsequent cessation of the reparatory processes is controlled by cells of the EMTU and infiltrating inflammatory cells. For example, eosinophils help mediate the inflammatory process by producing anti-inflammatory cytokines IL-4 and IL-13 (Ahdieh, Vandenbos, and Youakim 2001). If this process is not correctly regulated and the reparatory events are prolonged, a chronic inflammatory environment will manifest in the airways. Extensive ECM deposition, abnormal epithelial cell migration, uncontrolled cell proliferation and unregulated growth factor and cytokines release ultimately contributes to a disease phenotype in the lungs. Asthma, COPD, IPF, cancer and acute lung injury are disorders of the airways which present with pathophysiologies resembling different aspects of incorrect epithelial repair.

1.1.6 Lung Cancer

Lung cancer is the leading cause of cancer-related deaths in the USA. According to the American Cancer Society, it is forecast that about 221,200 new cases of lung cancer will be diagnosed in 2015 and that approximately 158,040 deaths will be

attributed to lung cancer. Tobacco smoke is the main risk factor for developing lung cancer and at least 80% of lung cancers are linked to smoking. Genetic inheritance, air pollution, radon and asbestos are also believed to elevate the risk of developing lung cancer (Challem 1997; Ger et al. 1992).

The two main types of lung cancer are small cell lung cancer (SCLC) and non-small cell lung cancer (NSCLC). SCLC is subdivided into the highly invasive small cell carcinoma (SCC) and combined small cell carcinoma (c-SCC). SCC is often termed "oat-cell carcinoma" as the cancer cells are small and flat with little cytoplasm and big nuclei. SCC forms metastatic sites very quickly and are thought to originate from PNECs (Jackman and Johnson 2005; Stovold et al. 2012, 2013). c-SCC is characterised by the presence of SCC alongside another non small cell-derived malignant tissue such as adenocarcinoma or large cell carcinomas (Wagner et al. 2009).

NSCLC is the most dominate form of lung cancer and 80-85% of all lung cancer cases fall into this category. The three main types of NSCLC include squamous cell carcinoma originating from epithelial cells, adencocarcinomas from secretory cells and large cell carcinomas such as large cell neuroendocrine carcinomas – which is similar to SCC (D'Addario et al. 2010). Surgical resection is the main treatment for NSCLC from stages I through to IIIA whereas combined chemotherapy and radiation are prescribed later stage NSCLC and for SCLC patients. Drugs such as the platinum based- cisplatin and etoposide are commonly used in chemotherapeutic treatment plans. In addition, recent advances in targeted therapy have seen drugs such as denosumab, a monoclonal antibody against receptor activated NFKB and crizotinib, a ROS1 and anaplastic lymphoma kinase (ALK)

inhibitor, being approved by the FDA for treatment of specific lung cancer subtypes (Scagliotti et al. 2012; Timm and Kolesar 2013).

Within a tumour a number of different cell subpopulations exist. As outlined in (Hanahan and Weinberg 2000), the cancer cells adopt specific properties in order to survive and thrive as a neoplastic legion. These include the ability to generate distant metastatic sites for increased tumour invasion, evade apoptosis and growth inhibitory signals, (3) develop sustained angiogenic potential, act as a source of autocrine growth factor signals and develop the capabilities of limitless replicative processes. While this list is not exhaustive and not all tumours acquire every characteristic, these six fundamental processes are central for cancer survival and tumour progression.

Tumour heterogeneity defines the differences in genotype and phenotype that exist between cancer cells in a single tumour (intra-tumour heterogeneity). These variations can also occur between different tumour sites in the body and similar tumour types occurring in different people (inter-tumour heterogeneity) (Burrell et al. 2013). Intra-tumour heterogeneity has been described as a branched evolutionary model enabling increased cancer cell survival following adoption of the six fundamental cancer cell properties. Heterogeneity can be introduced into the tumour population by genetic or non-genetic means. Genomic instability can introduce somatic point mutations leading to impaired DNA repair processes. This causes replication errors and alters chromosomal numbers which propagate between tumour subpopulations. Epigenetics play a role in non-genetic-induced tumour heterogeneity via silencing of tumour suppressor genes. Additionally, the tumour microenvironment affects cancer cell phenotype and different signals determine altered cell fate. Tumour heterogeneity is also introduced by dynamic

phenotypic switching events between the different cancer subpopulations (Ferrao et al. 2015; Marusyk, Almendro, and Polyak 2012).

In normal non-neoplastic tissues a hierarchy exists whereby a stem cell gives rise to committed progenitor cells which in turn produce lineage-restricted fully differentiated cells (Figure 1.0.7). Progenitor cells are capable of de-differentiating into stem cell in certain conditions. The field of directed de-differentiation of committed lung epithelial cells has received much attention recently and re-programming experiments have highlighted the potential use of committed cells in lung regeneration (Huang et al. 2014; Tata et al. 2013).

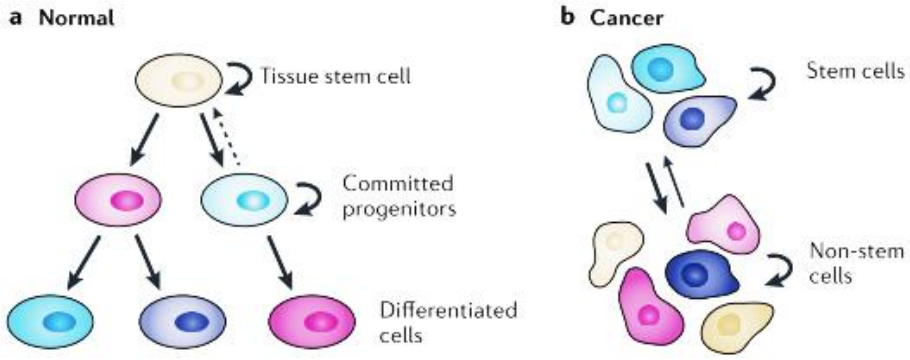

Figure 1.0.7 Differentiation hierarchies in normal and cancer cells

(Marusyk et al. 2012)

In neoplastic tissues, similar differentiation hierarchies exist. Stem cell and non-stem cell populations exist in the tumour and interconversion between the two occurs more frequently (Figure 1.0.7) (Marusyk et al. 2012).

Both SCLC and NSCLC actively form metastatic foci, particularly the more invasive SCLC (Jackman and Johnson 2005). One of the central dogmas regarding

tumour progression and metastasis formation is the clonal selection theory. This theory is centred on the existence of a cancer stem cell in the body of a tumour that is capable of undergoing metastasis to establish a new tumour at a distant site (Talmadge 2007). Subsequent differentiation and expansion of the metastatic population leads to the formation of complex heterogenous tumours at these new sites (Fidler 2003; McMorrow et al. 1988). Furthermore, karyotypic analysis of multiple metastatic sites originating from a primary tumour have revealed individual phenotypes specific to each metastatic site. This suggests that primary tumours can possess numerous clonal stem cell subpopulations capable of establishing new neoplastic legions each with different characteristics and properties (Talmadge et al. 1984).

Another dogma regarding the development of metastatic foci is the process of phenotypic switching. This phenomenon allows non-invasive benign tumour cells to adopt a more migratory and mesenchymal phenotype. These cells are then capable of detaching from the primary tumour to facilitate the formation of novel tumour sites at a different location in the body (Jonathan M. Lee et al. 2006; Li et al. 2015). Phenotypic switching can be driven by environmental stresses, growth factor signalling and transcriptional reprogramming and causes an epithelial-to-mesenchymal transition (EMT) in the cells (Ferrao et al. 2015; Kemper et al. 2014). Recently, a zebrafish-melanoma xenograft model was used to illustrate that metastatic foci can also form due to collective cooperation between intrinsically invasive cells and benign non-invasive cells (Chapman et al. 2014). In addition, different types of cancer cells favour metastasis formation in specific locations in the body and tend to repeatedly migrate to these regions. Thus, it is believed that the microenvironment plays an important role in establishing novel metastatic sites.

This is termed the "seed and soil" hypothesis (Fidler 2003). EMT is explored further in section 1.3.

1.1.7 Inflammatory lung disease

Asthma is an inflammatory airway disease characterised by broncho-constriction, wheezing and shortness of breath. According to the American Academy of Allergy Asthma and Inflammation (AAAAI), the incidence of asthma in US population has risen from 1 in 14 in 2001 to 1 in every 12 in 2009 (Center for Disease Control and Prevention 2011). Atopy, allergens, environmental pollutants and genetic inheritance are all risk factors for asthma (Knight and Holgate 2003; Saetta and Turato 2001).

At a structural level the EMTU of an asthmatic patient is both more susceptible to damage compared to a healthy individual and experiences impaired repair responses following injury (Knight and Holgate 2003). The EMTU is the central unit undergoing remodelling during asthma. Changes to the EMTU include mucus cell hyperplasia and metaplasia causing excessive mucus production, basement membrane thickening, ECM deposition, narrowing of the airway lumen, elevated smooth muscle mass, increased fibroblast proliferation and myofibroblast activation (Figure 1.0.8). All of these changes are mediated through abnormal growth factor signalling, inflammatory mediators, chemokines, cytokines and secretory products such as matrix metalloproteases (Bai and Knight 2005; Davies 2009; Saetta and Turato 2001).

At a cellular level, inflammation in asthma is mediated via the Th-2 response involving eosinophils, basophils and mast cells. Eosinophils exert their function via

secretion of inflammatory cytokines, eosinophil derived cationic proteins and growth factors such as TGF-B to promote collagen deposition (Gleich and Adolphson 1993a; Gundel, Letts, and Gleich 1991; Humbles et al. 2004). Differential eosinophilic infiltration has been reported throughout the airways in both the upper large airways and the smaller bronchioles (Carroll, Cooke, and James 1997). However, due to the mucus cell metaplasia and establishment of the Th-2 response that occurred in the absence of eosinophils in a mouse GATA-1 double knockout, additional inflammatory cells are believed to play a significant role in asthma pathology (Humbles et al. 2004). There is evidence that neutrophils are also involved in asthma and the once accepted paradigm segregating COPD and asthma based on neutrophil versus eosinophil infiltration is blurring. Different asthmatic endotypes are now accepted including allergic bronchopulmonary mycosis and neutrophilic asthma (Lötvall et al. 2011; Walford and Doherty 2014).

A novel study from Harvard School of Public Health, has highlighted the role of jamming and unjamming in an experimental model of asthma using human bronchial epithelial cells (Park et al. 2015). Cell movements in healthy cultures are minimal and each cell is tightly compacted with its immediate neighbours. However, in a model of bronchospasm, cell movement changes drastically and cells move in fluid-like swirling patterns. Interestingly, using a vortex model and shape indexing, this jamming and unjamming has been attributed to changes in epithelial cell shape as opposed to the expression of cell adhesion molecules. This study contributes to our knowledge about the biological processes involves in the tissue remodelling in asthma and adds a new mechanical dimension to the etiology of asthma's disease phenotype.

A

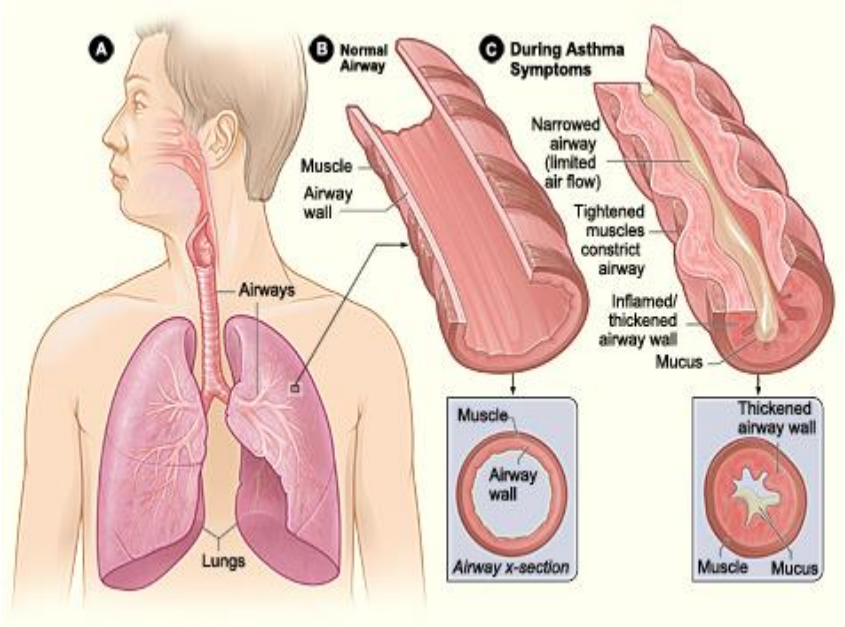

B

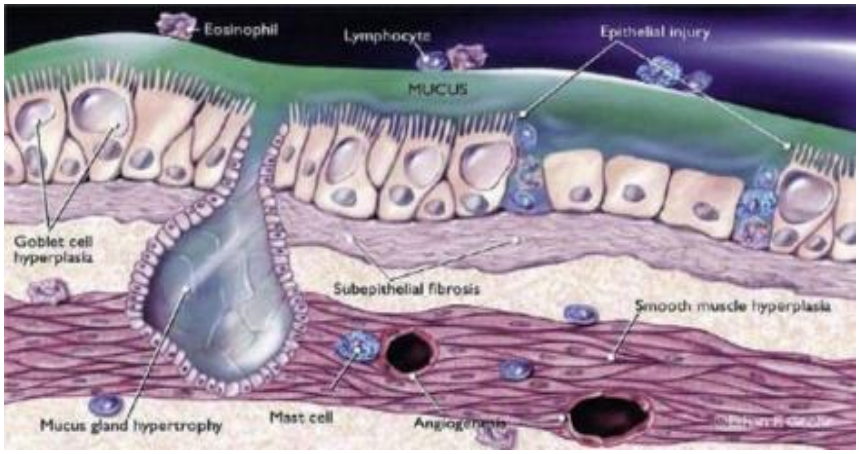

Figure 1.0.8 The asthma phenotype

(A) The changes in the asthmatic airway compared to healthy airways. Image obtained from NHLBI GOV http://www.nhlbi.nih.gov/health/health-topics/topics/asthma (B) The structural and cellular changes that occur in asthmatic airways include epithelial damage, BMZ thickening via subepithelial fibrosis, smooth muscle hyperplasia, excessive mucus production and inflammatory infiltration (Leonardi et al. 2013)

1.1.8 The DLKP cell line

The DLKP human cell line was established from a lymph node metastasis of a primary lung tumour, described as a "poorly differentiated squamous carcinoma". When grown in culture the DLKP parental population was observed to contain morphologically heterogenous sub-populations. The DLKP line was sub-cloned and three distinct clonal populations DLKP-SQ (squamous phenotype), DLKP-M (mesenchymal phenotype) and DLKP-I (intermediate) were established (Figure 1.0.9) (Law et al., 1992; Mcbride et al, 1998). This was achieved by serial dilutions to isolate individual cell colonies. DLKP-SQ cells grow as relatively small, squamous, cuboidal cells and form compact colonies in culture. The colonies display a "cobblestone"-like appearance with bright distinct boundaries between each individual cell. DLKP-SQ account for approximately 70% of the original parental population. DLKP-I cells are smaller than DLKP-SQ and account for approximately 25% of the parental population. DLKP-I cells also grow as colonies but no individual cell boundaries are evident between the cells. A bright outer boundary is present around the colony. DLKP-M cells are the largest of the three DLKP clones and represent approximately 5% of the parental population. DLKP-M cells possess extended cytoplasmic projections and do not grown in colonies. Instead, DLKP-M cells appear mesenchymal and mobile (Mcbride et al. 1998)

When grown in culture, spontaneous interconversion events have been observed between DLKP-I clones and both DLKP-SQ and DLKP-M. No conversion between DLKP-SQ and DLKP-M cells was evident and thus DLKP-I cells were deemed as a potential intermediate and stem-cell like population capable of switching phenotype between the two clones.

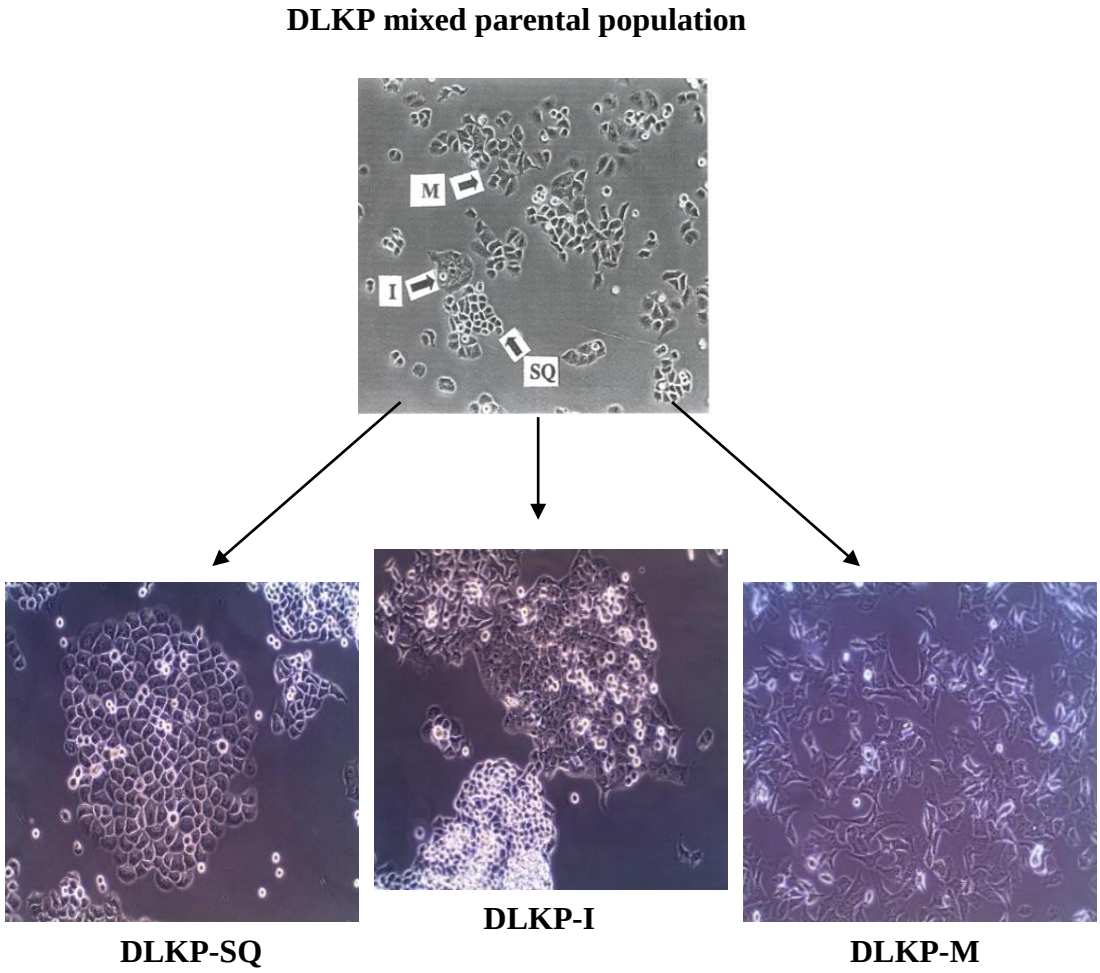

Figure 1.0.9 DLKP lung cancer cell line

DLKP parental populations contained DLKP-SQ, DLKP-I and DLKP-M clones which are morphological distinct and interconvert in culture.

1.2 Bone Morphogenetic Signalling

Bone morphogenetic proteins (BMPs) are a conserved family of signalling molecules that were first described by Prof. Martin Urist in the 1960s. He documented the osteoinductive capabilities of BMPs in the muscle pouches of rabbits (Urist 1965). Since then, BMPs have been referred to as "body morphogenetic proteins" based on their involvement with many different organs, structures and signalling cascades in the body (Wagner et al. 2010).

Decapentaplegic (Dpp) is the BMP homolog expressed in Drosphila embryo and is vital for the correct dorsal-ventral patterning of limbs and organs (Ferguson and Anderson 1992). In zebrafish and Xenopus, BMP signalling is responsible for directing ectodermal and mesodermal tissue to the correct cell fate, in a concentration dependent manner (O'Connor et al. 2006; Wilson et al. 1997; Zhang, Lander, and Nie 2007). In mice, knockout models have highlighted the vital function of BMP signalling in the formation of bones, endoderm patterning of the liver, lungs, gut and pancreas as well as ectoderm-derived organ development such as the brain and the skin (Monteiro et al. 2008; Wang et al. 1990). This essential developmental role is conserved in humans and many diseases are attributed to incorrect BMP signalling events including neurological and ophthalmic diseases, pulmonary aerterial hypertension (PAH), fibrodysplasia ossificans progressiva (FOP), osteoarthritis (OA), juvenile polyposis (JP) and cancers of the lung and colorectum (Figure 1.0.10) (Wang et al. 2014).

The signals involved in the BMP pathway and the molecules responsible for regulating pathway expression are discussed in this section. In addition, the role of BMP signalling in cancer and inflammatory diseases is highlighted.

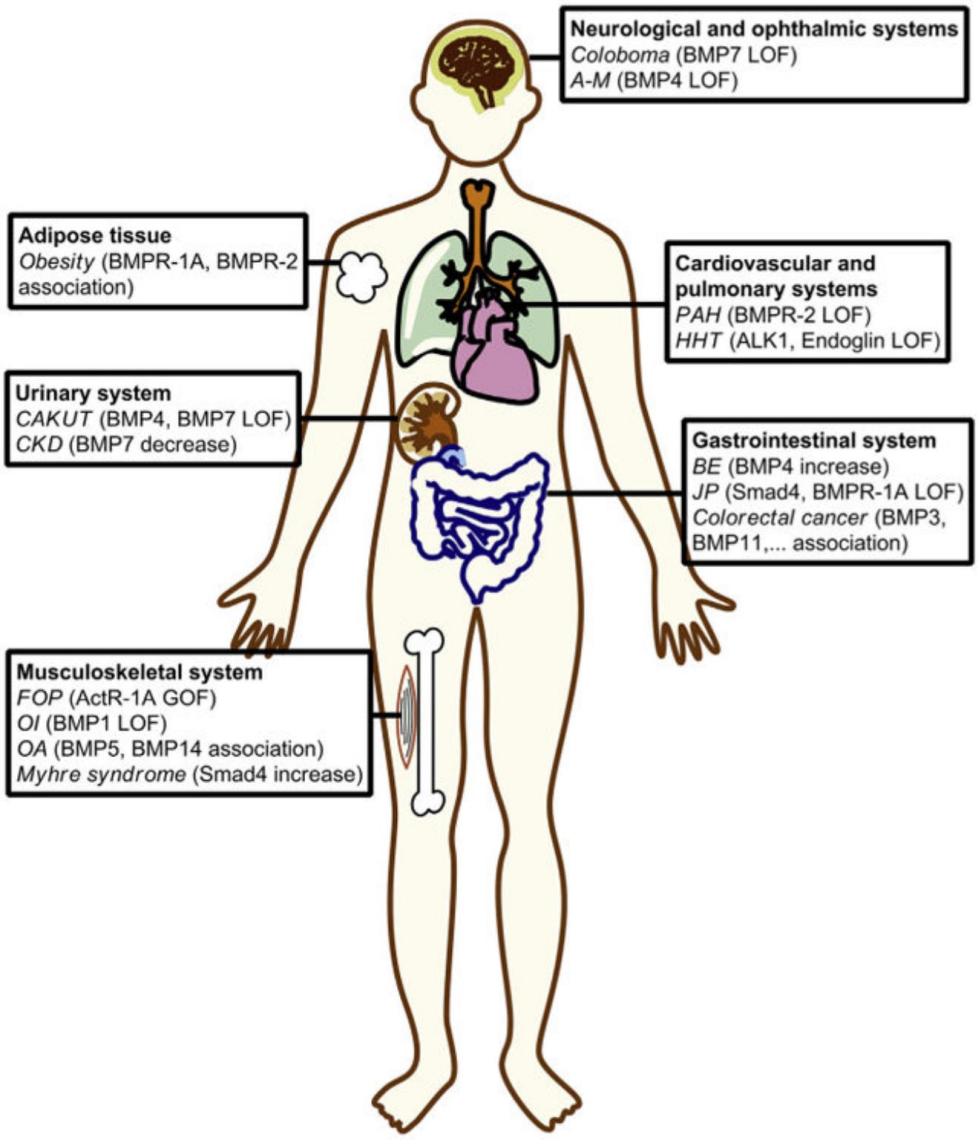

Figure 1.0.10 Human diseases associated with aberrant BMP signalling

Mutations in BMP receptors, SMAD signalling components and BMP ligands are associated with numerous diseases in the human body (Wang et al. 2014)

1.2.1 BMP signal transduction

BMPs are members of the transforming growth factor (TGF) superfamily of signalling proteins. Other family members include the activin/inhibins, Mullerian inhibiting hormones (MIH), TGF β and growth and differentiation factors (GDFs) (Kingsley 1994). To date, more than twenty BMP family members have been identified and these are subdivided to four groups based on amino acid sequence similarity. BMP-2 and BMP-4 are the best studied family members. These proteins have 83% homology and are grouped together (Wozney 1989). BMP-7 is known as osteogenic protein-1 (OP-1) and together with BMP-5, -6, -8 forms a second group known as the osteogenic protein group. Thirdly, BMP-9 and -10 are classed together while GDF-5, -6 and -7 form the final group (Miyazono, Kamiya, and Morikawa 2010).

BMP ligands bind to type I and type II receptors on the cell membrane of BMP-responsive cells. Both types of receptor possess a relatively short extracellular domain, a single transmembrane spanning domain and an intracellular cytoplasmic domain which contains a serine/threonine kinase domain (Miyazono et al. 2010). Type I receptors include BMPRIa/Alk-3, BMPRIb/Alk-6, ActR-I/Alk-2 and Alk-1 which is specific to endothelial cells. Type II receptors possess a constitutively active kinase domain and include BMPRII, ActR-IIa/ACVRIIa and ActR-IIb/ACVRIIb. BMP ligands bind weakly to type I receptors in the absence of type II receptors while type II receptors positively enhance the binding of ligands (Koenig et al. 1994; Rosenzweig et al. 1995). While some overlap does exist, generally BMPRIa and BMPRIb are involved in BMP-2, BMP-4 and BMP-7 signalling while BMP-6 preferentially binds to Alk-2 and BMPRIb (ten Dijke et al.

1994). Co-receptors, such as the repulsive guidance molecule family (RGM) members RGM-b and RGM-c, commonly known as Dragon and hemojuevelin, respectively, can amplify signalling of certain BMP ligands (Babitt et al. 2006; Nohe et al. 2002; Samad et al. 2005; Xia et al. 2010).

A variety of SMAD-dependent and SMAD-independent pathways can be activated following ligand-induced receptor activation. In canonical BMP signalling, three groups of SMAD proteins have been described based on their role in pathway activation: receptor-regulated SMAD-1, -2, -3, -5, - 8 (RSMADs); common mediator SMAD 4 (co-SMAD) and inhibitory SMAD-6, -7 (iSMADs). BMPs and MIH activate SMAD-1, -5, and/or -8 signalling while TGFβ ligands activate SMAD-2 and -3 via Alk-2, -4, -5 and -7 receptors (Miyazono, Maeda, and Imamura 2005).

R-SMADs contain highly conserved N- and C-terminal domains known as Mothers against decapentaplegic (Mad) homology (MH)-1 and MH-2 (Figure 1.0.11). A variable linker region joins these two domains. This linker region contains motifs that can be phosphorylated by mitogen-activated protein kinases (MAPK) and glycogen synthase kinase (GSK) as part of the non-canonical BMP pathway (Massague 2003). The linker also contain a Proline-Proline-x-Tyrosine (PPXY) motif. This PY motif is involved in interactions with proteins containing two conserved tryptophan residues spaced 20-22 amino acids apart (WW) such as the SMAD-ubiquitin regulatory factors (Smurfs).

A

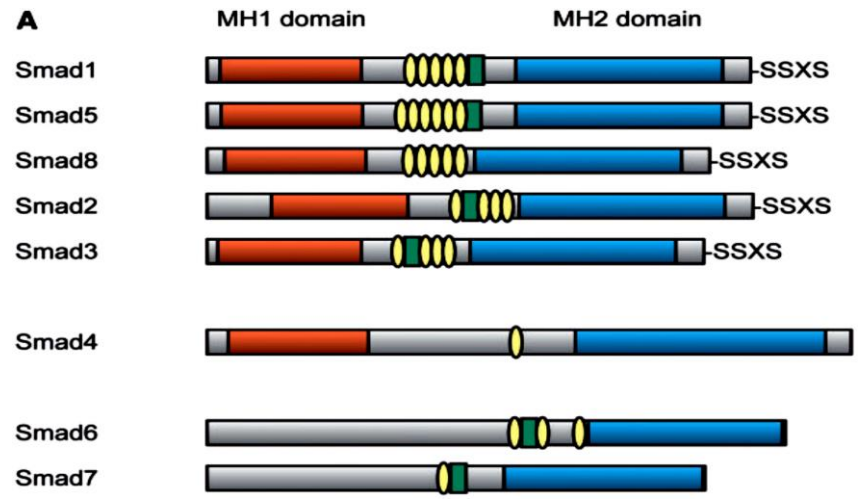

B

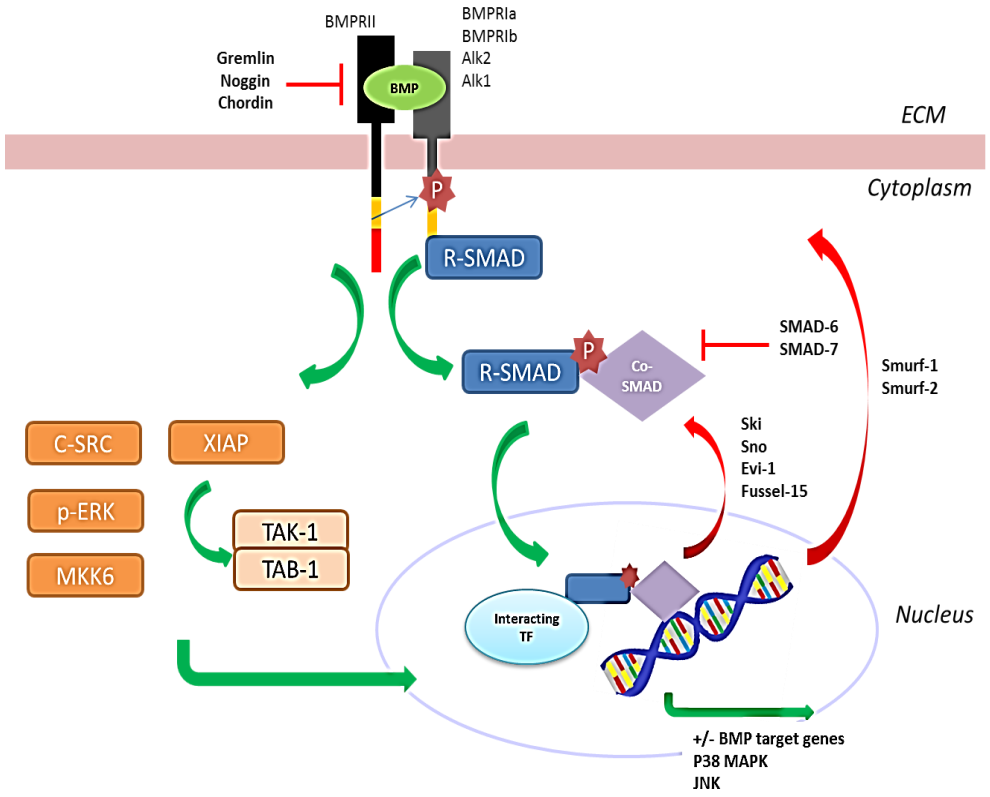

Figure 1.0.11 SMAD molecules and the BMP signalling cascade

Depiction of R-SMADs, coSMAD and iSMAD molecules including MH-1 and MH-2 domains with SSXS motifs. Circle represent motif that can be phosphorylated by MAP kinases. Square represent PY motifs (Miyazono et al. 2010) (B) Non canonical (left) and canonical (right) BMP signalling cascade. BMP ligand-mediated activation of membrane bound receptors causes downstream activation of R-SMAD and subsequent association with coSMAD for nuclear translocation.

The MH-2 domain is present in all SMAD proteins however, in RSMADs, a conserved phosphorylatable Ser-Ser-X-Ser (SSXS) motif is present at the C-terminal end. This motif is involved in canonical BMP signalling. co-SMAD4 proteins contain a MH-1 domain but iSMADs do not (Miyazono et al. 2010). The MH-2 domain is responsible for receptor interaction whereas MH-1 facilitates nuclear translocation and interaction with DNA and DNA-binding proteins (Shi et al. 1998; Yamashita et al. 1996).

BMP ligands bind to the extracellular domain of the constituently active type II receptor at the cell membrane and cause trans-phosphorylation of the type I receptor. This results in phosphorylation of the SSXS motif at the C-terminal end of R-SMADs (Huse and Chen 1999). Phosphorylated RSMADs (pSMAD) undergo a conformation change which releases the complex from the receptor. This allows pSMAD to form complexes with SMAD4 via the MH-2 domains and translocate to the nucleus. Both R-SMADs and co-SMAD4 contain signals to facilitate trafficking to and from the nucleus via its nuclear localisation signal (NLS) (Zhan Xiao, Latek, and Lodish 2003; Xiao et al. 2001). The NLS motif is recognised by importin which signals directly to nucleoporins to facilitate the passage of the complex across the nuclear envelope and into the nucleus (Görlich and Kutay 1999; Zhan. Xiao, Latek, and Lodish 2003). Interestingly, SMAD proteins can enter the nucleus independently of importins, by directly interacting with nucleoporins via their conserved MH2 domain (Xu et al. 2003). Here, they modulate BMP-specific gene transcription by directly binding to SMAD- and BMP-responsive elements and recruiting transcriptional repressors/co-repressors/activators or activating DNA binding proteins (Figure 1.0.11). (Hayashi et al. 2007; Heldin, Miyazono, and ten Dijke 1997; Ogata et al. 1993; Shi and Massagué 2003; J. Yang et al. 2013; Ying

et al. 2003). BMP signalling affects transcription via interaction with Runx family which regulate bone formation and Inhibitors of differentiation (Id) genes which are involved in cell differentiation and proliferation events (Nakahiro et al. 2010; Phimphilai et al. 2006; Zaidi et al. 2002).

Non-canonical BMP signalling occurs via MAPK, GSK and Akt/Protein kinase B pathways (Gallea et al. 2001). In Xenopus tissue, BMP type I and II receptors activated the mitogen-activated protein kinase (MAPK) pathway through TAK-1 and its activator TAB-1 via X-IAP. In C2C12 cells, BMP2 has been shown to activate the small Rho-GTPase Cdc42 mediator and PI3K signalling during cell migration and actin cytoskeletal rearrangement (Gamell et al. 2008; Zhang 2009). In human umbilical vein endothelial cells, BMP-4 stimulation induced phosphorylation of ERK 1/2 in a dose- and time-dependent manner and capillary sprout formation was dependent on BMP-4 induced ERK pathway activation (Figure 1.0.11) (Zhou et al. 2007)

1.2.2 BMP pathway regulation

BMP signalling is tightly controlled both extra- and intracellularly (Figure 1.0.11). Outside the cell, several extracellular proteins act as ligand traps to prevent receptor activation. These include α2-HS-glycoprotein (Ahsg), BMP binding endothelial cell precursor-derived regulator (BMPER), Connective Tissue Growth Factor (CTGF), dorsomorphin and members of the secreted protein families Gremlin, Noggin, Chordin and DAN/Cerberus (Moser et al. 2003; Rittenberg et al. 2005), (Moser et al. 2003; Rittenberg et al. 2005). Ligands are also sequestered outside the cells by soluble forms of type I receptor extracellular domains (Natsume et al. 1997). At the cell membrane, BAMBI acts as a pseudoreceptor as it lacks an internal

serine-threonine kinase domain (Onichtchouk et al. 1999). By forming dimers with Type I receptors it prevents the formation of functional receptor complexes thus preventing ligand activation of downstream signalling (Onichtchouk et al. 1999).

Inside the cell, iSMADs are important for negatively regulating the SMAD-dependent pathway. SMAD-6 preferentially inhibits BMP-mediated signalling while SMAD-7 inhibits with both BMP and TGFβ pathways. iSMADs physically compete with R-SMAD complexes at the activated type I receptor, preventing co-SMAD complex formation and interrupting gene transcription (Heldin et al. 1997). iSMADs also act as cofactors for the targeted ubiquitin-mediated degradation of type I BMP receptors and R-SMADs by recruiting Smurf-1. Smurf-1 is an E3 protein ubiquitin ligase which induces proteosomal degradation of Type 1 BMP receptors (Murakami et al. 2010). SMAD-7 also binds to Smurf-2 to mediate proteosomal digestion of TGF- β receptor complexes (Kavsak et al. 2000; Murakami et al. 2003; Tajima et al. 2003). Lefty, another intracellular antagonist of BMP signalling, inhibits phosphorylation RSMADs and subsequent nuclear translocation of the coSMAD complex (Ulloa and Tabibzadeh 2001).

SMAD8b is a splice variant of the R-SMAD, SMAD-8. SMAD8b lacks the SXSS motif in its MH2 domain and this renders the protein incapable of propagating downstream signal activation following ligand activation. Therefore, SMAD8b acts as a dominant negative regulator of BMP signalling (Nishita, Ueno, and Shibuya 1999). Using a PCR array, Nishita et al., examined coexpression of SMAD8 and SMAD8b mRNA in human tissues and demonstrated SMAD8b expression in placenta, kidney, heart and brain tissue. The results also highlighted that the balance between SMAD8 and SMAD8b may tissue-specific.

Following nuclear translocation of the R-SMAD-coSMAD4 complex, transcriptional co-repressors including c-Ski, SnoN and Evi-1 are activated (Luo et al. 1999; Moustakas, Souchelnytskyi, and Heldin 2001). These molecules recruit histone deactelyases to downregulate target genes. In addition, c-Ski, SnoN compete with SMAD-4 and Evi-1 binds to SMAD-2,-3-1 to repress TGF-B and BMP signalling. Fussel-15 and Fussel-18 have also been shown to inhibit intracellular BMP by binding to coSMAD-4 and preventing RSMAD complex formation (Arndt et al. 2007; Fischer et al. 2012).

1.2.3 BMP signalling and lung development

During lung development, the processes of branching and epithelial cell differentiation are controlled by complex signalling molecule cascades. The Notch family of signalling molecules are involved in regulating basal and ciliated cell expansion in the airways (Rock et al. 2013; Tsao et al. 2009). Wnt is a key orchestrator of proximal-distal lung patterning and induces expression of other signalling molecules from the endoderm and underlying mesoderm (Cohen et al. 2007). Wnt represses proximal epithelial differentiation and promotes distal epithelial differentiation via regulation of other growth factors such as FGF and BMP-4 in the distal branching regions of the developing lungs (Shu et al. 2005). FGF-10 is present in the mesenchyme and acts as a chemoattractant for directional growth of distal endoderm-derived lung buds (Park et al. 1998). Targeted ablation of FGF-10 in developing mouse lungs using a dominant negative FGFR2 under the control of SP-c promoter resulted in the complete loss of alveolar cell populations in the distal epithelium and an abundance of secretory columnar epithelial cells (Peters et al. 1994).

BMP-4 is strongly expressed at the distal tips of the developing lung bud and weakly expressed in proximal regions. Three main functions of BMP signalling have been highlighted in the developing lungs. Firstly, using various gain and loss of function systems in mice, BMP-4 has been shown to direct distal epithelial cell differentiation and repress the proximal epithelial cell programme (Bellusci et al. 1996; Hyatt, Shangguan, and Shannon 2002; Lu et al. 2001; Weaver et al. 1999). Secondly, loss of BMP-4 using a floxed SP-C promoter-driven system during mouse lung patterning resulted in malformed, terminal cystic-like sacs at the lung tips. This highlighted the role of BMP-4 in orchestrating correct branching morphogenesis (Bellusci et al. 1996). Thirdly, deletion of BMPRIa using a SFTPC-Cre transgene caused reduced epithelial cell expansion and high levels of epithelial cell apoptosis. This demonstrated that BMP signalling is a positive regulator of proliferation in the developing lung (Eblaghie et al. 2006).

Studies of mouse lungs in the late saccular and alveolar developmental stages indicated that BMP signalling remains active in the airways up to, and potentially after post natal day 28. High levels of BMP receptors, R-SMADs and pSMAD 1/58 were detected in whole cell protein extracted from 28 day old mouse lungs. SMAD-1 and 4 localisation also modulated as development progressed with reduced institial staining and increased epithelial expression (Alejandre-Alcázar et al. 2007). During late lung development, BMPRII, Alk-3 and Alk-6 also become localised to the epithelium of large airways and their previous expression in alveolar septae is greatly depleted (Alejandre-Alcázar et al. 2007). The role of BMP signalling in adult healthy lungs remained largely unexplored.

1.2.4 BMP signalling and cancer

BMP ligands and receptors are overexpressed in numerous cancer tissues including BMP-2 in lung, BMP-7 in breast, BMP-2 and BMP-4 in ovarian, BMP-6, BMPRIa and BMPRIb in prostate and BMPRIa in colorectal tumours (Feeley et al. 2005; Hardwick et al. 2008; Karhu and Kuukasja 2006; Langenfeld et al. 2003; McLean and Buckanovich 2013; Yuen et al. 2008). In NSCLC tumours resected from human patients, 98% expressed higher levels of BMP-2 ligand compared to normal lung tissue. Similarly, 100% of the 15 NSCLC samples expressed abnormal levels of BMP-6 ligand (Langenfeld et al. 2005). In bone metastasis from primary colorectal tumours, BMP-6 was highly overexpressed compared to both normal prostate tissue and primary tumours (Ye and Park 2009).

In terms of defining the definite role of BMP signalling in cancer, studies show that the BMP effect appears to be both spatially and temporally-regulated. Juvenile polyposis (JP) is an autosomal dominant disorder that predisposes patients to developing colorectal and gastric cancer. BMPRIa and SMAD-4 mutations cause approximately 50% of JP cases. This suggested that the loss of BMP signalling contributes to cancer formation and that a basal level of BMP signalling is required for health (Howe et al. 2004). Following a review of the literature Harwick et al. (2008) suggested a dual role for BMP signalling. In hamartomas, which are benign tumours in the body, the loss of BMP signalling initiates carcinogenesis. In adenocarcinomas the loss of BMP signalling contributes to the progression of the tumours to carcinomas in patients with sporadic colorectal cancer (Hardwick et al. 2008; Kodach et al. 2008). In both cases however, decreased BMP signalling was correlated to worsened prognosis.

Conversely, elevated BMP signalling has been linked to increased tumour invasiveness and reduced patients survival rates. In breast cancer, poorly differentiated oestrogen-receptor positive tumours expressed high levels of BMPRIb. The elevated receptor expression level was correlated to high tumour grade, cancer cell proliferation, tumour plasticity and overall, a poor patient prognosis (Helms et al. 2005). In gastric cancer cell lines AGS and SNU-638, BMP-2 signalling induced elevated invasiveness, motility and MMP-9 expression via the non-canonical BMP pathway. Furthermore, following analysis of 178 gastric tumour biopsies, BMP-2 was associated with poor patient outcome and increased metastasis formation (Kang et al. 2011). In NSCLC, high serum levels of BMP-2 was also associated with decreased patient survival (Fei et al. 2013). While a comprehensive analysis of the downstream signalling cascades stimulated by abberant BMP signalling has not been fully elucidated, Id genes may be responsible for the increased tumourigenic properties seen in some cases of excessive BMP signal activation (Ruzinova and Benezra 2003; Sikder et al. 2003)

Taking the two opposing effects of aberrant BMP signalling in different cancer types, it would appear that a basal level of BMP signal activation is required to maintain homeostatic conditions in the body. When the correct basal level of BMP signalling is lost, tumours formation can occur as seen in JP. Conversely, when BMP signalling is overactive, tumour formation can occur as seen in gastric and breast cancers. Although no definitive role for aberrant BMP signalling in cancer has been globally assigned, clinicians are warned against treating patients with BMP due to the growing number of studies suggesting associations with tumour initiation, progression and metastasis formation. (Thawani et al. 2010).

1.2.5 BMP signalling and inflammation

Inflammation is a normal physiological process which facilitates correct repair in the body following injury. Inflammatory mediators infiltrate the site of infection or damage and release cytokines, chemokines and stimulate growth factor release by the resident cells. These events culminate in tissue repair and restoration of homeostatic conditions. However, in chronic inflammatory states, the tissues become damaged due to prolonged exposure to inflammatory mediators and their effector molecules. The reactivation of developmental pathways during inflammation is a common phenomenon and further perpetuates the inflammatory phenotype (Beers and Morrisey 2011; Helbing et al. 2013). As BMP signalling is important in developmental processes it is believed that this signalling pathway is reactivated during injury and repair. The role of BMP signalling and inflammation has received growing attention in the past number of years and BMPs have been implicated in the inflammatory processes in a wide range of tissues.

A recent study investigating the role of BMPs in stomach inflammation has highlighted an anti-inflammatory role for BMP signalling. Mice overexpressing the BMP inhibitor noggin controlled by a BMP-responsive element displayed elevated H. pylori-induced inflammation and epithelial cell proliferation. Stomach dysplasia was evident alongside elevated expression of STAT3. In addition, BMP-2,-4 and -7 treatment of canine gastric epithelial cells inhibited both baseline and TNF-α stimulated Il-8 production (Takabayashi et al. 2014). This anti-inflammatory role is supported by evidence that BMP-7 treatment reduces inflammation in rats exposed to 2, 4, 6-trinitrobenzene sulfonic acid – a known experimental inducer of colitis. BMP-7 treatment reduced the expression of pro-inflammatory cytokines IL-6 and

TNF-β and fibrotic deposition mediated by TGF-β signalling (Maric et al. 2003, 2012).

In kidney formation, BMP signalling via BMP-7 specifically, facilitates correct epithelial cells differentiation and BMP-7 expression is present in podocytes, distal tubules and collecting duct to maintain correct kidney function in adults. Loss of BMP-7 expression occurs in early onset kidney fibrosis which indicates an important protective role for BMP signalling against fibrogenic renal diseases (Mitu and Hirschberg 2008; Simon et al. 2013). Furthermore, BMP-7 treatment of proximal tubule epithelial cells reduced basal and TNF-α induced pro-inflammatory cytokine (IL-6, IL-1β) release. Again, these results support an anti-inflammatory role for BMP signalling and particularly BMP-7 (Gould et al. 2002). These results also highlight potential a divergent role between different BMP ligands. BMP-7 may be involved in the anti-inflammatory response and act as a negative regulator of fibrogenic events (Maric et al. 2003). Conversely, BMP-2,-4 and-6 have been shown to contribute to pro-inflammatory, fibrotic events in the skin and joints (Kaiser et al. 1998; Lories and Luyten 2009; Stelnicki et al. 1998).

In lung injury and inflammation, BMP signalling is reactivated. Four studies have examined the expression of BMP signalling during allergic airway inflammation. Rosendahl et al., reported that BMP signal activation occured following ovalbumin (OVA)-induced airway injury in mice. Immunohistochemistry of healthy unchallenged mouse lungs did not reveal pSMAD 1/5 activation in the bronchial epithelium however, some alveolar and sub-epithelial fibroblast cells expressed pSMAD 1/5. Alk-2, BMPRIa and BMPRIb were expressed in the epithelium of healthy mouse airways. High expression levels of BMP-2, BMP-5 and moderate BMP-4,-6 and -7 expression were also found in the healthy airways, by western

blot. These results indicate that homeostatic BMP signalling is present in healthy airways.

Immunohistochemical staining of inflamed bronchial epithelial cells and scattered alveolar cells following OVA challenge revealed higher levels of pSMAD 1/5. In addition, BMPRIa, BMPRIb and Alk2 receptor expression were elevated in the injured airways in conjunction with increased BMP-2, -4 and -6 expression (Rosendahl et al. 2002). Interestingly, BMP-7 and BMP-5 expression were decreased following OVA challenge. These results suggest a divergent role for BMP ligands during inflammation similar to cancer.

The second study was carried out by Kariyawasam et al., and investigated BMP signalling in healthy and mild asthmatic human patients before and after allergen challenge (Kariyawasam et al. 2008). Normal non-allergic individuals expressed BMP ligands BMP-2, -4 and -7 and BMP receptors Alk-2, BMPRIa, BMPRIb and BMPRII on epithelial airway cells. While no difference in ligand expression was present in asthmatic patients, a significant decrease in Alk-2, BMPRIb and BMPRII was reported compared to normal-non allergic individuals. Immunohistochemical staining revealed that 40% of the healthy airway epithelial cells expressed pSMAD 1/5 compared to 3.8% in the asthmatic airways. This difference could be attributed to the reduced membrane-bound receptor expression. Alternatively, a different BMP ligand may be differentially expressed between healthy and asthmatic airways.

Asthmatic airways displayed marked upregulation of Alk-2 and BMPRIb at day 1 and day 7 post-allergen challenge. No change in BMP-2 or BMP-4 expression occurred whereas BMP-7 protein expression increased significantly in the epithelial

cells 7 days after allergen challenge. Furthermore, BMP-7 staining of inflammatory cell phenotypes revealed that eosinophils are the main source of this ligand in the allergen challenged airways. BMP-7 was shown to co-localize with Major Basic Protein (MBP) + eosinophils. Given these results, the authors concluded that BMP signalling is present in homeostatic airways and reduced in the inflammatory airway disease asthma. BMP signalling is reactivated in the airways following induced airway injury and the authors hypothesised a protective, anti-inflammatory function of BMP signalling attributed to BMP-7 expression (Kariyawasam et al. 2008).

Thirdly, Sountoulidis et al., examined BMP signalling expression during branching morphogenesis and lung formation using a GFP tagged BRE allele in C57/bl mice. Moreover, they examined the expression of the fluorescent tag in airway epithelial cells following naphthalene and bleomycin injury in adult mouse lungs. The study highlighted the role of BMP signalling in the distal lung bud tips during branching morphogenesis and subsequent pathway activation in airway and alveolar epithelial cells during late stage development. Following epithelial cell injury using naphthalene, which depletes club cell populations in the airways, the eGFP reporter was localised to NEBs and regions of the terminal bronchioles where airway epithelial cell progenitors reside. Following bleomycin injury, BRE-driven eGFP expression occurred in SpC+ cuboidal epithelial cells, a progenitor population capable of self-renewal and differentiation into both AEC I and AEC II. Overall, the authors concluded that BMP pathway activation maintains undifferentiated progenitor cell states in the developing airways to prevent premature exhaustion of the epithelial cell pool prior to the completion of lung development. Moreover, the authors speculated that BMP signalling activation following injury is involved in reparatory event in the airways (Sountoulidis et al. 2012).

Finally, a recent study in LPS treated BMP-4 +/- mutant mouse lungs indicated that BMP-4 plays a protective role against inflammation and bacterial infection. Mutant mice displayed more severe lung inflammation following LPS or *P. aeruginosa* challenge. In addition, following siRNA knockdown of BMP-4 in human airway epithelial cells, higher levels of Il-8 were produced following LPS and TNF α stimulation indicating an anti-inflammatory function of BMP signalling mediated by BMP-4 expression. Conversely, BMP-4 +/+ mutant mice displayed incorrect reparatory processes and reduced lung function which could be attributed to increased airway remodelling and airway epithelial cell migration (Li et al. 2014). This study married the positive and negative aspects of BMP signalling during inflammation whereby BMP pathway activation could act as an anti-inflammatory mediator while also disrupting normal epithelial repair.

1.3 Epithelial to Mesenchymal Transition

Epithelial to mesenchymal transition (T) is a biological process where epithelial cells undergo phenotypic changes to lose their polarised shape and many of their epithelial characteristics, detach from the basement membrane and become migratory, mesenchymal cells (Kalluri and Weinberg 2009). EMT is involved in organogenesis, wound healing and tumour progression. The types of EMT, characteristics of a cell undergoing EMT, growth factors responsible for initiating the process and its involvement in phenotypic switching will be discussed here.

1.3.1 Types of EMT

EMT is involved in different biological processes and three distinct subtypes of the EMT process have been assigned (Figure 1.0.12). The structural differences and cellular complexities involved in each type have yet to be elucidated however each EMT type is functionally distinct (Kalluri and Weinberg 2009).

Type 1 EMT occurs during embryonic development. In the very early stages of implantation, EMT takes place in the trophoectodermal cells of the parietal endoderm to allow for correct penetration of the endometrium and attachment of the placenta. This facilitates the essential nutrient and gas exchange function of the placenta to occur and development of the embryo to proceed (Acloque et al. 2009; Aplin et al. 1998). Type 1 EMT also occurs during gastrulation and leads to the characterisation of the three germ layers, ectoderm, mesoderm and endoderm, Ectodermal cells at the edge of the developing epiblast, undergo EMT and migrate from the edge of the primitive streak. Internalisation of the migrating cells generates mesoderm which gives rise to cardiac cells, hematopoetic cells, the urogenital

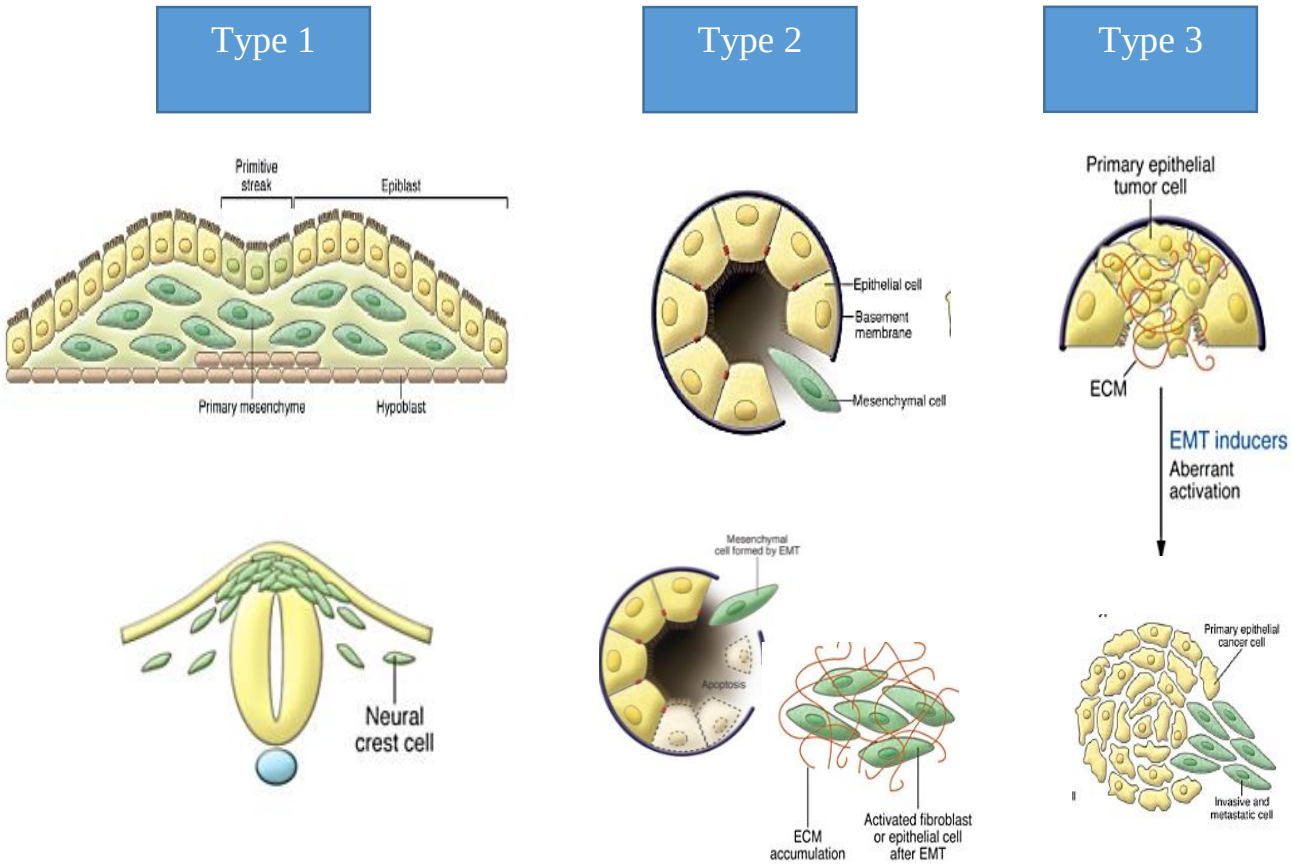

Figure 1.0.12 Different types of EMT

Type I EMT is involved in embryonic development and cell patterning events. Type 2 EMT facilitates wound repair and is linked to fibrosis due to prolonged inflammation, Type 3 EMT causes tumour cell metastasis formation and invasion of cancer cells into the blood to migrate to new sites. Modified from (Acloque et al. 2009; Kalluri and Weinberg 2009)

tract, bones, skeletal muscle and tendons. Subsequent MET of these internalised epiblast cells generates the digestive tract and epithelial lining of the organs. The external ectodermal cells remain in their epithelial cell state and are involved in neural crest EMT and the generation of cells of the nervous system, skeletal and cartilage precursors of the head and the epidermis (Acloque et al. 2009; Shannon and Hyatt 2004). Type 1 EMT is not involved in fibrosis or the invasion of cells to other regions of the body.

Type 2 EMT is involved in wound healing and tissue repair. Unlike type 1 EMT, this normal reparatory process involves the recruitment of fibrogenic cells and inflammatory mediators. If inflammation doesn't cease once its reparatory function is complete or if the primary insult is not attenuated, this type of EMT can be sustained in the cells which results in organ fibrosis and severe organ damage. Type 2 EMT occurs mainly in normal restitution events of the lung, liver, kidney and intestine and thus, is also linked to the onset of fibrosis in these organs (Acloque et al. 2009). Both endothelial and epithelial cells can undergo EMT in these organs (Kalluri and Weinberg 2009; Jonathan M Lee et al. 2006)

Type 3 EMT relates to cancer cell progression and metastasis formation. The dissemination of epithelial cancer cells from the primary tumour and migration to distant metastatic foci requires distinct changes in cell phenotype. EMT is involved in this process. EMT in the tumour cells facilitates tumour cell detachment, intravasation and migration in the circulatory system and the establishment of a nascent tumour site at a distant location in the body. This process is believed to involve a mesenchymal-to-epithelial (MET) process where the mesenchymal cells revert to their epithelial phenotype to promote tumour establishment in the new location (Kalluri and Weinberg 2009).

1.3.2 Characteristics of EMT

During EMT extensive changes in epithelial cell phenotype occur which lead to the adoption of mesenchymal cell features and increased cell invasiveness (Figure 1.0.13). Mesenchymal cells lack cell polarity, have a spindle-shaped extended morphology, are capable of migrating and do not express the typical epithelial cell adherens and junctional complexes (Hay 2005). Instead of apical-basal regions in the epithelial cells, mesenchymal cell have ventral-dorsal organisation with a leading edge morphology and extending filopodia to allow movement. Compared to the rigid quasi-immobility of the epithelial sheet, mesenchymal cells can migrate individually and are capable of resisting anoikis.

A hallmark of EMT is the disassembly of the E-cadherin mediated cell adherens junction. Tight junction and desmosomal protein expression is also altered during EMT. The loss of E-cadherin can occur through genetic and non-genetic mechanisms. Transcriptional downregulation of E-cadherin gene occurs via the induction of transcription factors Snail, Slug, Twist, SIP/Zeb and E47. These molecules bind to the E-cadherin promoter and repress transcriptional activity (Bryant and Stow 2004). Post-transcriptional downregulation by dysadherin disrupts the E-cadherin complex and promotes EMT progression (Ino et al. 2002; Nam, Hirohashi, and Wakefield 2007). Post-translational mechanisms of E-cadherin downregulation to induce EMT have also been described. Tyrosine phosphorylation of γ- and β-catenin by receptor tyrosine kinases (RTK) causes dissociation of the complex and induction of EMT. Phosphorylated catenins are flagged for proteosomal degradation and this prevents them from forming junction adhesion complexes. Ligand-mediated receptor activation of EGFR and HGFR

have been implicated in this process (Bremnes et al. 2002; Shiozaki et al. 1995). Epigenetic silencing of the E-cadherin gene via hypermethylation of CpG islands in the E-cadherin reporter has also been reported in many invasive cancer tumours such as the larynx, bladder and colorectum (Azarschab et al. 2003; Kanazawa et al. 2002; Nojima et al. 2001). Finally, enzymatic cleavage of the E-cadherin by MMPs, stromelysin-1, calpain, presenilin, ADAM-10 and ADAM-15 all introduce instability in the cell adherens junction and ultimately result in loosened intracellular junctions and the induction of EMT (Huguenin et al. 2008; Krampert et al. 2004; Maretzky et al. 2005; Rios-Doria et al. 2003).

Mesenchymal cells express different cell markers and intracellular molecules to account for the altered expression of desmosomal and tight junction proteins and the loss of E-cadherin (Chidgey and Dawson 2007; Kyuno et al. 2014). Proteins lost during EMT include E-cadherin as described, ZO-1, occuldin and demoplakin. Membrane bound N-cadherin and integrin α4β6 and intracellular fibroblast-specific protein 1 (FSP1), fibronectin, vimentin and α-SMA are commonly upregulated by mesenchymal cells (Jonathan M Lee et al. 2006). N-cadherin provides much weaker cell adhesion between cells and *in vitro* force measurements in the mouse sarcoma cell line S180 revealed that a significantly higher force is required to separate cells joined by E-cadherin complexes compared to N-cadherin (Chu et al. 2004).

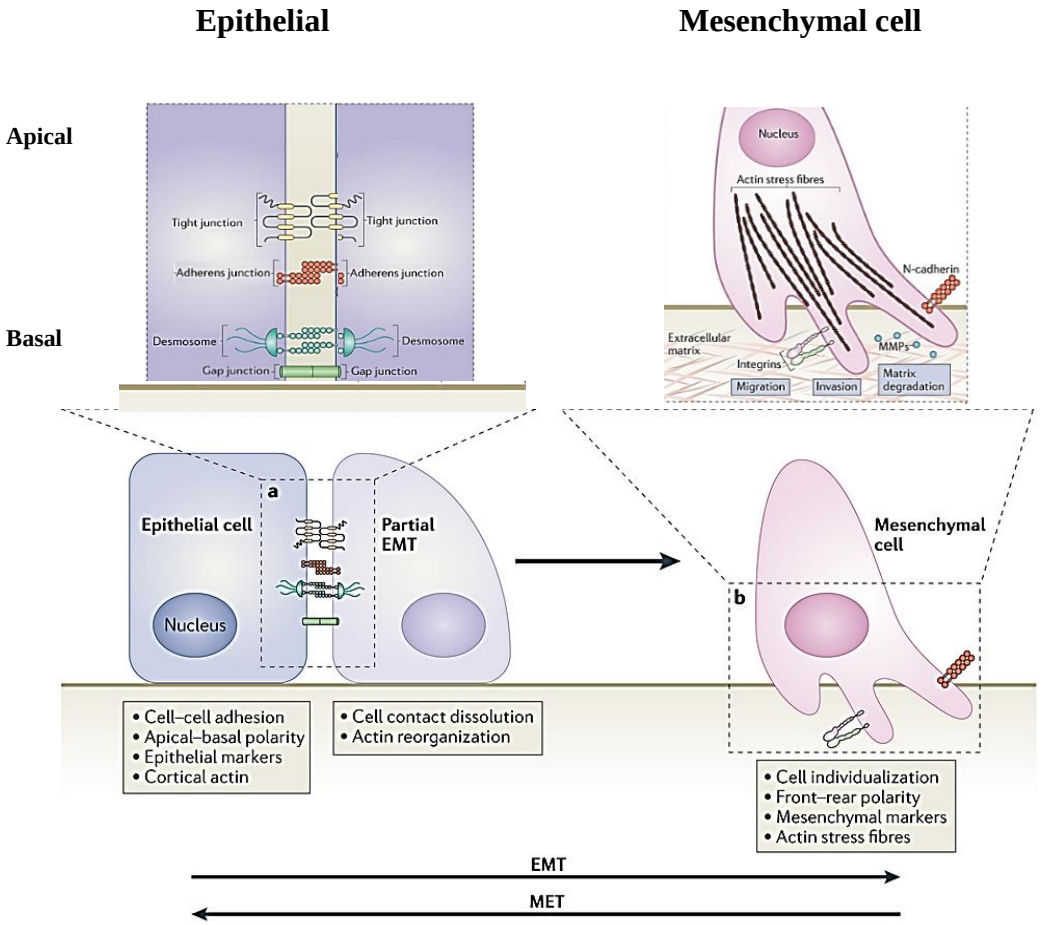

Figure 1.0.13 Epithelial to mesenchymal transition

Epithelial cells express tight junctions, desmosomes, gap junctions and adherens junctions to maintain the rigid, protective epithelial barrier. During EMT, these adhesive complexes are down regulated and the cell adopts a motile, invasive and migratory phenotype. Elevated expression of integrins and N-cadherin occurs alongside production of MMP for matrix degradation. The process of MET involves the reversal of this process. Modified from (Lamouille, Xu, and Derynck 2014)

Moreover, N-cadherin promotes cell mobility (Figure 1.0.12) (Cavallaro and Christofori 2004). The expression of α4β6-integrin increases cell invasiveness while maintaining the cell's ability to interact with the surround ECM (Mamuya and Duncan 2012; Maschler et al. 2005).

Changes in actin expression also occur during EMT. As previously outlined, the actin cytoskeleton is connected to tight junctions and cell adherens junctions. Actin maintains cell polarity in epithelial cells and loss of this apical-basal polarised phenotype during EMT results in a switch from cortical actin organisation to actin stress fibre formation, as depicted in Figure 1.0.13 (Vallenius 2013). The generation of filopodia and extended cytoplasmic processes facilitating cell migration also requires extensive actin remodelling. This is orchestrated by actin-myosin contraction and extension events (Haynes et al. 2011). The appearance of peri-nuclear actin bundles is also common in cells undergoing EMT (Gay et al. 2011).

Following the onset of the mesenchymal cell phenotype, the cell must excise itself from the tightly knit epithelial cell layer and migrate through the basement membrane and into the blood vessels. This occurs in type 2 and 3 EMT. Mesenchymal cells must express the necessary membrane-degrading molecules required to carry out this function. The cells produce MMP (MMP-2,3,9,14) and urokinase plasminogen-associated receptor (uPAR) which cause focal damage to laminin and type IV collagen in the basement membrane. This facilitates intravasation, cell migration and dissemination from original epithelial cell sites (Gupta et al. 2011; Jonathan M. Lee et al. 2006; Marudamuthu et al. 2015; Sillat et al. 2012).

The phenomenon of partial EMT has also been described in cancer. This intermediate EMT state is a hybrid metastable phenotype along the EMT-MET axis

whereby the cells express both epithelial and mesenchymal cell markers such as E-cadherin, keratins, vimentin and MMPs (Jonathan M Lee et al. 2006; Savagner 2010) . Partial EMT has been coined as "epithelial mesenchymal plasticity" (EMP) and allows cancer cells to fluctuate between organised, partly polarised epithelial cells and more mobile, individual mesenchymal cells expressing residual cadherins proteins (Van Denderen and Thompson 2013; Pinto et al. 2013; Thompson and Haviv 2011).

1.3.3 MET

Following EMT, the cells undergo the reversal of the process where epithelial-associated genes are upregulated and the epithelial cell phenotype is adopted once again. This is called mesenchymal to epithelial transition (MET). MET involves the loss of cell motility, re-establishment of cell polarity, increased expression of cortical actin and the reacquisition of E-cadherin and other cell adhesion molecules at the cell membrane (Figure 1.0.13).

The best studied examples of MET in development are kidney formation and the developing vertebrate somites. Reciprocal communication between the developing uteric bud epithelium and the nephrogenic mesenchyme occurs during kidney development. The nephrogenic mesenchyme condenses around the developing uteric bud following bud branching and MET occurs to form the nephron. BMP-7, wilms tumor 1 (Wt1) and paired box 2 (Pax2) are involved in this MET event (Lipschutz 1998; Plisov et al. 2000). During somitogenesis, the presomitic mesoderm undergoes MET to epithelialise the boundary of each somite. This process involved the small Rho-GTPase Cdc42 and rac1 (Ferrer-Vaquer, Viotti, and Hadjantonakis 2010).

During epithelial cell repair, it is postulated that while EMT induces normal epithelial cell restitution following injury, the onset of MET is an important step to prevent prolonged EMT and the formation of fibrotic legions (McCormack and O'Dea 2013). BMP-7 has been shown to induce MET in adult renal fibroblasts via re-expression of E-cadherin and decreasing cell motility and type 1 collagen secretion (Zeisberg, Shah, and Kalluri 2005). HGF binding to c-met also reduces TGF-β signalling to restore epithelial cell phenotype and decrease the amount of MMP-9 in tubular epithelial cells (Yang and Liu 2002).

MET in cancer is receiving more attention in recent years. The fact that metastatic tumours generally resemble the primary tumour population from which they arose led to the notion that mesenchymal cancer cells lose their metastatic properties and subsequently re-epithelialise during the process of neoplastic colonisation. It is understood that MET is involved in this process enabling the establishment and stabilisation of novel tumour sites. In a study of primary E-cadherin-negative breast cancer tumours, metastatic foci of the liver, lung and brain were found to be E-cadherin positive. The authors concluded that the metastatic tumour microenvironment can induce MET and the induction of epithelial-related markers to promote cancer survival (Chao, Shepard, and Wells 2010). Re-epithelialisation could also allow mitotic events to occur in the nascent tumour site which would be advantageous for cancer growth. Studies in mice have shown that the loss of the transcriptional co-repressors Twist1 and Snail1, responsible for downregulating E-cadherin, is associated with increased cell proliferation (Tsai and Yang 2013; Tsai et al. 2012).

At present, it is unclear if different types of MET exist in the body, what signalling molecules are involved in the induction of MET and if these differ spatially and

temporally. In addition, it is not known whether the loss of EMT-related signals during development, epithelial wound repair or cancer cell metastasis is sufficient for the induction of MET or if specific MET signalling molecules exist. Further characterisation of the EMP phenotype may aid in elucidating MET processes in cancer.

1.3.4 Growth factors and EMT

The Wingless (Wnt) family of signalling molecules are involved in all three types of EMT. Wnt signals are transduced by the frizzled family of receptors and LDL-receptor-related proteins 5 and 6 (LRP) coreceptors. In the absence of ligand binding, β-catenin is associated with the glycogen synthase kinase 3 (GSK3β) complex consisting of adenomatous polyposis coli (APC) and AXIN. β catenin is phosphorylated by GSK3β and this complex is actively ubiquitinated which results in proteosomal degradation. In the nucleus, Wnt target genes are inhibited due to interaction with the transcription factors and co-repressors T-cell factor (TCF) and Lymphoid enhancer-binding protein (LEF). Other β –catenin molecules are associated with adherens junctional complexes, offering protection from this degradative pathway. Following Wnt ligand binding, the receptor-associated Dishelleved (Dsh) protein is phosphorylated. This leads to the recruitment of AXIN to the cytoplasmic tail of LRP5/6 and the dissociation of the GSK3β complex. The activation of Dsh inhibits the phosphorylation of β-catenin by GSK3β which prevents degradation. Finally, unphosphorylated β-catenin accumulates in the cytoplasm and is either recruited for the formation of adhesion junction or translocated to the nucleus where is interacts with nuclear TCF and LEF, inhibiting

their transcriptional repression function (Komiya and Habas 2008; Moon et al. 2004).

Wnt signalling is essential to type 1 EMT and knockout studies of Wnt3 and Wnt8c resulted in the incorrect formation of the germ layers and the primitive streak. Exogenous introduction of Wnt8c lead to the development of numerous ectopic primitive streaks (Liu et al. 1999; Pöpperl et al. 1997). Wnt interacts with different growth factor families during type 1 EMT such as the TGF- β family particularly Nodal and Vg1. Nodal signalling is involved in controlling the invagination of cells during gastrulation (Varlet, Collignon, and Robertson 1997). Vg1 is involved in primitive steak formation and interacts with Wnt8c (Skromne and Stern 2001).

FGF receptors are involved in primitive streak formation via the phosphorylation of β-catenin and the induction of the E-cadherin transcriptional repressor, Snail. Furthermore, FGFR double-knockout mice have shown that while primitive streak formation begins in the absence of FGFR, its expression is vital for the normal progression of embryonic patterning (Ciruna and Rossant 2001). TGF- β and Wnt have also been shown to induce E-cadherin downregulation by inducing the expression of transcriptional repressors (Acloque et al. 2009).

BMP signalling is essential to type I EMT events for example, BMP-4 homozygote knockout mice do not form a mesoderm and die between e6.5 and e9.6. In heart mitral valve formation, BMP signalling mediated through BMP-2 induces EMT in the myocardium and endocardium of the atrioventricular canal (McCormack and O'Dea 2013; Winnier et al. 1995).

Similar pathways are activated in type 2 EMT. In the repair of renal tissue, Wnt induces EMT and prolonged Wnt signalling is associated with renal fibrosis

(Galichon and Hertig 2011; Jiang et al. 2013). During tissue regeneration in the lungs, TGF-β and BMP-4 have been shown to induce EMT in cultured mouse and human airway epithelial cells to facilitate epithelial restitution (McCormack, Molloy, and ODea 2013; Molloy et al. 2008). Conversely, BMP-7 has been shown to elicit the opposite effect on EMT progression and attenuates kidney, liver lung and intestinal fibrosis (Maric et al. 2012; Mitu and Hirschberg 2008; G. Yang et al. 2013). HGF also reduces TGF-β signalling to restore epithelial cell phenotype and decrease the amount of MMP-9 in tubule epithelial cells (Yang and Liu 2002).

In cancer cell progression and metastasis formation via type 3 EMT, the same signalling molecules of organogenesis and repair are involved. Conflicting reports exist regarding BMPs involvement in cancer progression and as previously outlined, both spatial and temporal properties appear to modulate the effect the BMP pathway. Exogenous TGF-β can induce type 3 EMT in human mammary gland epithelial cells, epidermal keratinocytes and murine mammary epithelial cells treated (Valcourt et al. 2005). Prolonged TGF- β signalling promotes type 3 EMT tumour formation and carcinogenesis in head and neck, breast and colorectal cancer (Derynck, Akhurst, and Balmain 2001).

Other RTKs are involved in type 3 EMT to facilitate metastasis of primary tumours. In breast tumour cells, N-cadherin expression in the cells prevents FGFR-1 ligand induced trafficking and the subsequent reduction in cell signalling. In the presence of N-cadherin, FGF-2 led to sustained activation of membrane-bound FGFR-1 which caused upregulation of MMP-9, the enzyme involved in focal degradation of the basement membrane. This signalling axis facilitated a more invasive and migratory phenotype in the tumour cells (Suyama et al. 2002).

In summary, a complex interplay of growth factors is involved in mediating EMT in cells. Growth factors facilitate epithelial and mesenchymal transition events and facilitate correct morphogenesis during development and cell repair following injury. In cases where abnormal growth factor signalling occurs due to overstimulation of the inflammatory system or otherwise, excessive growth factor signalling may lead to fibrosis and the development of malignant cancer tissues.

1.3.5 EMT and phenotypic switching in cancer

Numerous studies have shown that the EMT process is involved in phenotypic switching in cancer. Similar to the plasticity of the EMT-MET axis in the developing embryo, the phenotypic switching in cancer cells occurs readily between subpopulations. E-cadherin downregulation is the hallmark of EMT and occurs at the invasive front of many solid tumours (Perl et al. 1998). The progression of EMT in the tumour cell leads to reduced cell polarity and the loss of intercellular junctions ultimately resulting in more invasive, mesenchymal and migratory cells. The cell are capable of detaching from the solid primary tumour and invading the circulatory system before undergoing MET and developing nascent tumour sites (Li et al, 2015; Thiery et al, 2009; Thiery, 2002).

1.3.6 Experimental aims

BMP signalling is involved in lung morphogenesis. This signalling pathway is also believed to be reactivated during lung epithelium inflammation, repair and restitution. Altered BMP signalling has been shown to occur in both malignant and inflammatory diseases; however the role of BMP signalling in these processes is poorly understood. The main aim of this work was to gain a better insight into BMP

pathway activation in both healthy and diseased lungs. We aimed to determine the role of BMPs in EMT-mediated phenotypic switching. We hypothesised that BMP signalling is capable of inducing phenotypic switching in lung cancer cell populations. In addition, we hypothesised that BMP signalling is active in healthy adult airways and that signalling is sustained to mediate homeostasis in the lung epithelium. Finally, we hypothesised that BMP signalling is altered in inflammatory airways diseases and during active epithelial repair.

Our lab has shown that BMP signalling can induce a migratory phenotype in airway epithelial cells during epithelial restitution (McCormack et al. 2013). Our first objective aimed to determine the role of BMP signalling in EMT and phenotypic switching in lung cancer cells. We speculated that the heterogeneous lung tumour cell line DLKP would be a suitable model to study EMT-mediated phenotypic switching. We aimed to characterise the DLKP clones more extensively to determine what stage of EMT each clone represented. Subsequently the DLKP clones were treated with recombinant BMP-4 and gremlin to examine the effect of altered BMP signalling on cell morphology and the expression of epithelial and mesenchymal markers. In addition, the role of E-cadherin gene processing was investigated in DLKP-SQ and DLKP-M clones with the aim to determine the significance of the cadherin axis in heterogeneous cell populations. E-cadherin reporter plasmids, previously designed by Dr. Joanne Masterson in the O'Dea Lab, were transfected into the DLKP clones by myself and Dr. Emer Molloy to examine the effect of E-cadherin gene overexpression in the clones.

The second objective was to investigate whether a BMP signalling gradient exists in adult airways. For these studies, a healthy porcine lung model was chosen as the most readily-available clinically relevant large animal model. Following

histological analysis of the porcine airways, the expression of BMP receptors, BMP ligands, SMAD signalling molecules and BMP antagonists was determined by PCR and western blot in the descending left cranial pig bronchus.

Based on the resulting data, hypotheses would be developed around the role of BMP signalling in proximal versus distal airways. A porcine tracheal explant model was developed to investigate the function of BMP signalling. Primary porcine tracheal explants were treated with recombinant BMP-4 *in vitro* to examine the effect of BMP signalling on epithelial cell phenotype and downstream signal activation.

Finally, we aimed to determine if BMP signalling was present and active in non-human primates and if BMP signalling was altered during allergic airway disease and subsequently, during epithelial repair. To address this aim, we used an established model of allergic airway disease in a rhesus macaque model. The expression of BMP signalling components was examined by immunofluorescence in the left cranial bronchus of healthy, asthmatic and recovering rhesus macaques.

Overall, the aim of this research was to provide novel insights into the expression patterns of BMP signalling in healthy airways and to gain further insight into the role of BMP signalling in the pathophysiology of allergic airway disease and lung cancer.

2 Chapter 2

Material and methods

2.1 Materials

2.1.1 Reagents

Product	Company	Address
1kb ladder	Invitrogen	Dublin, Ireland
4-20% mini-precast TGX	BioRad	Herts, UK
7AAD Viability stain	eBioscience	Hatfield, UK
Acetic acid	Sigma	Dublin, Ireland
Agarose	Sigma	Dublin, Ireland
Alcian blue	Sigma	Dublin, Ireland
Amicon ultra 0.5ml 10k	Millipore	Cork, Ireland
Antigen unmasking solution (citrate)	Vector Labs	Peterborough, UK
Bench Top 100bp ladder	Promega	Madison, WI, USA
B-mercaptoethanol	Sigma	Dublin, Ireland
BMP-4	Immunotools	Friesoythe, Germany
QuickStart ™ Bradford assay reagent	BioRad	Herts, UK

Bovine Serum Albumin	Sigma	Dublin, Ireland
cDNA synthesis kit with Superscript® III RT	Thermo fisher scientific	Loughborough, UK
Chloroform	Sigma	Dublin, Ireland
Complete mini EDTA-free protease inhibitor	Roche	West Sussex, UK
Faramount mounting medium	DAKO	Glostrup, Denmark
DAPI	Sigma	Dublin, Ireland
dNTPs (dATP, dCTP, dGTP, dTTP)	Promega	Madison, WI, USA
Dimethyl sulfoxide DMSO	Sigma	Dublin, Ireland
DMEM Hams- F12 Medium	Sigma	Dublin, Ireland
Dnase for cDNA synthesis	Invitrogen	Dublin, Ireland
DPX mounting medium	Sigma	Dublin, Ireland
Eosin Y Solution	Sigma	Dublin, Ireland
Ethanol, 200 proof	Sigma	Dublin, Ireland
Ethyline diamine tetra-acetic acid EDTA	Sigma	Dublin, Ireland
Foetal calf serum	Sigma	Dublin, Ireland
10% formalin, neutral buffered solution	Sigma	Dublin, Ireland

G 418	Sigma	Dublin, Ireland
Gentamycin	Sigma	Dublin, Ireland
GelRed nucleic acid stain	BioTium	Hayward, CA, USA
GoTaq Flexi DNA polymerase kit	Promega	Madison, WI, USA
Gremlin	R&D Systems	Minneapolis, MN, USA
Happy Cell ® advanced suspension medium	Brennan & Co.	Dublin, Ireland
Harris Haemotoxylin Solution	Sigma	Dublin, Ireland
Hydrochloric acid	Sigma	Dublin, Ireland
Isopropanol	Sigma	Dublin, Ireland
L-Glutamine	Gibco	Loughborough, UK
Magic Mark	Invitrogen	Dublin, Ireland
Marvel – non-fat dried milkd	Dunnes Stores	Dublin, Ireland
Methanol	Sigma	Dublin, Ireland
MicroAmp Fast 96 well reaction plate	Applied Biosystems	Carlsbad, CA, USA
Mini Protean Comb – 10 well 0.75mm	BioRad	Herts, UK
Mini protean precast TGX	BioRad	Herts, UK
Mr Frosty	Nalgene	Loughborough, UK

MTS cell proliferation kit	Promega	Madison, WI, USA
NaCl	Sigma	Dublin, Ireland
Nitrocellulose Transfer Kit	BioRad	Herts, UK
Nuclease free water	Promega	Madison, WI, USA
Oligo dT 12-18 primer	Invitrogen	Dublin, Ireland
Optical adhesive covers	Applied biosciences	Carlsbad, CA, USA
Phosphate Buffered Saline tablets	Sigma	Dublin, Ireland
Penicillin-Streptomycin	Gibco	Loughborough, UK
Periodic Acid	Sigma	Dublin, Ireland
Polyacryl carrier	MRC	Cincinnati, OH, USA
QiaShredder	Qiagen	West Sussex, UK
Restore Western Blot stripping buffer	ThermoFisher	Carlsbad, CA, USA
RIPA buffer	Sigma	Dublin, Ireland
Rnase away	Invitrogen	Dublin, Ireland
RnaseOut – RNAse inhibitor	Invitrogen	Dublin, Ireland
RPMI 1640 media	Life Technologies	Carlsbad, CA, USA
Schiff Reagent	Sigma	Dublin, Ireland
SeeBlue molecular weight ladder	Invitrogen	Dublin, Ireland

Sodium Chloride (NaCl)	Sigma	Dublin, Ireland
Superscript III reverse transcriptase	Invitrogen	Dublin, Ireland
SYBR green – Jump start Taq ready	Sigma	Dublin, Ireland
Tris – hydoxymethyl aminomethane	VWR	Dublin, Ireland
2x Tris Glycine SDS Buffer	Invitrogen	Dublin, Ireland
10X Tris Glycine running buffer	BioRad	Herts, UK
TriZol Reagent	Invitrogen	Dublin, Ireland
Trypsin-EDTA	Sigma	Dublin, Ireland
Tween-20	Sigma	Dublin, Ireland
WesternBright ECL HRP substrate	Advansta	Menlo Park, CA, USA
Xylene	Sigma	Dublin, Ireland

2.1.2 Instruments

Instrument	Company	Address
Accuri C6 Cytometer	BD Biosciences	Oxford, UK
Centrifuge 5804	Eppendorf	Hauppauge, NY, USA
Centrifuge 5817 R	Eppendorf	Hauppauge, NY, USA
Gel Doc Imaging system	BioRad	Herts, UK
G:BOX Chemi XT4	Syngene	Cambridge, UK
GeneSys Software	Syngene	Cambridge, UK
GloMax multidetection platform	Promega	
MiniProtean 3.0 electrophoresis rig	BioRad	Herts, UK
Olympus BX61 fluorescent microscope	Olympus	Melville, NY, USA
Olympus CK40 light microscope	Olympus	Germany
Olympus IX81 Fluorescent microscope	Mason technologies	Dublin, Ireland
Olympus QI Click 12vbit CCD camera	Mason technologies	Dublin, Ireland
PowerPac™ basic power supply	BioRad	Herts, UK
Quantity-One® Software	Fannin Scientific	Dublin, Ireland
StepOnePlus™ Real-time PCR systems	Thermo Scientific	Paisley, UK
Thermal Cycler – PTC 100	MJ Research	Waltman, MA, USA
Trans-Blot™ turbo transfer system	BioRad	Herts, UK
Citadel ™ 2000 tissue processor	Thermo Scientific	Pasiley, UK

2.1.3 Antibodies

Antibody	Clone	Raised In	If Conc	WB Conc	Size	Company Catalogue
Actin	20-33	Rabbit	1/100	1/2000 TBSt	43kDA	Sigma A5060
Afadin	D1Y3Z	Rabbit		1/1000 mTBSt	205kDA	Cell Signalling 13531
β-catenin	14	Mouse	1/200	1/500 TBS	92kDA	BD Biosci 610153
BMPR-Ia	H60	Rabbit	1/20	1/200 TBSt	66kDA	Santa Cruz Sc-20736
CD2AP	n/a	Rabbit		1/1000 mTBSt	80kDA	Cell Signalling 2135
Claudin-1	D5H1D	Rabbit		1/1000 mTBSt	20kDA	Cell Signalling 13255
E-cadherin	36	Mouse	1/200	1/2000 TBS	120kDA	BD Biosci 610182
ERK 1/2	n/a	Rabbit		1/1000	42kDA, 44kDA	Cell Signalling 9102
GAPDH	6C5	Mouse		1/1000 TBSt	37kDA	Santa Cruz Sc-32233
N-cadherin	32	Mouse	1/200	1/2000 TBS	130kDA	BD Biosci 610920
Pan-Cytokeratin	c-11	Mouse	1/150	1/1000 TBS	45kda K18 52kDA K8 54kDA K13 56kDA K10 56kDA K6 58kDA K5	Sigma P2871
p-ERK 1/2	n/a	Rabbit		1/1000	42kDA, 44kDA	Cell Signalling 9101
pSmad 1/5/8	41D10	Rabbit	1/50	1/1000	60kDA	Cell Signalling D5B10
Smad -1	A4	Mouse	1/50	1/200	56kDA	Santa Cruz Sc-7965
Smad 1/5/8	N18-R	Rabbit	1/50	1/200	52-56kDA	Santa Cruz Sc-6031

Antibody	Clone	Raised In	If Conc	WB Conc	Size	Company Catalogue
Smad-5	D20		1/50	1/200	56kDA	Santa Cruz Sc-7443
Smad-6	H150	Rabbit	1/50	1/1000	54kDA	Santa Cruz Sc-13048
Smad-7	Z8-B	Mouse	1/50	1/250	51kDA	Santa Cruz Sc-101152
Vimentin	13.2	Mouse	1/2000	1/1000 TBS	53kDA	Sigma V5255
YFP		Rabbit	1/3000	1/3000 TBS	26kDA	Abcam A6556
ZO-1	D7D12	Rabbit		1/1000 mTBSt	200kDA	Cell signalling 8193
α SMA	1A4	Mouse	1/3000	1/2000	42kDA	Sigma A2547

2.1.4 Primers

Gene	Sp.	Sequence	Product (bp)	Temp. (°C)	$MgCl^2$ (nM)
BMPRIa	Hu	F: 5'-ATGACCAGGGAGAAACCACA-3' R: 5' – ATTCTATTGTCCGGCGTAGC -3'	105	55	1.5
BMPRIb	Hu	F: 5'- ACTCAAGGCAAACCAGCAAT -3' R: 5'- TCTGTTCAAGCTCTCGTCCA -3'	204	58	1.5
BMPRII	Hu	F: 5'- GCCCGCTTTATAGTTGGAGA -3' R: 5'- TCTGTTCAAGCTCTCGTCCA -3'	144	55	1.5
SMAD7	Hu	F: 5'- TCCAGATACCCGATGGATTT -3' R: 5'- GGGCCAGATAATTCGTTCC -3'	94	55	1.5
SMAD6	Hu	F: 5'- GTCGTACACCGCATAGAGG -3' R: 5'- GCCACTGGATCTGTCCGATT-3'	157	55	1.5
BMP-4	Hu	F: 5'- TACATGCGGGATCTTTACCG -3' R: 5'- ATGTTCTTCGTGGTGGAAGC -3'	132	55	1.5
ID-1	Hu/ Ms	F: 5'- GCAAAGTGAGCAAGGTGGAG -3' R: 5'- ATCGTCGGCTGGAACACAT -3'	191	55	1.5
N-cadherin	Hu/ Mk	F: 5'- TGTTTTGGACCGAGAATCAC -3' R: 5'- TAACACTTGAGGGGCATTGT -3'	148	55	1.5
GAPDH	Hu/ Mse	F: 5'- CTGCACCACCAACTGCTTAG -3' R: 5'-CCAGGAAATGAGCTTGACAAA-3'	487	55	1.5
E-cadherin	Hu/ Mse	F: 5'- GGCTGGACCGAGAGAGTT -3' R: 5'- CTGCTTGGCCTCAAAATCC -3'	350	58	1.5

Gene	Sp.	Sequence	Product (bp)	Temp. (°C)	$MgCl^2$ (nM)
BMPRIa	Pig	F: 5'- ATGCAAGGATTCACCGAAAG-3' R: 5'-TGCAGACAGCCATAGAAACG-3'	164	58	1.5
BMPRIb	Pig	F: 5'- AAATGTGGGCACCAAGAAAG-3' R:5'- ACAGGCATCCCAGAGTCATC-3'	171	58	1.5
BMPRII	Pig	F:5'- GAAGACTGTTGGGACCAGGA-3' R:5'- GGTTGCGCTCATTCTGCATA-3'	151	58	1.5
BMP-2	Pig	F:5'- CTTGCTAGTCACTTTCGGCC-3' R:5'- TCATTCCAGCCCACATCACT-3'	150	58	1.5
BMP-4	Pig	F:5'- GGCTGGAATGACTGGATTGT -3' R:5'- ACTCAGTTCGGTGGGAACAC-3'	158	58	1.5
BMP-7	Pig	F:5'- CTTCTCCTACCCCTACAAG-3' R:5'- GGAAGAACTCTTTGTCGTG-3'	119	55	1.5
SMAD-4	Pig	F:5'- CTATGAACGAGTTGTATCACC-3' R:5'- ATCCTTCACCAACATACCTG-3'	166	55	1.5
SMAD-6	Pig	F:5'- ACCCCATCTTCGTCAACTCC-3' R:5'- TGATGAACTGCCGGGAGTAG -3'	225	58	1.5
SMAD-7	Pig	F:5'- GGGGCTTTCAGATTCCCAAC-3' R:5'- TCCAAGGCAAAAGCCATTCC-3'	166	58	1.5
BAMBI	Pig	F:5'- AAACAGGCACGAAACCACTC-3' R:5'- TTGGAGGAAGTCAGCTCCTG-3'	191	58	1.5
E-cadherin	Pig	F:-5'- CATCTTCAACCCAACCTCGT-3' R:5'-: ACGCCTTCATTGGTTACTGG-3'	167	58	1.5
GAPDH	Pig	F:5'- GTCGGTTGTGGATCTGACCT-3' R:5'- AGCTTGACGAAGTGGTCGTT-3'	191	58	1.5
Gremlin	Pig	F:5'- CATGTGACGGAGCGCAAATA-3' R:5'- GTTCAGGGCAGTTGAGTGTG -3'	238	55	1.5

Gene	**Sp.**	**Sequence**	**Product (bp)**	**Temp. (°C)**	**$MgCl^2$ (nM)**
Noggin	Pig	F:5'TGGAGTTCTCCGAGAGGGTT-3' R:5'-CATGAGCGCTTACTGAAGCA-3'	166	58	1.5
Id-1 (set1)	Pig	F:5'-TCATCGACTACATCTGGGA-3' R:5'-GGAACACATGCTGTCTCTG-3'	130	58	1.5
Id-2 (set 2)	Pig	F:5'-CATCGACTACATCTGGGAC-3' R:5'-GAACACATGCTGTCTCTGC-3'	128	58	1.5
AQP-5	Pig	F:5'- GTGGTGGAAATGATTCTGAC-3' R:-5'- GAAGTAGATCCCCACAAGG-3'	127	58	1.5
EpCAM	Pig	F:5'- GACCTACTGGATCATCATTG-3' R:5'- TGATTACCTCCTTGAGTGC-3'	74	58	1.5

Gene	Sp.	Sequence	Product (bp)	Temp. (°C)	$MgCl^2$ (nM)
FOXA1	Pig	F:5'- CAGGATGTTAGGGACTGTG-R' R:5'- GGTATTCATGGTCATGTAGG-R'	160	58	1.5
ITGA6	Pig	F:5'- CCCTCTCAGACTCAGTAAC-R' R:5'-GACGGAGATCAATTCTGTTAG-3'	72	55	1.5
SFTPC	Pig	F:5'- CTGAGATGGTCCTAGAGATG-3' R:5'- ACTAGAGCCAATGGAGAAG-3'	85	55	1.5
K-18	Pig	F:5'- TGAAGACTATCGAGGAACTG-3' R:5'- CTCCGTCTCATACTTGACTC-3'	106	58	
ID-2	Pig	F:5'- CGATGAGCCTGCTGTACAAC-3' R:5'- GTGCAGGCTGACAATAGTGG-3'	173	58	1.5
GATA-6	Pig	F:5'-TGTGCAATGCTTGTGGACTC-3' R:5'-GGAAGTTGGAGTCATGGGGA-3'	164	58	1.5
SOX-9	Pig	F:5'- TTCGAGCAAGAATAAGCCGC-3' R:5'- CGCGGCTGGTACTTGTAATC-3'	240	58	1.5

Methods

2.2 Tissue culture

2.2.1 Cell lines

The human DLKP cell line was kindly provided by Prof. Martin Clynes, Dublin City University (Mcbride et al. 1998). The cells were derived from a lymph node metastasis of a primary tumour. The lung tumour was termed a "poorly differentiated squamous cell carcinoma" as described in (Law et al. 1992) . The parental DLKP line was subsequently cloned to three distinct populations DLKP-SQ, DLKP-M and DLKP-I as described (Mcbride et al. 1998). The cells were routinely cultured in a 1:1 mixture of DMEM: Hams-F12 medium supplemented with 5% fetal bovine serum and 2mM L-Glutamine. Cell culture medium for DLKP-SQ Eprom, DLKP- SQ Em^2, DLKP-M Eprom and DLKP-M Em^2 was supplemented with 200 ug/ml G418. Cells were maintained in a humified atmosphere at 5% CO_2 at 37 °C. Experiments were carried out within seven passages.

2.2.2 Sub-culture

DLKP cell lines were subcultured when the T-75 flask reached between 80-100% confluency. The culture medium was pipetted from the flask and the cells were rinsed with sterile 1XPBS solution. Trypsin-EDTA (0.5% w/v) was added to the flask which was incubated at 37 °C until the cells had completely detached from the flask – not exceeding 15 mins. Detachment of the cells was visualised using a light microscope. An equal volume of 5% serum-containing medium was added to

the flask to neutralise the trypsin enzyme. The entire content of the flask was transferred to a 30ml sterlin and spun at 259 x g for 5 mins in a bench top centrifuge. Following centrifugation, the supernatant was discarded and the cell pellet was resuspended in fresh medium. The cells were then used to re-seed culture flasks or for experimental set up.

2.2.3 Cell freezing

Cells were frozen to liquid nitrogen to maintain cell stocks. Freezing medium was prepared which consisted of 8ml DMEM:F12, 1ml FBS, 1ml DMSO. This medium was stored on ice and protected from the light. When the cells reached 60-70% confluency, the flask was trypsinised as above, and the resulting pellet was resuspended in 1ml freezing solution, in a dropwise fashion. The cell suspension was transferred to a cryovile and stored in Mr. Frosty apparatus at -80 °C overnight. The Mr. Frosty apparatus contains isopropanol which slowly freezes the cells at 1 degree /minute. The cryoviles were transferred to liquid nitrogen for long term storage.

2.2.4 Cell thawing

The freezing solution used during liquid nitrogen preparation is toxic to cells at room temperature – due to its dehydrating effect on the cells. Prior to the removal of cells from liquid nitrogen, a 10% serum-containing medium was prepared and incubated at 37 °C (1:1 DMEM/F12, 10% FBS, 2 mM L-Glutamine). A small beaker of dH_20 was heated to 37 °C. The cryovial was removed from liquid nitrogen and placed on ice. Cells were thawed by placing the cryovile in the heated water and swirling gently. Once the cells had thawed, the solution was quickly transferred

to the medium-containing sterilin. The cells were centrifuged at 259 x g for 5 mins. The supernatant was discarded and the cells were resuspended in 10% medium and placed in a tissue culture flask. The flask was placed in a 37 °C humidified environment with 5% CO_2. The culture medium was replaced between 8-17 hours later to remove any residual DMSO and dead cells.

2.2.5 Cell counting

Following trypsinising, cells were suspended in 10ml medium. A glass haemocytometer was used to carry out a cell count to determine the number of cells per millilitre of medium. The haemocytometer was cleaned with ethanol and a coverslip was mounted by applying pressure with the fingertips. Newton's rings were observed to ensure the correct depth between the haemocytometer and the coverslip. Approximately 10ul of cell suspension was pipetted onto the haemocytometer and the volume was drawn under the coverslip by capillary action. Cells present in each of the four corner were counted and an average cell concentration was obtained. This number was indicative of the number of cells x 10^4 per ml of the original cell solution.

2.2.6 Expansion of Eprom- and Em^2-expressing DLKP-SQ and DLKP-M cells

DLKP-SQ and DLKP-M cells were transfected with E-cadherin reported plasmids designed by Dr. Joanne Masterson in the O'Dea lab. The first contained the mouse E-cadherin promoter-CAT construct subcloned into the plasmid vector pEYFP-1. This plasmid was called Eprom. The second construct contained the full length

mouse E-cadherin gene from the pBATEM2 construct subcloned into the plasmid vector pEYFP-1. This plasmid was called Em^2.

Populations of DLKP-SQ and DLKP-M cells transfected with Eprom and Em^2 plasmids were grown in T-75 flasks by Dr. Emer Molloy. Cells were trypsinised and a cell suspension of 2 x 10^4 cells/ml was prepared of the mixed populations of DLKP-SQ Eprom, DLKP-SQ Em^2, DLKP-M Eprom and DLKP-M Em^2. DMEM-F12 culture medium containing 400ug/ml G418 was prepared and cells were diluted according to the Corning ® Cell cloning by serial dilution in 96 well plate protocol. In brief, 100ul was pipetted into all wells in a 96 well plate except A1. 200ul of the cell suspension was added to A1 and a serial dilution along column 1 was carried out. A subsequent serial dilution across each row was carried out using a multi-channel pipette. Medium was added so that each well contained 200ul of medium (see appendix Figure 8.0.1). The plate was left to incubate overnight at 37 °C in a humidified environment with 5% CO_2. Clonal cells growing as a single colony were detected by brightfield microscopy and fluorescent microscopy was used to validate fluorescent colonies. Once characterised, all fluorescent colonies were expanded and cells were transferred from 96 well plate to 24 well plate, 6 well plate, T-25 culture flask and finally to a T-75 culture flask. FACS was carried out to quantify the level of fluorescence in the DLKP-SQ Eprom, DLKP-SQ Em^2, DLKP-M Eprom and DLKP-M Em^2 cells. This work was carried out by Dr. Emer Molloy, see appendix Figure 8.0.1.

This clonal expansion protocol was repeated at the beginning of this project to prepare a purified population of DLKP-SQ Eprom cells as the stocks of this subclone had expired.

2.2.7 Spheroid cell culture

Cells were counted and suspended in 2x Happy Cell® Medium at the correct seeding density for a chamber well slide or a 24-well plate. 250ul of this cell suspension was added to the plate. A 1:1 mix of 2x Happy Cell ® Medium and DMEM-F12 medium was prepared and supplemented with 2% FBS, 2mM L-Glutamine and 200units/ml Pen-strep. 250ul of this cell medium was pipetted on top of the cell suspension of DLKP-SQ, DLKP-M, DLKP-SQ Eprom, DLKP-M Eprom, DLKP-SQ Em^2 or DLKP-M Em^2. Cells grown in Happy Cell ® medium began to form 3D spheroids after 4 days in culture.

2.2.8 Acquisition of bright field images

Phase contrast images were obtained using an Olympus CK40 light microscope.

2.3 Primary porcine tracheal explant ALI culture

2.3.1 Porcine tracheal tissue preparation

Pig lungs were collected from the local abattoir and transported on ice to the lab. Wash medium had been previously prepared and incubated at 37 °C – 1:1 RPMI DMEM-F12 medium supplemented with 200units/ml penicillin and streptomycin, 2.5ug/ml amphotericin, 50ug/ml gentamycin and 10mM L-glutamine. A bunsen burner was present on the bench once the lungs were removed from the ice to enhance sterility. The trachea was detached from the mouthparts and cut at the carina. The tracheal tissue was cleaned of all adventitia, connective tissues, blood and mucus. The trachea was cut along the trachealis (the cartilaginous axis) and divided into longitudinal sections. Each tissue section was submerged in sterile PBS

before being placed in wash medium. The tissue was rocked then for 5 minutes at room temperature before being placed at 37 °C for 40 minutes. Three washes were carried out over a period of 3 hours using fresh medium each time. All residual connective tissue attached to the exterior to the trachea was removed following each wash. The tracheal sections were cut into small explants, approximately 10mm x 10mm in size which consisted of cartilage, respiratory mucosa and respiratory epithelium.

2.3.2 Sub-culture on agar plugs

Tracheal sections were removed from the wash medium and placed on 1% w/v agarose plugs with the epithelium facing upwards. The plugs were 5mm in height and were placed in the centre the well in a 12-well plate. 2ml of culture medium was added to the well so the plug and the basal surface of the tracheal explant were bathed in medium. Culture medium contained all components of the wash medium with 10mM L-Glutamine. A serum control containing 10% FBS was prepared for all experiments.The primary porcine tracheal explant culture protocol was developed in collaboration with Dr. Peter Riddell (O'Dea Lab).

2.4 BMP Stimulation

2.4.1 Reconstitution of recombinant BMP-4

Human BMP-4 recombinant protein was purchased from Immunotools. The protein was reconstituted in 1ml DMEM-Hams F12 medium to yield a concentration of 10ug/ml. This stock solution was aliquoted into sterile Eppendorfs

and stored at -20 °C. A working concentration of 100ng/ml was used in all experiments.

2.4.2 Reconstitution of gremlin

Recombinant mouse gremlin was purchased from R&D systems. 50ug was reconstituted in 200ul of a 4mM HCL solution to yield a 250ug/ml solution. This stock solution was aliquoted into sterile Eppendorfs and stored at -20 °C. A working concentration of 3ug/ml was used in all experiments.

2.4.3 BMP-4 or gremlin stimulation of DLKP-SQ, DLKP-M, DLKP-I cell lines

Cells were trypsinised, counted and seeded as above. Reduced serum-containing medium (0.25% FBS) was added to the cells overnight to reduce the levels of any residual growth factors present in the serum. Medium was replaced after 24hrs with fresh medium (0.25% FBS) containing 100ng/ml BMP-4 or 3 ug/ml Gremlin. Cultures were maintained at 37 °C in a humidified incubator with 5% CO_2.

2.4.4 BMP-4 stimulation of pig tracheal explants

Serum-containing and serum-free medium supplemented with 100ng/ml BMP-4 was added to the wells containing the agar plugs and tracheal explants. Cultures were maintained at 37 °C in a humidified incubator with 5% CO_2.

2.5 Rhesus macaques model of allergic airway disease

The following procedures with rhesus macaques animals and tissues were carried out by trained staff at the California National Primate Research Centre (CNPRC) based at the University of California, Davis, USA prior to the present study.

2.5.1 Selection of non-human primates

All rhesus macaques in this study (*Macaca mulatta*) were chosen from the breeding colony at the California National Primate Research Centre at the University of California, Davis. All housing and care of the animals was in compliance with the provisions outlined by the Institute of Laboratory Animal Resources and followed the regulations of the Association for Assessment and Accreditation of Laboratory Animal Care (AAALAC). The Institute of Animal Use and Care Committee reviewed and approved all animal experimental protocols prior to commencement. Neonates were removed from the mothers and following 2 days of bottle-feeding, they were randomly assigned to groups and placed in social cohorts within chamber nurseries for a further 28 days. Body weights within social groups were comparable and the animals were chosen based on negative intradermal skin test reactivity to *Dermatophagoides farinae* which is a common house dust mite allergen (HDMA).

2.5.2 Asthma model

The rhesus macaques chosen for the study were moved to specially designed air chambers. Each exposure chamber had a turnover of 30 filtered air changes per hour. All animals were diligently checked and monitored by trained CNPRC animal technician, care, research and veterinary staff.

The animal test groups were exposed to HDMA + O_3 (n=6). The HDMA was supplied by Greer Laboratories (Lenoir NC) was used for inoculation and aerosolization in the treatment chambers as previously described (Schelegle, Walby, et al. 2003). Ozone generation and supply was carried out as previously described (Schelegle, Miller, et al. 2003). Over a 5 day period, O_3 was supplied to the chamber for 8hr per day at 0.5ppm in combination with aerosolized *D. farinae* during days 3, 4 and 5. HDMA was supplied to the chambers for 2.5hr/day at 1mg/ml. These animals had been previously sensitized to *D. farinae* in alum at 14 days old via subcutaneous inoculation and intramuscular injection of heat-killed *Bortetella pertussis* cells. At 28 days old an additional dose of HDMA in alum was provided. Following the 5 day treatment period, filtered air was supplied to the chamber for a further 9 days. This cycle of 14 days was repeated 11 times resulting in a 5 month exposure period.

2.5.3 Regeneration model

A separate cohort of animal was exposed to filtered air for a 6 month period following the initial 5 month HDMA + O_3 exposure period. This was to assess the potential recovery of the lungs. These monkeys were exposed to HDMA + O_3 for 2hours at monthly intervals to maintain sensitivity. Each exposure animal group (n=6) has a corresponding control animal group (n=6) housed in filtered air for the duration of the study.

2.5.4 Necropsy and tissue preparation

Following the period of six or twelve month treatment in HDMA + O_3 or filtered air, the animals were sedated by an intramuscular injection of Telazol (8mg/kg) and

anaesthetized intravenously with Diprivan (0.2/0.2mg/kg/min). Sodium pentobarbital was supplied intravenously to deeply anaesthetise the already sedated animals. Following tracheal intubation, the animal underwent exsanguination via the systemic aorta.

Following necropsy, the left cranial lobe was fixed in 1% paraformaldehyde. After fixation, the lobes were isotrophically oriented using an orientor and cut into 5-mm slabs. A smooth fractionator was used to sample the tissue (Gundersen et al. 1988). The tissue was embedded in paraffin and cut into 5-µm serial sections and stored at ambient temperature prior to deparaffinisation and immunofluorescence.

2.6 RNA Isolation

2.6.1 RNA Harvest from cells cultured in 24 well plates

Culture medium was removed from the well. In the fume hood, 250µl Trizol© was added to each well, swirled and incubated at room temperature for 2-3minutes. All Trizol© solution for each time point was then pipetted from well and placed in a labelled eppendorf. Samples were stored at -20°C before phase separation and RNA isolation was carried out.

2.6.2 RNA Isolation

Once the homogenate was thawed, all samples and materials were moved to the fume hood and 5µl of Polyacryl Carrier is added to every tube. This is a polymer used to aid visualisation of the RNA pellet. 200µl Chloroform was added to each tube and the samples were shaken vigorously for 15seconds before an incubation period of 10minutes at room temperature. The tubes were centrifuged at 1,200rcf at

4°C for 15minutes. The aqueous RNA phase was transferred to new labelled tubes (350-450µl).

2.6.3 RNA Precipitation and purification

To the tube containing RNA, 500µl Isopropanol was added and the tubes were vortexed. Following incubation at room temperature for 5-10minutes, the tubes were centrifuged at 1,200rcf at 4°C for 15minutes. A pellet was seen at the bottom of each tube. The supernatant was removed into a waste bottle using a P1000. A small volume was left and the pellet was left undisturbed. 1ml of 75% ethanol was added to wash the pellet in each tube. The tubes were vortexed prior to centrifugation at 7,500g at 4°C for 5minutes. The ethanol was removed and the wash steps were then repeated twice more. Following the final centrifugation, all traces of ethanol were removed and the tubes were left to air dry in the fume hood for 4-5minutes.The pellet was dissolved in 40µl nuclease-free water. The concentration of RNA was determined using a NanoDrop Spectrophotometer. All samples were stored at -80°C.

2.7 Polymerase Chain Reaction

2.7.1 DNAse treatment

RNA samples were treated with DNase to remove any DNA contamination. As an additional control, genomic samples of each sample were prepared. These samples did not receive cDNA synthesis reagents but received equal volumes of DEPC water in their place. Any amplification which occurred in the subsequent PCR was present due to DNA contamination and amplification of genomic DNA.

For each sample of RNA (500ng – 1µg), 1µl 10X DNase buffer and 1µl DNase enzyme were added. The volume of the tube was adjusted to 10µl with DEPC water. The samples were incubated at room temperature for 20minutes to allow full degradation of the DNA.

To deactivate the DNase enzyme, 1µl EDTA was added to all samples and all samples were heated to 65°C for 10minutes.

2.7.2 cDNA synthesis

Following heat-deactivation of DNase, 1µl oligod$T_{(12-18)}$ primers and 1µl 10mM dNTPs were added to the samples. The genomic samples did not receive any oligodT and dNTPs. The solution was heated to 65°C for 5minutes before being cooled to 4°C and transferred to ice.

The cDNAmastermix was then prepared for each sample as follows:

4µl 5X First-Strand buffer

1µl 0.1M DTT

1µlRNaseOUT Recombinant RNase Inhibitor

1µl Superscript III Reverse Transcriptase

The reagents were mixed by pipetting gently up and down and 7µl of the mastermix was added to each of the active samples. An equal volume of DEPC-water was added to the genomic samples. The solution was incubated at 50°C for 60minutes on a PCR machine. To deactivate the reaction, the temperature was raised to 70°C for 15minutes.

2.7.3 Primer design

Primers were designed using the NCBI database http://www.ncbi.nlm.nih.gov/pubmed. Once coding sequences for the gene of interest were obtained, "Primer3" software from the Whitehead Institute for Biomedical Research was used to generate specific primer sets. http://primer3.ut.ee/. Each primer set was verified using a Basic Line Alignment Search Tool blast.ncbi.nlm.nih.gov

Primers were reconstituted in DEPC water to give 100uM concentration. This volume was added to DEPC water to give a working concentration @ 10ul primer + 56.6ul primer (1:6.66)= 15uM OR 10ul primer + 90ul DEPC (1:10) =10uM OR 10ul primer + 10ul DEPC (1:2)=50uM

This working stock solution was diluted by 50 when added to the PCR mastermix (0.5ul to 25ul) giving 300nM, 200nM or 1000nM concentration respectively.

2.7.4 Reverse Transcriptase PCR

Firstly, 500µl micro-centrifuge tubes were labelled appropriately. A master-mix was prepared on ice as outlined below. The reagents were multiplied for the necessary sample number.

Volume (µl)	Reagent	Final Concentration
5	5X Green GoTaq Flexi buffer	1x
1-2.25	25mM $MgCl_2$ solution	1-2.25mM
4	1.25mM dNTP	200µM each nucleotide
0.5	10-15µM Upstream primer	200-300nM
0.5	10-15µM Downstream primer	200-300nM
0.125	(5U/ µl) GoTaq DNA Polymerase	0.025U/µl
To 25	DEPC	

A total of 24.5µl of the master mix was added to each tube to which 0.5µl of the cDNA samples was added. The tubes were placed in the PCR machine and the appropriate programme was initiated. Initial denaturation for 2minutes at 95°C was followed by denaturation at 95°C for 1minute. The temperature was brought to 42-60°C for annealing of the primers. Extension followed at 72°C for 1min/kb and final extension at the same temperature for 5 minutes. Following 25-35cycles, the samples were incubated at 4°C.

For the primers –Electrophoresis

The PCR products were separated by agarose gel electrophoresis. A 1X TAE buffer (40 mM Tris, 0.35 % v/v Acetic Acid, 0.5 mM EDTA) was poured into the electrophoresis apparatus A 1.5% w/v agarose gel was prepared with 100ml 1X TAE and 1.5g agarose powder. The solution was heated to dissolve and 10µl GelRed is added for DNA visualisation. A volume of 20µl of the PCR sample was added to each well and gel electrophoresis was carried out at 95V for 45minutes. A 100bp or 1Kb DNA ladder was ran on the gel simultaneously to verify product size. Visualisation was carried out under UV light using a Biorad GelDoc System. PCR product was quantified using QuantityOne densitometry software.

2.7.5 Real Time Quantitative PCR

Quantitative PCR was carried out using the Applied Biosystems, StepOne Thermocycler. A mastermix containing 1 µl of cDNA, 5 µl SYBR green JumpStart Taq and primers at 400nM. The 10 µl SYBR mix was added to 96well plate and An initial denaturation step of 10 min at 95 ºC was carried out, followed by 40 cycles of 95ºC for 45 sec, annealing at 58ºC for 45 sec and extension for 1 min at 72ºC. A

final extension of 72ºC for 5 minutes was carried out on the final cycle. The samples were then cooled to 4ºC.

The relative quantity of amplified PCR product was calculated using the 2^ -ΔΔCt method. Each sample ΔCt was compared to its GAPDH control, to generate the fold difference in PCR product. All samples and GAPDH controls were ran in duplicate.

GAPDH was chosen as a good housekeeping gene based on previous experiments in the lab (Dr. Emer Molloy, PhD thesis). In addition, actin and β-tubulin have been shown to be changed during EMT and as a GAPDH is an enzyme involved in glycolysis we believed it to be a more suitable housekeeping gene for experiments involving BMP-induced EMT-like processes.

2.8 Immunofluorescence

2.8.1 Methanol fixation

This method of preservation was used on cell cultures growing in chamberwell slides prior to immunofluorescent staining. Medium was removed from each well and ice-cold PBS was used to rinse the cells three times. Methanol stored at -20ºC was gently pipetted down the well wall to fix the cells. The samples were incubated at -20ºC for five minutes. Methanol was blotted off and the samples were covered in parafilm and stored at -20ºC if not used immediately.

2.8.2 Formaldehyde fixation

This method of preservation was used on pig airways prior to immunofluorescent staining and histology. The samples were submerged in 10% formalin, neutral buffered solution for 24hrs at room temperature. The samples were then placed in

plastic cassettes and loaded into the Thermo Scientific ™ Citadel 2000 tissue processor for overnight fixation. A series of dehydration steps in alcohol solutions and xylene were carried out over an 8 hour period. Once the final dehydration step was complete, the sample were incubated in molten paraffin wax.

All cassettes were removed from the Thermo Scientific ™ Citadel 2000 tissue processor and placed in molten paraffin wax baths prior to embedding. The baths has been heated to 65ºC. Small plastic moulds 15mm x 15mm were used to embed the samples in paraffin wax. The well of the moulds was filled with wax before submerging the sample in the wax. A new plastic cassette was placed on top of the mould. The samples were labelled and allowed to cool. Once hardened, the plastic moulds were removed and the samples embedded in wax and fixed to the cassettes were stored at 4 ºC.

A manual microtome was used to cut the paraffin embedded samples. All samples were cut at 5uM. Each section was mounted on positivity charged glass slides and incubated at 65 ºC for one hour to dry the samples to the slide. Slides were stored in cases at room temperature.

2.8.3 Indirect immunofluorescence on cells

Cells were removed from -20ºC and allowed to come to room temperature. 1 x Tris-buffered saline (TBS: 0.01M-Tris, 0.15M-Nacl, pH 7.5) was added to each well for 5 minutes to equilibrate the cells. The TBS was removed by blotting and 1% bovine serum-Tris solution was added. The cells were incubated at room temperature for 30 minutes. This blocked non-specific binding sites such as Fc receptors on the surface of the cells.

Primary antibodies were prepared in TBS as per table. The primary antibody was pipetted onto each well and the chamberslides/plates were incubated at 4ºC overnight. Moist tissue was used as an incubating chamber to ensure the samples remained humidified during incubation. When overnight incubation was complete, primary antibody was blotted off the cells and the cells were washed three times in 0.1% v/v TBS-Tween20 solution. The cells were placed on a rocker at room temperature during each 5 minute wash.

Secondary antibodies were prepared in 1% blocking solution at a 1/200 dilution. Cells were incubated for 30 minutes at room temperature in the dark. Cells were washed three times prior to secondary antibody incubation. Cells were counterstained with DAPI at 1/10000 for 5 minutes in the dark at room temperature. DAPI was blotted off and the cells were mounted with a coverslip using DAKO® Faramount aqueous mounting medium. Cells were viewed using an inverted Olympus IX81 fluorescent microscope. All software settings were kept consistent throughout imaging of controls and samples. Controls were prepared for all antibodies. Antibody controls were prepared where the primary antibody was omitted from the staining protocol. This controlled for non-specific fluorescent antibody staining. Isotype controls were prepared where an irrelevant IgG was used. This controlled for non-specific primary antibody staining.

2.8.4 Indirect immunofluorescence on tissue

Paraffin-embedded samples on glass slides were de-waxed in xylene for 10 minutes (2 x 15minutes) in a chemical fume hood. The sections were rehydrated using a gradient of ethanol solutions. The slides were placed in 90% ethanol for 2 minutes, 75% ethanol, for 2 minutes, 75% ethanol for 2 minutes and dH_20 for 2 minutes. The

slides were then placed in a citrate based antigen retrieval solution (pH 6.0). The sections were boiled for 15 minutes (3 x 5 minutes). Sections were cooled in running tap water for 2-3 minutes. Once the slides had dried on the bench, an ImmEdge wax pen was used to encircle the tissue sections. The wax pen border was placed as close to the samples as possible to minimise the volume of antibody required. Blocking and antibody incubations were carried out as previously described. Briefly, the tissue sections were incubated in a 1% bovine serum solution to block non-specific receptors. Primary antibodies were incubated overnight at 4 ºC in TBS. Sections were subsequently washed in 0.1% v/v TBS/Tween-20. Secondary antibodies were made up in the blocking solution and sections were incubated for 30 minutes in the dark at room temperature. Following a TBS/Tween-20 wash, the cells were counterstained with DAPI. The slides were mounted with coverslips using DAKO faramount mounting medium.

2.9 Histology

2.9.1 H&E staining

Following formaldehyde fixation and paraffin embedding, the slides were moved to the chemical fume hood and de-waxed in xylene for 10 minutes (2 x 5minutes). The samples were rehydrated in 100% ethanol for 5 minutes, 95% ethanol for 2 minutes, 80% ethanol for 2 minutes and dH_20 for 2 minutes. The slides were then placed in Harris haemotoxylin solution for 3 minutes and then rinsed in tap water for 40 seconds. The slides were submerged in 1% acid alcohol (1ml HCL, 69.3ml Isopropanol, 1ml dH_20) for 5 minutes and rinsed in tap water for 5 minutes. The slides were then placed in Eosin Y solution (1g eosin powder, 1.6g Potassium

dichromate made up to 100ml dH_20) for 3 minutes and rinsed in tap water for 40 seconds. The slides were rehydrated in 80% ethanol for 5 minutes, 95% ethanol for 5 minutes and 100% ethanol for 5 minutes. The slides were mounted with a coverslip using DPX mounting medium and viewed using a Olympus CX40 light microscope.

2.9.2 PAS staining

Following formaldehyde fixation and paraffin embedding, the slides were moved to the chemical fume hood and de-waxed in xylene for 10 minutes (2 x 5minutes). The samples were rehydrated in 100% ethanol for 5 minutes, 95% ethanol for 2 minutes, 80% ethanol for 2 minutes and dH_20 for 2 minutes. The slides were placed in 1% Alcian Blue in aqueous acetic acid solution for 15 minutes and then rinsed in tap water for 2 minutes. The slides were rinsed in dH_20 before being placed in 0.5% Periodic Acid for 5 minutes. Following a rinse in dH_20 the slides were place in Schiff's reagent for 10 minutes and rinsed in tap water for 5 minutes. The samples were counter stained with Harris haematoxylin solution for 1 minute and rinsed in tap water for 2 minutes. Finally the slides were placed in 1% Acid alcohol for 20 seconds before a 5 minute wash in tap water. The slides were rehydrated in 80% ethanol for 5 minutes, 95% ethanol for 5 minutes and 100% ethanol for 5 minutes. The slides were mounted with a coverslip using DPX mounting medium and viewed using a Olympus CX40 light microscope.

2.10 Western Blotting

2.10.1 Protein harvest

Cells in T25 flasks, 24 well plates or 12 well inserts were washed in ice-cold phosphate buffered saline (PBS) and scraped with a cell scraper or a pipette tip. The cells were centrifuged at 259 x g for 5 minutes at 4ºC. The cell pellet was resuspended in chilled lysis buffer. Lysis buffer contained RIPA buffer (150 mM NaCl, 1.0% IGEPAL® CA-630, 0.5% sodium deoxycholate, 0.1% SDS, 50 mM Tris, pH 8.0) supplemented with 1x Complete Mini-Protease inhibitor cocktail. The samples were rocked for 15 minutes at 4ºC before being centrifuged at 12,000 x g for 5 minutes at 4ºC. The supernatant was collected and stored at -80ºC.

For pig tracheal explants, the samples were cut into small segments and homogenized in lysis buffer for one minute on ice. The samples were rocked for 15 minutes at 4ºC before being centrifuged at 12,000 x g for 5 minutes at 4ºC. The supernatant was collected and stored at -80ºC.

2.10.2 Bradford Quantification

Protein was quantified using a BioRad Bradford assay. A standard curve was prepared using bovine serum albumin ranging from 0 mg/ml to 1.4 mg/ml. Samples were diluted 1/10 and all samples and standards were prepared in duplicate in a 96 well plate. Bradford reagent was added to the samples in a 1/50 dilution and the samples were incubated for 5 minutes. Absorbance was read at 620nm. The quantity of protein in the samples was calculated using the standard curve.

2.10.3 Sample preparation

Following quantification of the samples, the samples were prepared for gel electrophoresis. A loading dye consisting of 1:20 solution of β-mercaptoethanol and 2x loading buffer (Tris base, HCl, acrylamide, bisacrylamide, TEMED, APS, and highly purified water) was prepared. 15ug of protein was added to an equal volume of loading dye and the samples were boiled for 5 minutes at 95ºC. This process denatures the protein and allows protein separation during gel electrophoresis. The samples were placed on ice following the boiling step.

2.10.4 Sodium Dodecyl Sulphate- Polyacrylamide Gel Electrophoresis (SDS-PAGE)

BioRad 4-20% mini-precast TGX gels were routinely used for gel electrophoresis. The gels were loaded into the cassettes and the chambers was filled with 1X Tris-Glycine-SDS buffer (25 mM Tris, 192 mM glycine and 0.1% SDS, pH approx. 8.6). A chemiluminescent protein standard, MagicMark™ was loaded on each gel to track the molecular weight of the proteins (125 mM Tris-HCl (pH 6.8), 10 mM DTT, 17.4% Glycerol, 3% SDS, and 0.025% Bromophenol Blue). A colorimetric SeeBlue® ladder was added in the final lane to track correct protein separation and transfer (Tris-HCl, Formamide, SDS, and Phenol Red). Samples were loaded into the wells and the gel was electrophoresed at 200V for 45 minutes.

2.10.5 Semi-dry transfer

In the final five minutes of electrophoresis, two stacks of blotting paper and a nitrocellulose membrane were cut to size and equilibrated in 1x Transfer Buffer.

One stack of blotting paper was placed onto the tray of the BioRad Trans-Blot® Turbo™ System. The nitrocellulose membrane was placed on top of the blotting paper stack. Once electrophoresis was complete, the gel was removed from the running chamber and placed onto the membrane-blotting paper stack. The final blotting paper stack was placed on top of the gel and a roller was pressed across the sample to remove any air bubbles. The lid of the tray was replaced and the tray was inserted into the machine. The Trans-Blot® Turbo ™ 7 minutes programme for mixed molecular weights was carried out at 2.5A constant.

2.10.6 Immunoblotting

Following transfer, the gels were removed from the stack and placed in InstantBlue (Solubilisers, Coomassie Brilliant Blue, Phosphoric Acid, Ethanol) which stained any residual proteins present on the gel. This provided an additional control for correct transfer. The bottom right hand corner of the nitrocellulose membrane was scored for orientation and placed in a blocking solution of 20% BSA or dried milk powder in TBS-0.1 % Tween20 (5mM Tris, 150mM NaCl) depending on the primary antibody of choice. Blocking was carried out for 1hr at room temperature with gentle rocking. Phosphorylated antibodies were always blocked in BSA solution as casein present in milk would induce excessive background staining. Primary antibodies were incubated for 1hr at room temperature or overnight at 4ºC. Once incubation was complete, the blot was washed for 15 minutes (3 x 5 minutes) in 0.1% TBS-Tween-20 on the rocker. Secondary antibodies coupled to horseradish perioxidase-labelled (HRP labelled) were added for 1hr at room temperature. All secondary antibodies were made up in the blocking solution. Following secondary

incubation, the blot was washed for 15 minutes (3 x 5minutes) in 0.1% TBS-Tween-20 on the rocker. The blot was placed in TBS solution before being developed.

2.10.7 Chemiluminescence

The blot was placed on cling film and the enhanced chemiluminescence (ECL) western blotting detection reagents WesternBrite were added for 2 minutes. Excessive solution was poured off the blot and the cling film was folded down on top of the blot. Visualisation of the proteins was carried out using a Syngene G-box Visualiser and the Genesys image acquisition software. The primate western blots were visualised using a Cell Biosciences FluorChem E.

2.11 Flow Cytometry

2.11.1 Sample preparation

Cells growing in flasks or wells were rinsed with 1ml PBS before trypsinisation, as outlined above. Following 10minutes at 37 °C, the appropriate volume of FBS was added to neutralise the reaction. Cells were transferred to FACS tubes and centrifuged at 259*g for 5minutes at 4 °C. The supernatant was discarded and the cells were resuspended in PBS. Centrifugation at 259*g for 5 minutes at 4 °C was repeated. The final cell pellet was resuspended in a small volume of PBS to be read on the Accuri FACS machine.

2.11.2 7AAD staining of pig tracheal explants

Tracheal explants were removed from the culture medium and the epithelium was microdissected from the underlying cartilage and connective tissue. The epithelium

was placed in trypsin for 3 minutes at 37 °C. Following digestion, 1ml of FBS was added to neutralise the reaction. The cells were rinsed through a 70uM nylon mesh using a 10ml syringe pump. The cell suspension was centrifuged at 300*g for 5 minutes and the supernatant was discarded. The pellet was resuspended in PBS to rinse. This washing step was repeated two times. Following final resuspension in 60ul PBS, 3ul of 7AAD was added to the suspension and the Eppendorf was incubated for 15 minutes at 4 °C. 100ul of FACS buffer (1x PBS + 2% FBS) was added to the tube and the cells were spun at 300*g for 5 minutes at 4 °C. The supernatant was discarded and the cell pellet was resuspended in 100uL FACS buffer to be read on the Accuri FACS machine. An un-stained control was prepared for all timepoints and treatments. This allowed accurate gating of the stained cell population.

2.12 Stereology

2.12.1 Sample preparation

Tissue mounted onto glass slides was processed for immunofluorescence as outlines in above in section 0

2.12.2 Generation of DIC super-image

A super-image of the entire epithelial surface on the slide was generated by determining the perimeter co-ordinates of the section. This super-image consisted of between 9 and 16 images stitched together by the software. A region of interest (ROI) was determined on the super-image by tracing around the epithelium and basal lamina using the marker tool in Stereology toolbox ®. This ROI was then

randomly sampled by the morphometric software, generating approximately 25 sample images per section. A DIC and a fluorescent image was captured for each sample image to facilitate stereologic quantification. Stereology toolbox version1.1, Morphometrix, Davis, CA was used.

2.12.3 Quantification of surface epithelial staining

Using point and intercept counting on a cycloid grid, the volume of fluorescently labelled cells per unit basal lamina was quantified. This has previously been described in detail (Coppens et al. 2009). In brief, by counting the volume of positive cells per unit volume of interstitial epithelium (Vv) on the fluorescent image and the surface length of basal lamina per unit volume of the interstitial epithelium (Sv) on the corresponding DIC image, the number of positive cells per unit length of basal lamina was calculated (Vs). The following equation was used where P= number of points counted, I= intersections, bl=basal lamina, epi=epithelium, l/p = length per point which was calculated as 86µm, txred= Alexa 568 positive stain).

Volume per volume Vv Calculation: $Vv_{txred/epi} = P_{txred} / (P_{epi} + P_{txred})$

Surface per volume Sv Calculation: $Sv_{bl/epi} = ((\Pi * I_{bl})/2) / ((l/p) * P_{epi})$

Volume per surface Vs Calculation: $Vs_{txred/bl} = Vv_{txred/epi} / Sv_{bl/epi}$

All exposure settings were maintained at constant milliseconds based on the negative secondary IgG control. The calculations were corrected for the grid size used. Statistical analysis was calculated using One-Way ANOVA tests and paired 2-tailed t-test in Prism Version 5.00. p values less than 0.05 were considered

significant. Immunofluorescent images and DIC images were captured on an Olympus BX61 and Metamorph software.

3 Chapter 3

The effect of BMP-related signalling on the lung cancer cell line DLKP

3.1 Introduction

Tumour heterogeneity defines the differences that exist between cancer cells in a tumour (intra-tumour heterogeneity). (Burrell et al. 2013). Tumour heterogeneity can arise by genetic or non-genetic means. Tumour heterogeneity is also introduced by dynamic phenotypic switching events between the different cancer subpopulations (Ferrao et al. 2015; Marusyk et al. 2012)

Phenotypic switching involves changes in cellular and molecular signalling events to adopt a more advantageous phenotype in a given environment. This can occur in heterogeneous tumour cells to facilitate evasion of chemotherapeutic stresses or to increase the survival of the cancer by forming metastatic tumours (Sharma et al. 2010). EMT has been implicated in the process of phenotypic switching in cancer and tumour progression. EMT makes tumour cells more invasive and causes them to be released into the circulation and establish distant metastatic sites (Lee et al, 2006; Pierre Savagner, 2007; Talmadge, 2007). EMT involves changing from an organised, polarised, adherent epithelial cell to an invasive, elongated mesenchymal cell. The process involves downregulation of the tumour-suppressor and adherens

junction protein E-cadherin and other cell adhesion proteins in conjunction with upregulation of matrix degrading enzymes (Kalluri and Weinberg 2009).

The DLKP lung cancer cell lines contains three distinct clonal subpopulations designated DLKP-SQ, DLKP-M and DLKP-I. DLKP-SQ cells grow in small squamous-shaped colonies. DLKP-M cells are larger and more mesenchymal with extended neurite-like processes. DLKP-I cells are the smallest of the three clones and grow in tightly packed colonies with a distinct outer boundary. Interestingly, when the parental population are grown in culture, interconversion events are evident between DLKP-SQ, DLKP-M and DLKP-I clones (Mcbride et al. 1998). These interconversion events resemble phenotypic switching in this heterogenous tumour population. In order to determine the role of EMT in phenotype switching between these two clonal populations, we investigated the effect of modulating the BMP signalling pathway.

Previous literature has shown that EMT is a critical process involved in embryogenesis and correct organ formation. During wound healing and normal reparative processes, epithelial cells downregulate adherens junction proteins and undergo EMT to migrate onto the damaged area and restore epithelial integrity. EMT is also linked to tumour progression and the formation metastases (Kalluri and Weinberg 2009). Our lab has previously demonstrated a relationship between EMT and the BMP pathway, reviewed in (McCormack and O'Dea 2013).. BMP mediated signalling can induce a mesenchymal and migratory phenotype in the normal bronchial epithelial cell line Beas2b and also in normal primary airway epithelial cells (AECs). Furthermore, BMPs increase the rate of cell migration of AECs during epithelial restitution (McCormack et al. 2013; Molloy et al. 2008). In this study we investigated the role of the BMP signalling in the induction of EMT

and the control of the phenotypic switching events that occur between the clonal subpopulations of the DLKP cell line.

Given the distinct morphological differences that exist between the DLKP clones and the spontaneous interconversion events that occur in parental DLKP cell culture, we hypothesise that the DLKP-SQ and DLKP-M clones may be an ideal model for investigating phenotypic switching between heterogeneous tumour populations. We propose that DLKP-SQ cells are a more "epithelial"-like clonal population that represent normal cells more closely than DLKP-M cells.

We hypothesise that by agonising and antagonising the BMP pathway we could induce phenotypic switching between these clonal populations (Figure 3.1). Following BMP-4 stimulation we hypothesise that DLKP-SQ cells would undergo EMT and resemble DLKP-M clones. Conversely, we speculate that DLKP-M cells treated with gremlin would undergo MET, or partial MET and convert to DLKP-SQ or DLKP-I cells. We hypothesise that there would be no change in DLKP-M cells treated with BMP-4 as they already represent a mesenchymal, migratory clonal population. Finally, given the spontaneous interconversion events which occurred between DLKP-SQ and DLKP-M cells in culture we hypothesised that DLKP-I cells represented a stem cell-like clone capable of readily undergoing phenotypic switching events. We hypothesise that DLKP-I would convert to the more mesenchymal DLKP-M cells following BMP-4 stimulation and DLKP-SQ cells following gremlin stimulation.

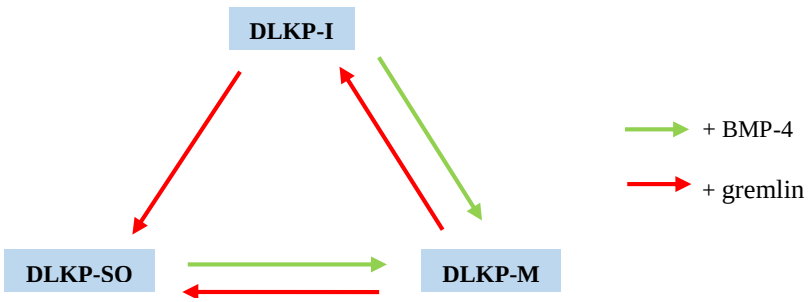

Figure 3.0.1 Hypothesis of BMP-mediated phenotypic switching in DLKP clones

3.1.1 Expression of tight junction proteins in DLKP-SQ, DLKP-M and DLKP-I clones

Given the morphological differences that exist between the DLKP-SQ, DLKP-M and DLKP-I clones, we hypothesised that the DLKP-SQ clones represent a more epithelial-like cell population. We hypothesised that DLKP-M have undergone phenotypic changes to become a more mesenchymal cell population. As tight junction proteins (TJP) are expressed in epithelial cells, we examined the expression levels of TJP in the DLKP clones by western blot.

Significant differences in the expression of TJP was observed between DLKP-SQ, DLKP-I and DLKP-M clones. DLKP-SQ and DLKP-I cells express afadin, ZO-1 and claudin-1 while DLKP-M cells do not. CD2AP was the only tight junction protein examined that was expressed in all DLKP cell lines (Figure 3.0.2). These results supported the hypothesis that DLKP-SQ represented a more differentiated, epithelial-like cell population compared to DLKP-M cells.

GAPDH was chosen as a suitable housekeeping gene as protein expression remained unchanged between experiments irrespective of treatments and stimulations. GAPDH was a more suitable than other common housekeeper genes such as actin or tubulin as their expression can change following BMP-4 treatment and during EMT.

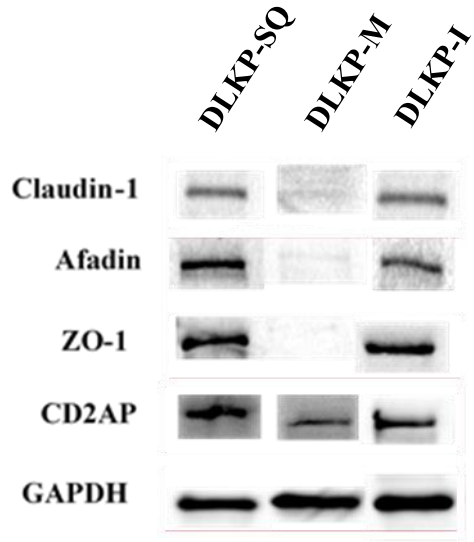

Figure 3.0.2 Western blot of tight junction proteins in DLKP-SQ, DLKP-M and DLKP-I cells

Representative western blots of claudin-1, afadin, ZO-1 and CD2AP in DLKP-SQ, DLKP-M and DLKP-I clones. There was no detectable expression of afadin, ZO-1 or claudin-1 in DLKP-M compared to DLKP-SQ and DLKP-M. CD2AP was expressed in all cell lines. GAPDH was used as a loading control, n=2.

3.1.2 Gene expression analysis of DLKP-SQ, DLKP-M, DLKP-I

Gene expression analysis was carried out on the DLKP clones to examine BMP receptor and ligand expression. This was carried out by our collaborators in DCU (Dr Helena Joyce). DLKP-SQ expressed the highest level of BMPRIa protein. DLKP-M expressed the highest level of BMPRII. Analysis of endogenous BMP-7 mRNA revealed that DLKP-SQ cells expressed higher levels of this BMP ligand compared to DLKP-I. Unfortunately no information was available for DLKP-M cells, but we hypothesise a similar level of expression to DLKP-I cells. In addition, DLKP-M and DLKP-I expressed higher levels of CRMP-1, α-integrin-V and scatter factor expression compared to DLKP-SQ (Figure 3.0.3, Appendix).

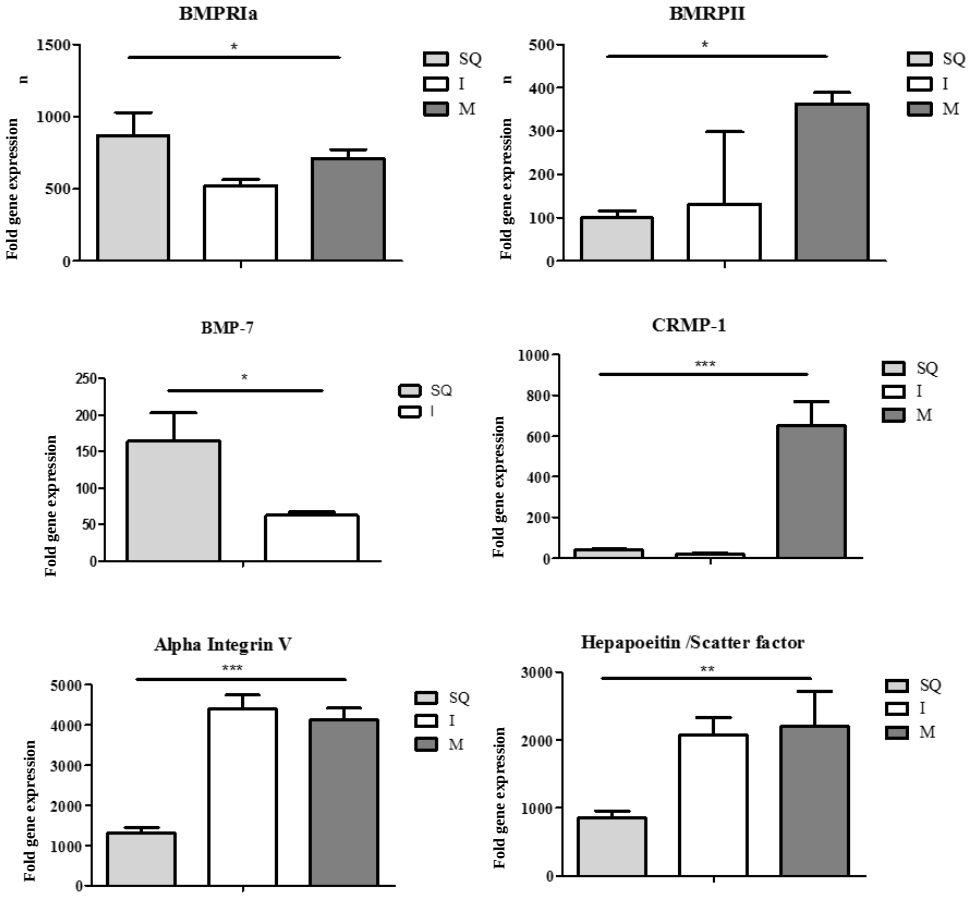

Figure 3.0.3 Gene expression analysis of DLKP clones

Gene expression analysis of endogenous mRNA expression of BMP receptors and mesenchymal markers was investigated in the three subclonal DLKP populations. This work was carried out by our collaborator Dr. Helena Joyce in DCU. DLKP-SQ expressed higher BMPRIa levels compared to DLKP-M and DLKP-I. DLKP-M expressed higher levels of BMPRII compared to DLKP-SQ and DLKP-I. DLKP-SQ expressed the lowest level of CRMP-1, α-integrin-V and scatter factor genes. Statistical significance was obtained using a One-way ANOVA test, * $p<0.05$, ** $p<0.005$, *** $p<0.0005$ n=3

3.1.3 BMP pathway activation in DLKP-SQ following BMP-4 stimulation

To assess whether DLKP-SQ clones respond to BMP stimulation, the cells were cultured in the presence of 100 ng/ml BMP-4 for 24 hrs. Serial dilution and timecourse experiments previously carried out in the O'Dea lab determined that this concentration of BMP-4 ligand was optimal (Dr. Natasha McCormack). The level of activation and localised expression of various SMAD signalling molecules were investigated by immunofluorescence. DLKP-SQ cells were also grown in the presence of 100 ng/ml BMP-4 for 2hr, 4hr and 24hr to assess ID-1, SMAD-6 and SMAD-7 mRNA expression.

The expression of SMAD-1 and SMAD-5 did not appear altered in response to BMP-4 treatment at 24 hrs (Figure 3.0.4). SMAD-1 and SMAD-5 were localised in the cytoplasm of the DLKP-SQ cells which remained unchanged following BMP-4 treatment. SMAD-4 was evident in the cytoplasm in untreated DLKP-SQ cells. Following 24 hrs, SMAD-4 was localised in the nucleus (Figure 3.0.4 i-l). Similarly, elevated nuclear expression of pSMAD 1/5/8 occurred in DLKP-SQ cells treated with BMP-4 compared to control cells. There was some evidence of nuclear pSMAD 1/5/8 localisation in the untreated DLKP-SQ cells (Figure 3.0.4 m-p). Larger images are presented in the appendix (Figure 8.0.11).

SMAD-6 expression was localised in the cytoplasm in the untreated DLKP-SQ cells whereas increased nuclear protein expression was present in cells stimulated for 24 hrs (Figure 3.0.4 q-t). SMAD-7 protein localisation was altered from the cytoplasm to the nucleus following BMP-4 stimulation for 24 hrs, as indicated by the white arrows (Figure 3.0.4 u-x).

The expression of ID-1, SMAD-6 and SMAD-7 mRNA was examined by rt-PCR. ID-1 expression increased in a time-dependent manner following BMP-4 stimulation. There was no significant change in SMAD-6 and SMAD-7 mRNA expression occurs following BMP-4 treatment (Figure 3.0.5).

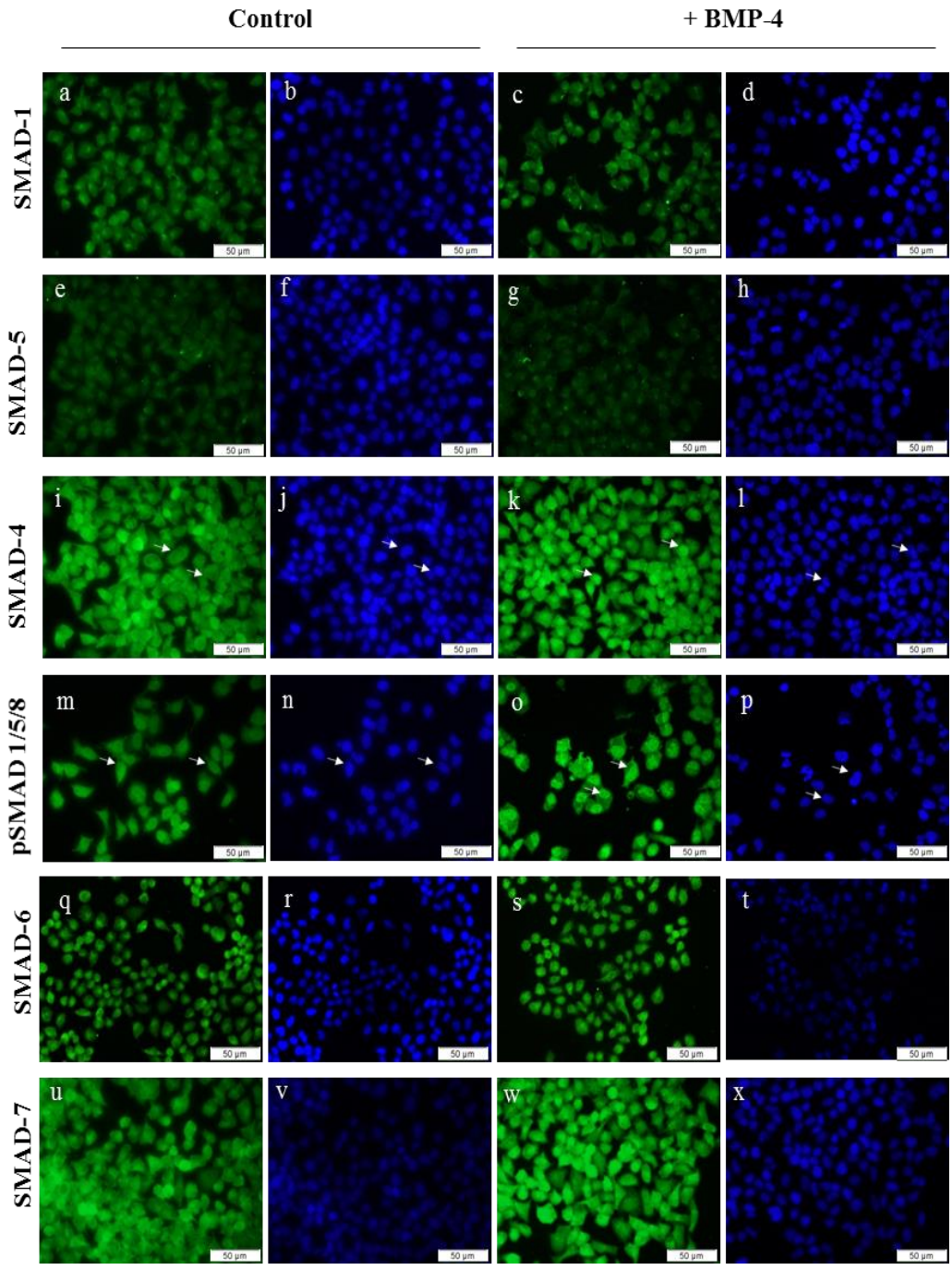

Figure 3.0.4 Immunofluorescence of intracellular SMAD signalling in DLKP-SQ cells following BMP-4 stimulation

Representative micrographs of SMAD-1 (a-d), SMAD-4 (e-h) , SMAD-5 (i-l) , pSMAD-1/5/8 (m-p), SMAD-6 (q-t) and SMAD-7 (u-x) localisation in DLKP-SQ cultured with 100ng/ml BMP-4 for 24 hrs. There is little evidence of altered SMAD-1 (a-d) and SMAD-5 (i-k) signalling following 24 hr BMP-4 treatment. Nuclear translocation of SMAD-4 (e-h) and pSMAD 1/5/8 (m-p) from the cytoplasm was evident following BMP-4 treatment, as indicated by the arrows. iSMADs SMAD-6 (q-t) and SMAD-7 (u-x) were expressed in the nucleus following BMP-4 treatment. All scale bars represent 50uM, white arrows indicate relative cytoplasmic or nuclear staining n=2. Additional images are included in the appendix.

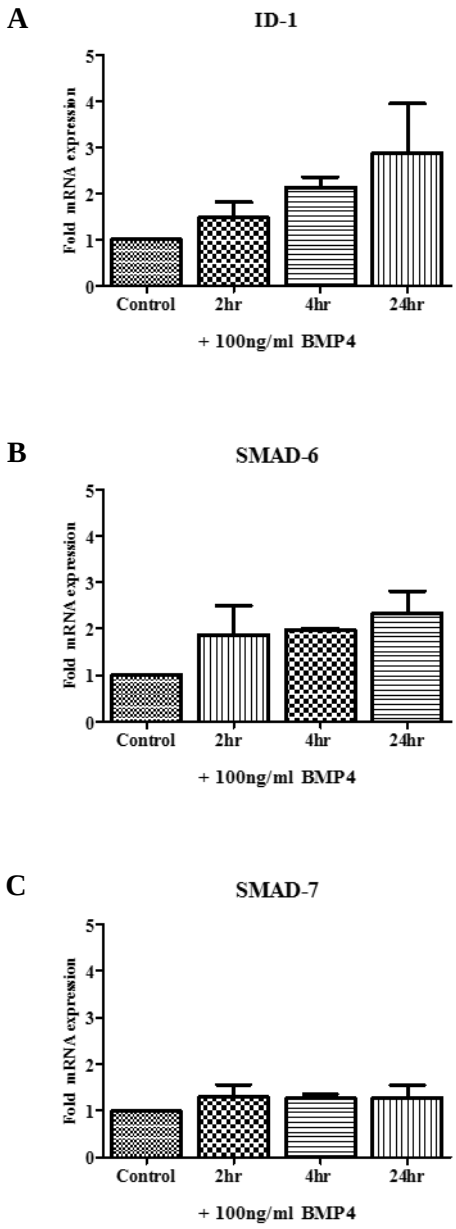

Figure 3.0.5 mRNA expression of ID-1, SMAD-6 and SMAD-7 following BMP-4 stimulation in DLKP-SQ cells

Representative graphs of quantified ID-1, SMAD-6 and SMAD-7 mRNA expression in DLKP-SQ cells following 2 hr, 4 hr, 24 hr treatment with 100 ng/ml BMP-4. (A) ID-1 is an early responder to the BMP-4 stimulation and increases in transcript expression can be seen in a time dependent manner. (B)(C) No significant change in SMAD-6 or SMAD-7 expression was evident following statistical anaylsis. n=3

3.1.4 BMP pathway activation in DLKP-M following BMP-4 stimulation

To assess whether DLKP-M clones are responsive to BMP signal activation, the cells were cultured in the presence of 100 ng/ml BMP-4 for 24 hrs. The level of activation and localised expression of various SMAD signalling molecules were investigated. DLKP-M cells were also grown in the presence of 100 ng/ml BMP-4 for 2hr, 4hr and 24hr to assess the level of ID-1, SMAD-6 and SMAD-7 mRNA expression.

SMAD-1 and SMAD-5 were detected in the cytoplasm and peri-nuclear region in both untreated and treated DLKP-M cells (Figure 3.0.6 a-h**).** Examination of SMAD-4 localisation showed increased nuclear translocation of SMAD-4 following 24 hr stimulation with 100 ng/ml BMP-4, as indicated by the white arrows (Figure 3.0.6 i-l). Similarly, bright nuclear pSMAD 1/5/8 expression was apparent in DLKP-M cells following 24 hr BMP-4 treatment (Figure 3.0.6 m-p). This increase in nuclear localisation of pSMAD 1/5/8 is highlighted by the white arrows. Similar to DLKP-SQ cells, endogenous nuclear pSMAD 1/5/8 was present in untreated DLKP-M cells. Elevated cytoplasmic and nuclear SMAD-6 staining was present in BMP-4 treated DLKP-M cells (Figure 3.0.6 q-t**).** Similarly, SMAD-7 was localised in the cytoplasm in untreated DLKP-M cells. Increased nuclear localisation of SMAD-7 occurred following BMP-4 stimulation (Figure 3.0.6 u-x). Larger images are presented in the appendix (Figure 8.0.12).

The expression of ID-1, SMAD-6 and SMAD-7 mRNA was examined by rt-PCR. ID-1 expression increased in a time-dependent manner following BMP-4

stimulation. There was no significant change in SMAD-6 and SMAD-7 mRNA expression occurs following BMP-4 treatment (Figure 3.0.7).

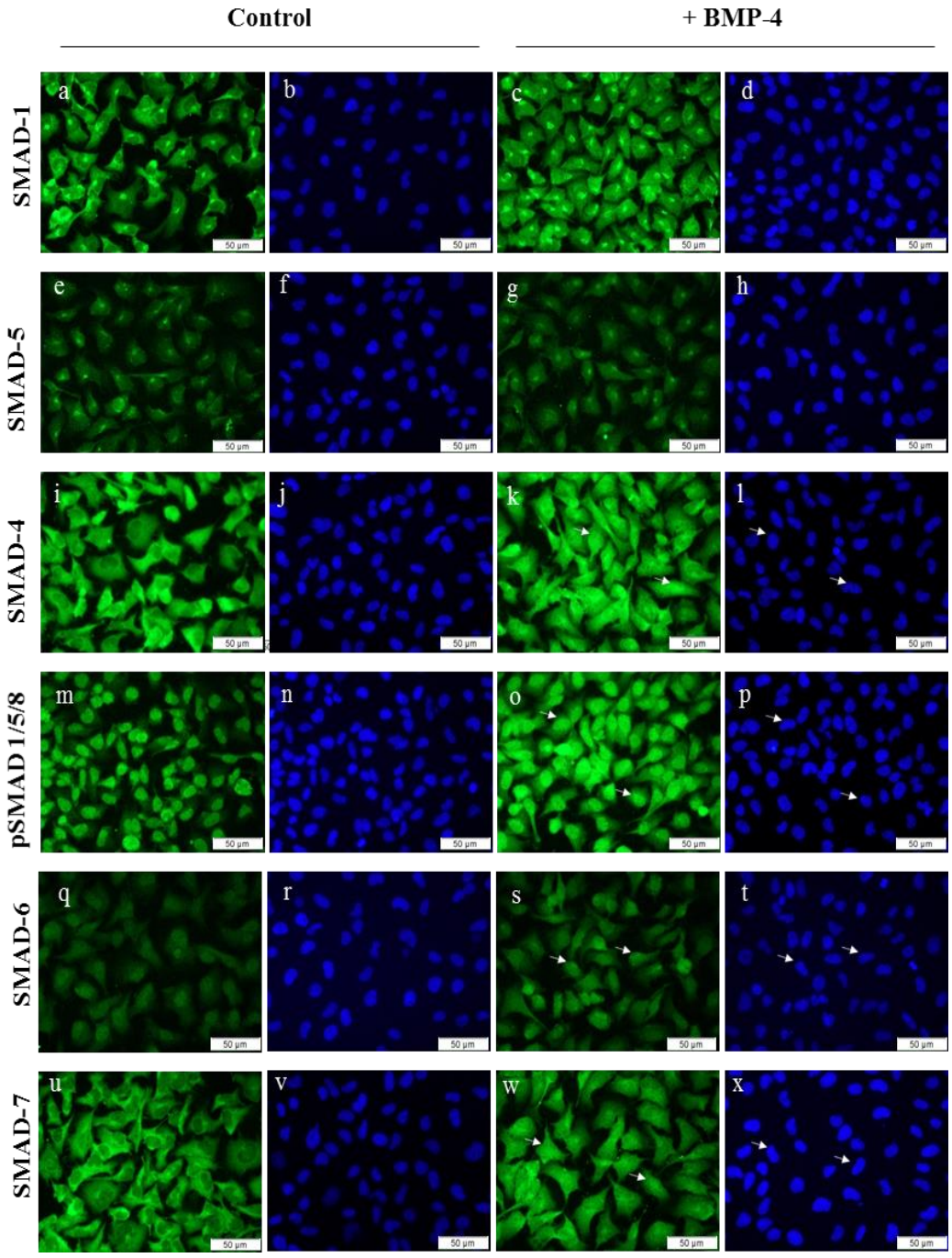

Figure 3.0.6 Immunofluorescence of intracellular SMAD signalling in DLKP-M cells following BMP-4 stimulation

Representative micrographs of SMAD-1 (a-d), SMAD-4 (e-h) , SMAD-5 (i-l) , pSMAD-1/5/8 (m-p), SMAD-6 (q-t) and SMAD-7 (u-x) localisation in DLKP-M cells cultured with 100ng/ml BMP-4 for 24 hrs. SMAD-1 was localised in the cytoplasm and around the nucleus in treated and untreated cells (a-d). There was no change in the weak peri-nuclear and cytoplasmic staining of SMAD-5 following treatment (e-h). Both SMAD-4 and pSMAD 1/5/8 localisation became nuclear following exposure to BMP-4 (i-l). SMAD-6 expression was increased in the cytoplasm with increased nuclear translocation (q-t). SMAD-7 was translocated from the cytoplasm to the nucleus. All scale bars represent 50uM, white arrows indicate relative cytoplasmic or nuclear staining, n=2

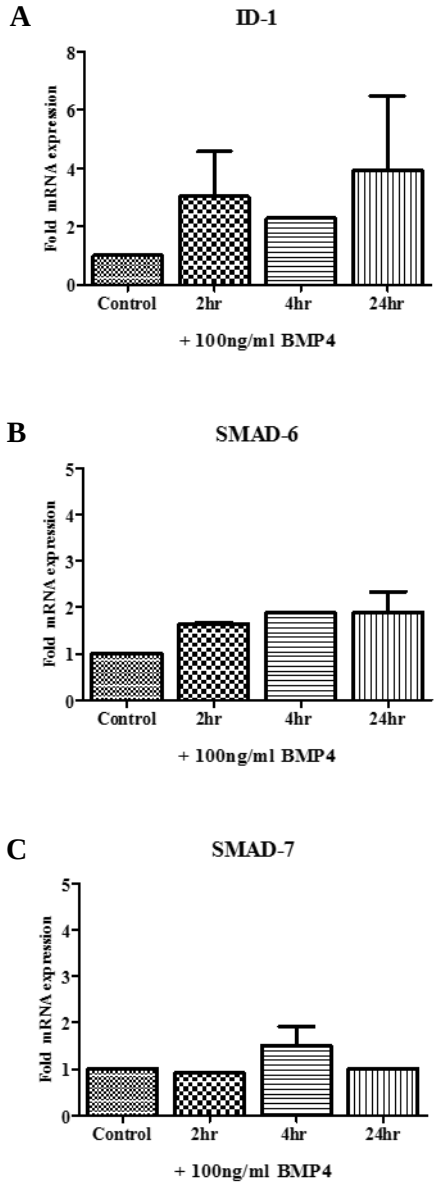

Figure 3.0.7 mRNA expression of ID-1, SMAD-6 and SMAD-7 following BMP-4 stimulation in DLKP-M cells

Representative graphs of quantified ID-1, SMAD-6 and SMAD-7 mRNA expression in DLKP-M cells following 2 hr, 4 hr, 24 hr treatment with 100 ng/ml BMP-4. (A) ID-1 increased in a time dependent manner following BMP-4 stimulation (B)(C) No change in SMAD-6 or SMAD-7 expression was evident following statistical analysis. n=3

3.1.5 BMP pathway activation in DLKP-I following BMP-4 stimulation

To assess whether DLKP-I cells BMP signals, the cells were cultured in the presence of 100 ng/ml BMP-4 for 24 hrs. The level of activation and localised expression of various SMAD signalling molecules were investigated. DLKP-I cells were also grown in the presence of 100 ng/ml BMP-4 for 2hr, 4hr and 24hr to assess the level of ID-1, SMAD-6 and SMAD-7 mRNA expression.

Similar to both DLKP-SQ and DLKP-M cells, SMAD-1 and SMAD-5 expression in DLKP-I remained unchanged following 24 hr BMP-4 treatment. SMAD-1 and SMAD-5 were detected in the cytoplasm and peri-nuclear straining could be seen in the untreated and treated cells alike (Figure 3.0.8 a-h). Increased nuclear localisation of SMAD-4 was detected following BMP-4 stimulation (Figure 3.0.8 i-l). Similarly, an elevated level of nuclear pSMAD 1/5/8 was present in BMP-4 treated cells (Figure 3.0.8 m-p). Elevated levels of both iSMADs were evident in the cytoplasm and nucleus following BMP-4 treatment (Figure 3.0.8 q-x). Larger images are presented in the appendix (Figure 8.0.13).

The expression of ID-1, SMAD-6 and SMAD-7 mRNA was examined by rt-PCR. ID-1 expression increased in a time-dependent manner following BMP-4 stimulation. There was no significant change in SMAD-6 and SMAD-7 mRNA expression occurs following BMP-4 treatment of DLKP-I cells (Figure 3.0.9).

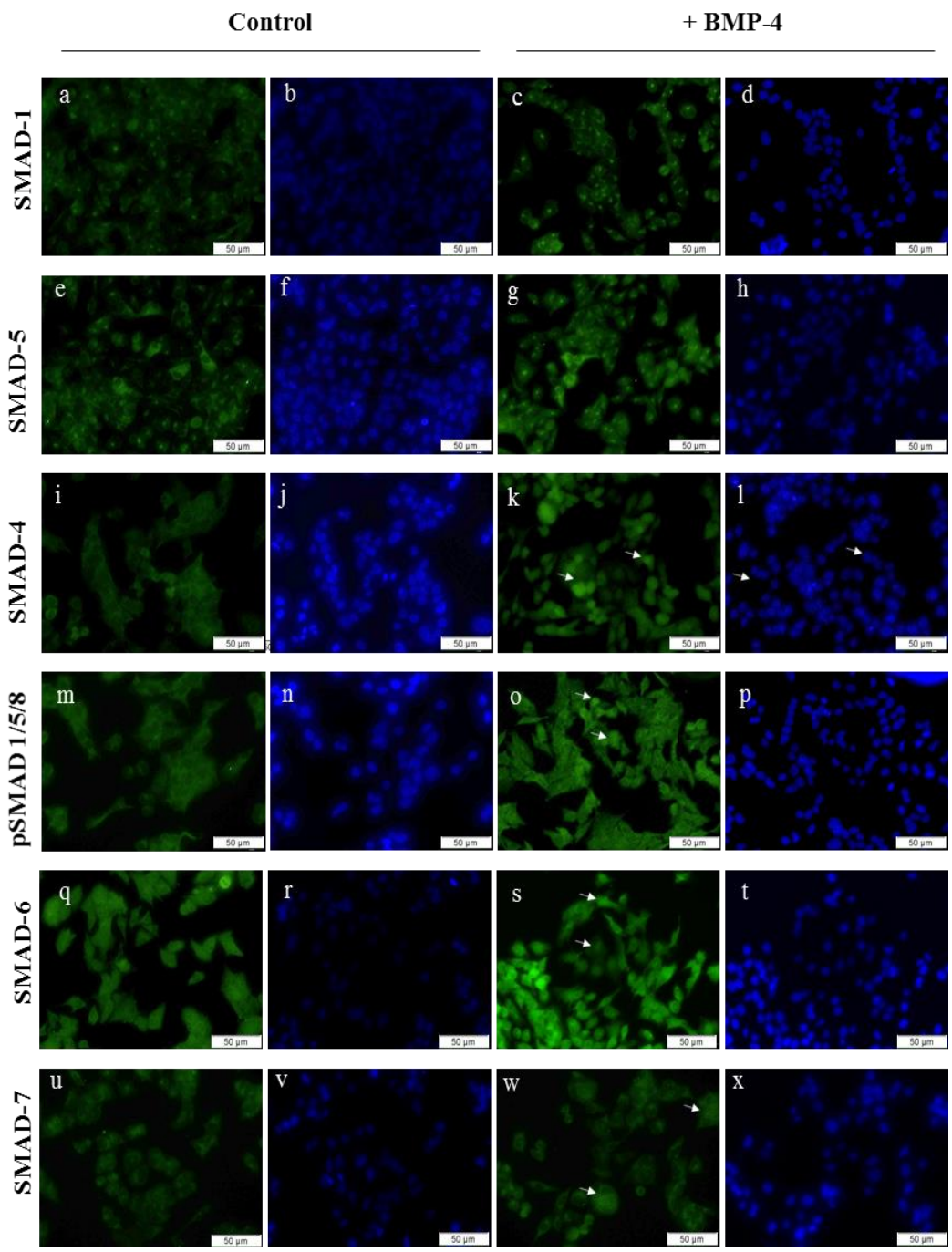

Figure 3.0.8 Immunofluorescence of intracellular SMAD signalling in DLKP-I cells following BMP-4 stimulation

Representative photomicrographs of SMAD-1 (a-d), SMAD-4 (e-h) , SMAD-5 (i-l) , pSMAD-1/5/8 (m-p), SMAD-6 (q-t) and SMAD-7 (u-x) localisation in DLKP-I cells cultured with 100ng/ml BMP-4 for 24 hrs. SMAD-1 was localised in peri-nuclear patterns and in the cytoplasm and expression was elevated in the same regions following BMP-4 treatment for 24 hrs (a-d). SMAD-5 was detected in the cytoplasm and in peri-nuclear regions in both the control cells and following BMP-4 treatment (e-h). There was evidence of elevated nuclear localisation of both SMAD-4 (i-l) and pSMAD 1/5/8 (m-p) following BMP-4 stimulation. SMAD-6 was localised in the nucleus in treated and untreated cells (q-r) SMAD-7 was present in cytoplasmic and nuclear localisation occurred following BMP-4 stimulation. All scale bars represent 50uM, white arrows indicate relative cytoplasmic or nuclear staining n=2

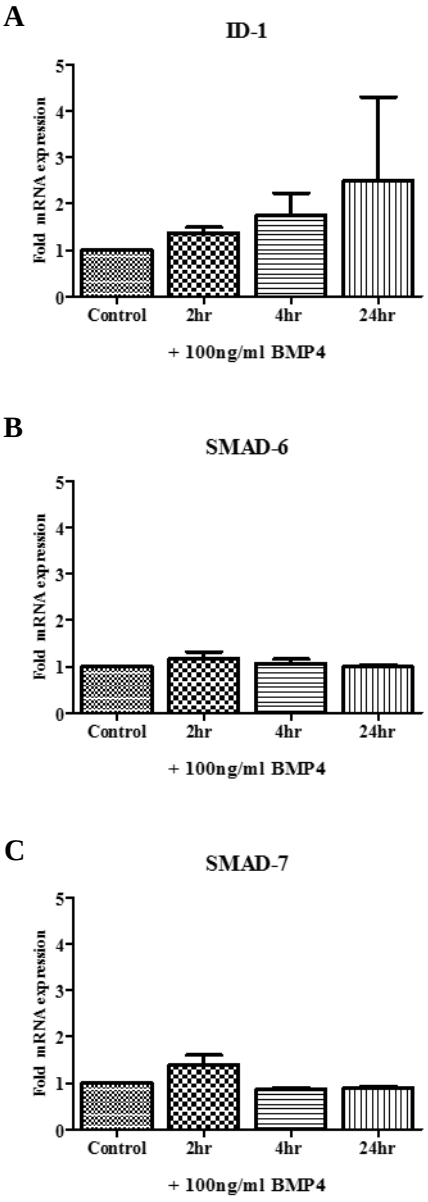

Figure 3.0.9 mRNA expression of ID-1, SMAD-6 and SMAD-7 following BMP-4 stimulation in DLKP-I cells

Representative graphs of quantified ID-1, SMAD-6 and SMAD-7 mRNA expression in DLKP-I cells following 2 hr, 4 hr, 24 hr treatment with 100 ng/ml BMP-4. (A) ID-1 mRNA expression increased in a time dependent manner following BMP-4 stimulation (B)(C) No change in SMAD-6 or SMAD-7 expression was evident following statistical analysis. n=3

3.1.6 Morphological changes in DLKP-SQ following BMP-4 and gremlin stimulation

Given the previous results that demonstrated DLKP-SQ cells are responsive to BMP-4 stimulation, we wanted to determine if BMP-4 induced EMT-mediated phenotypic switching in this squamous, epithelial-like population. Changes in morphology were assessed over 5 days (day 1, day 3 and day5) following stimulation with 100 ng/ml BMP-4 or 3 ng/ml gremlin. The cells were grown in 0.25% serum-containing medium as serum-free medium was suboptimal for growing DLKP clones (Mcbride et al. 1998).

DLKP-SQ treated with 100 ng/ml BMP-4 adopted a mesenchymal phenotype after one day in culture. The treated cells displayed reduced cell-cell contact compared to control cells and neurite-like extended cytoplasmic processes began to form, as highlighted by the white arrow in Figure 3.0.10 A. This mesenchymal transition was maintained to day 5 post-stimulation. BMP-4 has a half-life of approximately 48-72 hr suggesting autocrine BMP-4 activity may be present at day 5. The DLKP-SQ cells adopted a mesenchymal-like phenotype by day 5. Untreated DLKP-SQ growing in 0.25% medium grew in tightly packed colonies with characteristic "cobblestones" formations and cell-cell contact. No evidence of EMT was detected in the untreated cell populations at day 1, day 3 and day 5 (Figure 3.0.10).

DLKP-SQ cells treated with gremlin displayed similar morphology to untreated cells (Figure 3.0.10 B). Tightly packed "cobblestone"-like colonies grew in both treated and untreated cell populations. No apparent loss of cell contact was evident in gremlin-treated cells and no EMT was present.

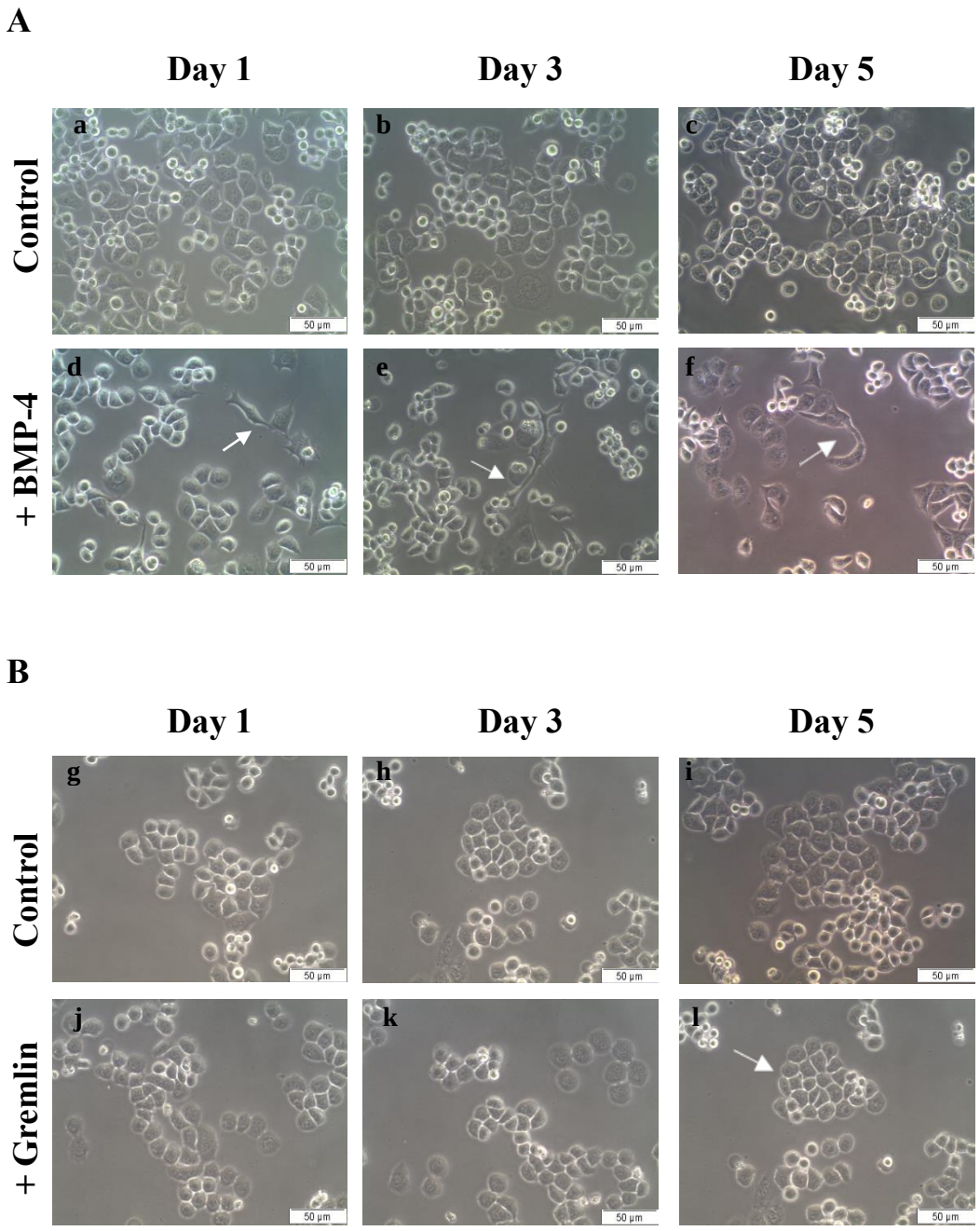

Figure 3.0.10 BMP-4 and gremlin treatment induced morphological changes in DLKP-SQ cells

Representative micrographs of DLKP-SQ at day 1, day 3 and day 5 in 0.25% serum containing medium with 100ng/ml BMP-4 and 3ng/ml gremlin. (A) Untreated cells were squamous with cobblestone-like morphology (a-c). BMP-4 treatment at day 1, day 3 and day 5 induced a mesenchymal-like cell phenotype and cytoplasmic extensions in DLKP-SQ cells (d-f) as indicated by the white arrows. (B) Untreated DLKP-SQ cells were squamous with distinct cell boundaries (g-i). Gremlin treatment at day 1, day 3 and day 5 maintained the squamous-like phenotype and prevented the formation of any mesenchymal extensions as seen following BMP-4 treatment (j-l). All scales bars represent 50uM, n=3

3.1.7 Morphological changes in DLKP-M following BMP-4 and gremlin stimulation

Previous results here demonstrated that DLKP-M cells are responsive to BMP-4 induced SMAD signalling and downstream target activation. To assess the role of BMP-4 in EMT-mediated phenotypic switching, changes in DLKP-M morphology were assessed over 5 days (day 1, day 3 and day5) following treatment with 100 ng/ml BMP-4 or 3 ng/ml gremlin. The cells were grown in 0.25% serum-containing medium as serum-free medium had previously been deemed suboptimal for growing DLKP clones (Mcbride et al. 1998).

Untreated DLKP-M cells grew as large, mesenchymal-like cells with extended neurite-like processes in reduced serum conditions. Following BMP-4 simulation a striking change in cell morphology was detected. DLKP-M cells began to join together and lose their individual cell morphology by day 1. On day 3, large colonies of DLKP-M cells had formed with bright, distinct outer boundaries. The individual cell membranes were no longer distinguishable and the colony appeared as one mass of cells. On day 5, the colonies of DLKP-M had undergone extensive morphological changes and the bulbous structure indicated that cell piling and aggregation had taken place. A distinct cell boundary was evident around the colony (Figure 3.0.11 A).

Morphological changes in DLKP-M cells following treatment with 3 ng/ml gremlin for 1, 3 and 5 days were examined by brightfield microscopy. An increase in cell contact between gremlin treated DLKP-M cells was detected at day 5 and smaller, tightly packed colonies emerged (Figure 3.0.11 B).

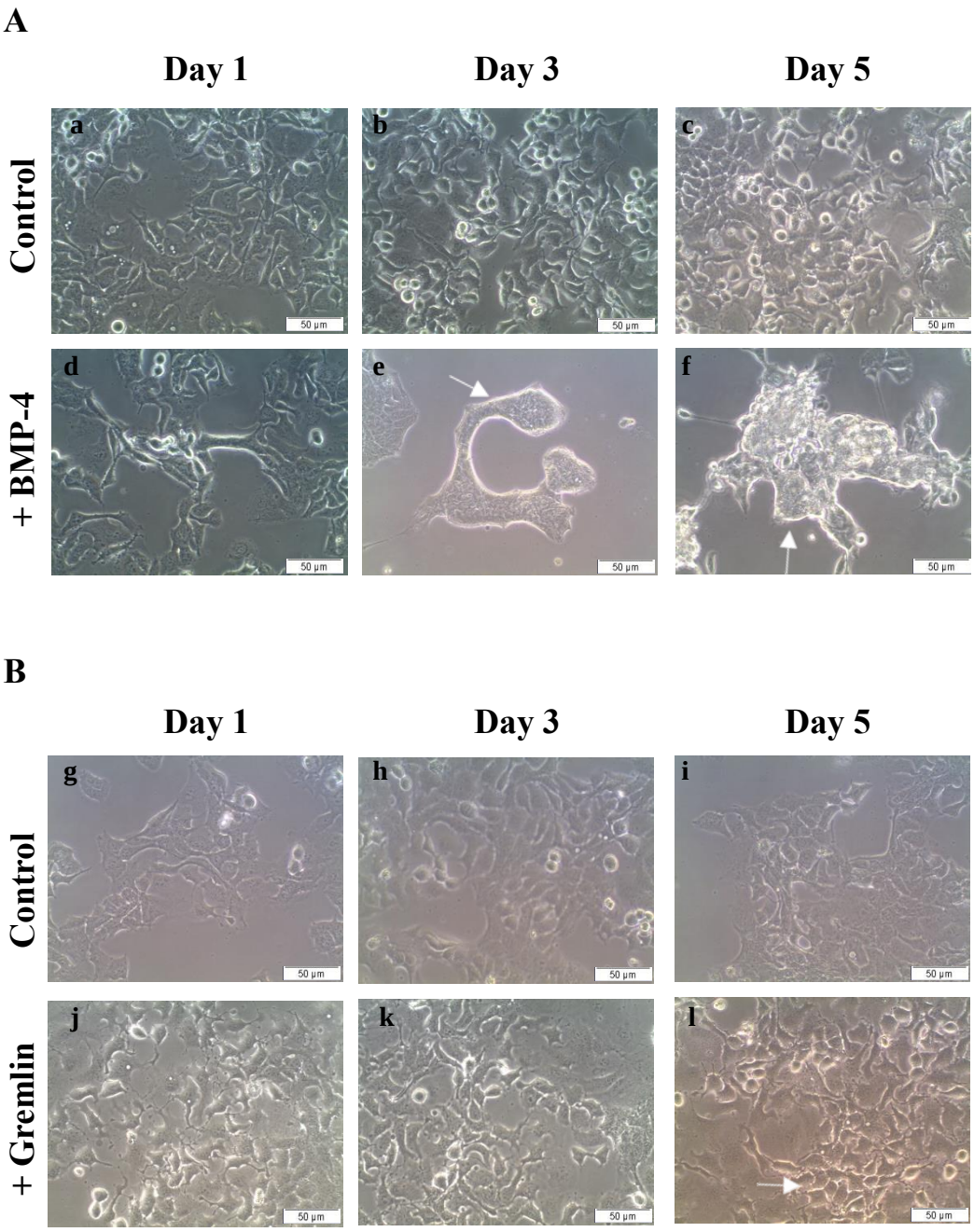

Figure 3.0.11 BMP-4 and gremlin treatment induced morphological changes in DLKP-M cells

Representative micrographs of DLKP-M at day 1, day 3 and day 5 in 0.25% serum containing medium with 100ng/ml BMP-4 and 3ng/ml gremlin. (A) Untreated cells had a mesenchymal-like phenotype with extended processes (a-c). BMP-4 treatment caused the cells to form colonies with distinct outer boundaries. By day 5, a mass had formed with a bright outer boundary (d-f). (B) Untreated DLKP-M cells were mesenchymal with extended neurite-like processes (g-i). DLKP-M cells following gremlin treatment for 1,3 and 5 days become more isolated from the surrounding cells with shorter cell processes (j-l). All scales bars represent 50uM, n=3

3.1.8 Morphological changes in DLKP-I following BMP-4 and gremlin stimulation

Previous results presented here established that DLKP-I cells are responsive to BMP-4 induced SMAD signalling. To assess the role of BMP-4 in EMT-mediated phenotypic switching, changes in DLKP-I morphology were assessed over 5 days (day 1, day 3 and day5) following treatment with 100 ng/ml BMP-4 or 3 ng/ml Gremlin. The cells were grown in 0.25% serum-containing medium as serum-free medium was deemed suboptimal for growing DLKP clones (Mcbride et al. 1998).

DLKP-I cells grew in small tightly packed colonies that displayed indistinct boundaries between individual cells but a bright, well-defined border between colonies. Cells treated with BMP-4 formed larger colonies with defined boundaries. The cells resembled DLKP-M cells treated with BMP-4 (Figure 3.0.12 A).

Growing DLKP-I cells in the presence of 3 ng/ml Gremlin for up to five days induced a significant change in morphology. DLKP-I displayed increased cell-cell contact and formed small, tightly packed colonies that resemble the “cobblestone” morphology of DLKP-SQ cells (Figure 3.0.12 B).

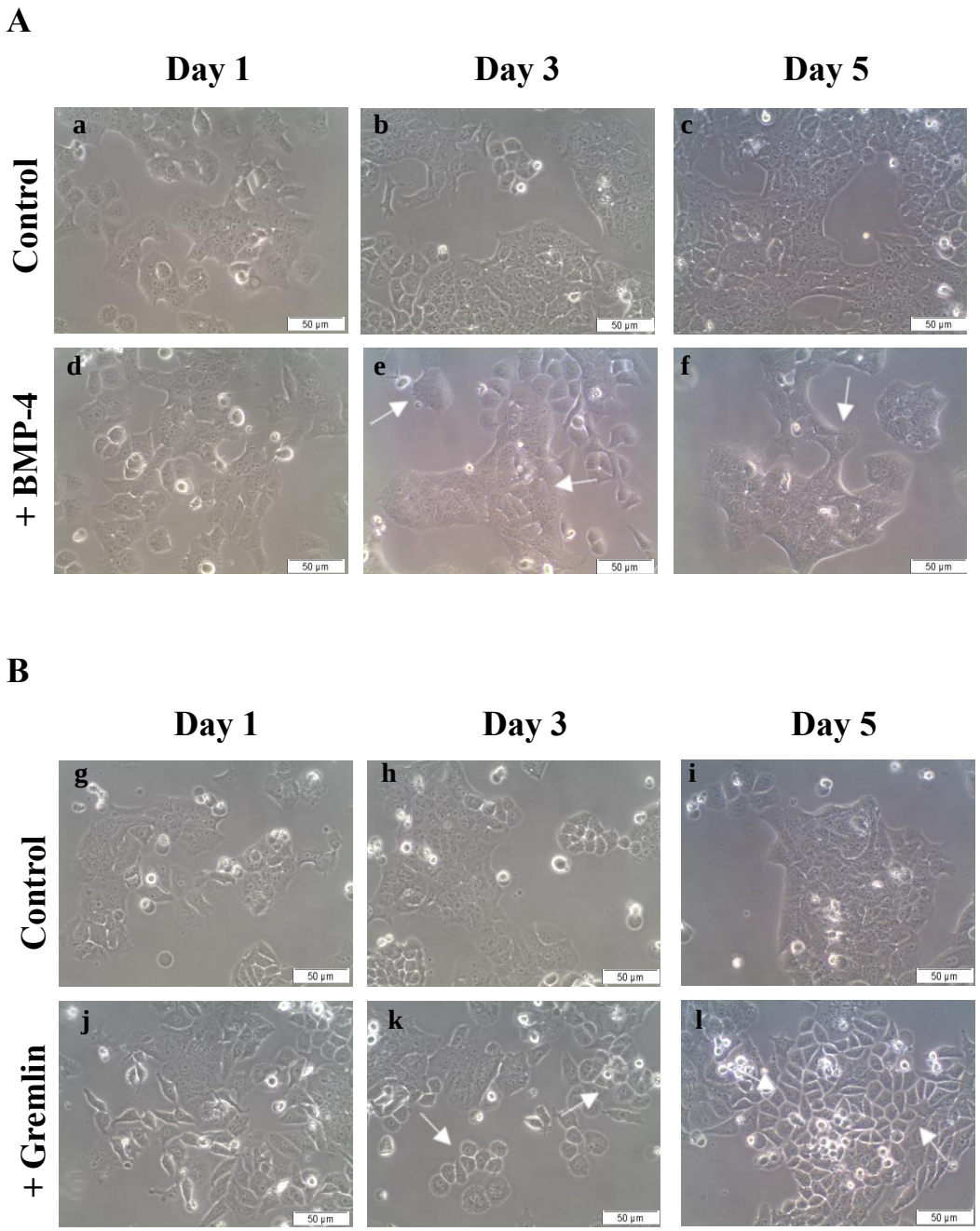

Figure 3.0.12 BMP-4 and gremlin treatment induced morphological changes in DLKP-I cells

Representative micrographs of DLKP-I at day 1, day 3 and day 5 in 0.25% serum containing medium with 100ng/ml BMP-4 and 3ng/ml Gremlin. (A) Untreated DLKP-I cells grew in tightly packed colonies with indistinct cell boundaries between the cells. There is evidence of some DLKP-SQ and DLKP-M at the periphery of the colonies (a-c). BMP-4 treatment caused the cells to form more colonies (d-f). (B) Untreated DLKP-I cells grew in packed colonies with some conversion to DLKP-SQ and DLKP-M at the periphery of the colonies (g-i). DLKP-I cells following gremlin treatment for 1,3 and 5 days adopted DLKP-SQ phenotype and grew as tightly packed squamous-like colonies with distinct cell boundaries (j-l). All scales bars represent 50uM, n=3

3.1.9 Expression of EMT markers in DLKP-SQ following BMP-4 stimulation

Following the observation that BMP-4 treatment caused morphological changes in DLKP-SQ towards a more mesenchymal cell phenotype that resembled the DLKP-M clone, we investigated if the expression and localisation of EMT-related structural proteins were altered in this process. Immunofluorescence performed at day 1, day 3 and day 5 and targets included vimentin, α –smooth muscle actin (SMA), β-catenin, N-cadherin, E-cadherin and actin.

Untreated DLKP-SQ cells displayed weak cytoplasmic vimentin staining at day 1, 3 and 5 however, following BMP-4 stimulation, elevated vimentin protein expression was detected at all time points (Figure 3.0.13-15 a-d). Vimentin was localised at the extended processes of the DLKP-SQ cells treated with BMP-4 ligand. The increase in vimentin expression following BMP-4 treatment was examined by western blot. Increased vimentin expression was detected at all time points and significantly higher protein expression was confirmed at day 3 and day 5 by densitometry (Figure 3.0.16).

Weak cytoplasmic staining of α –SMA was detected in the DLKP-SQ untreated populations at all time points. Following BMP-4 stimulation, slight increases in α –SMA protein expression were detected by immunofluorescence (Figure 3.0.13-15 c-h).

No change in β-catenin, N-cadherin or E-cadherin was detected at any of the time points following BMP-4 stimulation (Figure 3.0.13-15 i-l, m-p, q-t). Weak cytoplasmic staining of the three epithelial-like cell markers was evident in both treated and untreated cell.

Localisation of the cytoskeletal marker actin was investigated by immunofluorescence. Evidence of peri-nuclear actin staining was detected in DLKP-SQ cells treated with BMP-4 at all time points compared to cytoplasmic staining in untreated cells (Figure 3.0.13-15 u-x).

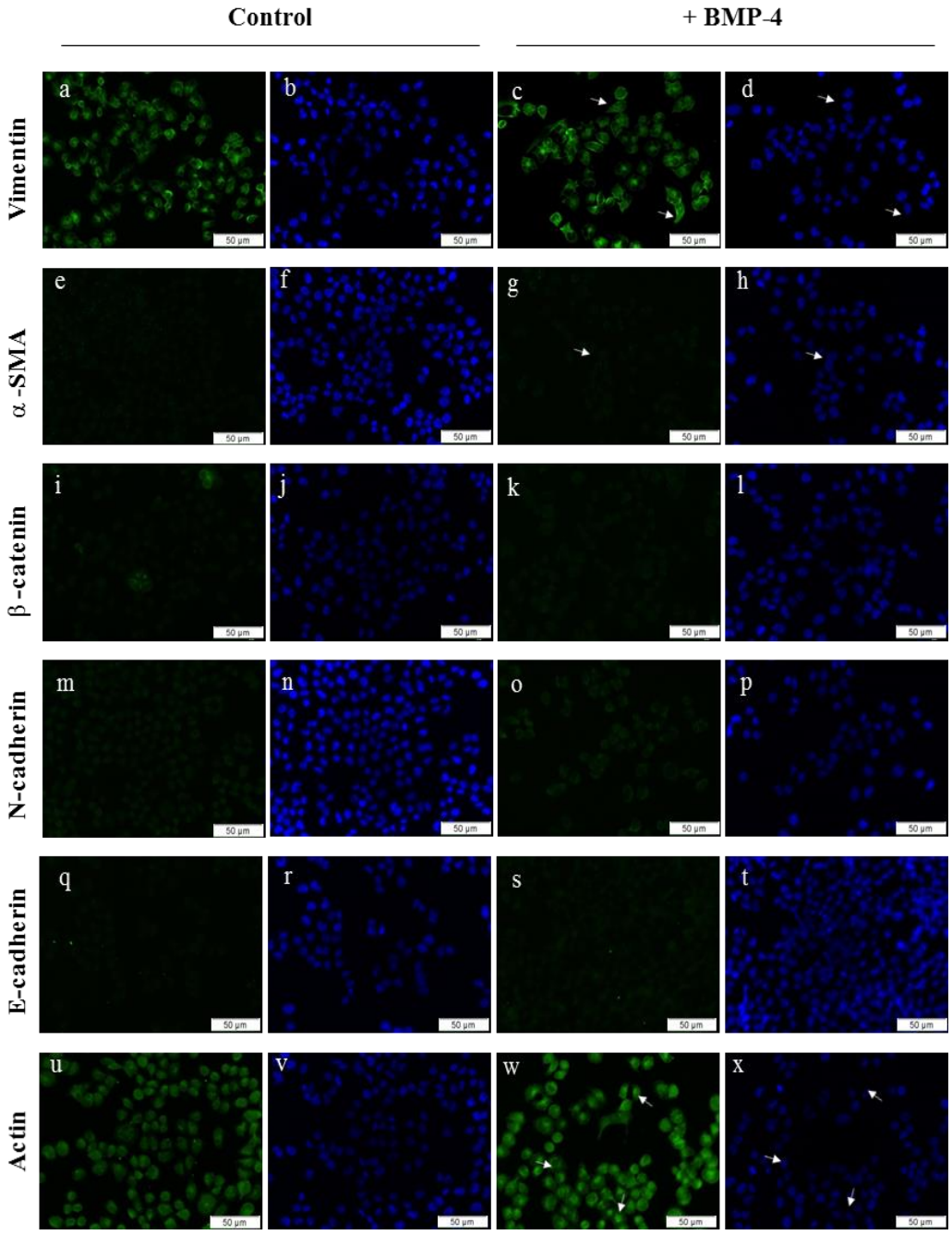

Figure 3.0.13 BMP-4 treatment induced changes in EMT marker localisation in DLKP-SQ cells at day 1

Representative micrographs of vimentin, α -SMA, β-catenin, N-cadherin, E-cadherin and actin localisation in DLKP-SQ at day 1 post stimulation with 100ng/ml BMP-4 in 0.25% serum containing medium. Elevated levels cytoplasmic vimentin and α –SMA were present following BMP-4 treatment. Peri-nuclear staining of actin was detected in treated cells. No change in β-catenin, N-cadherin and E-cadherin was detected following BMP-4 stimulation. Changes in expression are highlighted by the white arrows, scale bars represent 50uM, n=2.

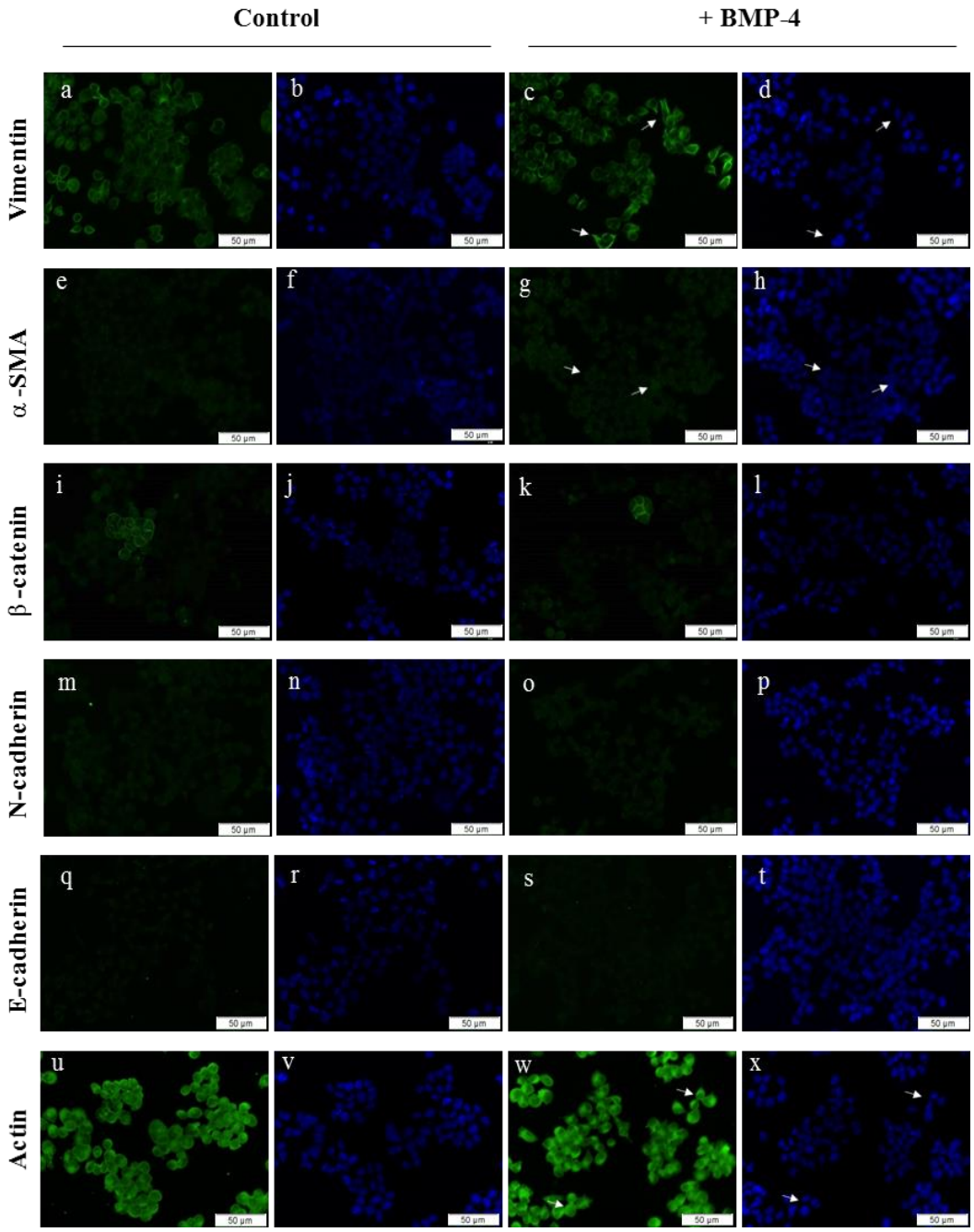

Figure 3.0.14 BMP-4 treatment induced changes in EMT marker localisation in DLKP-SQ cells at day 3

Representative micrographs of vimentin, α -SMA, β-catenin, N-cadherin, E-cadherin and actin localisation in DLKP-SQ at day 3 in 0.25% serum containing medium with 100ng/ml BMP-4. Elevated levels cytoplasmic vimentin and α –SMA were detected following BMP-4 treatment. Peri-nuclear staining of actin was present in treated cells. No change in β-catenin, N-cadherin and E-cadherin was detected following BMP-4 stimulation. Changes in expression are highlighted by the white arrows, scale bars represent 50uM, n=2

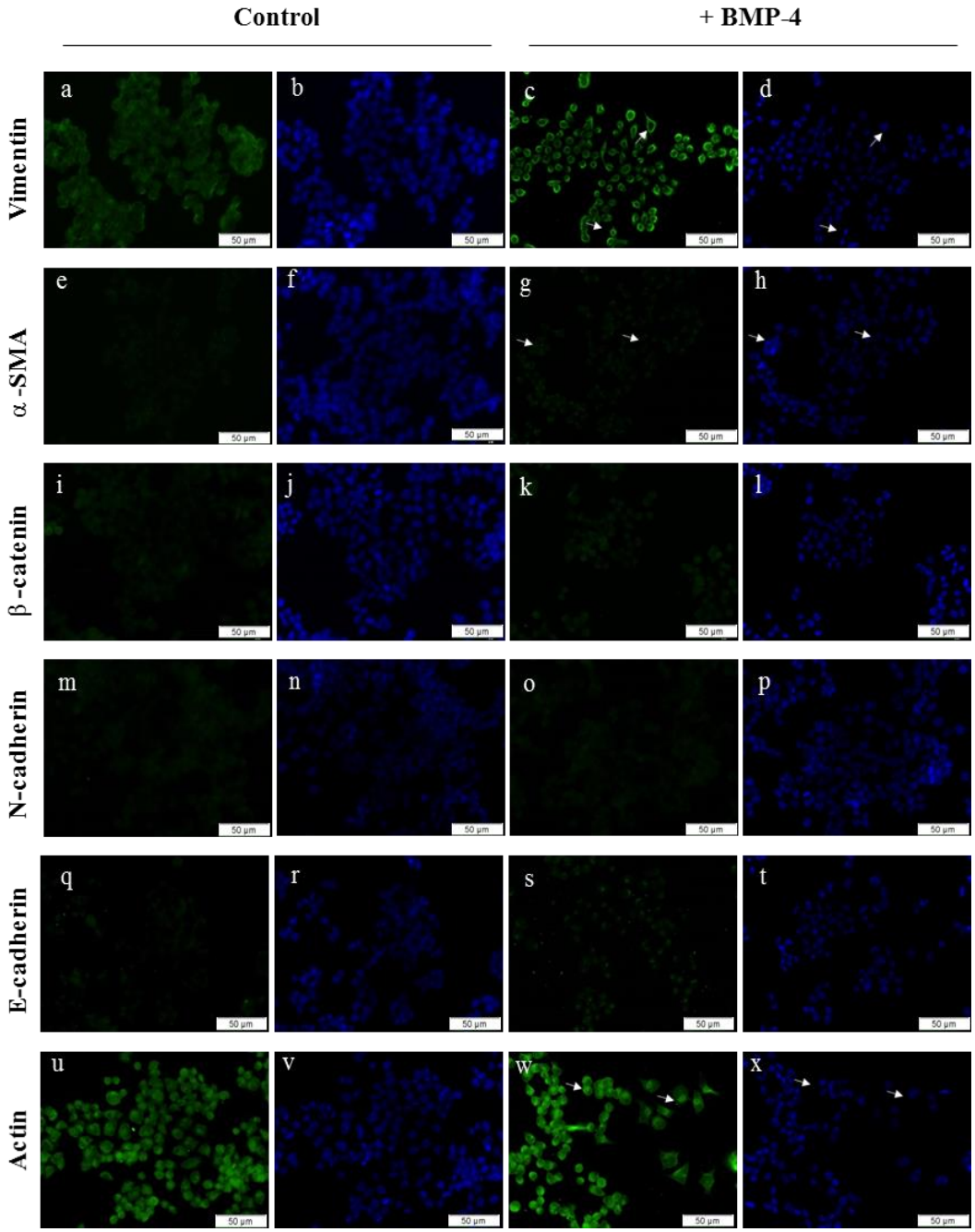

Figure 3.0.15 BMP-4 treatment induced changes in EMT marker localisation in DLKP-SQ cells at day 5

Representative micrographs of vimentin, α -SMA, β-catenin, N-cadherin, E-cadherin and actin localisation in DLKP-SQ at day 5 in 0.25% serum containing medium with 100ng/ml BMP-4. Elevated levels of cytoplasmic vimentin and α – SMA were detected following BMP-4 treatment. Peri-nuclear staining of actin was evident in treated cells. No change in β-catenin, N-cadherin and E-cadherin was seen following BMP-4 stimulation. Changes in expression are highlighted by the white arrows, scale bars represent 50uM, n=2.

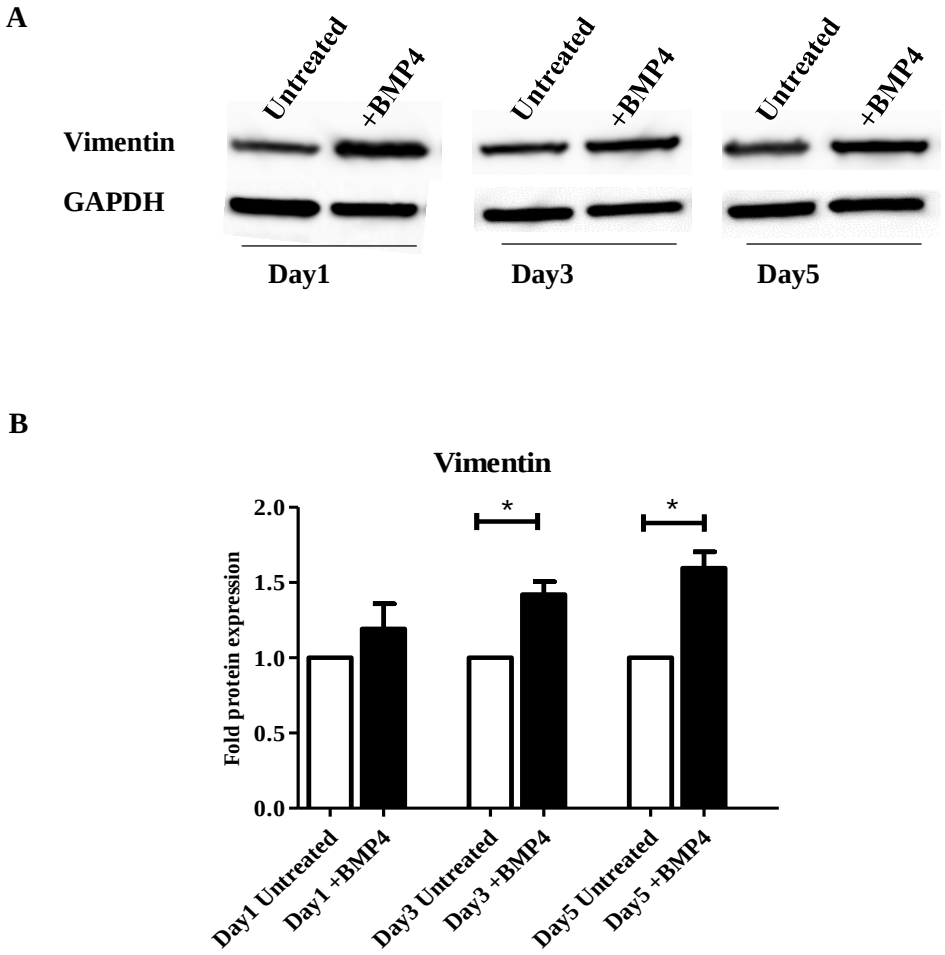

Figure 3.0.16 BMP-4 treatment induced elevated vimentin expression in DLKP-SQ

(A) Representative blots of vimentin at day1, day3 and day5 in DLKP-SQ cells treated with 100ng/ml BMP-4. (B) Densitometry revealed a statistically significant increase in expression at day 3 and day 5, * = $p<0.05$, n=3

3.1.10 Expression of EMT markers in DLKP-M following BMP-4 stimulation

Following the observation that BMP-4 treatment caused morphological changes in DLKP-M, we investigated if the expression and localisation of EMT-related structural proteins were altered. Immunofluorescence was performed at day 1, day 3 and day 5 and targets included vimentin, α-SMA, β-catenin, N-cadherin, E-cadherin and actin.

Elevated cytoplasmic vimentin expression was detected in DLKP-M cells following BMP-4 stimulation at day 1, day 3 and day 5, by immunofluorescence. Vimentin was present at the extended processes of the DLKP-M cells and at the boundary of the newly formed colonies (Figure 3.0.17 -19 a-d). The level of increased vimentin expression was determined by western blot and quantified by densitometry. Vimentin expression was significantly increased at day 5 (Figure 3.0.20).

Peri-nuclear and cytoplasmic staining of α-SMA was detected in DLKP-M cells at all time points (Figure 3.0.17-19 e-h). β-catenin was localised at the cell membrane as a "chickenwire"-like pattern in untreated and treated DLKP-M cells (Figure 3.0.17-19 i-l). Neither α-SMA or β-catenin localisation was altered following BMP-4 treatment. Western blotting revealed a significant increase in β-catenin protein expression in DLKP-M cells stimulated with BMP-4 at day 3 and day 5 (Figure 3.0.21).

N-cadherin was localised at the cell membrane of DLKP-M cells (Figure 3.0.17 m-p). Following BMP-4 treatment, no change in N-cadherin localisation was detected. A significant increase in N-cadherin expression at day 3 was determined by western blot and densitometry (Figure 3.0.22).

Weak cytoplasmic expression of E-cadherin was detected in untreated DLKP-M cells. No change in E-cadherin localisation or expression occurred in DLKP-M cells following BMP-4 treatment (Figure 3.0.17-19 q-t).

Finally, actin localisation was investigated by immunofluorescence. Cytoplasmic and peri-nuclear actin expression was present in untreated and treated DLKP-M cells at day 1, day3 and day 5 (Figure 3.0.17 u-v).

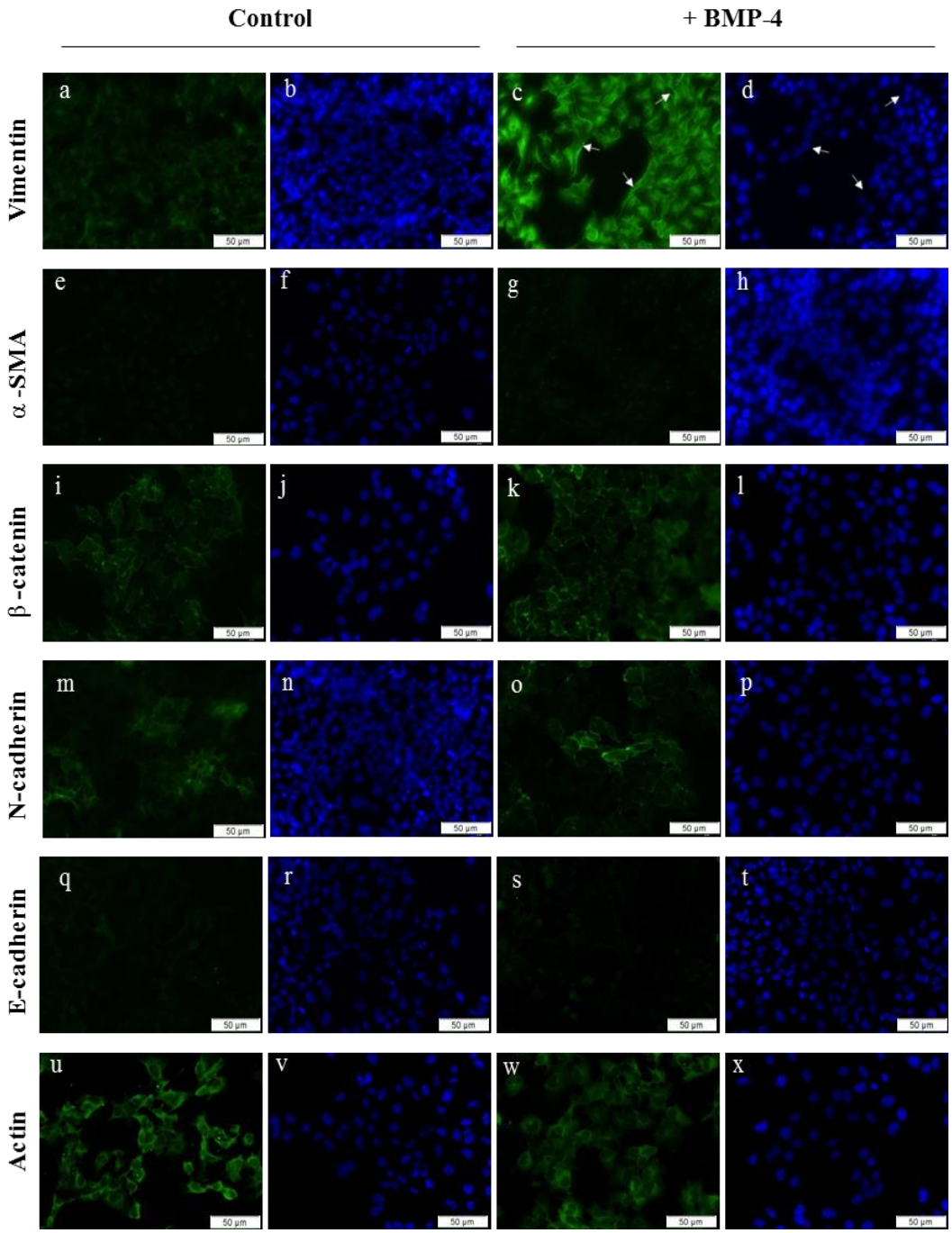

Figure 3.0.17 BMP-4 treatment induced changes in EMT marker localisation in DLKP-M cells at day 1

Representative micrographs of vimentin, α -SMA, β-catenin, N-cadherin, E-cadherin and actin localisation in DLKP-M at day 1 in 0.25% serum containing medium with 100ng/ml BMP-4. Increased expression of vimentin, α -SMA, β-catenin, N-cadherin was evident following BMP-4 treatment. Elevated peri-nuclear actin staining was detected in treated cells. No change in E-cadherin staining occurred. White arrows indicate changes in protein localisation, scale bars represent 50uM, n=2.

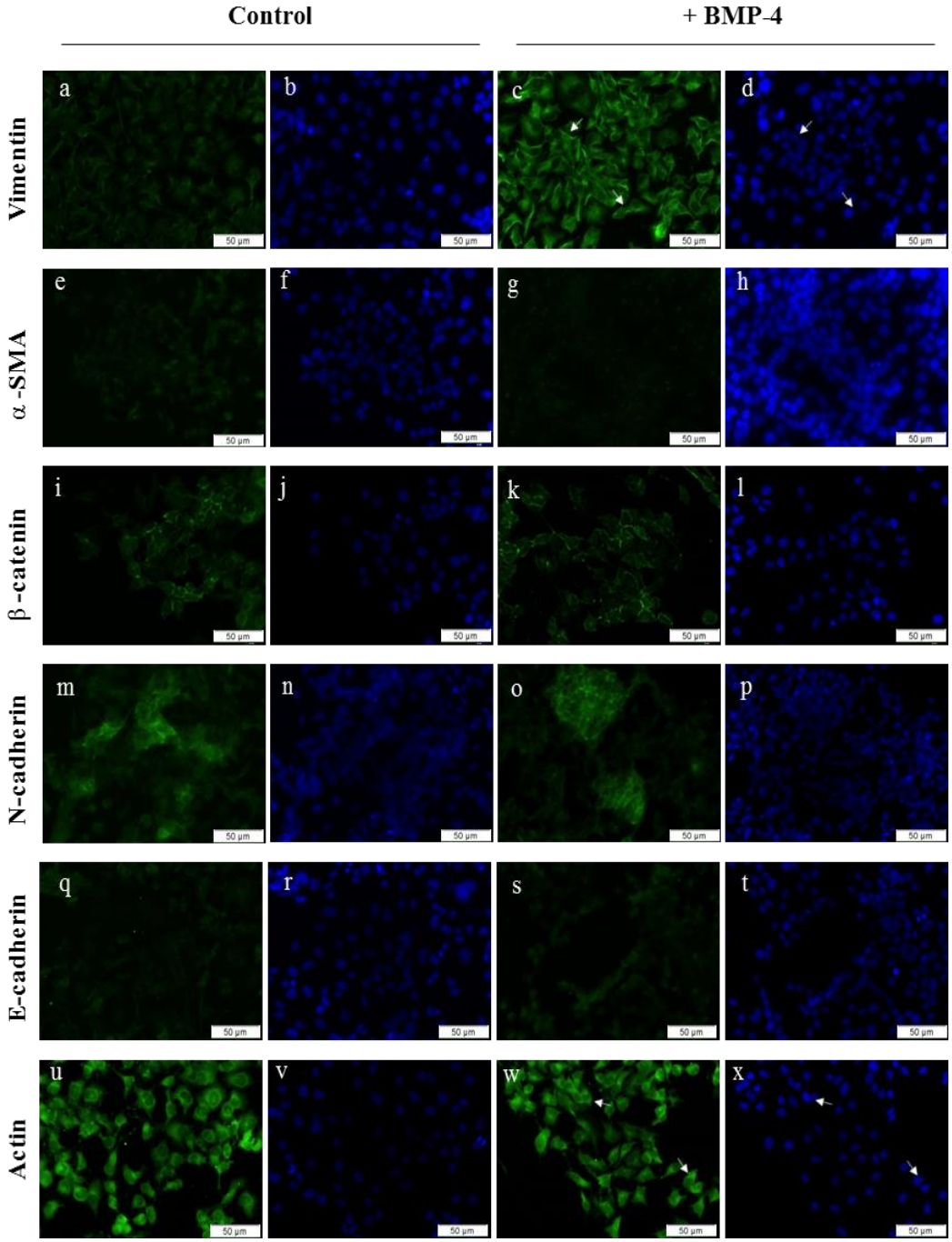

Figure 3.0.18 BMP-4 treatment induced changes in EMT marker localisation in DLKP-M cells at day 3

Representative micrographs of vimentin, α -SMA, β-catenin, N-cadherin, E-cadherin and actin localisation in DLKP-M at day 3 in 0.25% serum containing medium with 100ng/ml BMP-4. Increased expression of vimentin, α -SMA, β-catenin, N-cadherin was evident following BMP-4 treatment. Elevated peri-nuclear actin staining was present in treated cells. No change in E-cadherin staining occurred. White arrows indicate changes in protein localisation, scale bars represent 50uM, n=2.

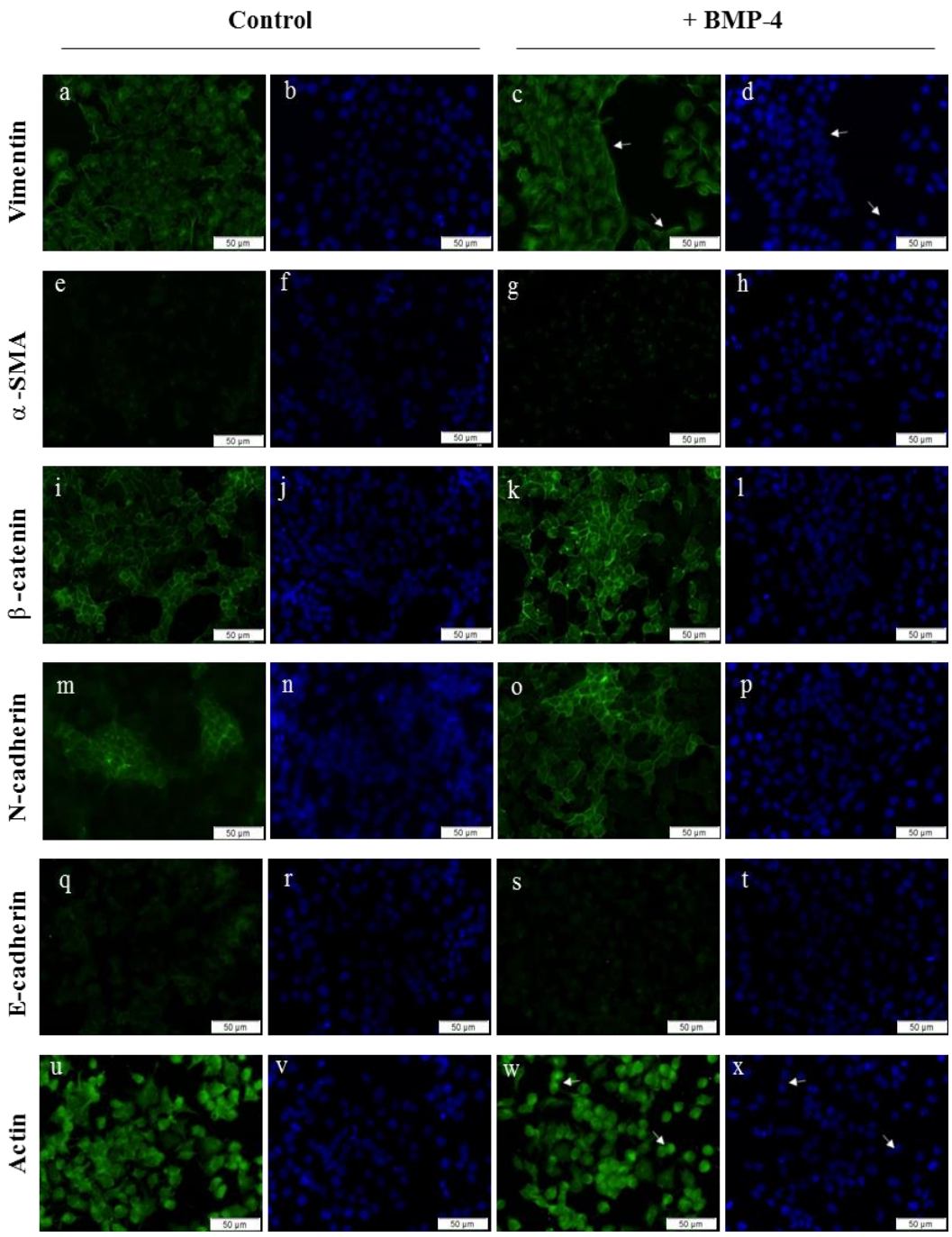

Figure 3.0.19 BMP-4 treatment induced changes in EMT marker localisation in DLKP-M cells at day 5

Representative micrographs of vimentin, α -SMA, β-catenin, N-cadherin, E-cadherin and actin localisation in DLKP-M at day 5 in 0.25% serum containing medium with 100ng/ml BMP-4. Increased expression of vimentin, α -SMA, β-catenin, N-cadherin was detected following BMP-4 treatment. Elevated peri-nuclear actin staining was present in treated cells. No change in E-cadherin staining occurred. White arrows indicate changes in protein localisation, scale bars represent 50uM, n=2.

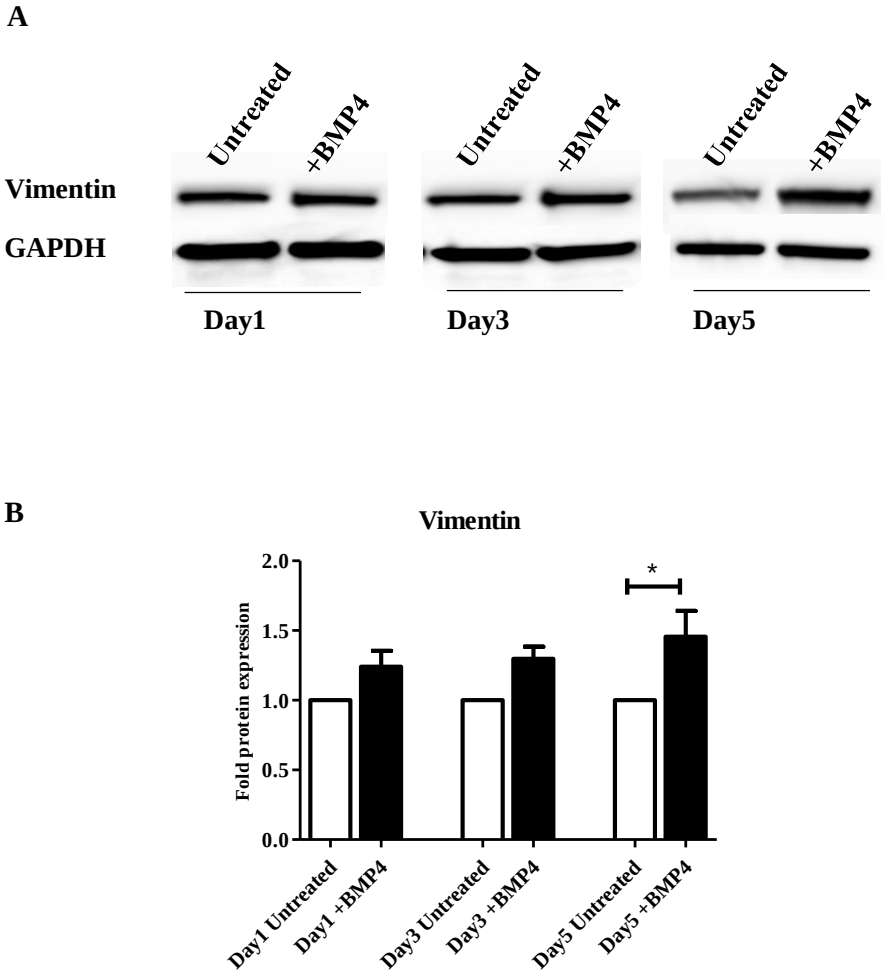

Figure 3.0.20 BMP-4 treatment induced elevated vimentin expression in DLKP-M

A) Representative blots of vimentin at day1, day3 and day5 in DLKP-M cells treated with 100ng/ml BMP-4. (B) Densitometry revealed a statistically significant increase in expression at day 5, * = $p<0.05$, n=3

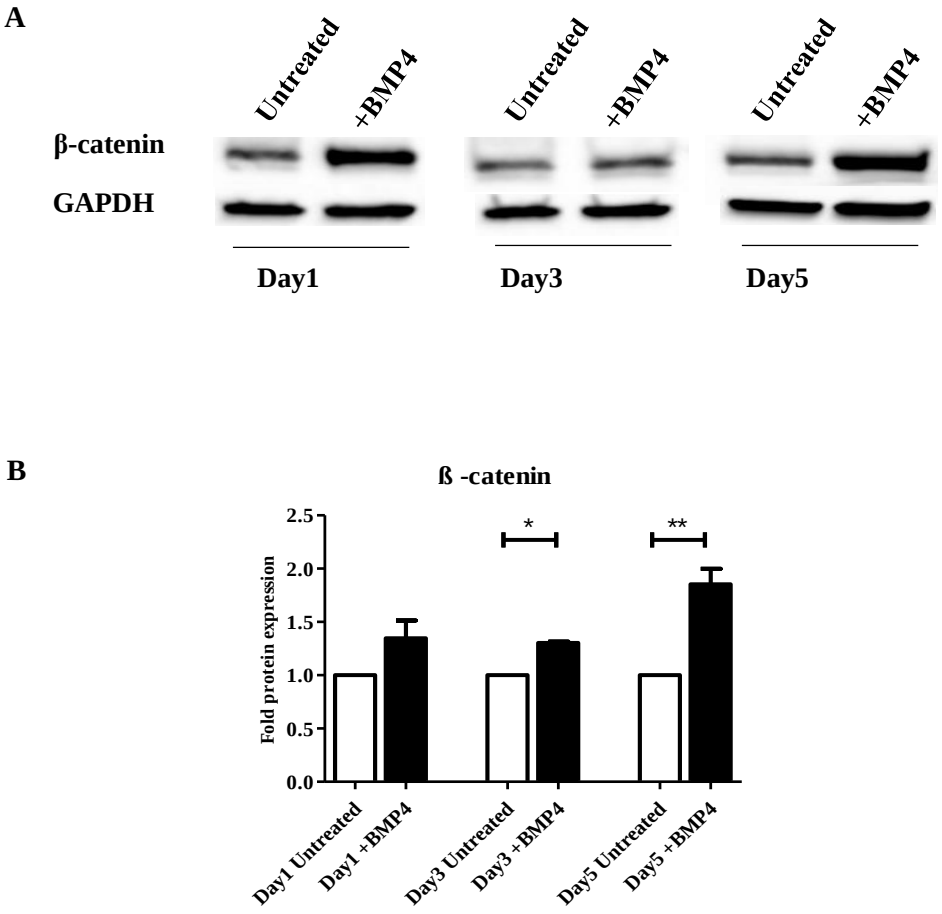

Figure 3.0.21 BMP-4 treatment induced elevated β -catenin expression in DLKP-M cells

(A) Representative blots of β-catenin at day1, day3 and day5 in DLKP-M cells treated with 100ng/ml BMP-4. Elevated protein expression was detected (B) Densitometry a revealed a statistically significant increase in protein expression at day 3 and day 5, * = $p<0.05$, n=3

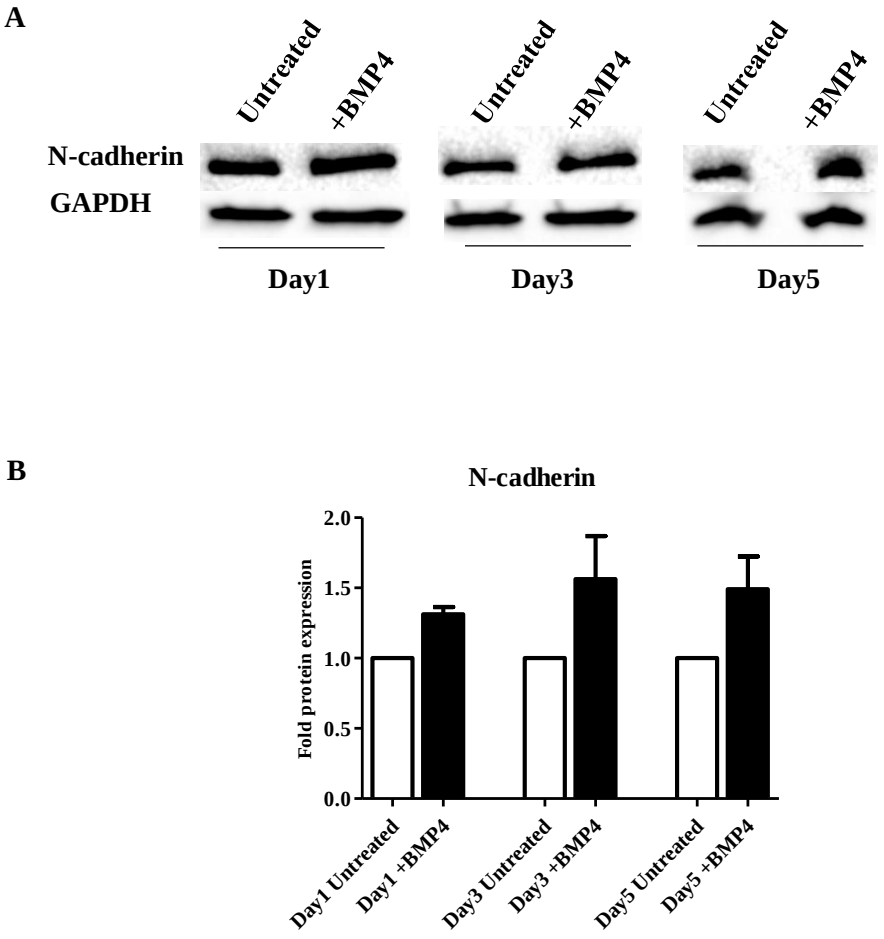

Figure 3.0.22 BMP-4 treatment induced elevated N-cadherin expression in DLKP-M cells

(A) Representative blots of N-cadherin at day1, day3 and day5 in DLKP-M cells treated with 100ng/ml BMP-4. Elevated protein expression was seen (B) Densitometry revealed a significant increase N-cadherin expression at day 3. *=$p<0.05$, n=3

3.1.11 Expression of EMT markers in DLKP-I following BMP-4 stimulation

Although BMP-4 treatment of DLKP-I cells did not induce extensive morphological changes compared to gremlin treatment, we wanted to investigate if the expression and localisation of EMT-related structural proteins were altered in response to the treatment. Immunofluorescence was performed at day 1, day 3 and day 5 and targets included vimentin, α-SMA, β-catenin, N-cadherin, E-cadherin and actin.

Vimentin was localised at the extensions of the membrane and along the border of the DLKP-I colonies. Increased vimentin expression was evident in immunofluorescence images at all time points (Figure 3.0.23-25 a-d). This observation was supported by western blotting and densitometry. A significant increase in vimentin protein expression in cells treated with BMP-4 was detected at day 5 (Figure 3.0.26).

Weak α-SMA expression was detected in the cytoplasm of untreated DLKP-I cells and there was evidence of peri-nuclear staining following BMP-4 treatment at day 1, day 3 and day 5 (Figure 3.0.23-25 e-f). β-catenin and N-cadherin were localised at the cell membrane of untreated DLKP-I cells (Figure 3.0.23-25 i, j, m, n). Following BMP-4 treatment, both β-catenin and N-cadherin remained localised at the cell membrane (Figure 3.0.23-25 k, l, o ,p). Western blotting revealed a significant increase in β-catenin protein expression following BMP-4 treatment at day 1 and day 5 (Figure 3.0.27). No difference in N-cadherin protein expression was revealed by western blot (Figure 3.0.28).

Similar to DLKP-SQ and DLKP-M cells no change in E-cadherin expression or localisation occurred in DLKP-I clones following BMP-4 treatment

Cytoplasmic actin staining was detected in untreated DLKP-I cells (Figure 3.0.23-25 u, v). There was evidence of nuclear translocation and peri-nuclear staining at day 1 and day 3 following BMP-4 treatment (Figure 3.0.23-25 w,x).

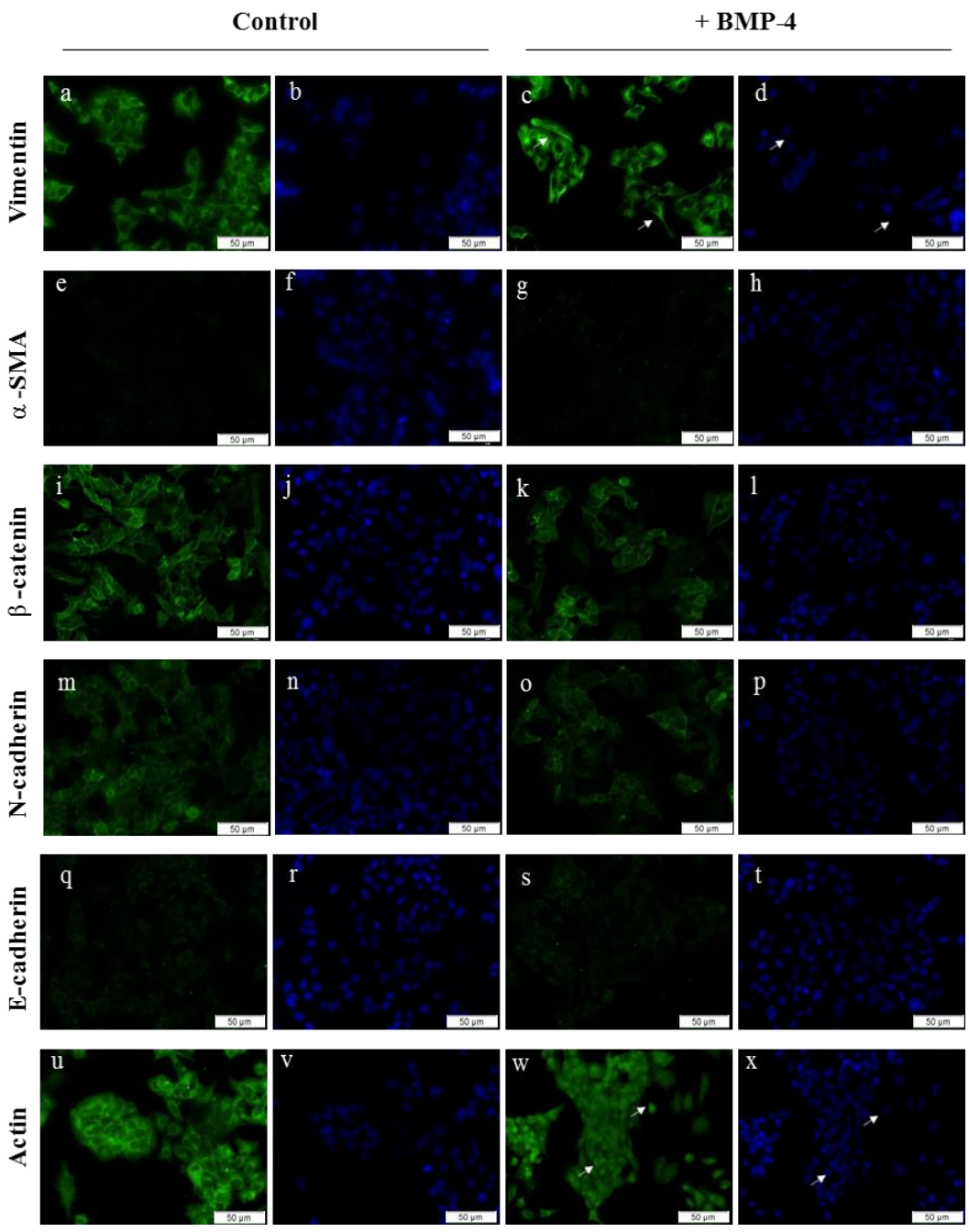

Figure 3.0.23 BMP-4 treatment induced changes in EMT marker localisation in DLKP-I cells at day 1

Representative micrographs of vimentin, α -SMA, β-catenin, N-cadherin, E-cadherin and actin localisation in DLKP-I at day 1 in 0.25% serum containing medium with 100ng/ml BMP-4.

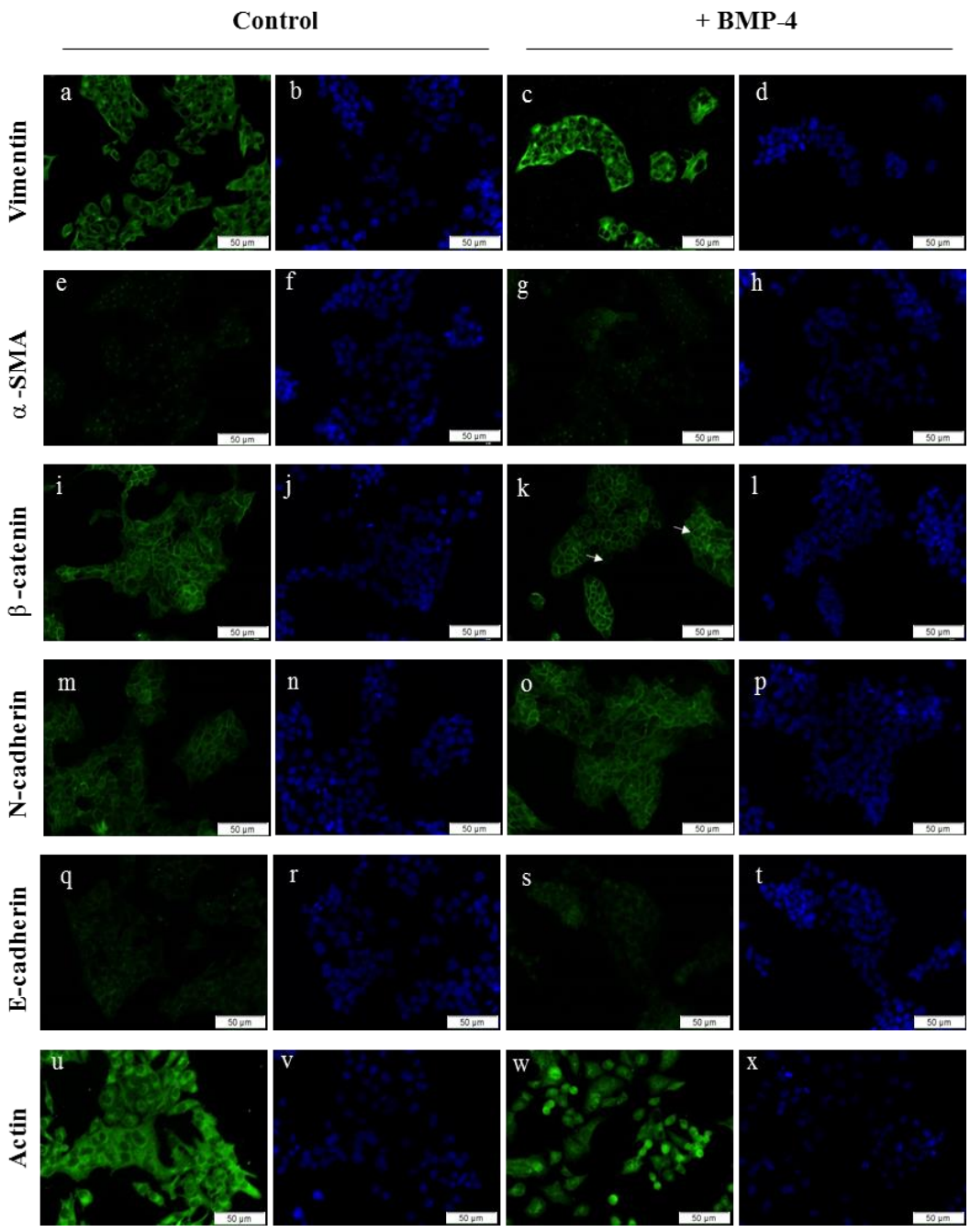

Figure 3.0.24 BMP-4 treatment induced changes in EMT marker localisation in DLKP-I cells at day 3

Representative micrographs of vimentin, α -SMA, β-catenin, N-cadherin, E-cadherin and actin localisation in DLKP-I at day 3 in 0.25% serum containing medium with 100ng/ml BMP-4.

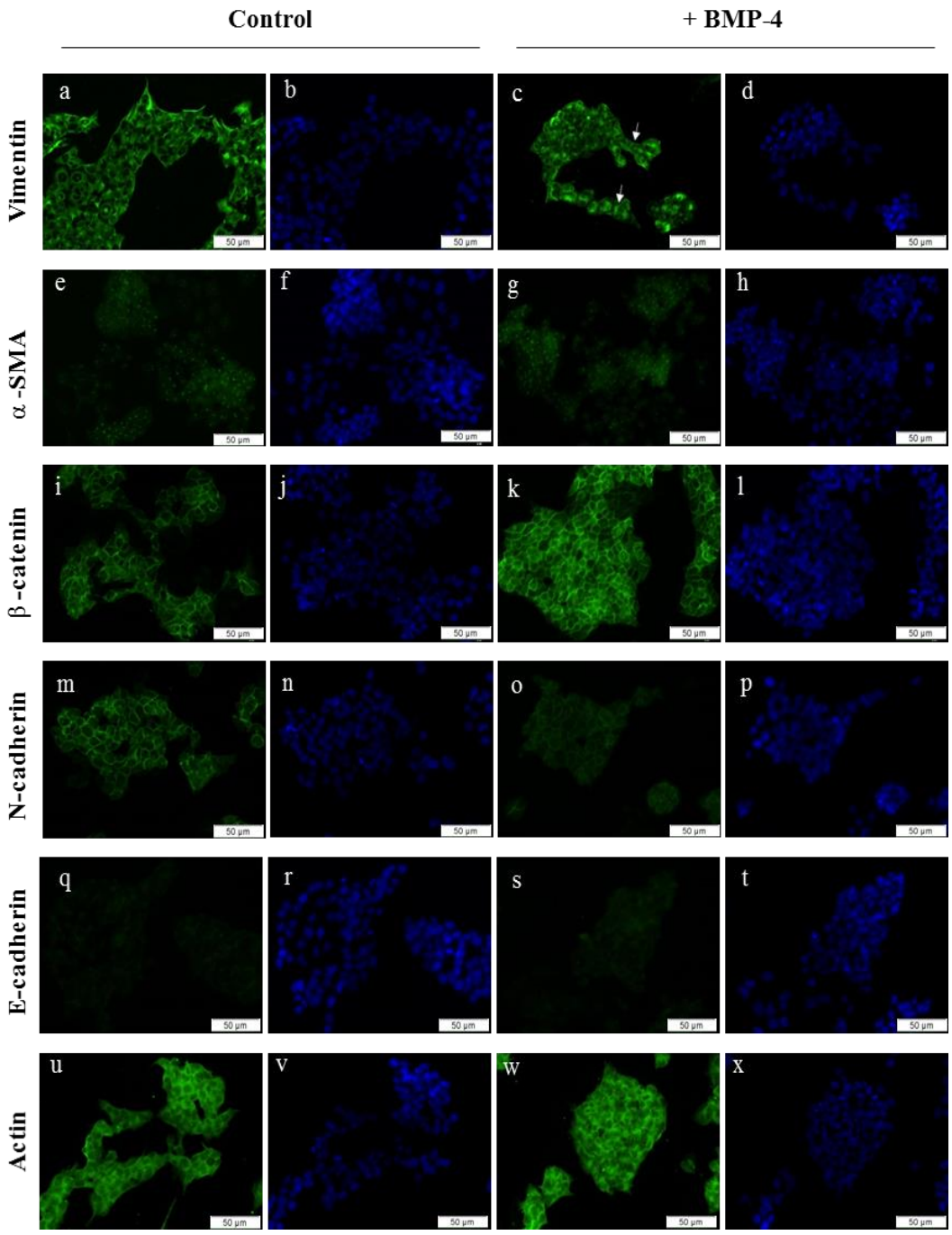

Figure 3.0.25 BMP-4 treatment induced changes in EMT marker localisation in DLKP-I cells at day 5

Representative micrographs of Vimentin, α -SMA, β-catenin, N-cadherin, E-cadherin and Actin localisation in DLKP-I at day 5 in 0.25% serum containing medium with 100ng/ml BMP-4.

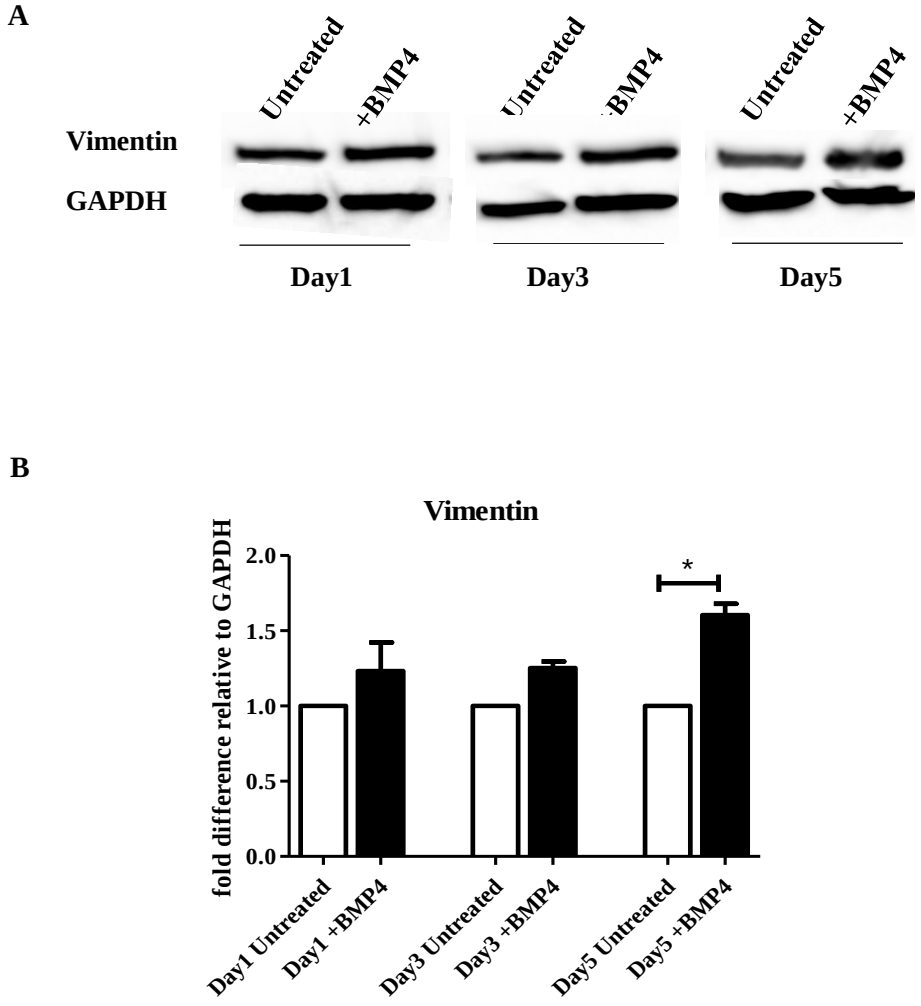

Figure 3.0.26 BMP-4 treatment induced increased vimentin expression in DLKP-I cells

(A) Representative blots of vimentin at day1, day3 and day5 in DLKP-I cells treated with 100ng/ml BMP-4. (B) Densitometry revealed a statistically significant increase in expression at day 5, * = $p<0.05$, n=3

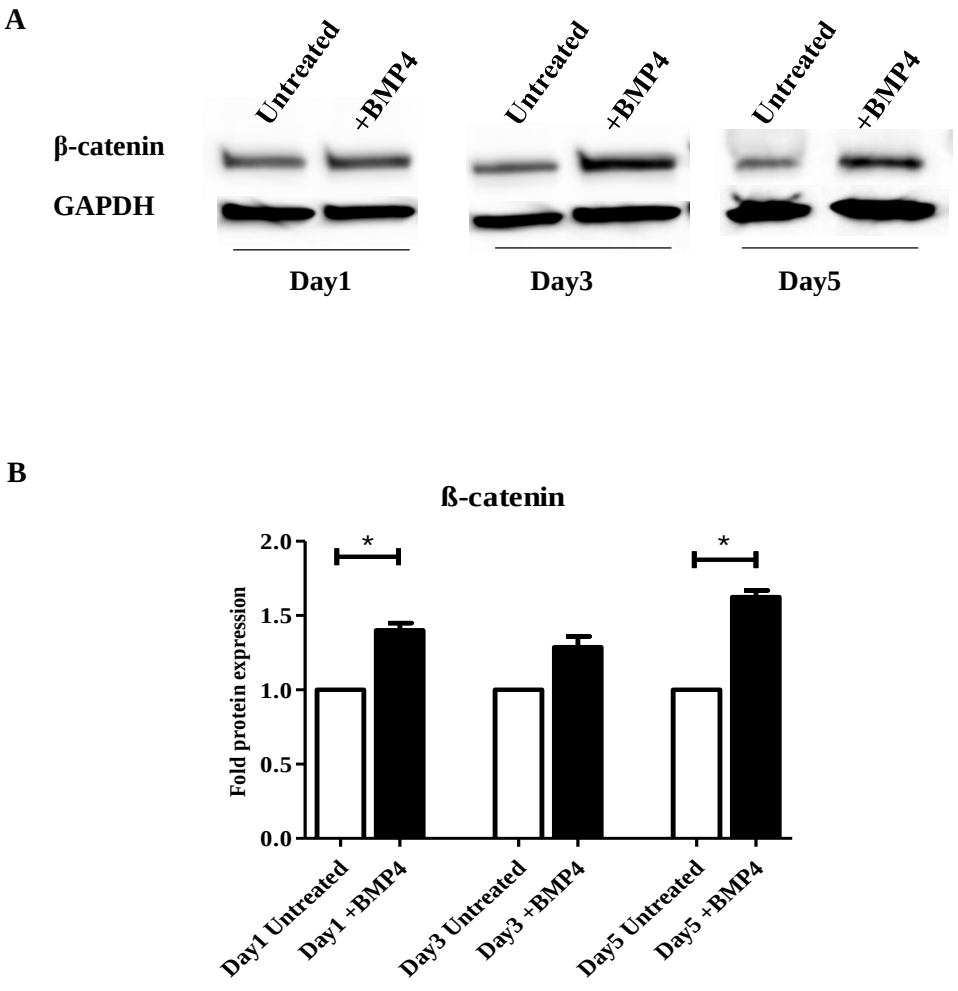

Figure 3.0.27 BMP-4 treatment induced an increase in *β* -catenin expression in DLKP-I cells

(A) Representative blots of β-catenin at day1, day3 and day5 in DLKP-I cells treated with 100ng/ml BMP-4. Elevated protein expression was seen (B) Densitometry revealed a statistically significant increase in expression at day 1 and day 5, * = $p<0.05$, n=3

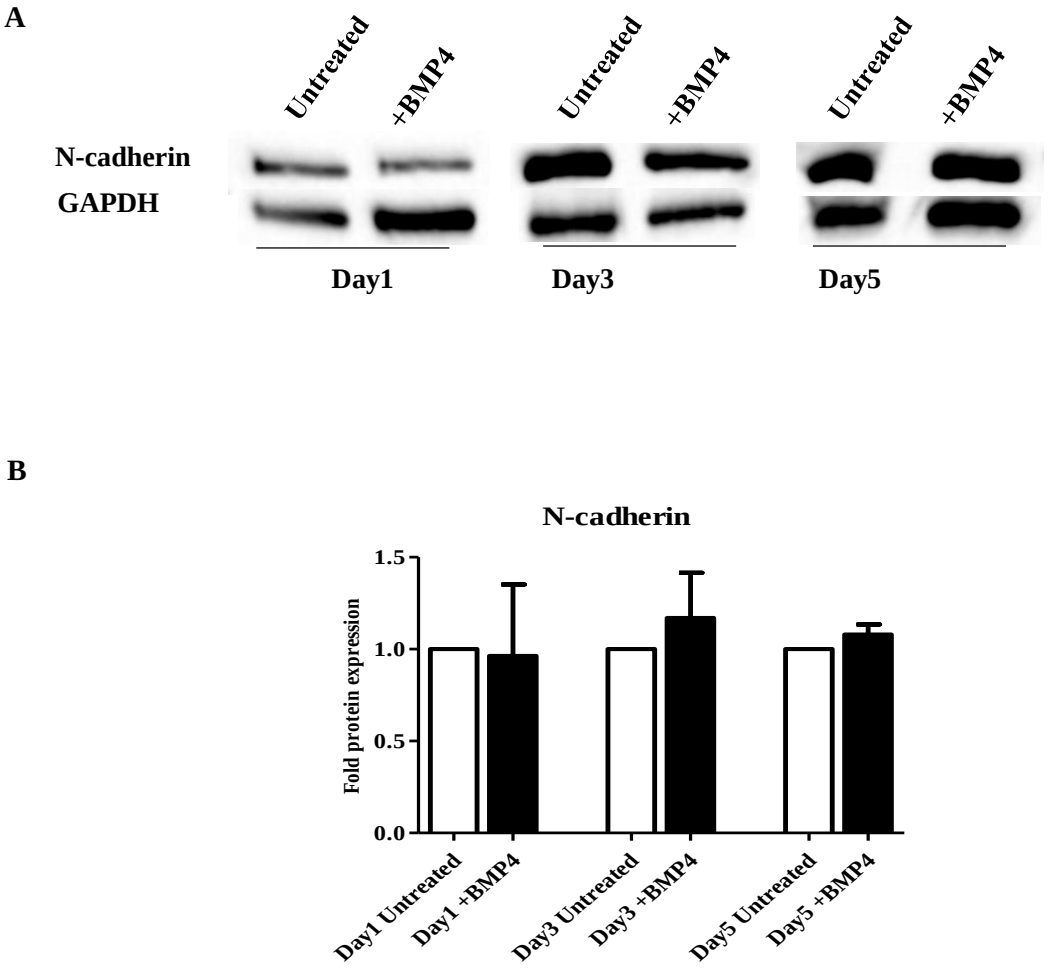

Figure 3.0.28 BMP-4 treatment did not induce an increase in N-cadherin expression in DLKP-I cells

(A) Representative blots of N-cadherin at day1, day3 and day5 in DLKP-I cells treated with 100ng/ml BMP-4. (B) Densitometry revealed no change in protein expression following treatment, * = $p<0.05$, n=3

3.1.12 Expression of EMT marker in DLKP-SQ, DLKP-M and DLKP-I following Gremlin stimulation

The results presented here have shown that BMP-4 can induce morphological changes and cause the upregulation of EMT markers in DLKP cell populations. Gremlin is also capable of inducing morphological changes in DLKP-M and DLKP-I populations. Next, we investigated the effect of gremlin stimulation on the expression of EMT-related structural proteins.

N-cadherin and vimentin expression were reduced in DLKP-M and DLKP-I following gremlin treatment. DLKP-SQ expressed low levels of β-catenin and did not express N-cadherin. No change in expression was detected in β-catenin or N-cadherin (Figure 3.0.29).

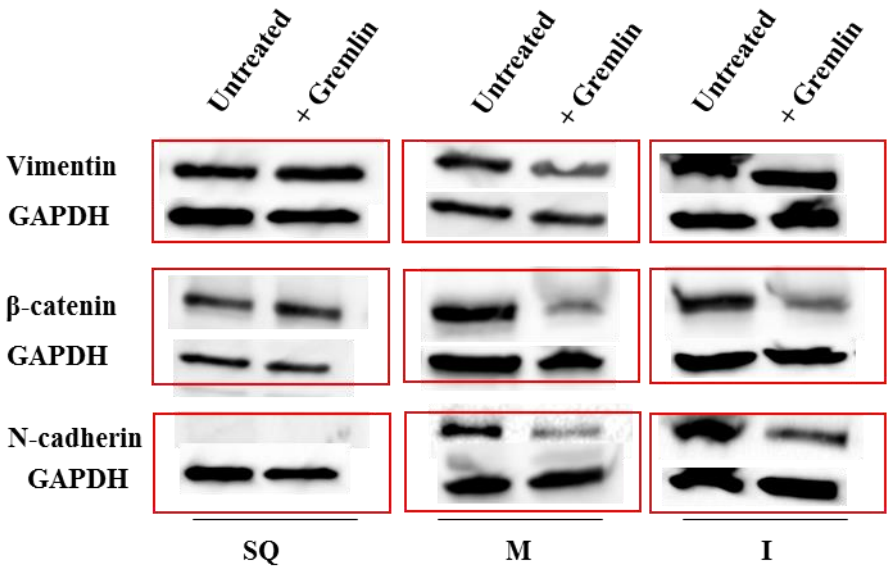

Figure 3.0.29 Gremlin treatment altered EMT-related structural protein expression in DLKP clones

Representative blots of vimentin, β-catenin and N-cadherin at day5 in DLKP-SQ, DLKP-M, DLKP-I cells treated with 3 ng/ml gremlin. Reduced β-catenin and N-cadherin expression was present in DLKP-M and DLKP-I cells following gremlin treatment. A reduction in vimentin expression was evident in DLKP-M cells. Red boxes indicate samples that were ran on the same gel. Each red box indicates a different gel therefore the expression of the EMT markers in SQ,M and I cannot be compared by density analysis. n=3.

3.2 Discussion

Our research group is interested in the mechanisms underlying the regulation of cell phenotypes in the airways. Phenotypic switching and trans-differentiation can be controlled by the EMT-MET process. EMT is classified into three main types in the body and result in very different biological consequences (Kalluri and Weinberg 2009). Our lab has previously demonstrated the relationship between EMT and the BMP pathway. In this study we investigated the role of the BMP signalling and type III EMT between heterogeneous clonal populations of the DLKP cell line. The results indicate that DLKP-SQ cell represent a more "normal" epithelial phenotype compared to mesenchymal-like DLKP-M cells. In addition, DLKP clonal populations were responsive to BMP-mediated signalling. BMP pathway activation induced EMT in this adult cancer model and abrogation of the BMP signalling pathway altered cell morphology, in a process resembling MET. Our results highlight the dynamic role of BMP signalling on the induction of phenotypic switching in this cell model.

We hypothesised that the DLKP-SQ clonal population resemble "normal" airway epithelial cells more closely than DLKP-M cells. In cultures of the parental cell line, spontaneous interconversion events occur between DLKP-SQ, DLKP-M and the intermediate DLKP-I clonal population. The cells are morphologically distinct and the changes between the small, cuboidal, tightly packed DLKP-SQ cells to the larger, extended mesenchymal-like DLKP-M cells appear to resemble a process morphologically similar to EMT (Mcbride et al. 1998). DLKP-I cells resemble a small stem cell-like colonies capable of interconverting to either DLKP-SQ or DLKP-M. Gene expression data showed that CRMP-1, α-integrin-V and scatter

factor expression were higher in DLKP-I and DLKP-M compared to DLKP-SQ cells. This highlighted again that DLKP-SQ were more associated to normal epithelial cells than the other two clones (Figure 3.0.3).

Furthermore, we examined the expression of tight junction proteins by western blotting. These proteins are involved in epithelial cell polarity, mediating the impermeable intercellular junctions between adjacent cells and ensuring that the integrity of the epithelial barrier is upheld (Acharya et al. 2004; Balda and Matter 2000; Hervé 2008; Tang and Brieher 2013). In addition, the loss of tight junction proteins is associated with increased cell invasiveness in cancer and the adoption of a more mesenchymal, migratory cell phenotype in breast cancer tumours (Costello et al. 2010; Ikenouchi et al. 2003). DLKP-SQ and DLKP-I expressed afadin, claudin-1 and ZO-1 whereas all three TJP were absent from DLKP-M clonal populations (Figure 3.0.2). The finding that CD2AP is present in DLKP-SQ, DLKP-M and DLKP-I clones highlighted that some maintenance of actin cytoskeletal interaction with cell adherens junctions is required in DLKP-M cells despite their evident loss of epithelial-related structural proteins. TJP could be downregulated in DLKP-M cells by the transcriptional co-repressor Snail which was show to bind directly to the promoter region of occuldin and claudin genes in epithelial cells, Eph4 and CSG1. Snail-induced downregulation of TJP caused the cells to adopt mesenchymal, mobile cell characteristics (Ikenouchi et al. 2003). In summary, these preliminary findings indicated that DLKP-SQ represent a more epithelial-like cell population compared to DLKP-M cells. In addition, DLKP-I cells may represent an EMP cell phenotype as they still possess epithelial-related tight junction proteins but also express mesenchymal-like markers.

We believe that BMP-2, -4 and -7 are key regulators of airway epithelial cell differentiation and phenotype in both health and disease. In this study, we investigated if DLKP clones are responsive to BMP-mediated signalling. BMP signal transduction occurs via phosphorylation of the R-SMAD complex at either SMAD-1, SMAD-5 or SMAD-8. This occurs following ligand binding and is the hallmark of active BMP signalling. R-SMADs and co-SMAD both contain a nuclear localisation signal (NLS) and a nuclear export signal (NES). These signals facilitate nucleocytoplasmic shuttling and allow SMAD interactions with DNA transcription factors in the nucleus to occur and the activation/repression of BMP specific genes to proceed (Zhan Xiao et al. 2003; Xiao et al. 2001). In experiments carried out by our collaborator in DCU, gene expression analysis revealed endogenous expression of the type I and type II BMP receptors in the DLKP clones. This indicated that the cells are responsive to BMP ligands. SMAD-1 and SMAD-5 were detected in the cytoplasm of untreated DLKP-SQ, -M and –I cells. In addition, nuclear localisation of pSMAD 1/5/8 occurred independent of SMAD-4 nuclear localisation in untreated DLKP-SQ, DLKP-M and DLKP-I cells. We speculate that nuclear translocation occurs via the NLS of the R-SMAD protein. This demonstrates that activated R-SMADs could play a role in regulating homeostatic gene expression. Following BMP-4 stimulation, elevated nuclear expression of pSMAD 1/5/8 and SMAD-4 was detected in the cells. We propose that the nuclear localisation of both of these signalling molecules in tandem in the DLKP cell lines maintains BMP pathway activation following BMP-4 treatment. Early studies have also highlighted this phenomenon in BMP signalling whereby nuclear translocation of activated R-SMADs does not require SMAD-4 in colon carcinoma cells, (Hoodless et al. 1999; Liu et al. 1997). Similar signalling events

occurs in human Beas-2b cells treated with BMP-2 and BMP-4 ligands (E. L Molloy, Shirley O'Dea lab).

iSMAD localisation was examined by immunofluorescence following 24 hr stimulation with BMP-4 in DLKP-SQ, DLKP-M and DLKP-I. In resting state cells, SMAD-6 was localised in the nuclei. Lower levels of SMAD-7 protein were found in the nuclei. While little is known about the NLS and NES of iSMADs this difference in protein localisation could be attributed to the altered rate of nuclear trafficking in the cells. Following BMP-4 stimulation, elevated iSMAD protein expression was present in the cytoplasm and nucleus of all three cell lines. The expression of SMAD-7 in the clones could indicate the presence of TGF- β signalling as SMAD-7 regulates both BMP and TGF signalling pathways.

The presence of nuclear iSMADs at 24 hrs post BMP-4 stimulation indicates sustained pathway regulation in these cells. This suggests the establishment of a negative feedback mechanism in the cells. While rt-PCR data demonstrated a time-dependent induction of ID-1 mRNA expression in DLKP cells, no significant difference in SMAD-6 or SMAD-7 expression was found following BMP-4 treatment. However, as described, immunofluorescence showed changes in protein localisation. This indicated that endogenous control of BMP signalling may be present in DLKP cells and that following BMP-4 treatment iSMADs alter their localisation to regulate the pathway.

In summary, the DLKP cell lines are responsive to BMP-4 mediated signalling and induce the nuclear translocation of p-SMAD 1/5/8 and SMAD-4 for the activation of BMP responsive genes. Our results indicate that endogenous BMP pathway regulation occurs in these cells and is mediated through iSMADs.

We hypothesised that by agonising and antagonising the BMP pathway we could induce EMT-mediated phenotypic switching between these clonal populations. EMT involves altered cell morphology, loss of cell polarity and upregulation of mesenchymal-associated proteins. Firstly, we hypothesised that DLKP-SQ cells would undergo EMT following BMP treatment and adopt a morphology similar to DLKP-M cells. Conversely, we hypothesised that DLKP-SQ cells treated with gremlin would remain unchanged. In these experiments, DLKP-SQ cells lost their cuboidal shape and no longer grew in tightly organised "cobblestone"- like colonies following BMP-4 stimulation. A ventral lateral polarity was established and the cell membrane became stretched with cytoplasmic extensions. The cells expressed an elevated level of vimentin protein which was localised at the newly formed extended mesenchymal processes. This cell phenotype resembled DLKP-M cells (Figure 3.0.10). Peri-nuclear staining of actin was also evident following BMP-4 treatment at day 1, day 3 and day 5. Both elevated vimentin expression and this actin staining pattern are associated with changes in cell architecture that occur during EMT (Gay et al. 2011). This indicated that BMP-4 stimulation induced EMT-like changes in DLKP-SQ cells.

Gremlin is a well-studied antagonist of the BMP pathway and binds to BMP ligands outside the cell to prevent receptor-mediated signal activation. No significant change in cell phenotype was detected following gremlin stimulation of DLKP-SQ cells for five days and no change in vimentin expression was evident by western blot. This indicated that DLKP-SQ cells may not produce endogenous BMP ligands (BMP-2, BMP-4 or BMP-7) to maintain cell phenotype as gremlin elicited no change in cell morphology. However endogenous BMP-7 mRNA expression was higher in DLKP-SQ compared to DLKP-I (Figure 3.0.3) A recent study in human

kidney tubule cells and HEK-293 cells showed that gremlin preferentially binds to BMP-2 and BMP-4 over BMP-7 (Church et al. 2015). Thus, we speculate that DLKP-SQ cells may produce endogenous BMP-7 as opposed to BMP-4 or BMP-2 thus there was no significant phenotypic alteration following gremlin treatment. As shown in a mouse model of chronic renal injury, BMP-7 has the ability to reverse epithelial to mesenchymal transition and elicit a more "normal" cell phenotype (Zeisberg et al. 2003). This supports our hypothesis that DLKP-SQ could be producing BMP-7 to maintain a squamous-like phenotype which is unaltered following gremlin treatment. Future experiments investigating endogenous expression of BMP ligands using PCR and western blotting would be an important step to begin elucidating this hypothesis.

To conclude, these results indicate that DLKP-SQ undergo EMT in response to BMP-4 treatment and that BMP-7 mediated signalling may be involved in maintaining DLKP-SQ cell phenotype.

Secondly, we hypothesised that DLKP-M cells would be unchanged following BMP-4 treatment and exposure to gremlin would induce MET and promote a DLKP-SQ-like phenotype. Contrary to our original hypothesis, DLKP-M cells treated with BMP-4 underwent extensive morphological changes. The cells formed large cell clusters and the extended neurite-like processes in the DLKP-M cells were no longer observed. Individual cell outline was no longer visible in the large colony and the outer border of these colonies were very distinct and resembled DLKP-I cells at day 3 following BMP-4 treatment. Furthermore, the cells expressed elevated levels of vimentin and N-cadherin, both common markers upregulated during EMT (Figure 3.0.20-21). Vimentin staining was localised along the distinct cell border of the newly formed DLKP-I-like colonies as seen by immunofluorescence. β-catenin

was also elevated in DLKP-M cells treated with BMP-4 at day 1, day 3 and day 5. Due to the lack of E-cadherin in these cells, we speculate that the elevated level of β-catenin is related to the increase in N-cadherin expression. β-catenin attaches to the cell adherens molecule N-cadherin at the cell adherens junction, linking the complex to α-catenin and subsequently to the cell cytoskeleton.

At day 5, the cells had developed from DLKP-I like colonies into a large fibrotic mass (Figure 3.0.11). Cell piling and aggregation were evident and long neurite-like processes were observed. BMP-4 has a half-life of between 24-48 hrs thus we speculate that endogenous BMP-4 production may be occurring at day 5 in these DLKP-M cell masses which could establish a feed-forward mechanism and results in further morphological changes and cell aggregation. DLKP-M cells also expressed the highest level of BMPR-II compared to DLKP-SQ and DLKP-I cells which could account for the cells' hyper-responsiveness to BMP-4 stimulation (Figure 3.0.3). Given the mesenchymal nature of the cells and change in morphology following BMP-4 treatment we hypothesise that this fibrotic mass could be induced by excessive EMT in these cancer cells, whereby these already mesenchymal cells begin to form colonies and pile on top of one another to form a tumour-like mass. BMP mediated EMT has been shown in primary airway epithelial cells and these results support the hypothesis that excessive EMT and the lack of MET could lead to tissue fibrosis. In this case, excessive EMT results in the formation of a tumour cell mass with what appears to be excessive cell proliferation and piling (McCormack et al. 2013). Future experiments should address this cell processes to elucidate the cellular events that occur following BMP-4 treatment.

When DLKP-M cells were treated with gremlin for up to five days, downregulation of vimentin, N-cadherin and β-catenin occurred in conjunction with a

morphological change that resembled DLKP-SQ cells. Increased cell-cell contact was evident and the larger DLKP-M cell shape was replaced by tightly packed, smaller cells in some regions of the culture. These changes indicated an MET process in DLKP-M cells mediated through removal of BMP ligands. We speculate that DLKP-M cells produce endogenous BMP ligands which maintain their mesenchymal cell phenotype.

In conclusion, these results showed that modulating BMP-4 mediated signalling in DLKP-M cells greatly alters cell morphology along the EMT-axis. BMP-4 mediated signalling can induce a fibrotic-like cell phenotype due to excessive signal activation and the potential establishment of an autocrine feed forward loop.

Finally, we hypothesised that DLKP-I cells represented an intermediate phenotype. Given the spontaneous interconversion events which occurred between DLKP-SQ and DLKP-M cells in culture we hypothesised that DLKP-I cells represented a stem cell-like clone capable of phenotypic switching. We postulated that DLKP-I cells would undergo EMT when treated with BMP-4 to adopt DLKP-M like phenotype and an MET process following gremlin treatment to adopt DLKP-SQ like phenotype. Following BMP-4 treatment, DLKP-M-like cells were observed the in DLKP-I cell culture. Cells began to form colonies that resembled DLKP-M cells treated with BMP-4. The individual cell membranes became indistinguishable within the large colonies (Figure 3.0.12). We speculate that these colonies would have developed into large fibrotic masses similar to DLKP-M cells treated with BMP-4 if the time points were increased.

Following gremlin treatment the cell-cell contact between DLKP-I colonies increased and individual cells became more distinct. The cells adopted a squamous,

"cobblestone"-like morphology and resembled DLKP-SQ clones (Figure 3.0.12). Decreased expression of vimentin, N-cadherin and β-catenin protein expression occurred in the DLKP-I cells following gremlin treatment which indicated an MET process. We postulate that the loss of β-catenin was related to disassembly of the ADJ, as DLKP-SQ cells do not expression N-cadherin or E-cadherin at the membrane. In addition, the fact that gremlin treatment elicited a change in morphology indicted that DLKP-I clones may produce endogenous BMP ligands which maintain their cell phenotype, specifically BMP-2 or BMP-4 as opposed to BMP-7. Thus, BMP ligands could be acting in an autocrine fashion and could dictate the morphology of the cells in the intermediate DLKP-I colonies. A BMP ligand gradient may exist in culture and cells further away from DLKP-I clusters may be exposed to lowered BMP-4 or BMP-2 mediated signalling and this causes phenotypic switching- for example, to DLKP-SQ cells. Higher levels of BMP-4 induce a DLKP-M phenotype. This speculation is confounded by the low level of nuclear localisation of SMAD-4 and pSMAD 1/5/8 in untreated DLKP-I cells. We postulate this potential autocrine activity may be also be partly controlled via non-canonical BMP, non-SMAD pathways or by other factors involved in controlling cell morphology.

We propose that DLKP-M have progressed along the EMT axis and committed to a mesenchymal-cell fate rather than the EMP-like status of DLKP-I cells. This would account for the DLKP-I interconversion events that occur readily in parental cell culture.

Taken together these results depict a dynamic model of EMT-mediated phenotypic switching which can be controlled by BMP agonists and inhibitors. We highlight a potential divergent role between BMP-4 and BMP-7 ligands in these cells. Our

results also indicate that different states of EMT are represented by the heterogeneous DLKP clonal populations. We propose that DLKP-SQ cells represent an early stage of EMT, DLKP-I cells represent an intermediate EMP-like cell and DLKP-M cells possess a mesenchymal-like cell which has progress further along the EMT axis. By increasing BMP pathway activation in these different clonal subpopulations via BMP-4 stimulation, it was possible to direct DLKP-SQ towards a DLKP-M-like mesenchymal phenotype. Likewise, inhibiting BMP pathway activation by administering gremlin led to DLKP-I conversion to DLKP-SQ clones. DLKP-M cells represented a mesenchymal population which were capable of excessive cell aggregation and formation of a fibrotic mass following BMP-4 stimulation. Conversely, DLKP-M cells adopted a DLKP-SQ phenotype following gremlin treatment.

Following on from our original hypothesis (Figure 3.1), we propose that a BMP gradient is responsible for phenotypic switching between the DLKP clones (Figure 3.0.30). Based on the results presented here we speculate that high levels of BMP-7 and low BMP-4 expression in DLKP-SQ maintain the squamous, epithelial-like cell phenotype. On the other hand, we postulate that endogenous BMP-4 or BMP-2 mediated signalling in DLKP-I and DLKP-M cells maintain their respective cell phenotypes. It is unknown if an intermediate cell phenotype exists between DLKP-SQ and DLKP-M but we propose that DLKP-I cells represent an EMP-like cell phenotype which expresses both epithelial and mesenchymal properties. Treatment of DLKP-I or DLKP-M cells with the BMP antagonist gremlin results in the loss of this endogenous signalling cascade and the cells convert to DLKP-SQ-like clones. We propose that DLKP-M cells are the most mesenchymal and invasive cell population of the three.

Further experiments should utilise BMP-2 and BMP-7 to investigate the effect of these ligands on motility and EMT. In addition the role of TGF-β has not been explore in DLKP cells lines. Firstly, the level of expression of endogenous TGF-β ligands and receptors would be investigated in DLKP cell lines. In addition, targeted inhibition of TGF-β / BMP signalling using siRNA or neutralising antibodies would provide a greater insight into the role of BMP and TGF-β signalling in EMT. By silencing BMP signalling in DLKP-M cells, their mesenchymal metastatic properties may be reversed. These experiments could also elucidate the role of BMP signalling with proliferation in DLKP cell populations.

Future experiments investigating BMP signalling and EMT should be carried out. Treatment experiments involving DLKP-M clones and BMP-4 could lead to important findings regarding growth factor induced EMT and fibrosis. The role of BMP signalling *in vivo* during tissue fibrosis would be of particular interest and could highlight BMP as a potential therapeutic target.

In conclusion our results have highlighted a role for BMP signalling in the induction of phenotypic switching between the clonal subpopulations of a heterogenous lung tumour. Furthermore, we have demonstrated the potential importance of BMP gradients in driving carcinogenic tumour properties and identified BMP-4 as an important target for cancer therapeutics

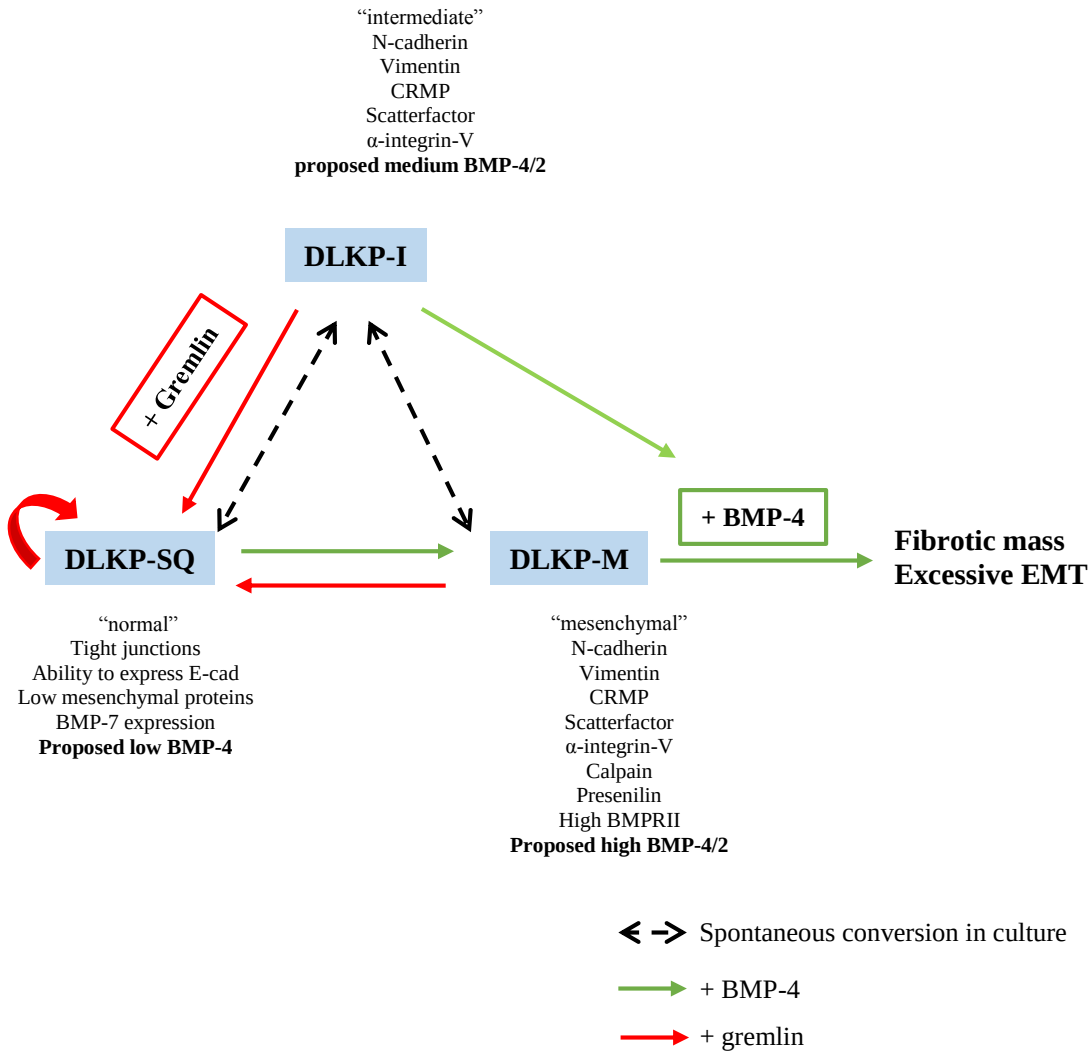

Figure 3.0.30 BMP gradients and EMT-mediated phenotypic switching in DLKP clones

Chapter 4

Investigation of E-cadherin gene processing in the heterogeneous lung cancer cell line DLKP

4.1 Introduction

We have provided evidence that DLKP-SQ cells represent a more "normal" epithelial cell population compared to the invasive, mesenchymal counterpart DLKP-M. We have demonstrated that DLKPSQ and DLKP-M are on the EMT-axis and that BMP-4 induced EMT-mediated phenotypic switching events between DLKP-SQ and DLKP-M cells. E-cadherin downregulation and N-cadherin upregulation is a well characterised hallmark of EMT (Gravdal et al. 2007). Interestingly, neither DLKP-SQ nor DLKP-M cells express membrane bound E-cadherin thus, we hypothesise that this heterogeneous cell population represents a very suitable model to investigate cadherin switching.

Two E-cadherin reporter plasmids have previously been designed in the O'Dea lab by Dr. Joanne Masterson (PhD, Masterson 2008). The first contained the mouse E-cadherin promoter construct subcloned into the plasmid vector pEYFP-1. This plasmid was called Eprom and transfection into MLE-12 and MAECs resulted in YFP protein expression in the cytoplasm. Eprom served as a control for E-cadherin

promoter efficacy. The second construct contained mouse E-cadherin cDNA from the pBATEM2 construct subcloned into the plasmid vector pEYFP-1. This plasmid was called Em^2. Transfection of Em^2 into Beas2b cells resulted in E-cadherin-YFP fusion protein expression at the cell membrane. Expression of the fusion protein at the membrane indicated that the cells contain the necessary machinery to facilitate correct E-cadherin mRNA translation and subsequent trafficking to the plasma membrane.

Transfection of both Eprom and Em^2 into DLKP-SQ and DLKP-M cells was originally carried out by Dr. Emer Molloy and stable clones were generated (Shirley O'Dea lab). Preliminary analysis of the subclones by Dr. Emer Molloy revealed no significant difference in proliferation or migration of DLKP-SQ Eprom, DLKP-SQ Em^2 , DLKP-M Eprom or DLKP-M Em^2 . Dr. Emer Molloy examined the DLKP-SQ subclones further and a change in actin localisation was evident in DLKP-SQ Em^2 cells compared to DLKP-SQ and DLKP-SQ Eprom cells. The same stable subclones prepared by Dr. Emer Molloy were used for this project except for DLKP-SQ Eprom subclones. An additional subcloning and expansion experiment protocol was carried out for DLKP-SQ Eprom cells as the stock of this subclone had expired. A mixed population of DLKP-SQ Eprom were subcloned by limiting dilutions in 96 well plates. Single fluorescent cells were identified and expanded in G418-containing medium to generate DLKP-SQ Eprom subclonal populations (see Appendix).

Given the preliminary data demonstrating evidence of altered cell phenotype but no change in cell proliferation following E-cadherin gene transfection, we hypothesise that a cadherin switch is a possible mechanism involved in phenotypic switching events between these two DLKP clonal populations. As neither cell line expresses

endogenous E-cadherin protein, we postulate that re-introduction of the E-cadherin gene would result in MET in DLKP-SQ and DLKP-M cells. We hypothesise that DLKP-M cells have undergone phenotypic re-programming to become a more invasive and mesenchymal population. Furthermore, we hypothesise that transfection of the E-cadherin gene into DLKP-M cells will cause conversion to DLKP-SQ cells.

4.1.1 Endogenous E-cadherin mRNA expression in DLKP-SQ and DLKP-M

The E-cadherin to N-cadherin switch is a hallmark of EMT and phenotypic switching events. We wanted to elucidate the phenotypic reprogramming events that have occurred in the DLKP clones and investigate if overexpression of an E-cadherin gene in the cells induces MET. Firstly, endogenous E-cadherin mRNA expression in DLKP-SQ and DLKP-M cells was determined by semi-quantitative rt-PCR. E-cadherin mRNA expression was inconsistent and irregular in both DLKP-SQ and DLKP-M cells (Figure 4.0.1).

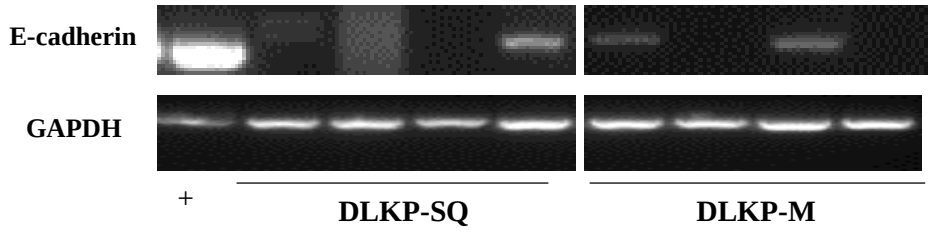

Figure 4.0.1 Endogenous E-cadherin expression in DLKP-SQ and DLKP-M cells

Representative image of endogenous E-cadherin expression in DLKP-SQ and DLKP-M clones grown in 5% serum-containing medium. E-cadherin mRNA expression was inconsistent in the clones. A549 was the positive control, GAPDH was used as a loading control.

4.1.2 Generation of DLKP-SQ and DLKP-M cell lines stably expressing Eprom and Em^2 reporter plasmids

All plasmid design and cloning was carried out by Dr. Joanna Masterson in the O'Dea lab. In brief, the E-cadherin promoter construct was sub-cloned into the pEYFP-1 plasmid, upstream of the YFP gene. This reporter plasmid is termed "Eprom" hereafter. To generate the E-cadherin-YFP construct, the mouse E-cadherin gene from pBATEM2 was inserted into the pEYFP-1 plasmid. This generated the E-cadherin-fluorescent fusion protein under the control of the E-cadherin promoter – termed Em^2, hereafter (Figure 4.0.2) (Behrens et al. 1991; Nose, Nagafuchi, and Takeichi 1988). Following clonal expansion and selection of fluorescence clones, FACS was carried out to analyse the expression of YFP fluorescent protein in the subclonal populations. This was carried out by Dr. Emer Molloy (see Appendix).

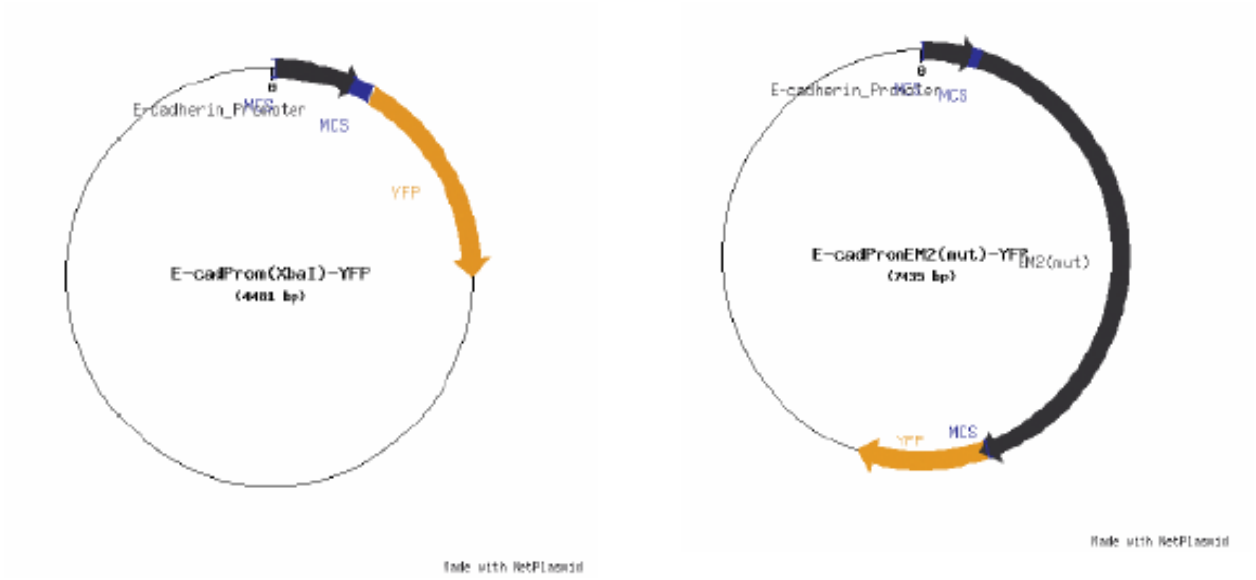

Eprom:
E-cadherin promoter driving YFP gene expression

Em^2:
E-cadherin promoter driving YFP-tagged E-cadherin gene expression

YFP protein

YFP

E-cadherin YFP fusion protein

E-cad | YFP

Figure 4.0.2 The Eprom and Em2 reporter plasmids

The Eprom plasmid contained the mouse E-cadherin promoter construct subcloned into the pEYFP-1 plasmid. When transfected into cells and following correct transcription and translation, the Eprom plasmid generated fluorescent YFP. The Em^2 plasmid contained the mouse E-cadherin gene from the pBATEM2 construct subcloned into the pEYFP-1 plasmid. When transfected into cells and following correct transcription and translation, the Em^2 reporter construct generated E-cadherin protein tagged with fluorescent YFP. These constructs were designed and constructed by Joanne Masterson, PhD (Shirley O' Dea lab). The transfection experiments were carried out by Dr. Emer Molloy (Shirley O'Dea lab).

4.1.3 3D culture of DLKP-SQ and DLKP-M clones

We utilised HappyCell® advanced suspension medium to investigate the effect of E-cadherin expression on cell growth patterns in a more biologically relevant 3D environment. Happy Cell ® is an optimised suspension DMEM-based media which facilitates 3D spheroid culture of cells. Both normal and neoplastic cells have been shown to grow as spheroids in suspension medium. DLKP-SQ cells did not grow complete spheroids in HappyCell® but instead formed small cell clusters. These cell aggregates had irregular shapes and formations. A similar growth pattern was evident in DLKP-SQ Eprom cell (Figure 4.0.3 A). These cells were fluorescent indicating the presence of YFP protein. In contrast to both DLKP-SQ and DLKP-SQ Eprom, DLKP-SQ Em^2 formed distinct, discrete spheroid bodies with a defined, smooth and regular boundary when cultured in Happy Cell ® medium. These spheroids were also fluorescent (Figure 4.0.3 A).

DLKP-M, DLKP-M Eprom and DLKP-M Em^2 cells grew as distinct spheroids in the HappyCell® advanced suspension medium (Figure 4.0.3 B). The DLKP-M spheroids possessed the same regular, smooth outer boundary as the DLKP- SQ Em^2 spheroids however, DLKP-M spheroids possessed extended neurite-like processes. The DLKP-M Eprom spheroids were fluorescent in contrast to the DLKP- M Em^2 spheroids (Figure 4.0.3 B).

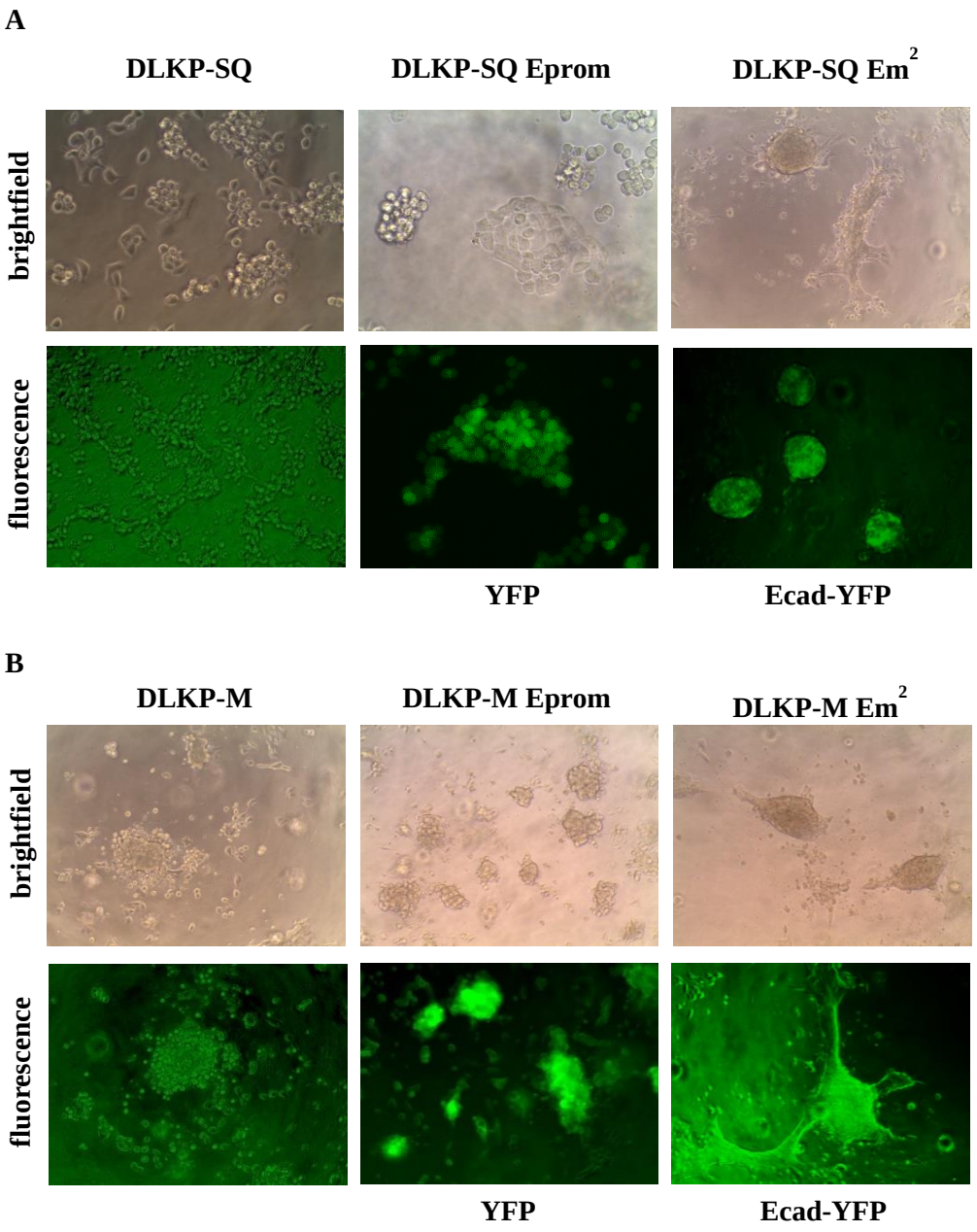

Figure 4.0.3 3D culture of DLKP-SQ and DLKP-M subclones

Representative micrographs of DLKP-SQ, DLKP-SQ Eprom, DLKP-SQ Em^2 and DLKP-M, DLKP-M Eprom, DLKP-M Em^2 grown in HappyCell® medium for nine days. (A) DLKP-SQ and DLKP-SQ Eprom grew in aggregated cell clusters but did not form spheroids. DLKP-SQ Eprom aggregates were fluorescent. DLKP-SQ Em^2 formed fluorescent discrete and compact spheroids with a defined outer boundary. (B) DLKP-M, DLKP-M Eprom and DLKP-M Em^2 cells formed distinct discrete spheroids in HappyCell® culture. The DLKP-M Eprom spheroids were fluorescent and the DLKP-M Em^2 were less fluorescent.. The DLKP-M spheroids possessed extended process and were larger than the DLKP-SQ Em^2 structures. Brightfield and fluorescent images were taken of different fields of view.

4.1.4 Expression of epithelial markers in DLKP-SQ clones grown in 3D culture

Given the evidence presented here that DLKP-SQ and DLKP-SQ Eprom populations formed aggregated cell clusters in Happy Cell ® suspension medium while DLKP-SQ Em^2 formed discrete compact spheroid with smooth, regular and defined outer boundaries, we wanted to investigate what cell adherens proteins were involved in the formation of the spheroids. The cells were grown on chamber-well slides for nine days in Happy Cell® before immunofluorescence was carried out. The cells were stained for YFP, E-cadherin and N-cadherin.

DLKP-SQ cell clusters did not express membrane-localised E-cadherin or N-cadherin when grown in Happy Cell ® suspension medium. E-cadherin and N-cadherin were expressed weakly in the cytoplasm. DLKP-SQ cells did not express YFP (Figure 4.0.4). Similar to DLKP-SQ cell aggregates, DLKP-SQ Eprom cell clusters expressed E-cadherin and N-cadherin weakly in the cytoplasm. YFP protein was present in the cytoplasm of DLKP-SQ Eprom, by immunofluorescence (Figure 4.0.5).

As previously noted, DLKP-SQ Em^2 developed large spheroid bodies in Happy Cell ® culture with a distinct, regular boundary. When protein localisation patterns were examined by immunofluorescence, E-cadherin-YFP fusion protein was expressed at the cell membrane. The spheroids did not express N-cadherin at the cell membrane (Figure 4.0.6). This indicated that E-cadherin protein expression was involved in spheroid formation in Happy Cell ® suspension culture.

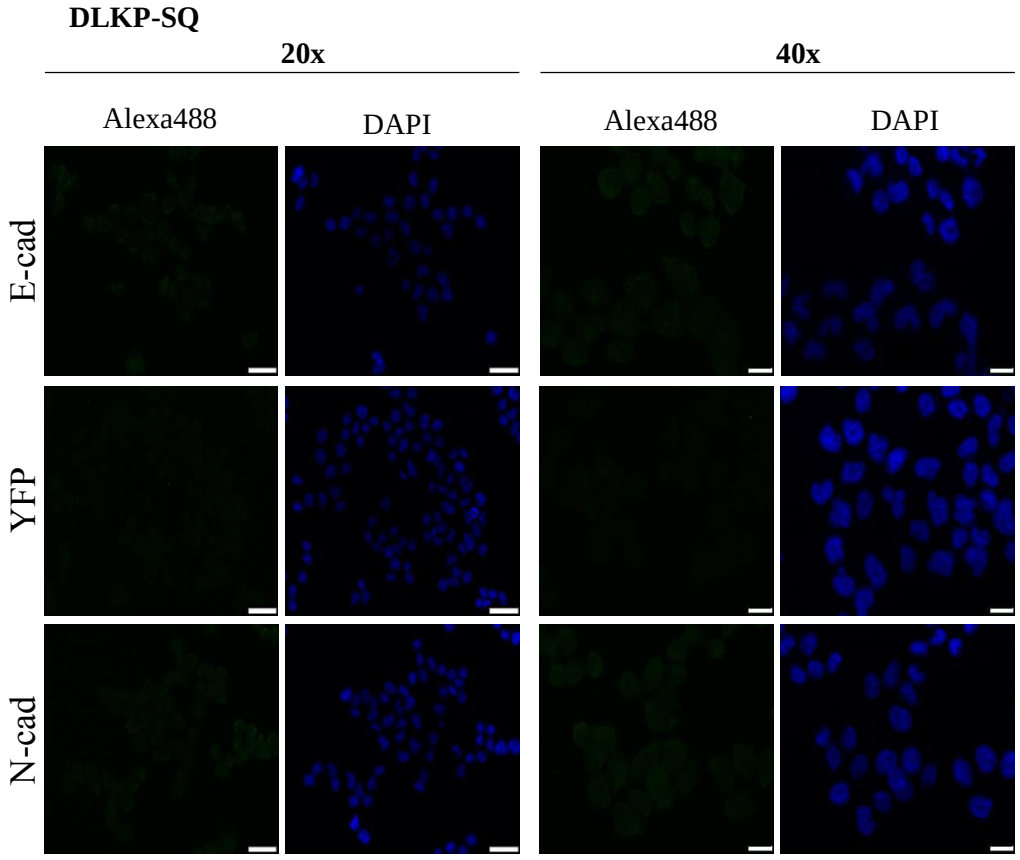

Figure 4.0.4 Immunofluorescence of DLKP-SQ spheroids

Representative micrographs of DLKP-SQ cells grown in HappyCell® medium for 9 days and stained for E-cadherin, YFP and N-cadherin. Very dull E-cadherin and N-cadherin expression was present in DLKP-SQ cels. DLKP-SQ cells were YFP-null. Cells were counterstained with DAPI. Scale bars represent 50uM and 20uM respectively

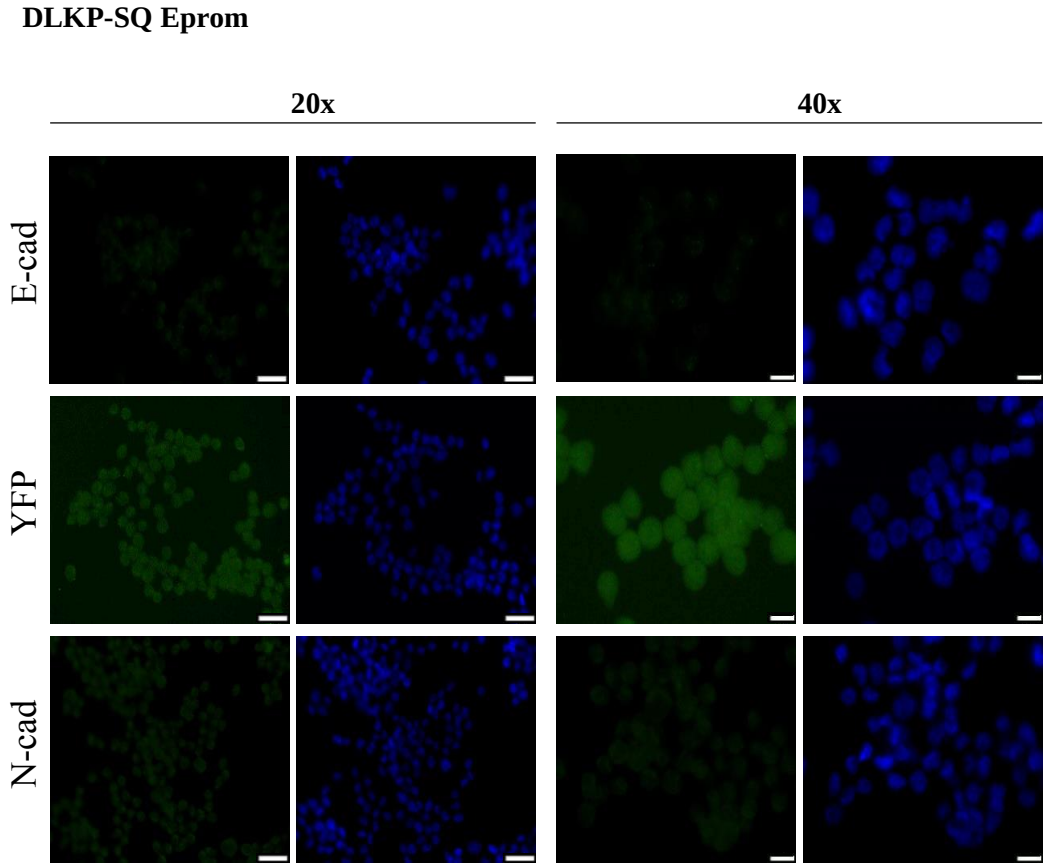

Figure 4.0.5 Immunofluorescence of DLKP-SQ Eprom spheroids

Representative micrographs of DLKP-SQ Eprom cells grown in HappyCell® medium for 9 days and stained for E-cadherin, YFP and N-cadherin. E-cadherin, YFP and N-cadherin expression was weak and cytoplasmic. Cells were counterstained with DAPI. Scale bars represent 50uM and 20uM respectively

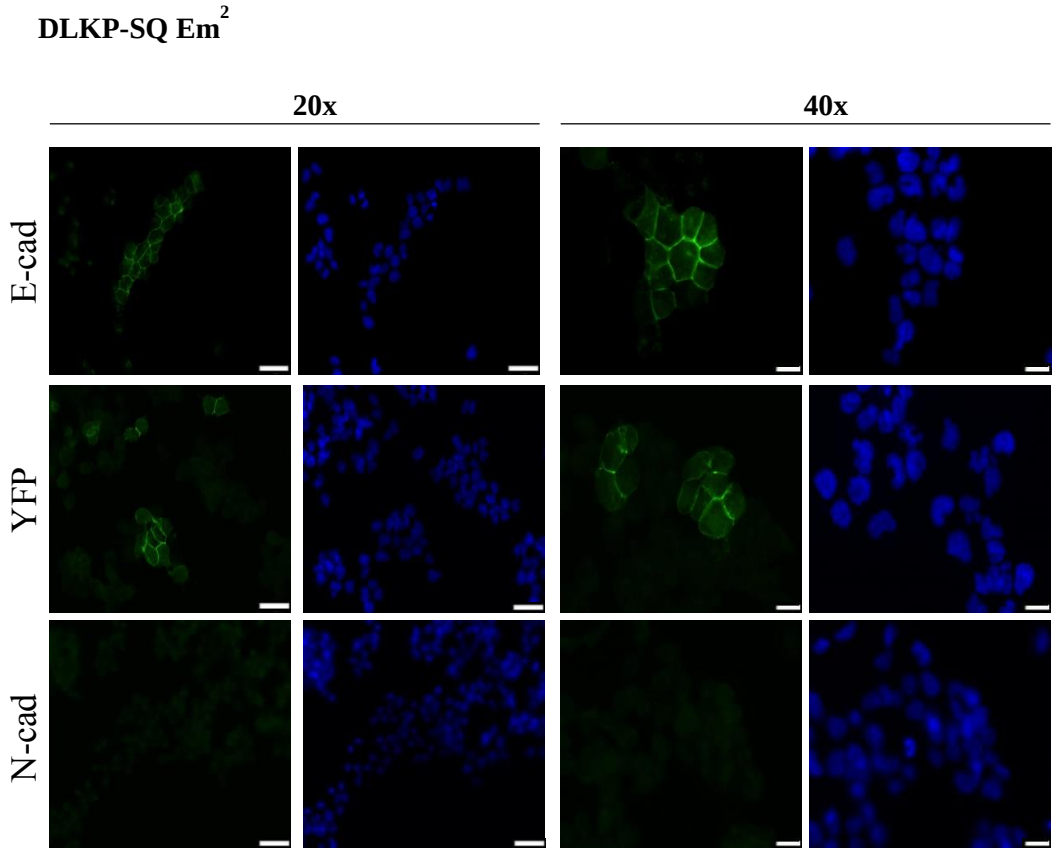

Figure 4.0.6 Immunofluorescence of DLKP-SQ EM^2 spheroid

Representative micrographs of DLKP-SQ Em^2 cells grown in HappyCell® medium for 9 days and stained for E-cadherin, YFP and N-cadherin. E-cadherin and YFP were localised at the cell membrane in a chicken-wire pattern. N-cadherin expression was weak and cytoplasmic. Cells were counterstained with DAPI. Scale bars represent 50uM and 20uM respectively.

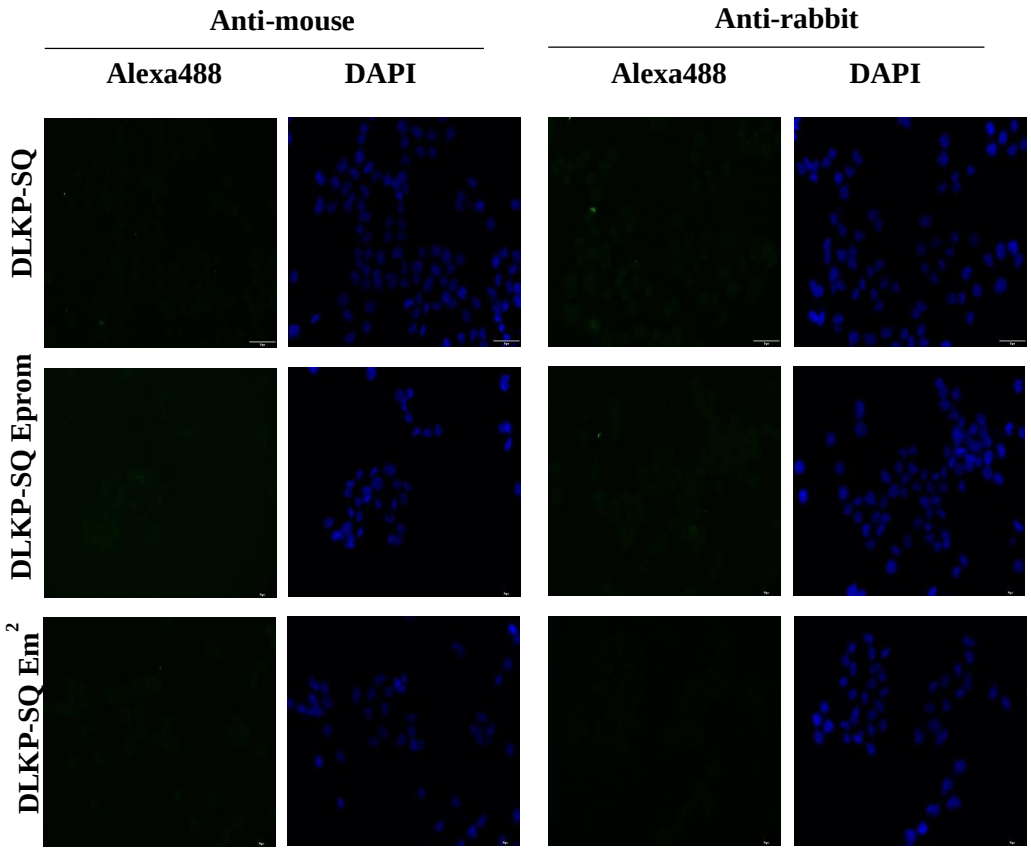

Figure 4. 0.7 Antibody controls

Representative micrographs of immunofluorescence controls of DLKP-SQ, DLKP-SQ Eprom and DLKP-SQ Em^2 cells. Secondary controls were incubated overnight in TBS in place of the omitted primary antibodies. The Alexa488-conjugated anti-mouse and Alexa488-conjugated anti-rabbit antibodies were then added. Cells were counterstained with DAPI. Scale bars represent 50uM and 20uM respectively.

4.1.5 Expression of epithelial markers in DLKP-M clones grown in 3D culture

Given the evidence presented here that all of the DLKP-M subclones grew as spheroids in HappyCell® medium, we wanted to investigate what cell adhesion molecules were involved in DLKP-M spheroid formation. The cells were grown on chamber-well slides for six days in Happy Cell® before immunofluorescence was carried out. The cells were stained for YFP, E-cadherin and N-cadherin.

Immunofluorescence of the DLKP-M cells showed that the cells expressed low levels of cytoplasmic E-cadherin. DLKP-M spheroids did not express YFP protein (Figure 4. 0.8). N-cadherin protein was expressed at the membrane of the DLKP-M spheroid in a characteristic "chicken-wire" pattern. Similar N-cadherin protein localisation was evident in DLKP-M Eprom and DLKP-M Em^2 cell spheroids. DLKP-M Eprom population expressed bright cytoplasmic YFP protein and dull cytoplasmic E-cadherin similar to DLKP-M spheroids (Figure 4.0.9). DLKP-M Em^2 expressed dull cytoplasmic YFP protein and no membrane bound E-cadherin, in striking contrast to DLKP-SQ Em^2 (Figure 4. 0.10). These results indicated that N-cadherin was involved in spheroid formation in DLKP-M, DLKP-M Eprom and DLKP-M Em^2 cells.

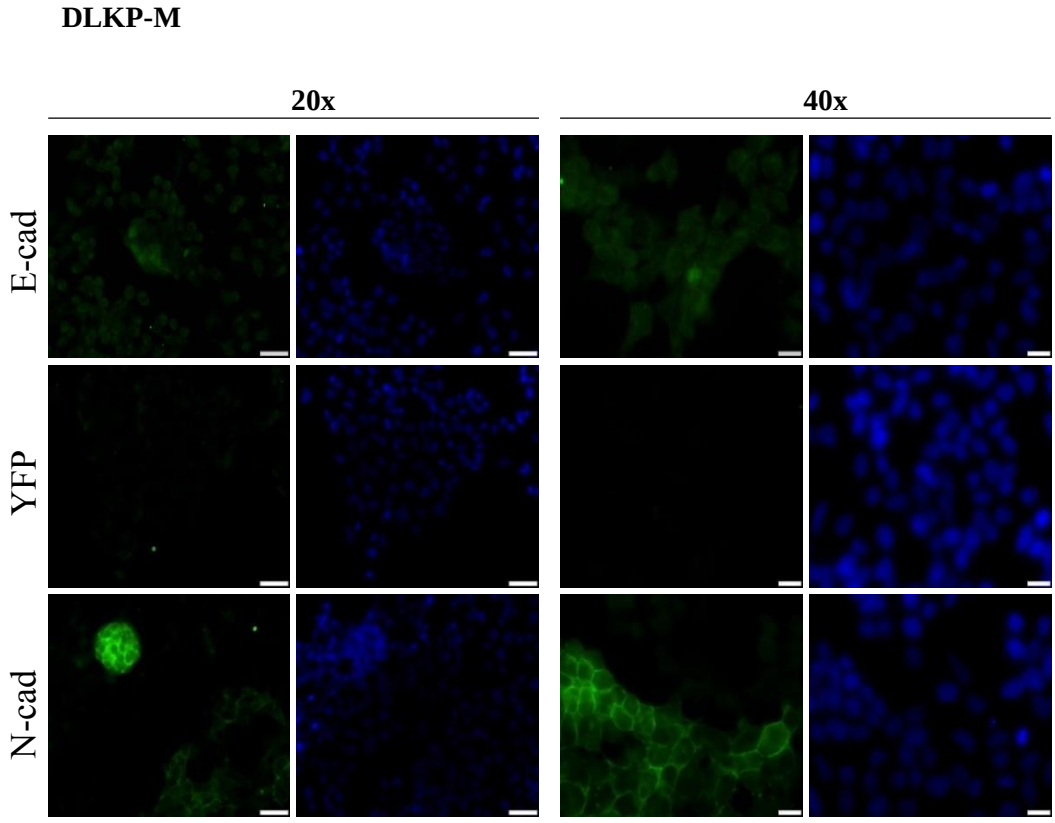

Figure 4. 0.8 Immunfluorescence of DLKP-M spheroids

Representative micrographs of DLKP-M cells grown in HappyCell® medium for 9 days and stained for E-cadherin, YFP and N-cadherin. E-cadherin expression was weak and cytoplasmic and the cells were negative for YFP. The DLKP-M spheroids expressed N-cadherin at the membrane. Cells were counterstained with DAPI. Scale bars represent 50uM and 20uM respectively.

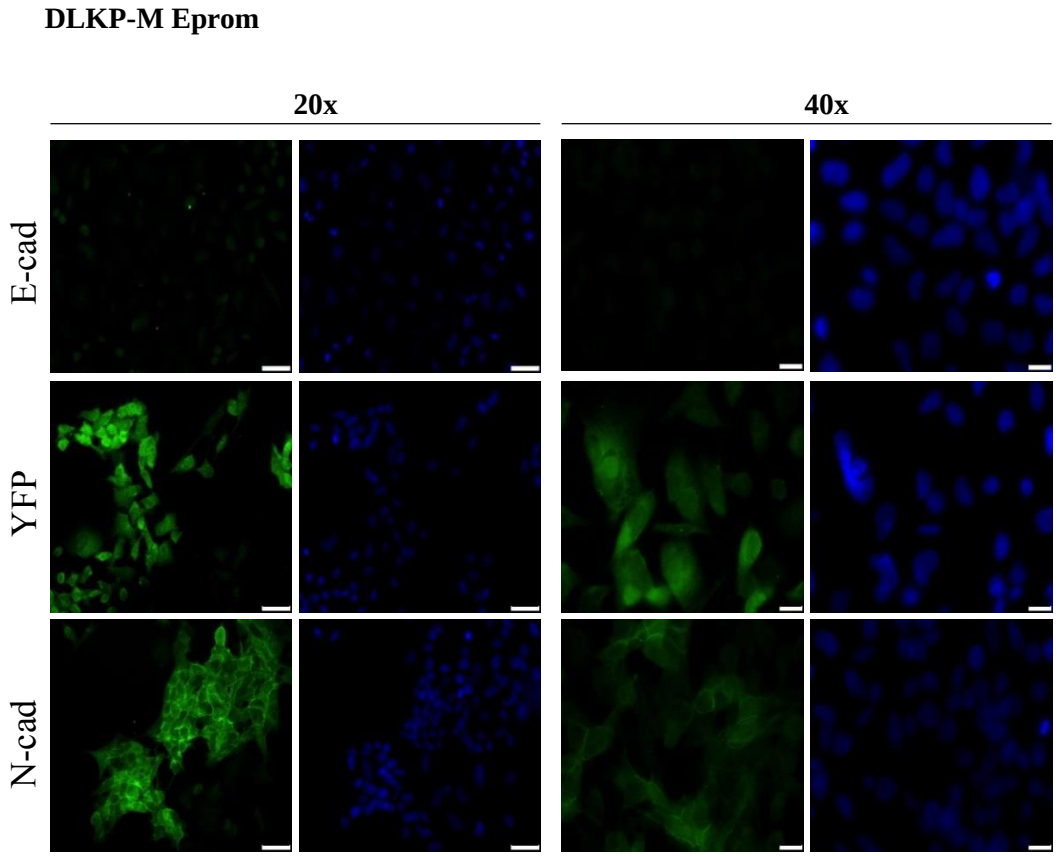

Figure 4.0.9 Immunofluorescence of DLKP-M Eprom spheroids

Representative micrographs of DLKP-M Eprom cells grown in HappyCell® medium for 9 days and stained for E-cadherin, YFP and N-cadherin. E-cadherin expression was weak and cytoplasmic. YFP was localised in the cytoplasm. N-cadherin was expressed at the cell membrane. Cells were counterstained with DAPI. Scale bars represent 50uM and 20uM respectively.

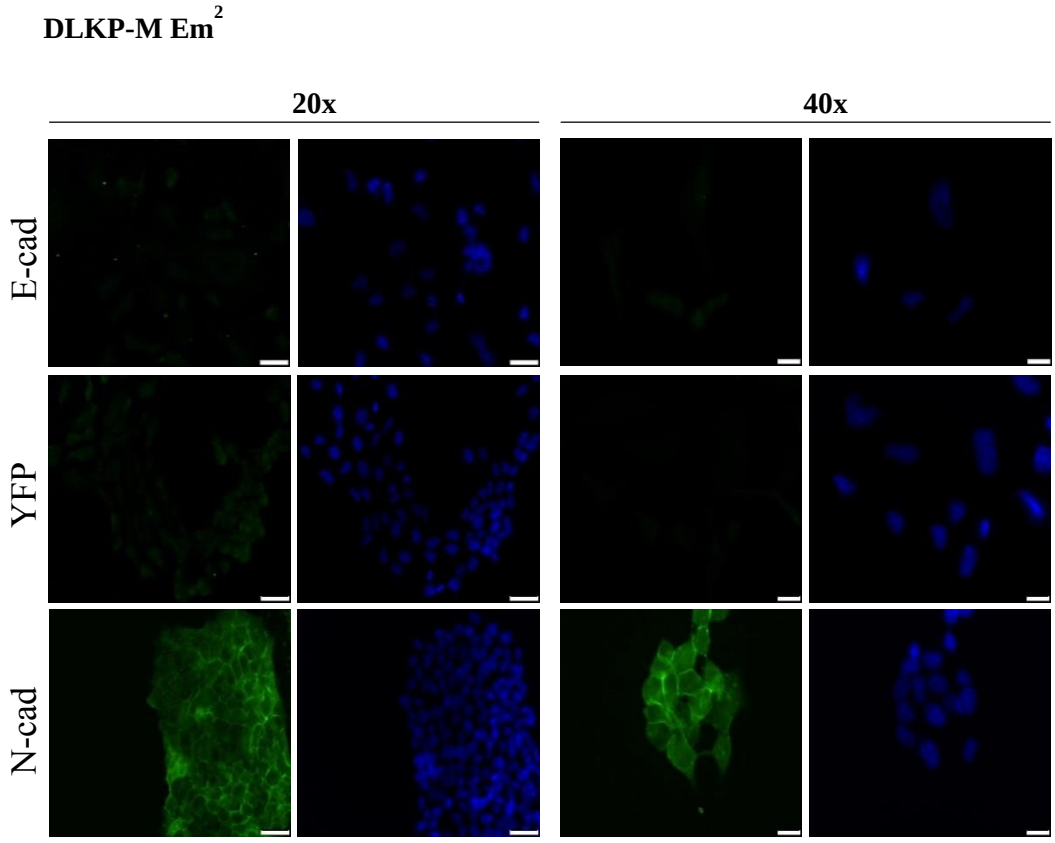

Figure 4. 0.10 Immunofluorescence of DLKP-M Em2 spheroids

Representative micrographs of DLKP-M Em^2 cells grown in HappyCell® medium for 9 days and stained for E-cadherin, YFP and N-cadherin. E-cadherin expression was weak and cytoplasmic. YFP was expressed weakly in cytoplasm. N-cadherin was expressed at the cell membrane in a chicken-wire pattern. Cells were counterstained with DAPI. Scale bars represent 50uM and 20uM respectively.

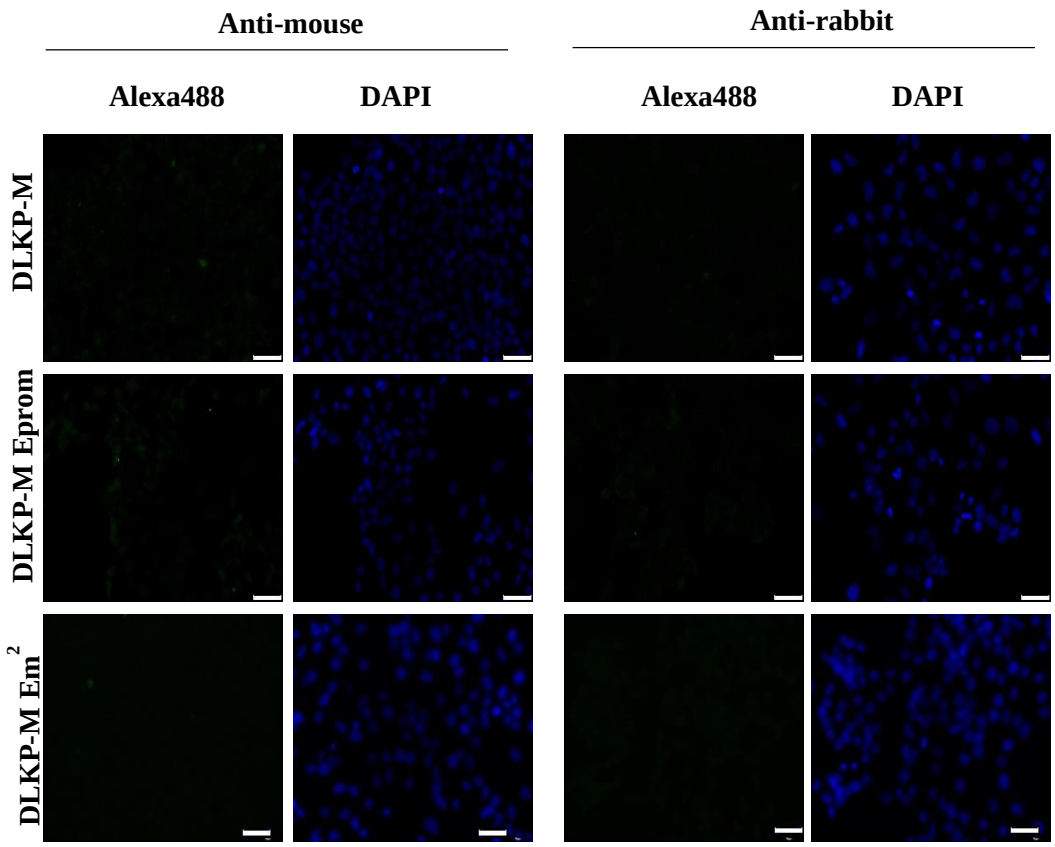

Figure 4.0.11 Antibody controls

Representative micrographs of immunofluorescence controls on DLKP-M, DLKP-M Eprom and DLKP-M Em^2 cells. Secondary controls were incubated overnight in TBS in place of the omitted primary antibodies. The Alexa488-conjugated anti-rabbit and Alexa488-conjugated anti-mouse antibodies were then added. Cells were counterstained with DAPI. Scale bars represent 50uM and 20uM respectively.

4.1.6 Expression of epithelial markers in DLKP-SQ, DLKP-SQ Eprom and DLKP-SQ Em^2 in 2D culture

We hypothesised that DLKP-SQ cells transfected with the E-cadherin reporter plasmid Em^2 would express E-cadherin at the cell membrane, undergo MET and that the expression of other epithelial-related markers would increase as a result. Immunofluorescence and western blotting were carried out to examine the localisation patterns and expression levels of E-cadherin, YFP, actin, β-catenin and cytokeratin in the subclonal populations. In these experiments, a monoclonal antibody generated against the C-terminal end of the full length E-cadherin protein (735/883) was used. The expected molecular weight was 120kDA. A polyclonal antibody against full length GFP was used. This antibody is reactive to YFP. The expected molecular weight was 27kDA.

Immunofluorescence showed that E-cadherin protein was localised at the cell membrane of the DLKP-SQ Em^2 cells (Figure 4.0.12). The characteristic "chicken-wire" like staining of E-cadherin at the cell membrane formed a distinct boundary between each cell. Cytoplasmic E-cadherin protein was visible in DLKP-SQ and DLKP-SQ Eprom cells and no membrane bound E-cadherin was present (Figure 4.0.12). E-cadherin protein expression was examined by western blotting, using both an E-cadherin antibody and an YFP antibody. E-cadherin expression was absent in DLKP-SQ and DLKP-SQ Eprom. In DLKP-SQ Em^2 cells a band was present at approx. 150kDA when whole cell protein was probed with either antibody (Figure 4. 0.13). This 150kDA size band is approximately equal to the molecular weights of E-cadherin and YFP combined. This indicated that the E-cadherin gene tagged with YFP was successfully transfected and that gene

incorporation, transcription, translation and processing to the membrane took place in DLKP-SQ Em^2 cells.

DLKP-SQ cells did not express YFP. Immunofluorescence showed that YFP was present in the cytoplasm of DLKP-SQ Eprom subclones and localised at the cell membrane of DLKP-SQ Em^2 subclones (Figure 4.0.12). Western blots probed with a YFP antibody revealed a 27kDA band in the whole cell protein extracted from DLKP-SQ Eprom cells (Figure 4. 0.13). DLKP-SQ Em^2 expressed a 150kDA size band, indicative of the E-cadherin-YFP fusion protein. These results confirmed that the E-cadherin promoter was successfully driving both YFP and E-cadherin-YFP transcription and subsequent protein production in DLKP-SQ Eprom and DLKP-SQ $Em^{2,}$ respectively.

Because membrane-bound E-cadherin protein was present in DLKP-SQ Em^2, the expression of other proteins associated with the epithelial phenotype and EMT progression such as actin, β-catenin and cytokeratins were investigated. Actin re-polarisation was evident in DLKP-SQ Em^2 cells (Figure 4.0.12). Compared to DLKP-SQ or DLKP-SQ Eprom cells, actin was localised at the cell membrane in DLKP-SQ Em^2 as indicated by the white arrows. In the DLKP-SQ and DLKP-SQ Eprom cells, actin was dispersed throughout the cytoplasm, as indicated by the white arrows. This result supported previous experiments carried out by Dr. Emer Molloy (O'Dea lab). The level of actin expression was investigated from whole cell protein extracted from the cells. Higher levels of actin protein were evident in DLKP-SQ Em^2 compared to DLKP-SQ and DLKP-SQ Eprom cells. This result was confirmed by densitometry (Figure 4. 0.13).

Immunofluorescence revealed β-catenin localisation at the cell membrane in DLKP-SQ Em^2 subclones. The white arrows highlight regions expressing membrane bound β-catenin (Figure 4.0.12). Low levels of membrane bound β-catenin was evident in DLKP-SQ and DLKP-SQ Eprom cells. A low level of β-catenin expression was also present in these cells by western blot (Figure 4. 0.13). Conversely, DLKP-SQ Em^2 displayed a significantly higher level of β-catenin protein expression by western blot. This result was confirmed by densitometry.

Finally, cytokeratin expression was investigated. A pan cytokeratin antibody detecting K 4, 5, 6, 8, 10 and 13 was used. There was evidence of cytokeratin re-organisation at the cell membrane in DLKP-SQ Em^2 cells following immunofluorescence. DLKP-SQ and DLKP-SQ Eprom cells displayed cytoplasmic cytokeratin expression with some non-uniform expression at the cell membrane (Figure 4.0.12). No detectable change of cytokeratin protein was found by western blot (Figure 4. 0.13).

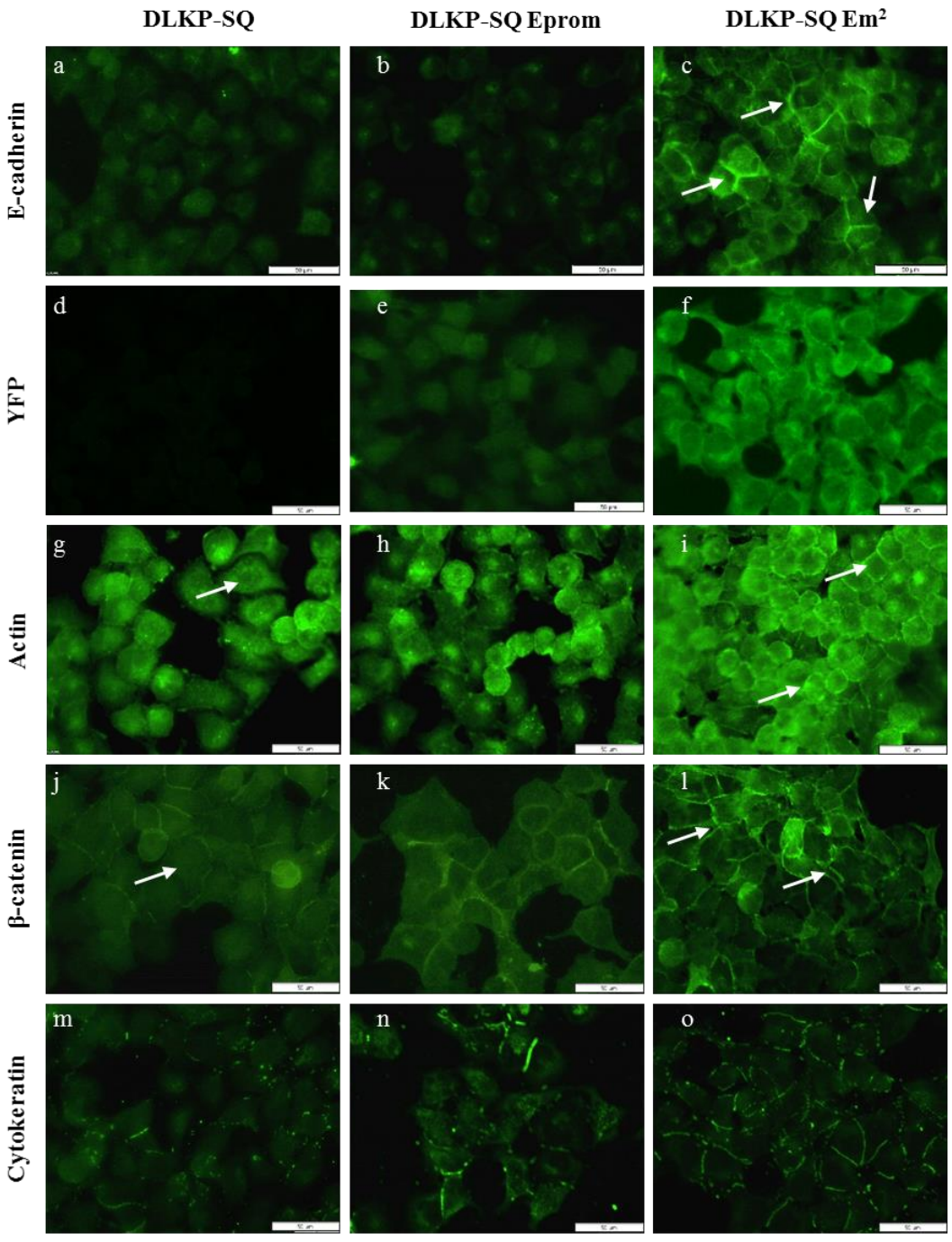
DLKP-SQ
DLKP-SQ Eprom
DLKP-SQ Em²
E-cadherin
YFP
Actin
β-catenin
Cytokeratin
a
b
c
d
e
f
g
h
i
j
k
l
m
n
o

Figure 4.0.12 DLKP-SQ subclones display alters adhesion junctions and cytoskeletal organisation

Representative micrographs of localisation patterns of E-cadherin, YFP, Actin, β-catenin and cytokeratin in DLKP-SQ cells transfected with Eprom and Em^2. E-cadherin was expressed at the membrane in DLKP-SQ Em^2 subclones as indicated by the white arrows (a-c). YFP was expressed in the cytoplasm of DLKP-SQ Eprom and at the membrane of Em^2 cells (d-f). Actin re-polarisation was evident in DLKP-SQ Em^2 compared to DLKP-SQ and DLKP-SQ Eprom, as indicated by the white arrows (g-i). β-catenin was re-organised in DLKP-SQ Em^2 and elevated expression at the membrane was present compared to DLKP-SQ cells or DLKP-SQ Eprom cells, as indicated by the white arrows (j-l). Cytokeratin expression localised at the cell membrane in DLKP-SQ Em^2 (m-o). All scale bars represent 50uM, n=2

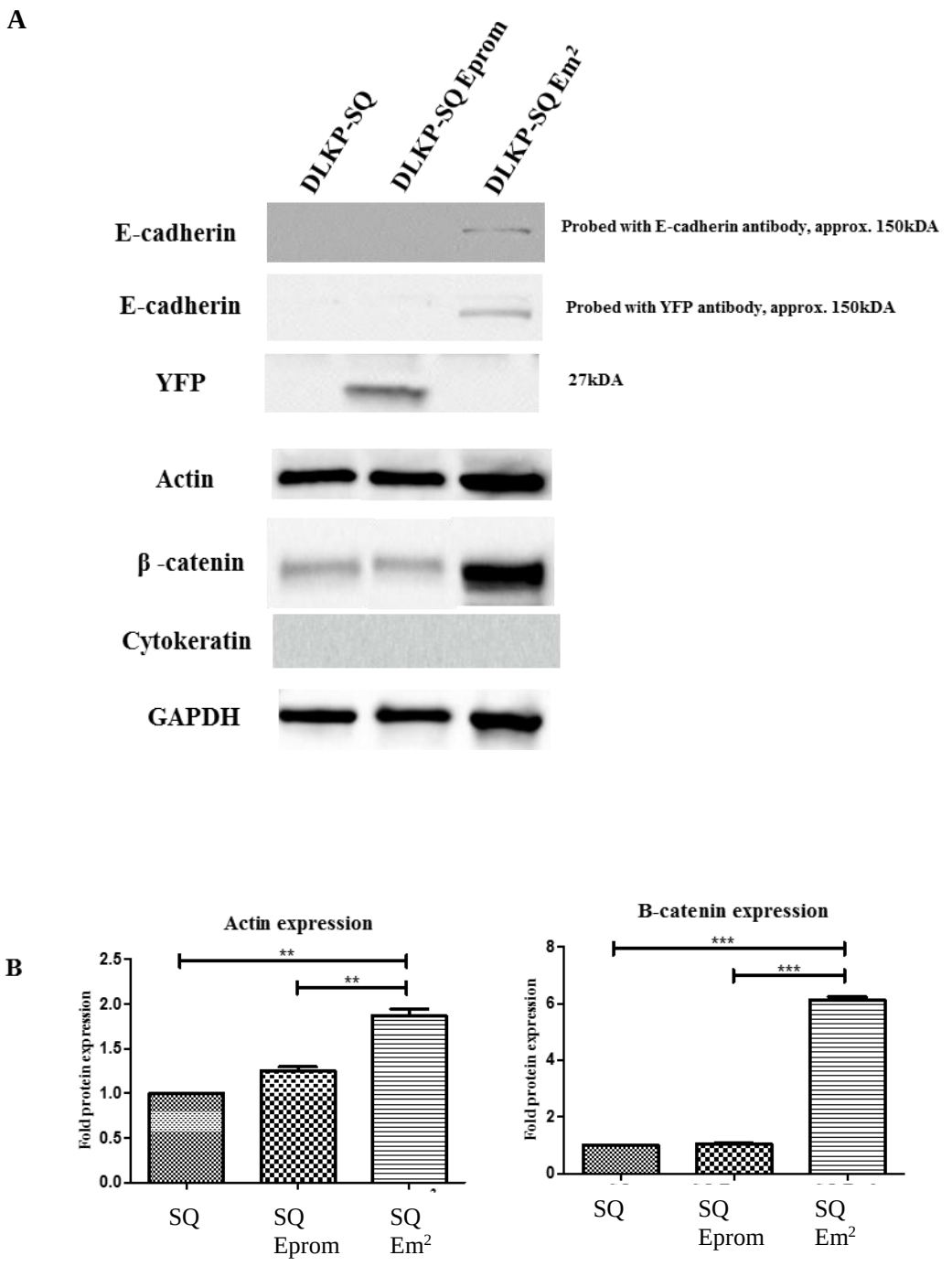

Figure 4. 0.13 Western blot of adherens and cytoskeletal proteins on DLKP-SQ, DLKP-SQ Eprom and DLKP-SQ Em2 cells

(A) Representative western blots of E-cadherin, YFP, actin, β–catenin and cytokeratin in DLKP-SQ, SQ Eprom and SQ Em^2. There was an increase in E-cadherin, actin and β–catenin expression in DLKP-SQ Em^2. DLKP-SQ Eprom expressed YFP. No change in any cytokeratin expression was detected between the cell lines. GAPDH was used as a loading control, n=2 (B) Densitometry showed a significant increase in actin and β–catenin protein in DLKP-SQ Em^2 compared to DLKP-SQ and DLKP-SQ Eprom cells. **p<0.005, ***p<0.0005, n=3

4.1.7 Expression of epithelial markers in DLKP-M, DLKP-M Eprom and DLKP-M Em^2

We hypothesised that DLKP-M cells, like DLKP-SQ, would incorporate the E-cadherin gene and that E-cadherin protein would be present at the cell membrane. This would cause DLKP-M cells to undergo MET and result in a more stable cell phenotype, reducing the mesenchymal and migratory properties of the cells. DLKP-M subclonal 3D culture data (presented in section 3.1.5) indicated that this was not the case. DLKP-M and DLKP-M subclones were grown in 2D cultures and immunofluorescence was carried out to investigate the localisation of epithelial cell markers. Western blotting was used to quantify any possible changes in protein expression.

When examined by immunofluorescent using an anti-E-cadherin antibody, weak cytoplasmic staining of E-cadherin protein was observed in DLKP-M, DLKP-M Eprom and DLKP-M Em^2. There was no evidence of membrane bound E-cadherin-YFP fusion protein in DLKP-M Em^2 subclones (Figure 4. 0.14). This was unexpected as the DLKP-M Em^2 cells previously displayed high levels fluorescence by FACS which indicating the presence of YFP protein (see Appendix). The level of E-cadherin protein expression was investigated by western blot. Both an E-cadherin and YFP antibody were used to probe all three cells lines. DLKP-M, DLKP-M Eprom and DLKP-M Em^2 showed no detectable levels of E-cadherin (Figure 4. 0.15).

When examined by immunofluorescence using a YFP antibody DLKP-M cells did not display YFP staining (Figure 4. 0.14). In contrast DLKP-M Eprom displayed cytoplasmic YFP expression indicating that the E-cadherin promoter was

functioning correctly and driving YFP transcription and downstream protein expression successfully. Western blotting supported this result and strong YFP protein expression was detected in DLKP-M Eprom cells (Figure 4. 0.15). DLKP-M Em^2 cells stained for YFP displayed very dull cytoplasmic protein expression (Figure 4. 0.14). However, this YFP protein was not detected by western blot of DLKP-M Em^2 cells (Figure 4. 0.15).

The expression of other proteins associated with the epithelial phenotype and EMT progression such as actin, β-catenin and cytokeratins were investigated in the DLKP-M subclonal populations. Immunofluorescence and western blotting for all three proteins in DLKP-M Eprom and DLKP-M Em^2 subclones did not indicate any change compared to DLKP-M clones (Figure 4. 0.14). Actin expression was dispersed throughout the cytoplasm with no evidence of re-polarisation and no increase in protein expression by western blot (Figure 4. 0.15). β-catenin protein expression was localised throughout the cytoplasm with some weak membrane localisation (Figure 4. 0.14). There was no change in β-catenin expression levels between the subclones by western blot (Figure 4. 0.15). Similarly with cytokeratin, no difference in protein localisation was evident by immunofluorescence and no increased in protein expression was present by western blot between DLKP-M and Eprom and Em^2 subclones. Cytokeratin protein expression was dispersed throughout the cytoplasm. No distinct pattern was discernible in the membrane staining (Figure 4. 0.14, Figure 4. 0.15).

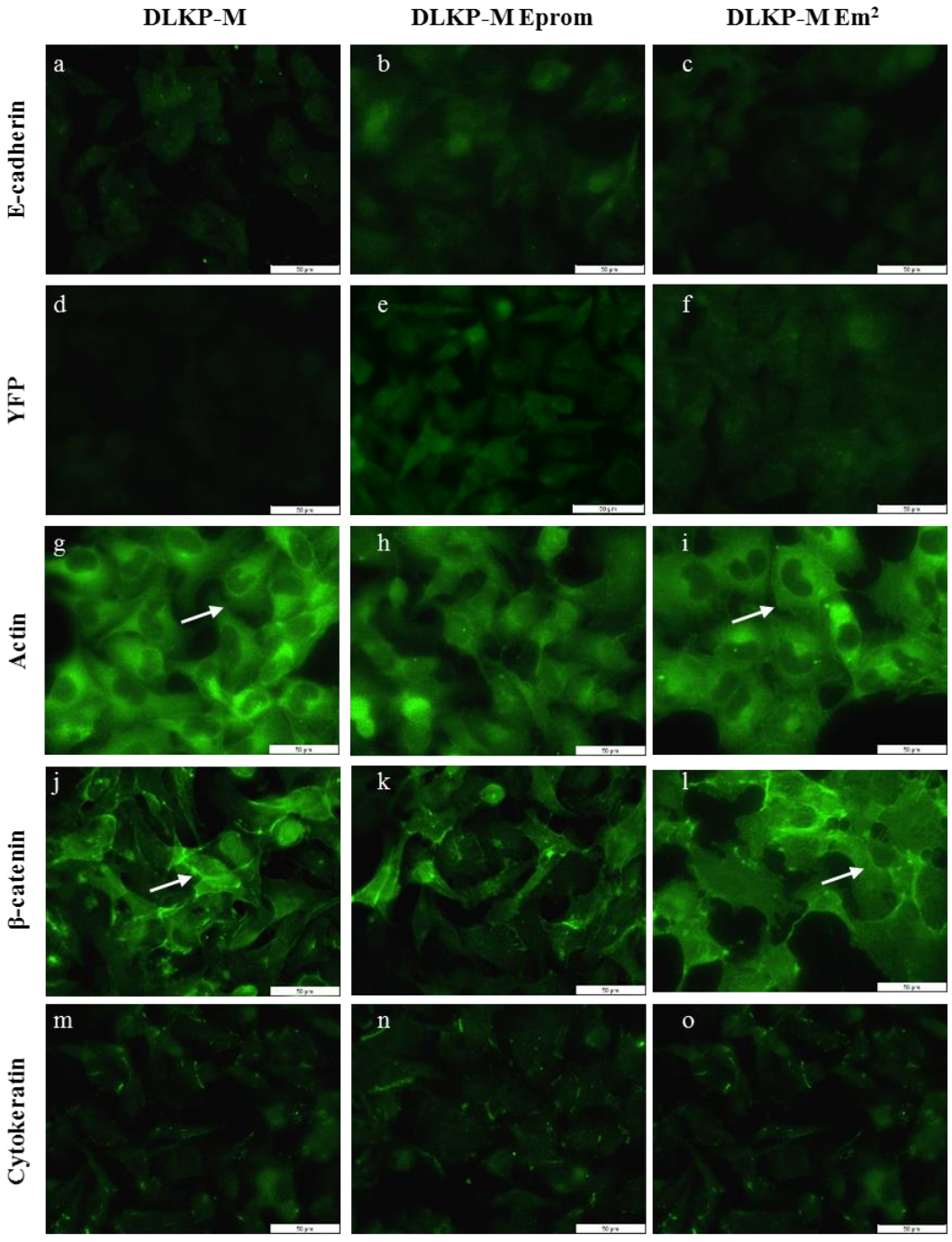
DLKP-M
DLKP-M Eprom
DLKP-M Em²
E-cadherin
YFP
Actin
β-catenin
Cytokeratin
a
b
c
d
e
f
g
h
i
j
k
l
m
n
o

Figure 4. 0.14 DLKP-M subclones do not display altered adhesion junction proteins and cytoskeletal organisation

Representative micrographs of localisation of E-cadherin, YFP, Actin, β-catenin and cytokeratin in DLKP-M, DLKP-M Eprom and DLKP-M Em^2 .E-cadherin was expressed in the cytoplasm of DLKP-M and DLKP-M Eprom and no change in E-cadherin localisation was evident in DLKP-M Em^2 (a-c). YFP was present in the cytoplasm of both DLKP-M Eprom and Em^2 cells (d-f). Actin was expressed in the cytoplasm of DLKP-M cells with no change in DLKP-M Eprom and Em^2 (g-i). β-catenin was localised at the membrane of DLKP-M, DLKP-M Eprom and Em^2 cells. (j-l). Cytokeratin expression was dull and cytoplasmic in DLKP-M, DLKP-M Eprom and DLKP-M Em^2 (m-o). All scale bars represent 50uM, n=2

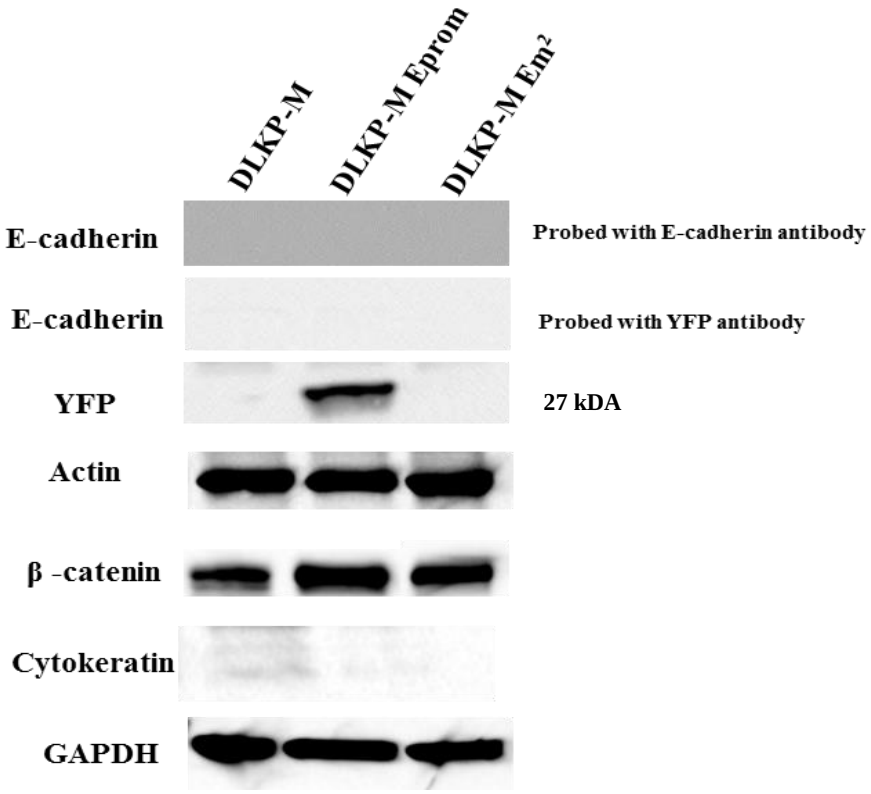

Figure 4. 0.15 Western blot of adherens and cytoskeletal proteins in DLKP-M, DLKP-M Eprom and DLKP-M Em^2 cells

Representative western blots of E-cadherin, YFP, Actin, β –catenin and cytokeratin in DLKP-M cells following transfection of Eprom and Em^2 constructs. There was no detectable E-cadherin bands in DLKP-M and DLKP-M Eprom cells and no increase in E-cadherin protein expression in DLKP-M Em^2. YFP protein was present in DLKP-M Eprom cells. There was no difference in Actin, β –catenin or cytokeratin expression. GAPDH was used as a loading control, n=3

4.1.8 Expression of tight junction proteins in DLKP-SQ and DLKP-M clones and subclones

Tight junction protein expression is indicative of the epithelial cell phenotype. We examined if any changes in TJP expression occurred following transfection of the E-cadherin gene in DLKP-SQ and DLKP-M cells.

Significant differences in the expression of TJP was observed between DLKP-SQ and DLKP-M clones, as previously stated (chapter 3). The DLKP-SQ cells expressed claudin-1, afadin and ZO-1 while DLKP-M cells do not. No change in TJP expression was observed following re-introduction of the E-cadherin gene. CD2AP was the only tight junction protein examined that was expressed in both DLKP-M and DLKP-SQ cell lines (Figure 3.0.2).

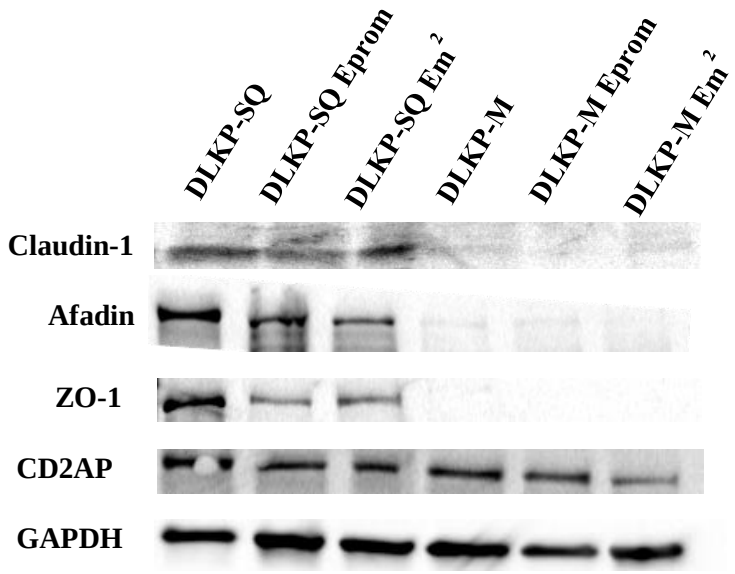

Figure 4.0.16 Western blot of tight junction proteins in DLKP-SQ, DLKP-SQ Eprom, DLKP-SQ Em2, DLKP-M, DLKP-M Eprom and DLKP-M Em2.

Representative western blots of and CD2AP in all DLKP-SQ and DLKP-M clones and subclones. There was no detectable expression of claudin-1, afadin or ZO-1 in DLKP-M, DLKP-M Eprom or DLKP-M Em^2 compared to DLKP-SQ, DLKP-SQ Eprom and DLKP-SQ Em^2. CD2AP was expressed in all cell lines. GAPDH was used as a loading control, n=2

4.1.9 E-cadherin cleavage enzyme expression in DLKP-SQ and DLKP-M clones

The results presented here indicated that DLKP-SQ and DLKP-M clones transfected with Em^2 resulted in very different processing events. E-cadherin-YFP fusion protein was successfully translated and processed to the cell membrane in DLKP-SQ Em^2 subclones. In contrast, immunofluorescence showed that the DLKP-M Em^2 subclones did not express E-cadherin-YFP fusion at the cell membrane and only weak cytoplasmic E-cadherin and YFP expression was detected by immunofluorescence (Figure 4. 0.14). However, flow cytometry data demonstrated that DLKP-M Em^2 subclones were fluorescent indicating that correct gene processing and translation of YFP is occurring in these cells (see Appendix).

Assuming that the YFP-E-cadheirn construct was still functioning correctly in the cells, we postulated that the E-cadherin-YFP gene was correctly translated in DLKP-M Em^2 subclones however, a possible cleavage event may be occurring intracellularly which prevents E-cadherin trafficking to the membrane in these cells. This would account for the low level of E-cadherin and YFP staining by immunofluorescence and the presence of fluorescence by FACS. The gene expression of E-cadherin cleavage enzymes calpain and presenilin were investigated by our collaborators in Dublin City University (Dr. Helena Joyce). Subsequent analysis of the results indicated a significant increase in both calpain and presenilin enzymes in DLKP-M compared to DLKP-SQ (Figure 4.0.17).

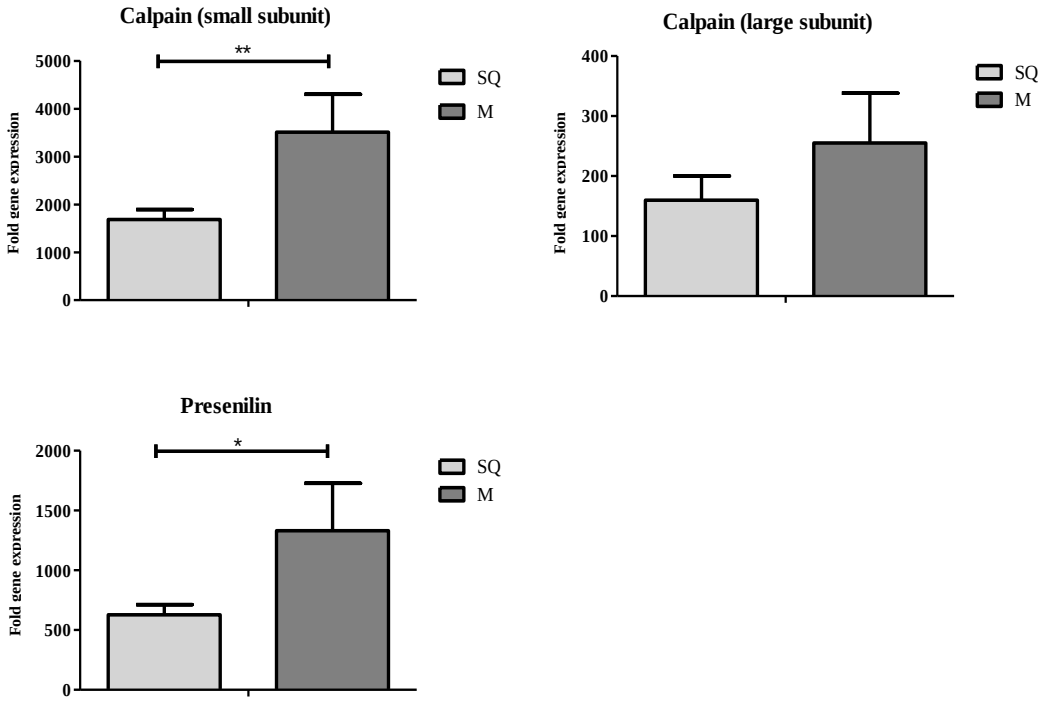

Figure 4.0.17 Gene expression of calpain and presenilin in DLKP-SQ and DLKP-M clones

Representative graphs of calpain and presenilin expression following gene expression analysis which was carried out in Dublin City University, Ireland. Higher levels of both calpain and presenilin expression were observed in DLKP-M cells compared to DLKP-SQ. * $p < 0.05$. ** < 0.005, n=3

4.2 Discussion

In multicellular organisms, phenotypic plasticity enables normal developmental processes and cellular functions to occur. This dynamic process is sustained in cancer and contributes to the formation of heterogeneous tumour populations (Scheel and Weinberg 2011). In this study, we investigated the cadherin switch in EMT-mediated phenotypic switching in a heterogeneous lung cancer cell line, DLKP.

Both of the DLKP clones studied here, DLKP-SQ and DLKP-M, were E-cadherin null and by using E-cadherin reporter plasmids we demonstrated that these subcloned populations differentially regulate the expression of an E-cadherin transgene. In contrast to DLKP-M cells, DLKP-SQ displayed similar morphology to epithelial cells, lacked E-cadherin processing enzymes and contained the machinery required to correctly process the exogenous E-cadherin gene and express E-cadherin protein at the cell membrane. The expression of membrane-localised E-cadherin protein in transfected DLKP-SQ cells enabled spheroid formation in 3D culture and increased the expression of epithelial-related structural proteins. DLKP-SQ maintained tight junction expression following E-cadherin transfection. No change in TJP expression occurred in DLKP-M subclones. DLKP-M cells expressed N-cadherin at the cell membrane which facilitated spheroid formation. This suggests that the DLKP-SQ clones represent a different stage of the EMT process and that DLKP-M cells have undergone phenotypic re-programming to adopt a more invasive mesenchymal phenotype capable of resisting MET via a switch to N-cadherin expression. Our results suggest that a cadherin switch is involved in EMT-mediated phenotypic switching in this model of lung cancer.

The loss of E-cadherin expression or function causes tumour progression and increased tumour invasiveness in head and neck, breast, lung and liver cancer. As a result, E-cadherin is known as a tumour suppressor protein (Ino et al. 2002; Mao et al. 2008; Wang et al. 2011). As described 1.1.4, E-cadherin is involved in homodimeric interepithelial ADJ complexes which maintains tight epithelial cell contact and the quasi-immobility of the epithelial sheath. E-cadherin acts as a negative regulator of cell motility in this way. In addition, the loss of E-cadherin at the cell membrane is a hallmark of EMT and the adoption of motile, invasive cell properties. Previous experiments in the lab using E-cadherin reporter plasmids (Eprom and Em^2) transfected into DLKP-SQ and DLKP-M cells showed that E-cadherin introduction did not have any effect on cell proliferation. Following six days in culture, proliferation rates remained unchanged between DLKP-SQ, DLKP-M and the subclonal populations (Dr. Emer Molloy, O'Dea lab, unpublished data). Additional experiments highlighted that despite not altering cell proliferation, introduction of the E-cadherin gene caused actin re-polarisation at the cell membrane of DLKP-SQ cells. This is a common characteristic of epithelial cells indicating that E-cadherin restoration could promote a switch in cell phenotype toward a more epithelial-like cell.

Given that E-cadherin is a tumour suppressor protein, downregulation of E-cadherin is involved in the induction of EMT-mediated tumour progression and the preliminary data from the lab regarding altered structural protein expression following E-cadherin restoration, we used the same reporter plasmids to investigate the role of EMT as a mechanism of phenotypic switching between DLKP-SQ and DLKP-M cells. The functionality of the reporter plasmids was determined by FACS following transfection and sub-cloning of DLKP-SQ and DLKP-M clones to

generate DLKP-SQ Eprom, DLKP-SQ Em^2, DLKP-M Eprom and DLKP-M Em^2. A significant increase in fluorescence was present in the transfected subclones compared to DLKP-SQ or DLKP-M cells. It is worth noting that reduced fluorescence was evident in the Em^2 subclones compared to Eprom subclones. The exact reason for this is unknown but we speculate that the reduced MFI could be attributed to the larger gene size in these cells compared to YFP.

Spheroid culture represents a more physiologically relevant culture environment and we hypothesised that the cells would form spheroids. DLKP-M and the subclones DLKP-M Eprom and DLKP-M Em^2 formed spheroids in 3D culture. However, further investigation into the cell adhesion molecules responsible for spheroid formation in DLKP-M cells demonstrated that the mesenchymal cell marker N-cadherin was involved (Figure 4. 0.10). This ADJ protein was localised at the membrane of the DLKP-M Em^2 cells by immunofluorescence. In addition, the spheroids possessed extended cytoplasmic processes and appeared to be larger than the DLKP-SQ Em^2 spheroids. N-cadherin expression was absent from DLKP-SQ and DLKP-SQ subclones. DLKP-SQ Em^2 subclones formed discrete, distinct spheroids with smooth regular boundaries with membrane-localised E-cadherin-YFP fusion protein expression (Figure 4.0.3). The expression of N-cadherin by the DLKP-M clones support the hypothesis that these cells have progressed further along the EMT axis to become more invasive and mesenchymal compared to E-cadherin. The switch between E-cadherin and N-cadherin expression is a characterised and well-characterised event during EMT and tumour progression (Gravdal et al. 2007; Hazan et al. 2004).

As DLKP-SQ cells are E- and N-cadherin null, the fact that no large spheroids form in the DLKP-SQ and DLKP-SQ Eprom suggests that interactions between cell

adherens molecules are required for the formation of spheroids *in vitro.* The presence of either E-cadherin in the case of DLKP-SQ Em^2 cells or N-cadherin in DLKP-M, DLKP-M Eprom and DLKP-M Em^2 cells appeared to mediate spheroid formation. Previous studies of the mouse mammary epithelial cell lines EpH4 and SCP2 also highlighted the role of the cell adherens junction proteins in spheroid formation (Somasiri et al., 2000).

Both normal and neoplastic tissues have been shown to form spheroids in different 3D culture techniques and our results indicate that the divergent populations DLKP-SQ and DLKP-M can both form spheroids, albeit by the presence of different cell adhesion molecules. The formation of spheroids in DLKP-SQ Em^2 cells can be viewed as a normal process driven by the epithelial cell adhesion molecule E-cadherin. Due to the size and nature of the DLKP-M spheroids, we hypothesise that these structures represent mesenchymal spheroids whose formation is mediated by N-cadherin. We conclude that these findings supported the hypothesis that DLKP-SQ cells represent a more epithelial-like cell phenotype and that DLKP-M have undergone phenotypic re-programming to downregulate tight junction protein expression, express mesenchymal cell markers and form large spheroid structures with extended neurite-like processes.

We hypothesised that E-cadherin introduction into DLKP-SQ cells would result in E-cadherin expression at the membrane and the subsequent induction of MET. E-cadherin protein tagged with YFP was localised at the cell membrane in both 3D and 2D cell cultures. E-cadherin was present as the characteristic "chicken-wire" pattern (Figure 4.0.6, Figure 4.0.12). To support this result, western blotting using both an E-cadherin and YFP antibody detected a 150kDA band, indicative of the E-cadherin-YFP fusion protein. These results show that the E-cadherin null DLKP-

SQ clonal cells have retained the machinery required to process the E-cadherin gene and correct transcription and translation results in membrane-bound protein expression of the E-cadherin protein.

MET is the reverse process of EMT. MET results in a more epithelial-associated cell phenotype characterised by expression of E-cadherin at the cell membrane and the loss of invasive mesenchymal properties. The process of MET and re-expression of E-cadherin has been observed in metastatic foci present in lung, liver and brain of primary E-cadherin negative breast cancer tumours (Chao et al. 2010). In addition, metastasis forming MDA-MB-231 mesenchymal cells underwent MET and re-expressed E-cadherin following injection into the fat pad of mice (Chao et al. 2010).. In our study, overexpression of the E-cadherin transgene in DLKP-SQ cells appeared to induce MET and caused increased epithelial-specific protein expression and reorganisation of the cytoskeletal architecture. Alongside the expression of E-cadherin, actin repolarisation and increased expression of membrane localised β-catenin was evident by immunofluorescence (Figure 4.0.12). Elevated levels of actin and β-catenin expression were also demonstrated by western blot and confirmed by densitometry. We postulate that the introduction of the E-cadherin gene stimulated increased actin and β-catenin production in the cells during the onset of MET. This enabled increased exocytosis of the cell adherens junction and increased stabilisation of the complex. High levels of actin and β-catenin facilitated association of the structural proteins with E-cadherin and recruitment to the ADJ to cause re-epithelialisation of DLKP-SQ cells.

We conclude that E-cadherin gene introduction and subsequent E-cadherin-YFP fusion protein expression at the cell membrane induced a more epithelial-like cell phenotype in the DLKP-SQ cells. This MET-like process caused by acquisition of

membrane-bound E-cadherin increased cell polarity by elevated actin expression, stimulated increased β-catenin expression and re-organised cytoskeletal architecture. Although the DLKP-SQ clones do not express endogenous E-cadherin protein and thus have developed a carcinogenic phenotype, the cells have maintained the ability to process the E-cadherin gene which links the EMT process with tumour progression in this clonal population.

Transfection of the E-cadherin gene tagged with YFP into DLKP-M cells did not result in a similar process. DLKP-M Em^2 cells did not express the E-cadherin-YFP fusion protein at the cell membrane and no detectable E-cadherin protein or YFP protein was detected by western blot (Figure 4. 0.15). This is in contrast to the obvious E-cadherin-YFP fusion protein expression in DLKP-SQ Em^2 cells. However, the presence of detectable fluorescence by FACS and the expression of weak cytoplasmic YFP protein by immunofluorescence in DLKP-M Em^2 cells suggested that YFP was being produced in these cells, if only at a low level.

The Em^2 reporter construct contained the full length mouse E-cadherin gene subcloned into the pEYFP-1 plasmid (Masterson 2008). The stop codon sequence of the E-cadherin gene was mutated to a glycine residue using site directed mutagenesis. This resulted in production of an E-cadherin-YFP fusion protein by transfected cells when correct transcription and translation occurred. As the YFP gene was downstream of the E-cadherin sequence and the E-cadherin gene lacked a functioning stop codon the production of YFP protein in the cells was dependent on E-cadherin protein production and vice versa. Analysis of the fluorescent data generated by DLKP-M Eprom cells demonstrated that the E-cadherin gene promoter was functioning correctly. These cells contained the Eprom construct in which the mouse E-cadherin promoter was driving YFP gene transcription. YFP

was localised in the cytoplasm of these cells by immunofluorescence and YFP protein was detected by western blot. This excluded any problems with transcription of the E-cadherin promoter in the DLKP-M Em^2 cells.

While DLKP-M Em^2 cells displayed weak E-cadherin expression in the cytoplasm by immunofluorescence, we postulated that this E-cadherin is not functional as it has not been processed correctly and exported to the membrane to form ADJ. Further evidence that no functional E-cadherin protein was produced in the DLKP-M Em^2 was provided by examining epithelial-related structural proteins by immunofluorescence (Figure 4. 0.14). Actin expression remained cytoplasmic and no repolarisation was evident in the DLKP-M Em^2 subclones. This was in direct contrast to DLKP-SQ Em^2 cells where cortical actin was localised at the cell membrane and levels of actin protein were increased compared to DLKP-SQ cells (Figure 4. 0.13). The level of β-catenin protein expression and β-catenin localisation also remained unchanged between DLKP-M, DLKP-M Eprom and DLKP-M Em^2. Again, this was the opposite of what was observed in the DLKP-SQ Em^2 subclone.

We originally hypothesised that DLKP-M would undergo MET following E-cadherin gene re-introduction and resemble DLKP-SQ cells more closely. Assuming the reported plasmid was still expressed correctly in these cells, we conclude that DLKP-M did not process the E-cadherin gene as hypothesised. Overexpression of E-cadherin in DLKP-M cells did not cause MET and there was no change in E-cadherin expression at the cell membrane, epithelial-associated protein expression or tight junction protein expression. We conclude that DLKP-M cells have undergone a cadherin switch to express the mesenchymal marker N-cadherin and may have lost or supressed the ability to correctly process the epithelial-related E-cadherin gene.

Given the results thus far, we hypothesised that the E-cadherin-YFP fusion protein was being produced in the DLKP-M Em^2 but that subsequent post-translational modifications prevented correct downstream processing of the fusion protein. Assuming that the FACS analysis was robust and that the Em^2 plasmid was functioning correctly, we speculated that post-translational cytoplasmic cleavage of the E-cadherin-YFP fusion protein was taking place. This would cause degradation of the E-cadherin protein and would account for the low level of both E-cadherin and YFP expression detected in the cytoplasm by immunofluorescence and the fluorescence evident in the DLKP-M Em^2 subclonal population by FACS. Post-translational control of E-cadherin occurs through a variety of different processes and these changes have been linked to neoplastic transformation and cancer progression, as reviewed in (Masterson and Dea 2007). While cleavage of pro-E-cadherin by the subtilisin-like proprotein convertase is essential for E-cadherin activation and trafficking to the cell membrane, additional cleavage events have been shown to disrupt E-cadherin mediated cell adhesion (Hirohashi 1998). Nascent E-cadherin is trafficked from the trans-Golgi network with catenins for incorporation as cell adherens junctions. In our cell model, it appears that E-cadherin is cleaved before exocytosis to the cell membrane occurs. We hypothesise that enzymes such as calpain or presensilin-1 (PS-1) could be involved in this intracellular cleavage event.

E-cadherin cleavage by calpain occurs upstream of the β- and α-catenin binding domains on the cytoplasmic tail of E-cadherin. The calpain cleavage site is between residues 782-787 which are present in the full length E-cadherin gene used in this construct (Rios-Doria et al. 2003). This cleavage event would release the full length YFP protein into the cytoplasm. The E-cadherin antibody used in these experiments

detects the C-terminal tail of the E-cadherin protein between residues 735-883. We postulate that a segment of the cleaved E-cadherin C-terminal tail is detected in the cytoplasm by this antibody following immunofluorescence (Figure 4. 0.14). The protein expression was possibly too weak to be detected by western blot. It is common for antibodies to detect shorter cleaved products and this E-cadherin antibody can detect the cleaved products such as 24kDA, 29kDA, 35kDA fragments which occur in MDCK cells following the addition of staurosporine (Steinhusen et al. 2001). We detected weak cytoplasmic staining of YFP by immunofluorescence in 2D culture using an antibody reactive to the full length YFP. This YFP protein was not detected by western blot. This could be because the YFP signal was too weak in DLKP-M Em^2 cells or perhaps the remaining C-terminal residues attached to the YFP protein following calpain cleavage resulted in protein degradation or masking of antibody epitopes.

The cytoplasmic processing and cleavage of E-cadherin-YFP fusion protein could also be due to PS-1. This enzyme has been shown to cleave E-cadherin between residues Leu731 and Arg732 at the interface with the cell membrane. These residues are present in the Em^2 E-cadherin reported construct used in these experiments. Cleavage by PS-1 disassembles the E-cadherin-catenin complex and prevents expression of the correct ADJ at the cell membrane. As previously stated the E-cadherin antibody used in these experiment detects the C-terminal tail of the E-cadherin protein between residues 735-883, which would be undisturbed following presenilin-mediated cleavage. This accounts for the dull cytoplasmic staining of E-cadherin found in the DLKP-M Em^2 cells as this hypothesis would cause cytoplasmic accumulation of the cleaved E-cadherin fragment (Figure 4. 0.14).

Our hypothesis regarding calpain- or presenilin-mediated cleavage of intercellular E-cadherin in DLKP-M Em^2 is supported by gene expression analysis of the DLKP clones. This work was carried out by our colleagues in Dublin City University and the results showed a significantly higher level of calpain and presenilin expression in DLKP-M cells compared to DLKP-SQ cells (Figure 4.0.17). This result also supports the hypothesis that DLKP-SQ cells are a more epithelial-associated cell population as they do not express a high level of this E-cadherin cleavage enzyme.

Alternatively, the Em^2 plasmid may have stopped functioning correctly in these cells. An important future experiment to address this question would be to isolate RNA from the DLKP-SQ Em^2 and DLKP-M Em^2 cells and carry out rt-PCR to confirm that the YFP message was still present. In addition, FACS analysis should be repeated to ensure that the same level of fluorescence was present in the cell population and that transient loss of the plasmid had not occurred over time. Additional clonal expansion experiments of the mixed populations of fluorescent DLKP-SQ and DLKP-M subclones would ensure that no discrepancies or errors have been introduced over the course of this project.

To conclude, the DLKP-M cell line appear to have developed a mechanism to suppress the expression of E-cadherin at the cell membrane thus preventing any EMT-mediated phenotypic switching. Assuming that the plasmids are functioning correctly, we speculate that DLKP-M cells could use E-cadherin cleavage enzymes to prevent normal E-cadherin membrane localisation. The ability to repress E-cadherin protein trafficking to the membrane prevented the cells from undergoing a MET-like process similar to DLKP-SQ Em^2 cells. These results also supported the hypothesis that DLKP-M clones represent a more invasive tumour grade that

have progressed along the EMT axis and exist as a mesenchymal, invasive population.

In summary, we have shown that DLKP-SQ and DLKP-M cells represent two different populations along the EMT axis. The changes that occur during EMT can induce phenotypic switching both in normal and neoplastic development and here, we have shown that a switch to N-cadherin expression during EMT is an important process involved in phenotypic switching between two heterogeneous subpopulations of a lung cancer cell line. The definition of an epithelial cell is one that possesses tight junctions, cell polarity between apical and lateral domains, maintains cell interactions with neighbouring cells and displays a pseudo-immobility between itself and the microenvironment (Savagner 2007). Based on these definitions, our results indicate that DLKP-SQ, as opposed to DLKP-M cells, possess more epithelial-associated traits. The ability of DLKP-SQ cells to successfully process the transfected E-cadherin transgene to induce E-cadherin protein expression at the cell membrane further supports this hypothesis.

Further characterisation of these clones would be beneficial and provide further insights into the re-programming events that have occurred to give rise to the different cell phenotypes. This would provide important information regarding potential therapeutic targets for cancer treatments.

Future experiments in this project should investigate the effect of the E-cadherin reporter plasmids in DLKP-I clones. These cells express N-cadherin, similar to DLKP-M but lack E-cadherin. They represent an EMP population between DLKP-SQ and DLKP-M on the EMT axis. Transfection of DLKP-I cells would further elucidate where on the cadherin axis this “intermediate” population exists. Future

experiments should also address the potential cleavage events and downregulation of the E-cadherin protein which occurs in DLKP-M cells following E-cadherin overexpression.

The DLKP cell line was harvested from a primary lymph node metastasis of a primary poorly differentiated lung cell carcinoma (Law et al. 1992). This finding itself demonstrates that the cells of the DLKP parental population must possess the ability to undergo EMT and disseminate from the primary lung tumour. These cells were capable of migrating through the body and interacting with extracellular matrix proteins to undergo some form of MET and establish a metastatic site at a new location, the lymph node in this instance. The results presented here and in chapter 3 demonstrate that the DLKP subpopulations are a unique and dynamic model of studying EMT-mediated phenotypic switching in heterogeneous lung cancer cell line (Figure 4.0.18). Understanding the mechanisms controlling this process is important for the development of more clinically relevant cancer therapeutics directed against heterogeneous tumours.

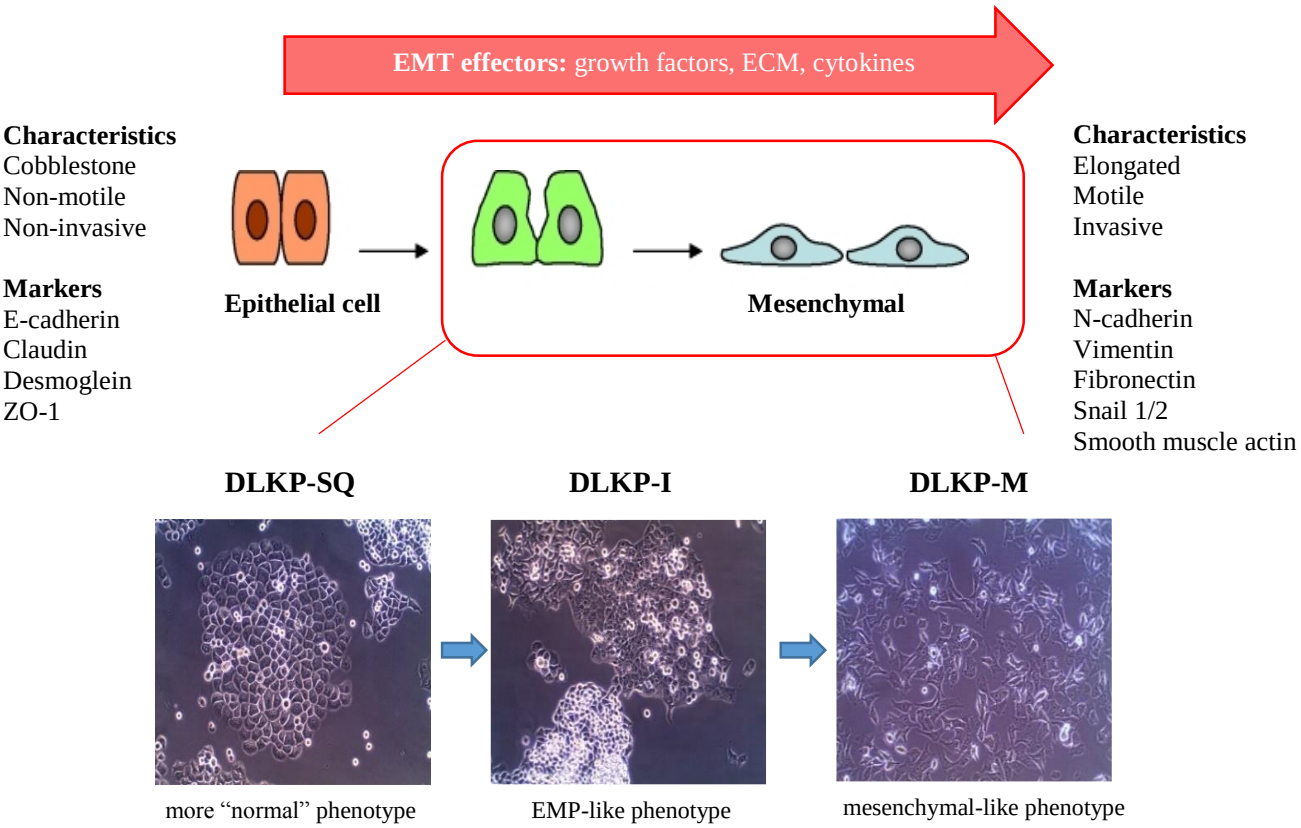

Figure 4.0.18 DLKP clones represent different stages of EMT

DLKP-SQ cells present a more "normal" epithelial phenotype in the early stages of EMT-mediated phenotypic switching. DLKP-I cells represent an EMP-like phenotype with a hybrid of epithelial and mesenchymal characteristics. DLKP-M cells represent late-stage EMT and possess mesenchymal-like markers and an elongated, motile phenotype. Modified from SpringerImages.

Chapter 5

Mapping the BMP Pathway in healthy porcine airways and investigating the role of a BMP signalling gradient in the lung epithelium

5.1 Introduction

The development of the lungs from an amniotic fluid-filled sac in the embryo to a complex arborized respiratory system responsible for oxygenation of the blood is a finely tuned and complicated process. Growth factors and morphogens such as Fibroblast Growth Factor (FGF), Wnt-βcatenin, Notch and Bone Morphogenetic Proteins (BMP) produced by the underlying mesoderm and developing endoderm form a complex signalling network co-ordinating this developmental processes. BMP signalling, specifically, orchestrates the branching events in the nascent lung and the correct epithelial cell distribution along the proximal-distal axis (Alejandre-Alcázar et al. 2007; Weaver et al. 1999; Weaver, Dunn, and Hogan 2000).

While BMP signalling in the developing lung has been extensively studied, BMP pathway expression in healthy airways remains largely unaddressed. A study by

Kariyawasam et al. 2008 demonstrated the presence of BMP ligands and receptors in the lung epithelium of healthy human subjects. Similar expression of BMP ligands, BMPRIb and BMPRII was found in the bronchial epithelium of healthy mice (Rosendahl et al. 2002). This is in contrast to studies of the mouse lung epithelium which showed a BRE-eGFP reporter was barely detectable and pSMAD 1/5/8 expression was absent in the airways of healthy adult mice (Sountoulidis et al. 2012). In inflammatory and fibrotic lung diseases, there is growing evidence that the BMP pathway becomes re-activated and is involved in the repair of the damaged epithelium and/or perpetuating the disease phenotype (Koli et al. 2006; Masterson et al. 2011; Mccormack et al. 2013; Rosendahl et al. 2002). Despite the importance of BMP signalling during epithelium repair and disease, BMP signalling during adult airway homeostasis and the concept of BMP signalling gradients existing along the respiratory tract remains largely unexplored.

We hypothesise that the BMP signalling pathway is active during adult lung homeostasis. We set out to map the expression of BMP ligands, SMAD signalling molecules and antagonists of the BMP pathway in the descending lung epithelium of a large animal model. In addition, we aim to investigate the function of BMP signalling gradients in the lung epithelium and explore the role of BMP signalling in differentiated lung epithelium.

To address our aim in a large animal model, we used porcine lungs due to the comparative lung size, physiology, anatomy and biochemistry between adult human and pig lungs (Judge et al. 2014; Rogers et al. 2008)

5.1.1 Examination of lung architecture and histology in the large porcine airways

Porcine lungs were used in this study due to the robust comparative lung biology between pigs and humans. The porcine lung shares similar morphological structure and architecture to the human lung with similar bronchial generations and an inverse relationship between airway diameter and length and bronchial tree bifurcations (Dondelinger et al. 1998; Maina and van Gils 2001).

Porcine lungs were obtained from two local abattoir at Rosderra Irish Meats, Edenderry, Co. Meath and Coogan Meats, Trim, Co. Meath. The porcine lungs were harvested from pigs weighing 70 kg reared in the Irish countryside prior to slaughter. The lungs were removed from the fully grown pigs and transported on ice to the lab in Maynooth University, Maynooth, Co. Kildare, Ireland. Once in the lab, the lungs were submerged in pre-warmed medium, each lobe was dissected and sterile water was used to flush out any residual mucus. Approximately five pig lungs were obtained to learn and improve the dissection technique and carry out the H&E and PAS staining and E-cadherin immunofluorescence.

The large porcine airways were dissected as per the map designed in the O'Dea lab previously by Dr. Eoin Judge (Figure 5.0.1) (Judge et al. 2014). This standardised classification of the porcine airways did not exist prior to the present study. Therefore, alternate classifications of the lung bronchi and bronchioles were assigned for the purpose of this study. The right lung consists of four lobes so the right bronchus was classified numerically according to each lobe, RB1-4. RB1 was described as cranial and caudal branches. The RB4 was separated to superior and inferior sections because of its length. Similar classifications were assigned for LB1

and LB2. Large airway dissections were carried out and subsequent H&E, PAS and immunofluorescence of the sections was performed.

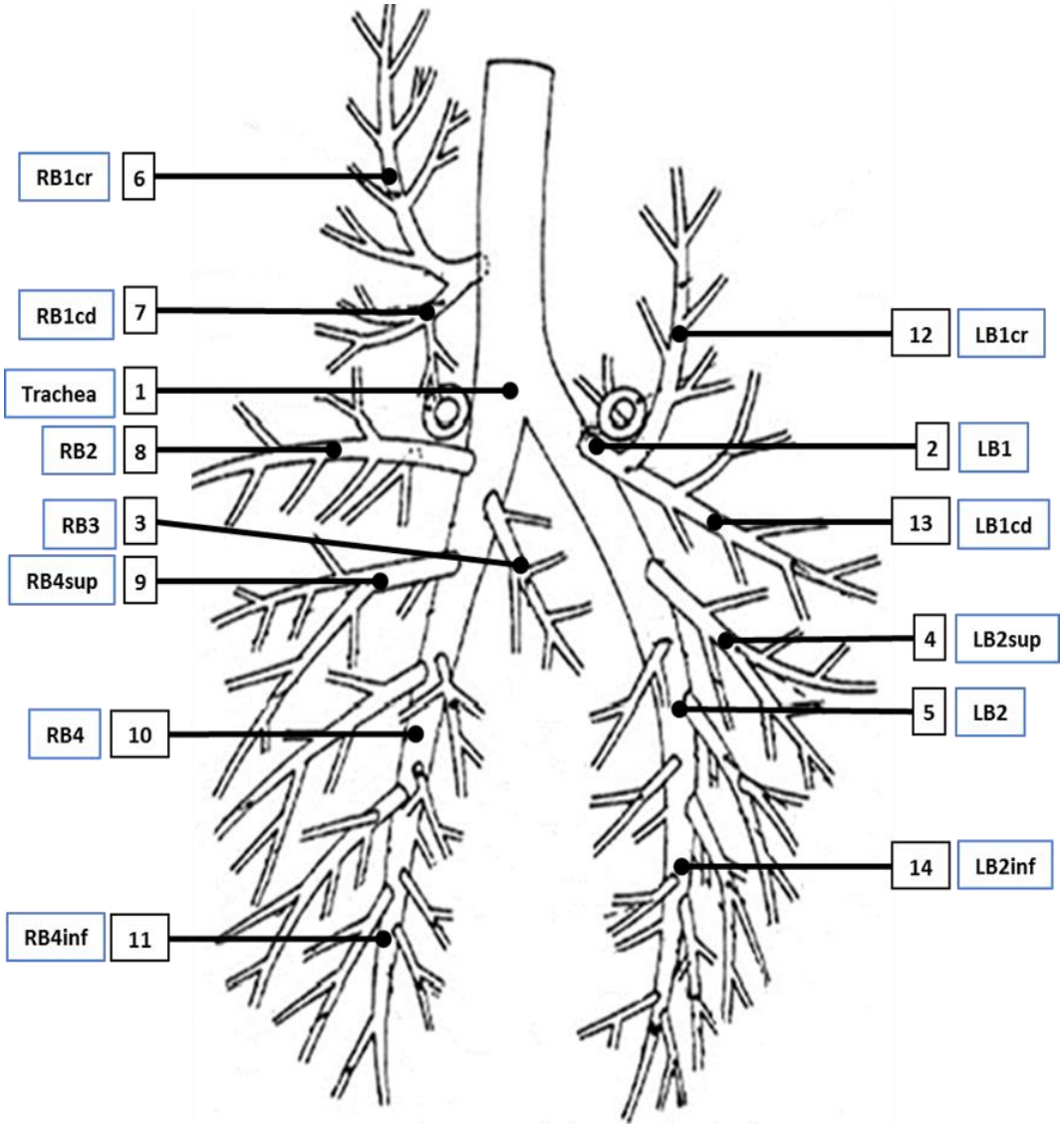

Figure 5.0.1 Map of the large airways in porcine lungs

The four bronchi in the right porcine lobe are divided 1-4. The two bronchi in the left porcine lobe are divided 1-2. Each section is assigned a number from 1-14 for ease of section identification. This map was designed previously in the O'Dea lab by Dr. Eoin Judge.

RB= right bronchus, LB= left bronchus, cr=cranial, cd = caudal, sup=superior, inf = inferior

Using H&E and PAS staining, the architecture of the lung epithelium throughout the airways was examined. The sections were arranged according to decreasing airway size. The progression from pseudostratified columnar epithelium in the trachea to ciliated columnar epithelium lining the small bronchi and bronchioles was observed. The complex nature of the descending lung epithelium was also evident in the sections and the diverse range of epithelial cells could be seen in the sections. Ciliated epithelial cells, basement membrane, basal cells, goblet cells, lamina propria, submucosal glands, smooth muscle cells and underlying connective tissue and cartilage were present in the sections (Figure 5.0.2 -3).

By using PAS staining techniques to detect polysaccharides and mucosubstances such as mucins in the lung epithelium, the frequency of goblet cells and submucosal glands in the descending porcine airways was examined. In the epithelium of the upper airways, there was a large volume of goblet cells and submucosal glands, as evidenced by the positive dark PAS stain (Figure 5.0.2).

The distribution of epithelial cells was examined in the large airways of the pig lung by immunostaining for E-cadherin expression (Figure 5.0.4). The tall, pseudostratified epithelial cells of the trachea and upper airways was clearly visible in sections 1-7. As the airways became narrower and the bronchi develop into smaller bronchioles, the tall pseudostratified epithelial cells developed into ciliated columnar cells, as seen in section 14. These experiments were also performed to optimise the techniques required for subsequent experiments in this study in addition to providing an extensive histological analysis of the lung epithelium in the descending airways of porcine lungs.

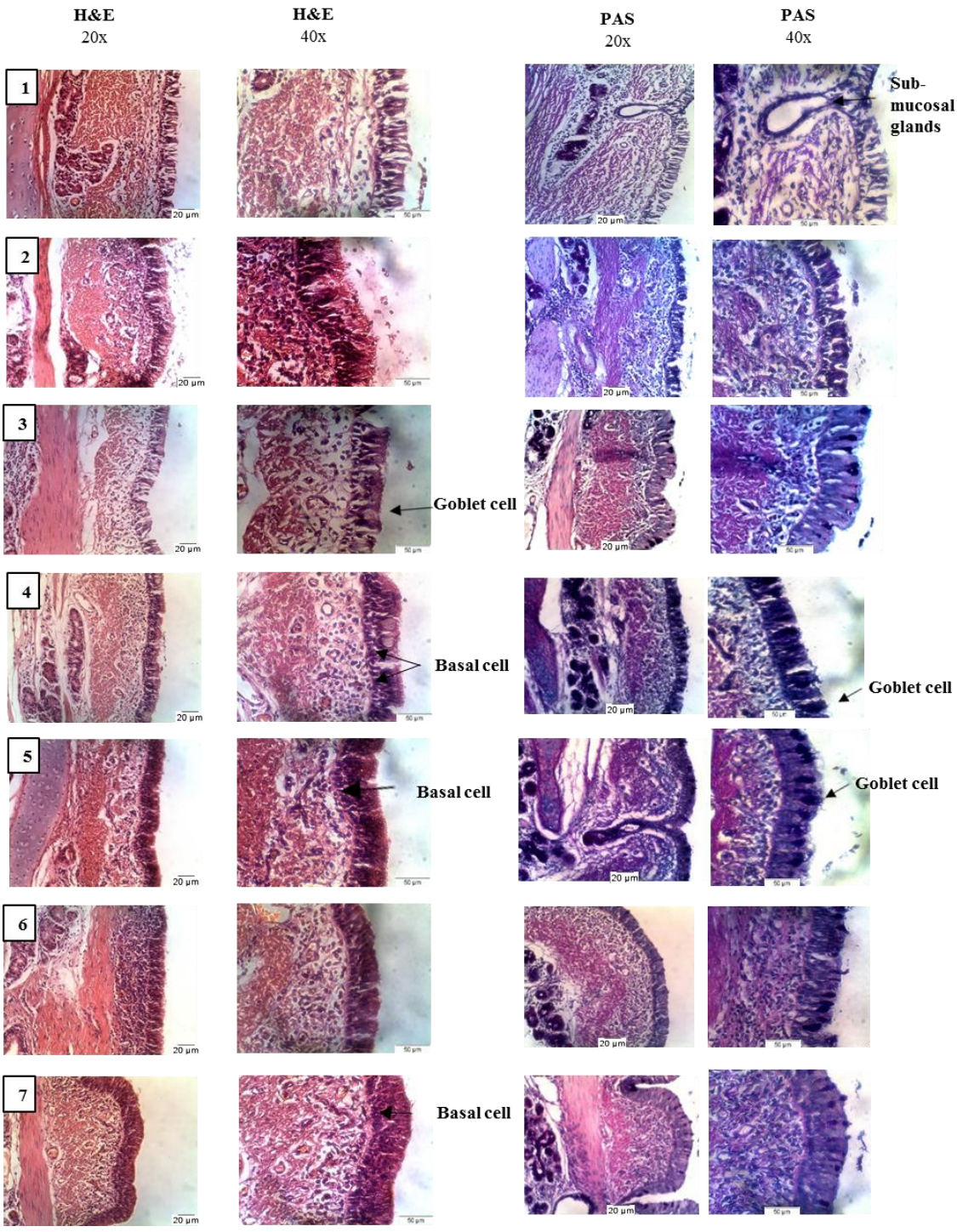

Figure 5.0.2 H&E and PAS staining of large porcine airways arranged according to decreasing size (part I/II)

Representative micrographs of H&E and PAS staining throughout the large porcine airways. Scale bars represent 20uM and 50uM respectively. Sections represent lung regions in figure 5.0.1.

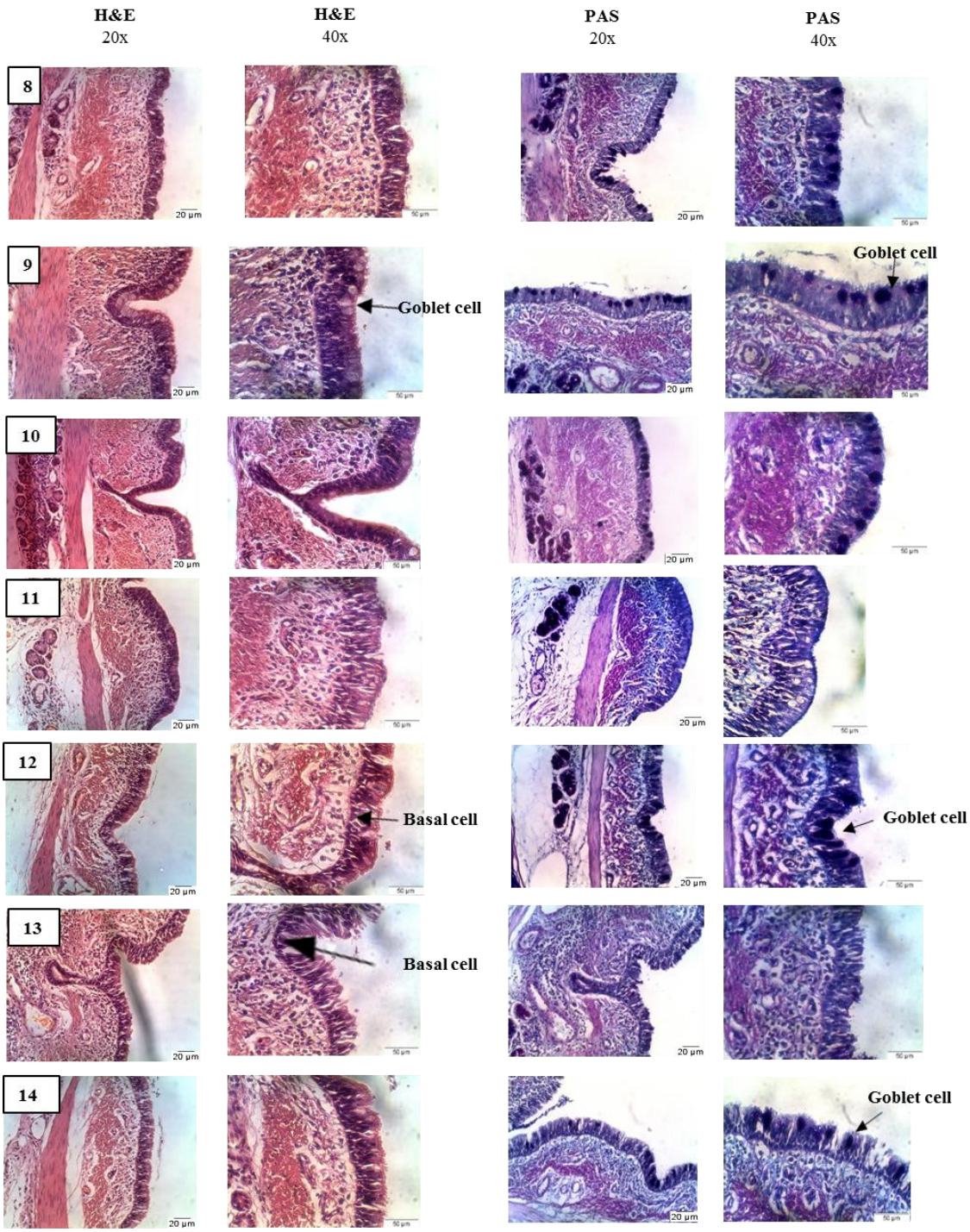

Figure 5.0.3 H&E and PAS staining of large porcine airways arranged according to decreasing size (part II/II)

Representative micrographs of H&E and PAS staining throughout the large porcine airways. Scale bars represent 20uM and 50uM respectively. Sections represent lung regions in figure 5.0.1.

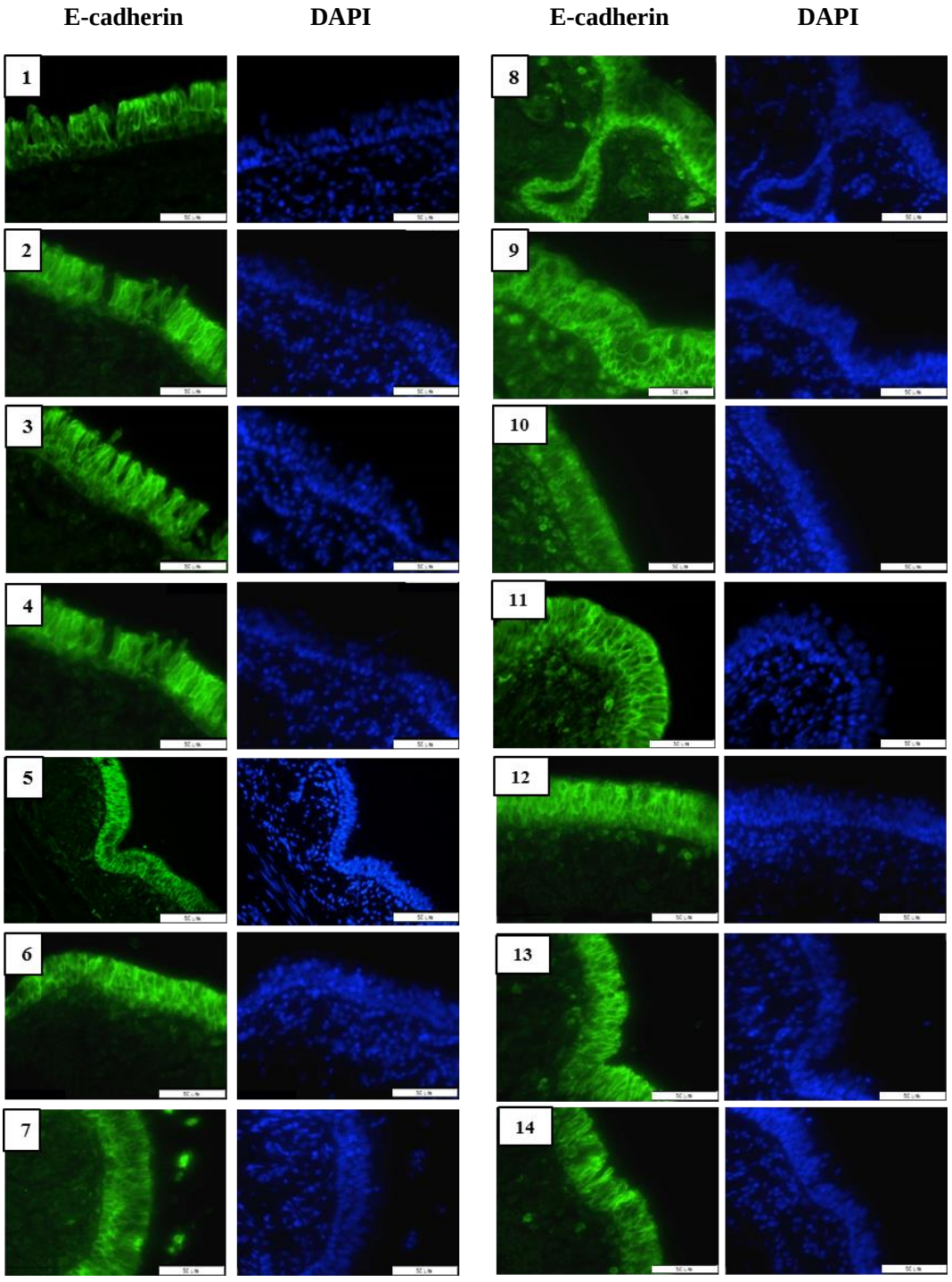

Figure 5.0.4 E-cadherin immunofluorescence staining of large porcine airways arranged according to decreasing size

Representative micrographs of E-cadherin immunofluorescence throughout the large porcine airways. The "chicken-wire" characteristic E-cadherin staining was detected in the descending epithelium. DAPI counterstain is shown in blue. Scale bars represent 50uM. Sections represent lung regions in figure 5.0.1.

5.1.2 Examination of lung architecture in the left cranial bronchus of porcine airways

The left cranial lobe was chosen for our study of the descending airways because of its similarities to the human left cranial lobe and the overlap with another study examining BMP signalling in the left cranial lobe of rhesus macaques (Lynn et al. 2015). To ensure that the tissue remained intact during the experimental procedure histological profiling was carried out on sequential sections of the left cranial bronchus. The sections were characterised as trachea, conduction airways (section2-5) and distal bronchioles (6-9) for the purpose of this study (Figure 5.0.5). Approximately five pig lungs were obtained to perfect the dissection of the left cranial lobe and carry out subsequent processing.

The epithelium and underlying connective tissue of the descending airways remained intact following dissection. Examination of the sections showed the presence of pseudostratified ciliated epithelium descending into ciliated columnar epithelium. There was a reduction in the frequency of goblet cells in the distal epithelium compared to the trachea and upper airways, as demonstrated by the positive dark PAS staining (Figure 5.0.6).

E-cadherin immunofluorescence served as an additional control to ensure that the epithelium remained intact following tissue processing. The characteristic "chicken-wire" pattern of staining around the cell membrane of the epithelial cells was detected by immunofluorescence (Figure 5.0.7). Small cuboidal basal cells lining the basement membrane were also evident in the sections. There was evidence of submucosal glands in the trachea and upper sections of the left bronchus, which are also E-cadherin positive.

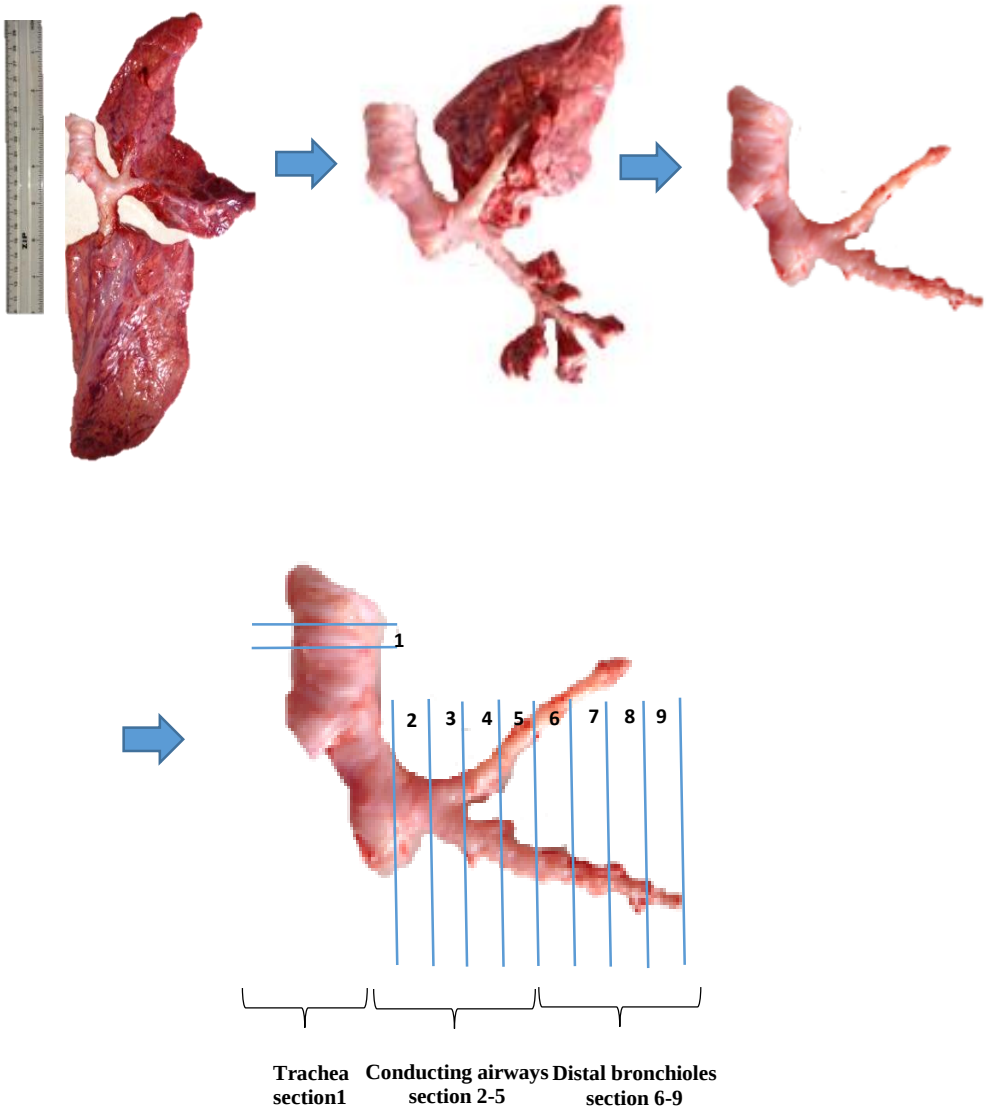

Figure 5.0.5 Sequential sections of the left cranial bronchus

Sequential sections were dissected from the left cranial lobe along the main stem bronchus. Each section was measured to 10mm and subsequently fixed in paraformaldehyde or prepared for RNA or protein harvest. The sequential sections were characterised as trachea, conduction airways (section2-5) and distal bronchioles (6-9) for the purpose of this study.

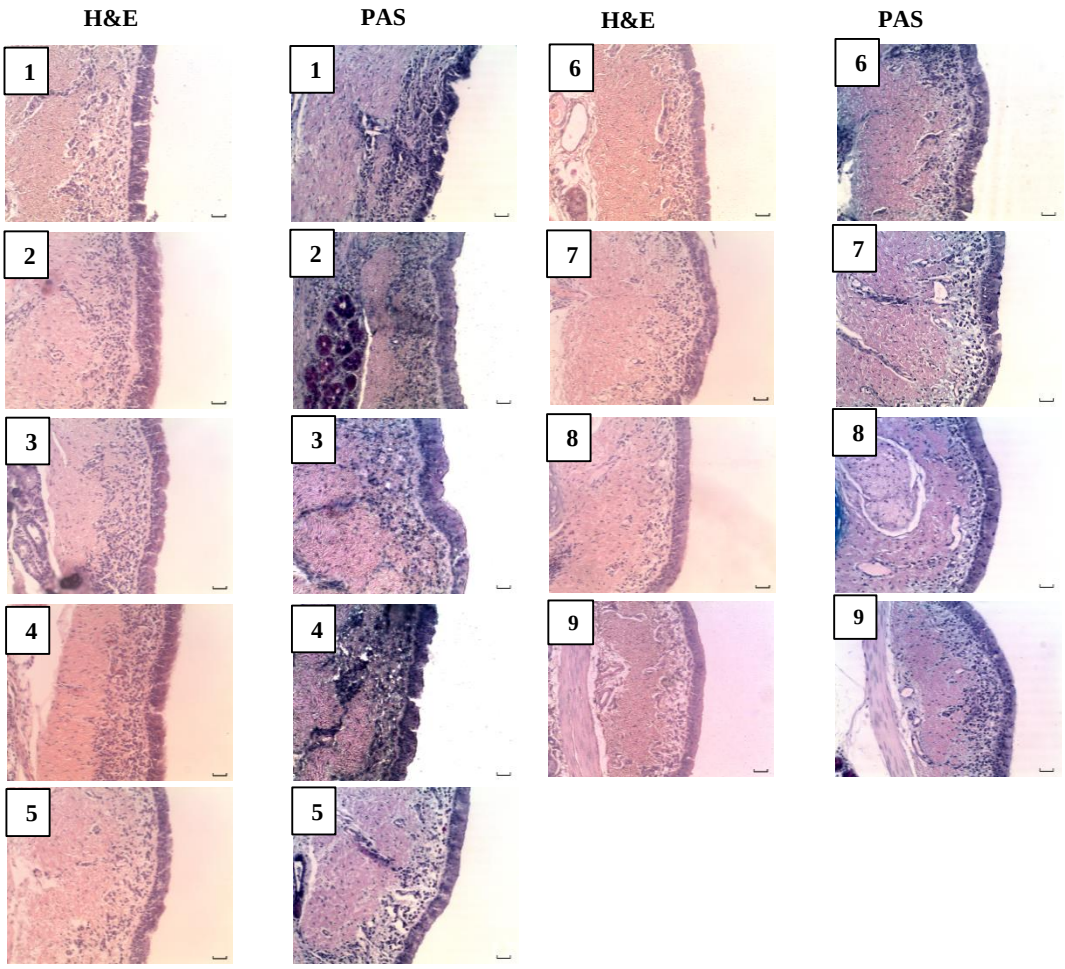

Figure 5.0.6 H&E and PAS staining of descending sections of the left cranial bronchus

Representative images of H&E and PAS staining in the descending left cranial bronchus. Scale bars represent 20uM. Sections represent lung regions in figure 5.0.5.

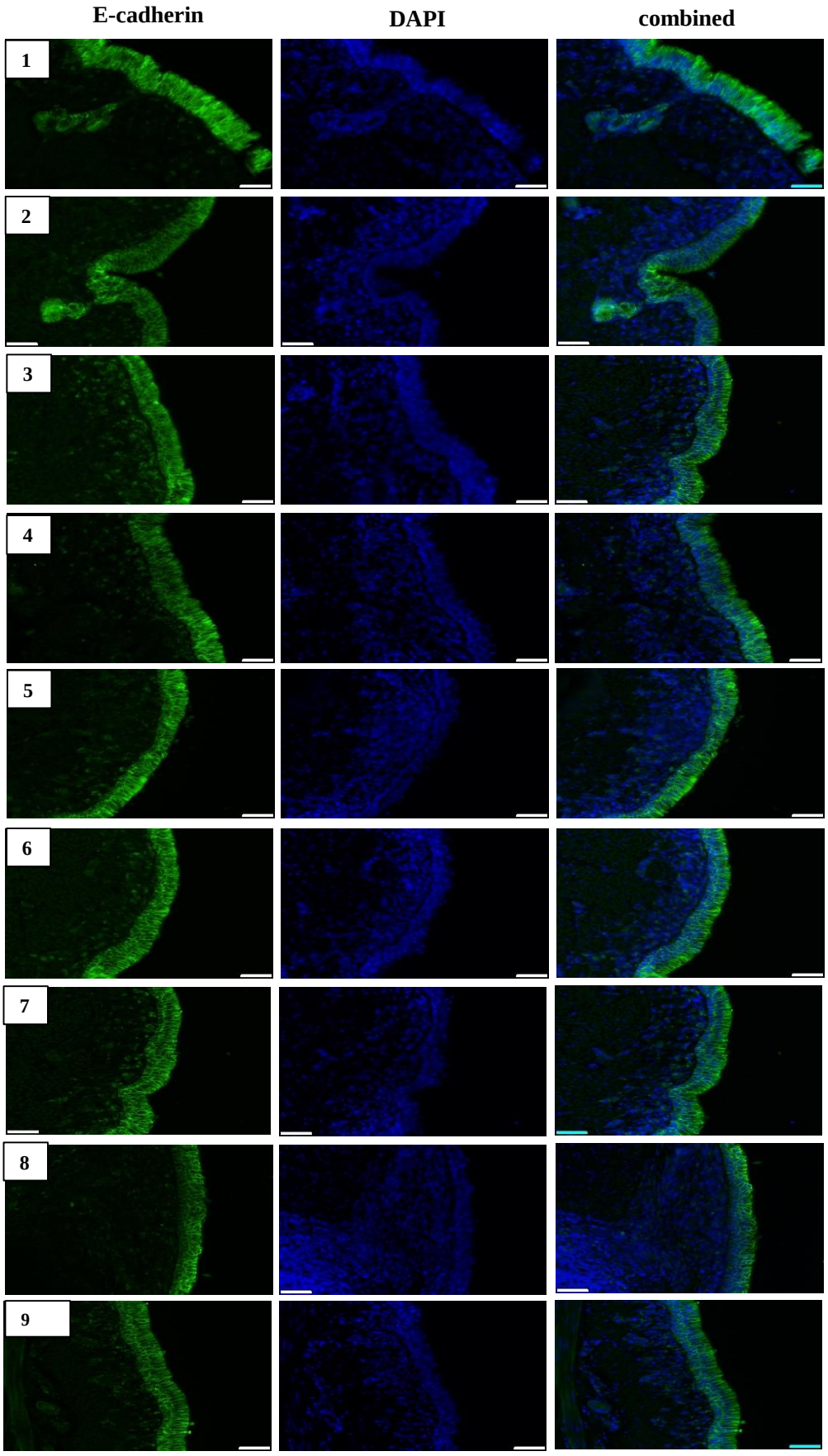

Figure 5.0.7 E-cadherin immunofluorescence staining of descending sections of the left cranial bronchus.

The intact epithelium was detected by the characteristic "chickenwire"-like E-cadherin staining. Scales bars represent 20uM. Sections represent lung regions in figure 5.0.5

5.1.3 Expression of the BMP pathway in healthy descending airways

BMP pathway expression in healthy adult airways remains poorly defined despite extensive research on developing lungs and the emerging role of BMP signalling in lung diseases. To address this question, we set out to map the BMP pathway in healthy adult lung epithelium. The descending lung epithelium in the left cranial porcine bronchus was used (Figure 5.0.5). Protein and RNA were extracted from sequential sections along the length of the left cranial bronchus and the expression of various BMP ligands, receptors, SMADs and pathway inhibitors were examined. The sequential sections were characterised as trachea, conduction airways (section2-5) and distal bronchioles (6-9) for the purpose of this study.

The expression of BMP-2, BMP-4 and BMP-7 mRNA were examined by qPCR, based on existing knowledge that these ligands are involved in lung morphogenesis and are expressed in the bronchial epithelium during inflammatory, fibrotic and malignant lung diseases. There was a significant difference in the expression of all three ligands between the tracheal epithelium and distal epithelium. BMP-2 expression was significantly ($p<0.05$) higher in the distal bronchioles and similarly, BMP-4 expression was significantly increased in conducting airways ($p< 0.05$) compared to the trachea. Conversely, BMP-7 mRNA expression was reduced in the distal bronchioles compared to the trachea ($p<0.005$) (Figure 5.0.8 A).

SMAD-6 and SMAD-7, the inhibitory SMAD proteins were expressed at a higher level in the trachea compared to the distal epithelium ($p<0.005$ and $p<0.05$, respectively). SMAD-4 also known as co-SMAD, is expressed throughout the

bronchial epithelium with elevated mRNA levels present in the trachea compared to the distal bronchioles ($p<0.05$) (Figure 5.0.8 B).

When BMP receptors mRNA expression was investigated in the descending epithelium of the left cranial lobe, there was no evident difference in BMPRIa expression. However, a significant decrease in BMPRIa receptor expression emerged between tracheal epithelium and distal bronchial epithelium ($p<0.05$) (Figure 5.0.8 C).

The levels of gremlin and another common BMP-antagonist called noggin were examined using q-PCR in the descending lung epithelium of the left cranial lobe. The results indicated a significant negative gradient in both BMP antagonist mRNA expression between the tracheal epithelium and the distal bronchial epithelium ($p<0.0005$) (Figure 5.0.8 D). There was also a significant decrease in gremlin and noggin signal expression between the trachea and the conducting airways ($p<0.0005$).

These results indicate that not only is the BMP pathway expressed in the healthy adult epithelium but that significant expression gradients of BMP ligands and antagonists exist throughout the airways.

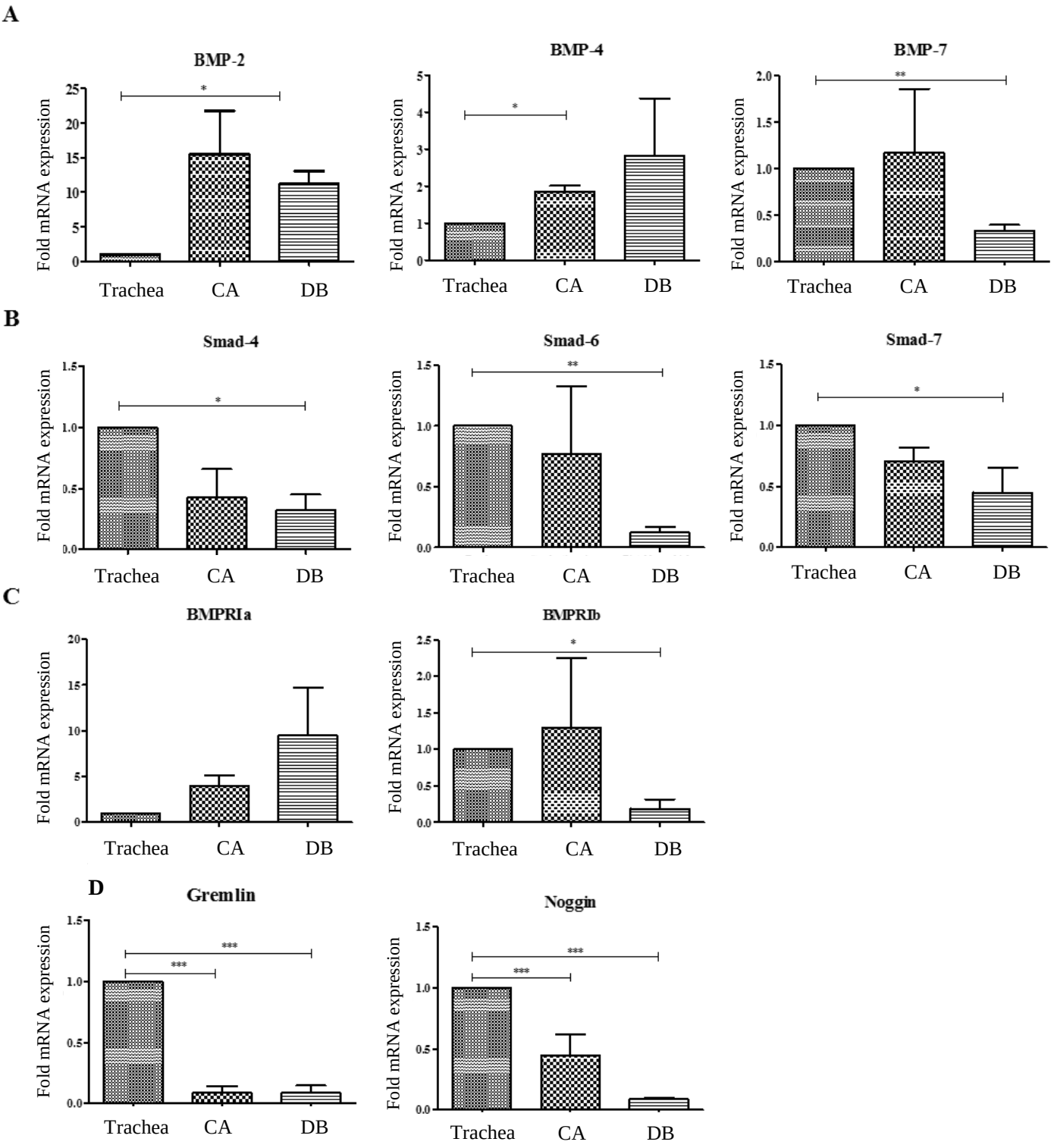
A
BMP-2
BMP-4
BMP-7
Fold mRNA expression
Trachea
CA
DB
B
Smad-4
Smad-6
Smad-7
C
BMPRIa
BMPRIb
D
Gremlin
Noggin

Figure 5.0.8 Quantitative PCR of BMP signalling components in the descending lung epithelium

Representative graphical analysis of q-PCR analysis of BMP ligands, SMADs, BMP receptors and BMP antagonists in the descending lung epithelium of the left cranial porcine bronchus. (A) The expression of BMP-2,-4 and -7 mRNA was significantly higher in the most distal region of the left cranial lobe. (B) SMAD-4 mRNA was present throughout the airways with reduced expression in the distal bronchioles. Inhibitory SMADs, SMAD-6 and SMAD-7 mRNA was significantly reduced in the epithelium of distal bronchioles compared to the trachea. (C) There was no BMPRIa gradient present in the airways. BMPRIb was significantly reduced in the distal epithelium compared to the trachea. (D) There were significantly elevated levels of BMP inhibitors present in the proximal airways epithelium compared to distal regions. n=3, * = $p < 0.05$, ** $p < 0.005$, Trachea = section1, CA, Conducting airways = sections 2,3,4,5 DB, distal bronchioles = sections 6,7,8,9

5.1.4 Expression of the BMP signalling proteins in healthy descending airways

Following characterisation of the BMP signalling pathway at the mRNA levels, the level of expression of BMP pathway signalling proteins were examined by western blot.

BMPRIa protein was expressed throughout the descending airways and no gradient in protein expression was detected (Figure 5.0.9 A). Investigation of SMAD-4 protein expression throughout the descending airways revealed a significant decrease in expression between the tracheal epithelium and the distal bronchioles (Figure 5.0.9 B). Unfortunately, there were no pig-specific antibodies available for the BMP ligands, BMPRIb, SMAD-6 or SMAD-7.

pSMAD 1/5/8 was expressed homogenously throughout the descending airways (Figure 5.0.9 C). Previous results here showed that SMAD-4 protein and mRNA expression was reduced in the distal bronchioles which indicated the presence of non-canonical BMP signalling, Thus, pERK 1/2 was examined by western blot. pERK 1/2 was expressed in the descending lung epithelium of the left cranial bronchus and no significant gradient in protein expression was evident (Figure 5.0.9 D).

These results provide further evidence that the BMP pathway is active during adult airway homeostasis.

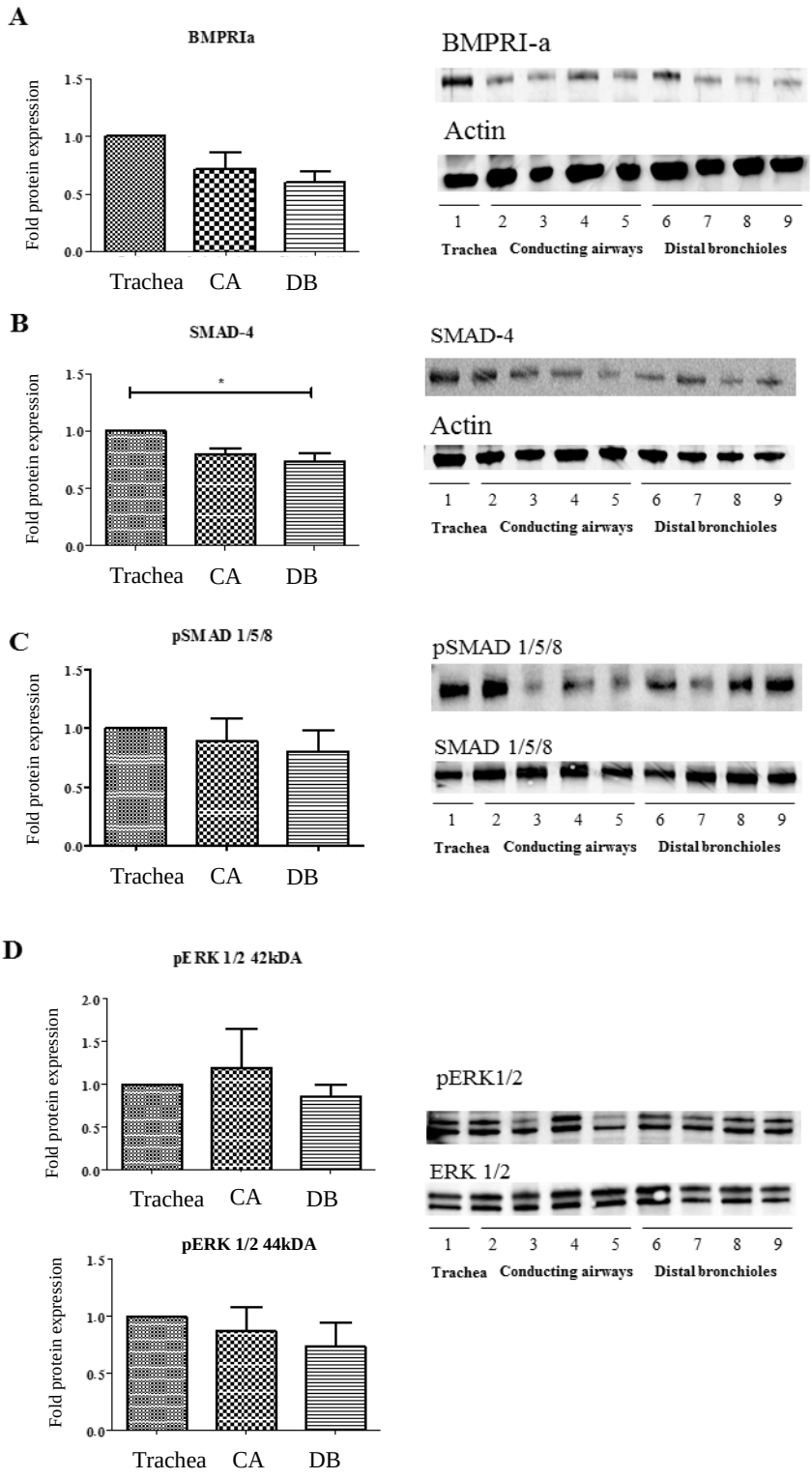

Figure 5.0.9 Expression of BMP signalling proteins in the descending left cranial porcine bronchus

Representative graphs of western blot analysis of BMPRIa, SMAD-4, pSMAD and pERK expression in the descending left cranial porcine bronchus. (A) No BMPRIa gradient existed in the descending bronchial epithelium. (B) SMAD-4 was differentially expressed between the trachea and the distal bronchioles ($p<0.05$) (C) No difference in pSMAD 1/5/8 expression was detected (D) No difference in pERK 1/2 was detected in the descending bronchial epithelium, n=3, * = $p < 0.05$, ** $p < 0.005$, Trachea = section1. CA, Conducting airways = sections 2,3,4,5. DB, distal bronchioles = sections 6,7,8,9

5.1.5 Establishing a porcine tracheal explant model *in vitro*

By mapping the BMP pathway using quantitative PCR and western blotting, a BMP signalling gradient was detected in the descending airways. BMP-2 and BMP-4 ligands were expressed at an elevated level in the distal bronchial epithelium compared to the trachea. In what appeared to be an inverse relationship, the BMP antagonists gremlin and noggin were expressed more abundantly in the tracheal epithelium and proximal airways compared to distal epithelial regions in the adult lung, (Figure 5.0.10). We hypothesised that this gradient was involved in maintaining epithelial homeostasis. To investigate this in adult porcine tracheal epithelium, an *in vitro* porcine tracheal explant model was designed.

The tracheal tissue of the pig was sectioned longitudinally along the trachealis. This is the band of smooth muscle that bridges the gap between both sides of the cartilaginous tracheal circumference. Following wash steps, the explants were grown in culture at air liquid interface (Figure 5.0.11).

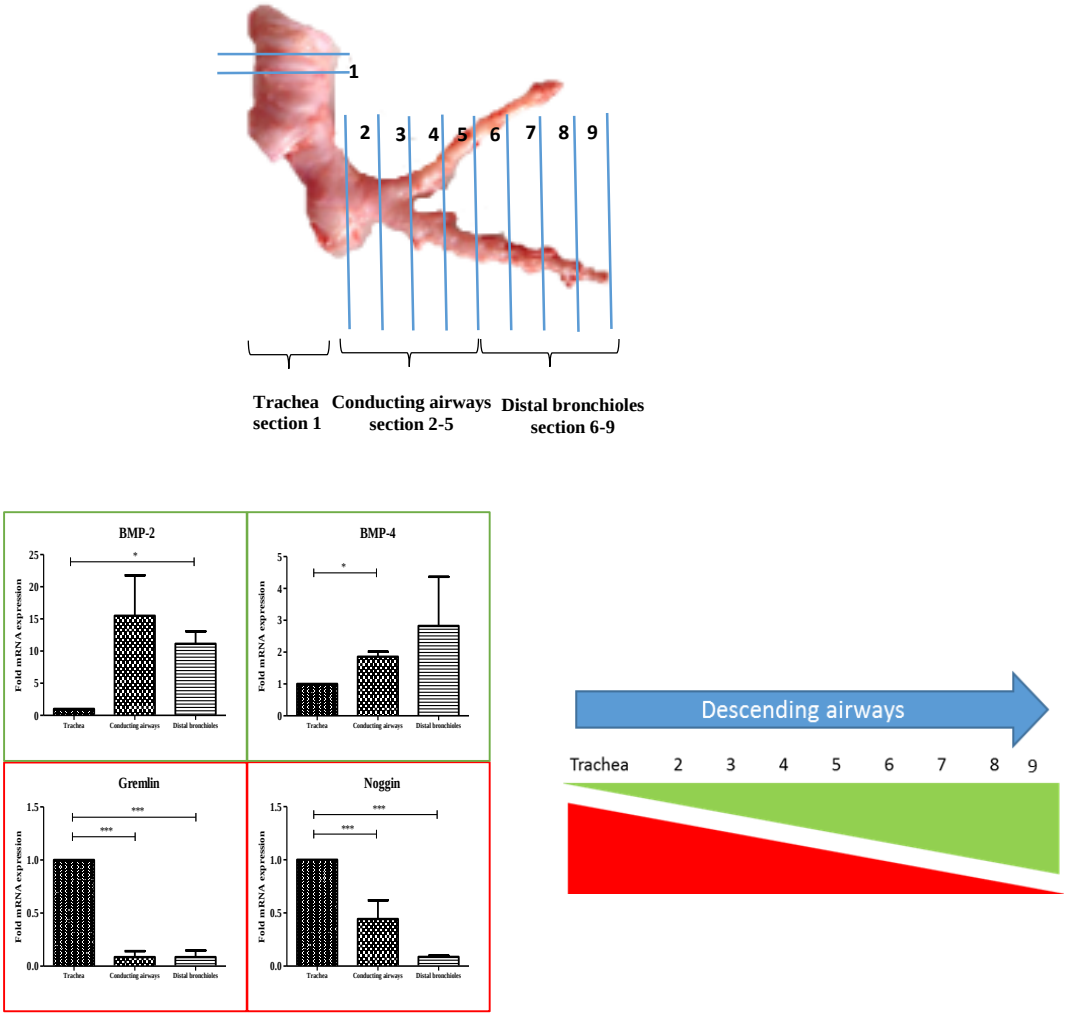

Figure 5.0.10 A BMP signalling gradient was detected in the descending porcine airways

Quantitative PCR and western blotting analysis revealed a gradient in BMP signalling in the descending airways. BMP ligands were higher in the proximal airways compared to the distal regions of the lungs. Conversely, extracellular BMP antagonists gremlin and noggin were higher in the tracheal epithelium compared to the distal bronchial epithelium. Trachea=section 1, conducting airways = section 2,3,4,5, distal bronchioles = sections 6,7,8,9

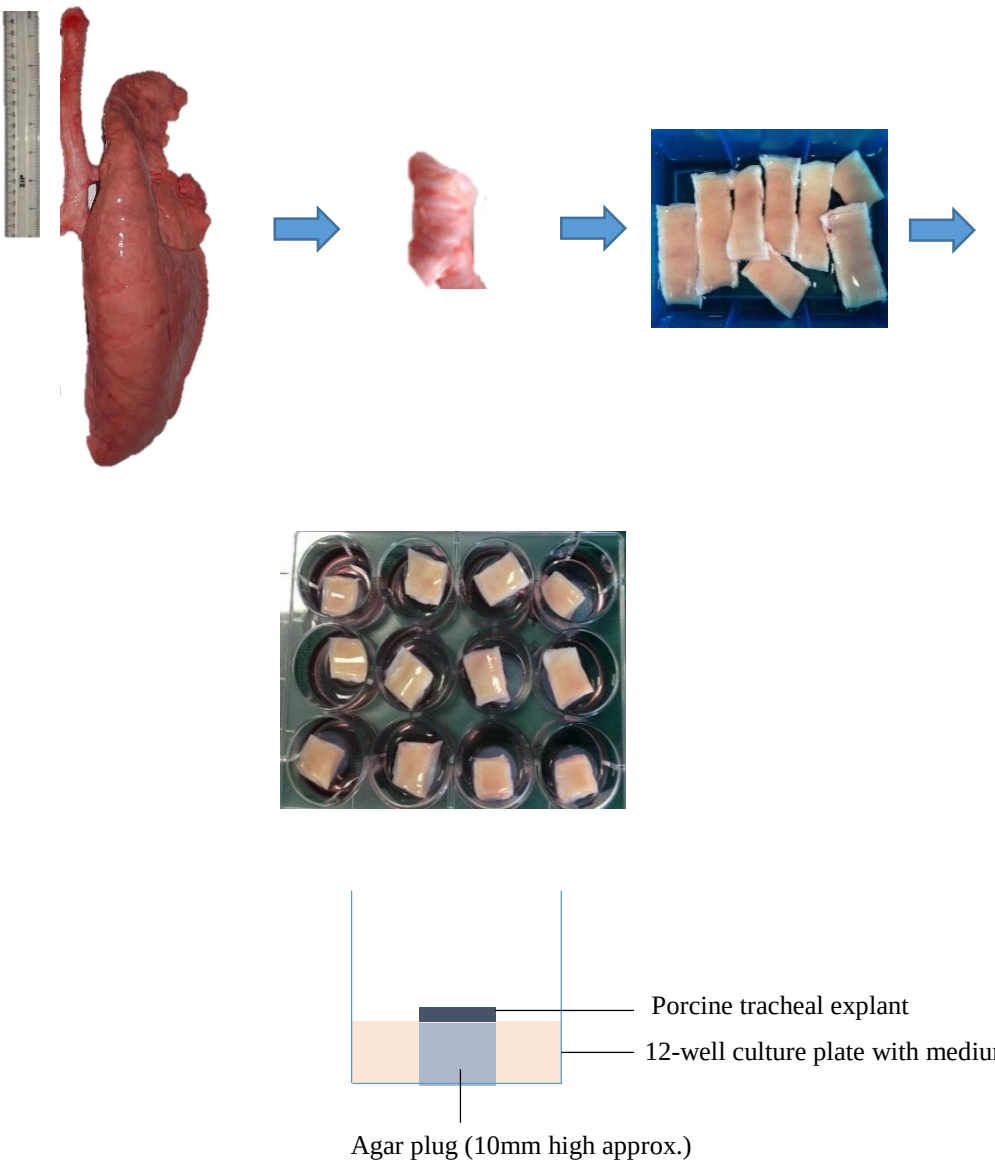

Figure 5.0.11 Establishing an *in vitro* porcine tracheal explant model

Longitudinal sections of trachea were sectioned and washed and dissected to small explant sections. These sections were placed on agar plugs in 12-well culture plates and grown for 2-3 days.

5.1.6 Examination of porcine tracheal explant architecture

Following establishment of explant culture conditions, the tracheal tissue was maintained at 37 °C for 48 hrs. Histological analysis by H&E and PAS staining and E-cadherin immunofluorescence was carried out to assess the architecture of the explant and to ensure the epithelial layers remained intact following the culture process.

The tracheal explants were fixed in formalin and embedded in wax after 48 hrs in culture. Subsequent H&E and PAS staining revealed that the epithelium was intact. The pseudo-stratified epithelium, a submucosal glands and lamina propria were evident following staining. The gland stained dark purple in the PAS stain due to presence of mucus and polysaccharides (Figure 5.0.12 A). Following E-cadherin immunofluorescence, the intact epithelium was clearly visible. The pseudostratified epithelium can identified by the tall E-cadherin positive epithelial cells situated on top of the small cuboidal basal cells (Figure 5.0.12 B***).*** The lamina propria does not stain for E-cadherin protein and there was evidence of E-cadherin positive submucosal gland in the lower magnification image of the tracheal explant.

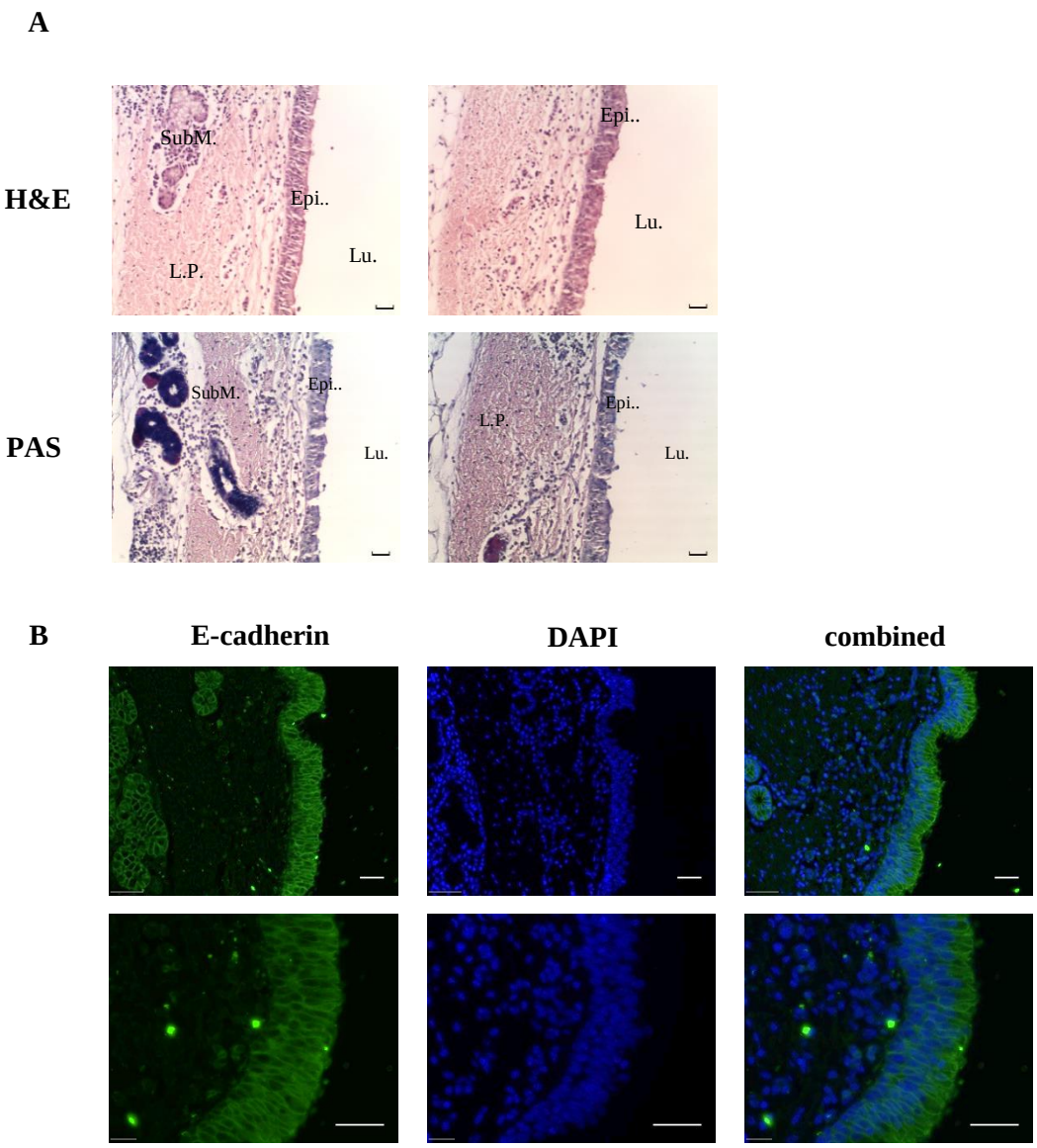

Figure 5.0.12 Histological analysis of porcine tracheal explants

(A) H&E and PAS histological staining revealed the pseudostratified epithelium, submucosal glands, lamina propria and underlying connective tissue of the porcine tracheal explant remain intact following 24 hr culture *in vitro*. There was no damage to the sections during culture and processing. (B) E-cadherin immunofluorescence of the tracheal explants showed the chickenwire pattern of the intact epithelium. Epi = epithelium, SubM = submucosal glands, LP = lamina propria, Lu = lumen. Sclae bars represent 20uM, 20uM and 50uM respectively.

5.1.7 Evaluation of viability of porcine tracheal explants

To assess for epithelial cell viability, uptake of the fluorescent nucleic acid intercalator 7AAD was examined.. The epithelial and submucosal layers of the tracheal explant were micro-dissected from the explant and prepared for enzyme digestion. The cells were then passed through a 70uM filter prior to incubation with the dye. FACS analysis revealed that approximately 85% of the tracheal explant cells remained viable following 48 hrs in culture (n=6) (Figure 5.0.13).

A

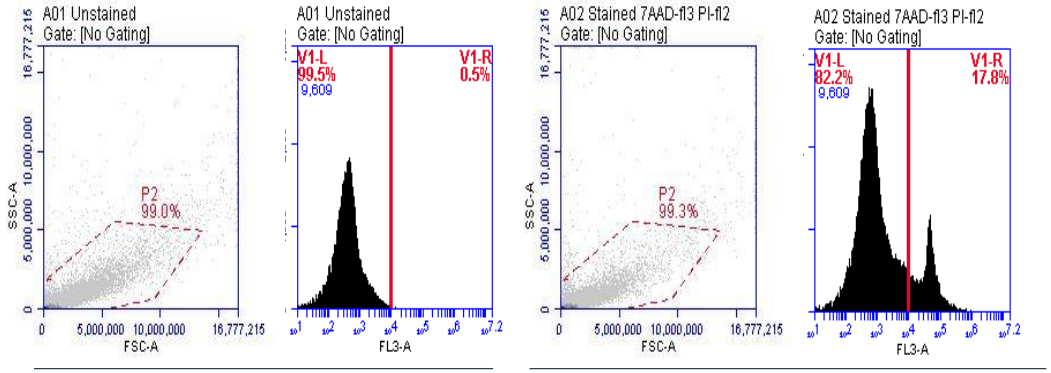

unstained stained – 82.2% viable

B

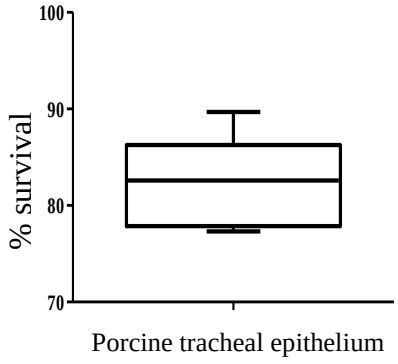

Porcine tracheal epithelium

Figure 5.0.13 Porcine tracheal explants remained viable after 48 hrs in culture

(A) Representative FACS data of porcine tracheal explant viability following 48 hrs in culture. 82.2% of the cells remained viable, as 17.8% were fluorescent due to uptake of the intercalated 7AAD stain (B) Graph depicting percentage cell survival following 48 hrs in culture (n=6).

5.1.8 BMP pathway activation following exogenous BMP-4 stimulation of porcine tracheal explants

Given that the epithelium of the tracheal explants were intact and the epithelial cells were viable following 48 hrs in culture, we wanted to confirm that the tissue was responsive to exogenous BMP ligand stimulation. The tracheal explants were grown in serum free conditions and treated with 100ng/ml BMP-4. The medium containing BMP-4 ligand was added into the chamber surrounding the agar plug and thus, any BMP-4 induced signalling was due to the activation of BMP receptors by growth factors present in the serum. This was chosen as the best method for BMP pathway activation in our culture model based on existing evidence that BMP receptors are present on the basal surface of polarised epithelial cells (Saitoh et al. 2013).

Following 24 hr stimulation with exogenous BMP-4 ligand, RNA was harvested and reverse-transcription-PCR was carried out. An increase in ID-1 expression was evident (Figure 5.0.14 A). pSMAD 1/5/8 was expressed endogenously in the tracheal explant, as detected by western blot. Exogenous treatment with BMP-4 induced an increase in pSMAD 1/5/8 expression in the tracheal explant. Densitometry analysis of the western blots revealed a significant increase in pSMAD 1/5/8 protein expression ($p<0.05$, $n=3$) (Figure 5.0.14 B).

Taken together these results indicate that the porcine tracheal explant system recapitulated a healthy porcine epithelium *in vivo.* The explants maintained their epithelial cell phenotype, were viable in the culture system and were responsive to BMP-4 ligand treatment during *in vitro* culturing.

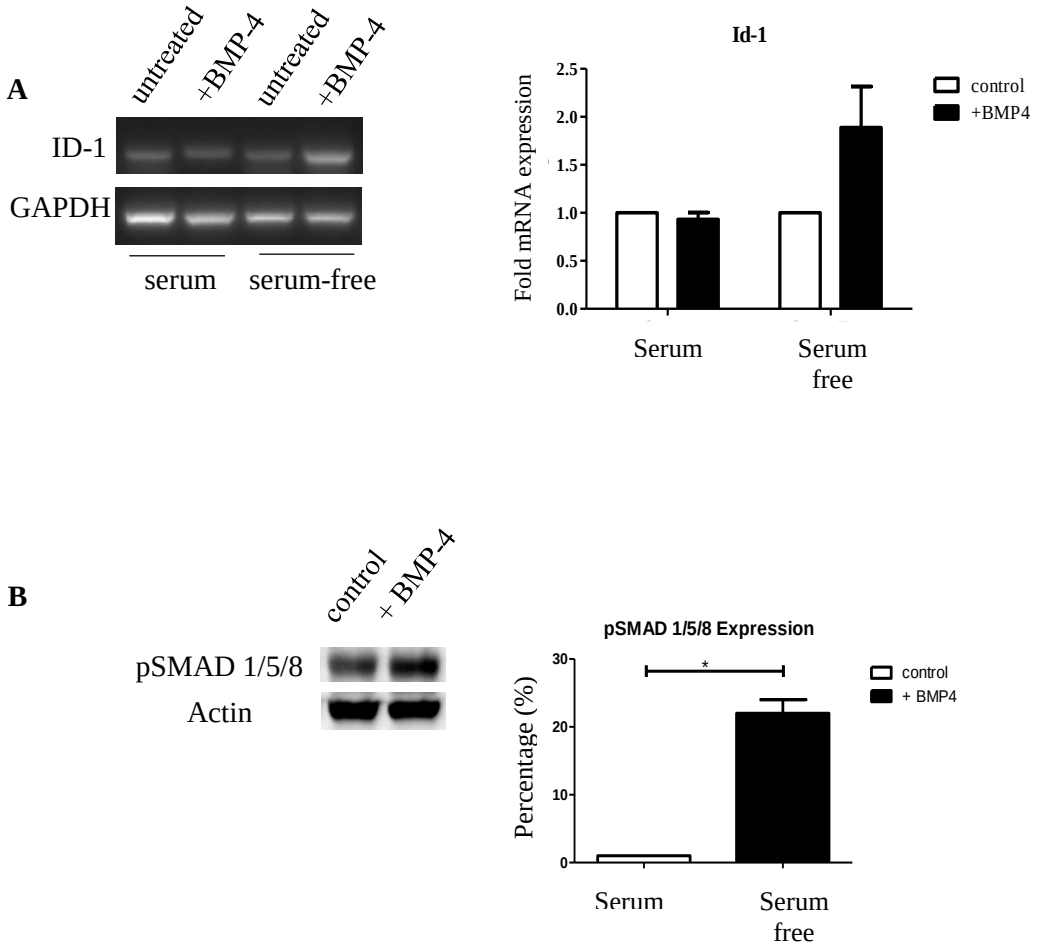

Figure 5.0.14 Porcine tracheal explants were responsive to exogenous BMP-4 treatment

Serum-free explants were supplied with medium containing 100ng/ml BMP-4 for 24 hrs. This medium was placed in the chamber surrounding the agar plug and bathed the basal surface of the explant. The epithelium of the explant was dissected away from the connective tissue and harvested for RNA and whole cell protein. (A) rt-PCR indicated an increase in Id-1 expression. A 10% serum containing control was included. (B) Analysis by Western blot and subsequent densitometry showed a significant increase in pSMAD 1/5/8 expression n=3, $p<0.05$

5.1.9 Expression of epithelial cell markers and transcription factors of the distal lung epithelium in porcine tracheal explants following 24 hr treatment with BMP-4

Given that BMP-4 is involved in distal epithelial cell expansion in lung morphogenesis and that BMP-4 mRNA was higher in distal lung epithelium in healthy porcine airways, we investigated whether BMP-4 exposure would result in expression of markers of distal cell phenotypes in the tracheal tissue.

Following 24 hr stimulation with 100 ng/ml BMP-4, RNA was harvested from the tracheal explants and rt-PCR was carried out with a range of primers designed for pig epithelial cell markers. There was a significant increase in mRNA expression of SFTPC, a marker of the distal epithelial alveolar cell and ITGA-6, a marker for basal cells in the lung epithelium ($p<0.05$) (Figure 5.0.15). There was no significant difference in the expression of EpCAM, K18, FOXA1 or AQP5 – markers of both bronchial and distal lung epithelium.

The expression levels of transcription factors responsible for distal epithelium differentiation SOX-9, ID-2 and GATA-6 were examined by rt-PCR. SOX-9, ID-2 and GATA-6 were expressed at a low level in the tracheal tissue explants. A significant increase in both SOX-9 and ID-2 expression occurred in the tracheal explants following treatment with BMP-4 ($p<0.05$) (Figure 5.0.16). A serum control was included in all experiments to rule out the induction of any BMP pathway activation by growth factors ubiquitously present in the serum.

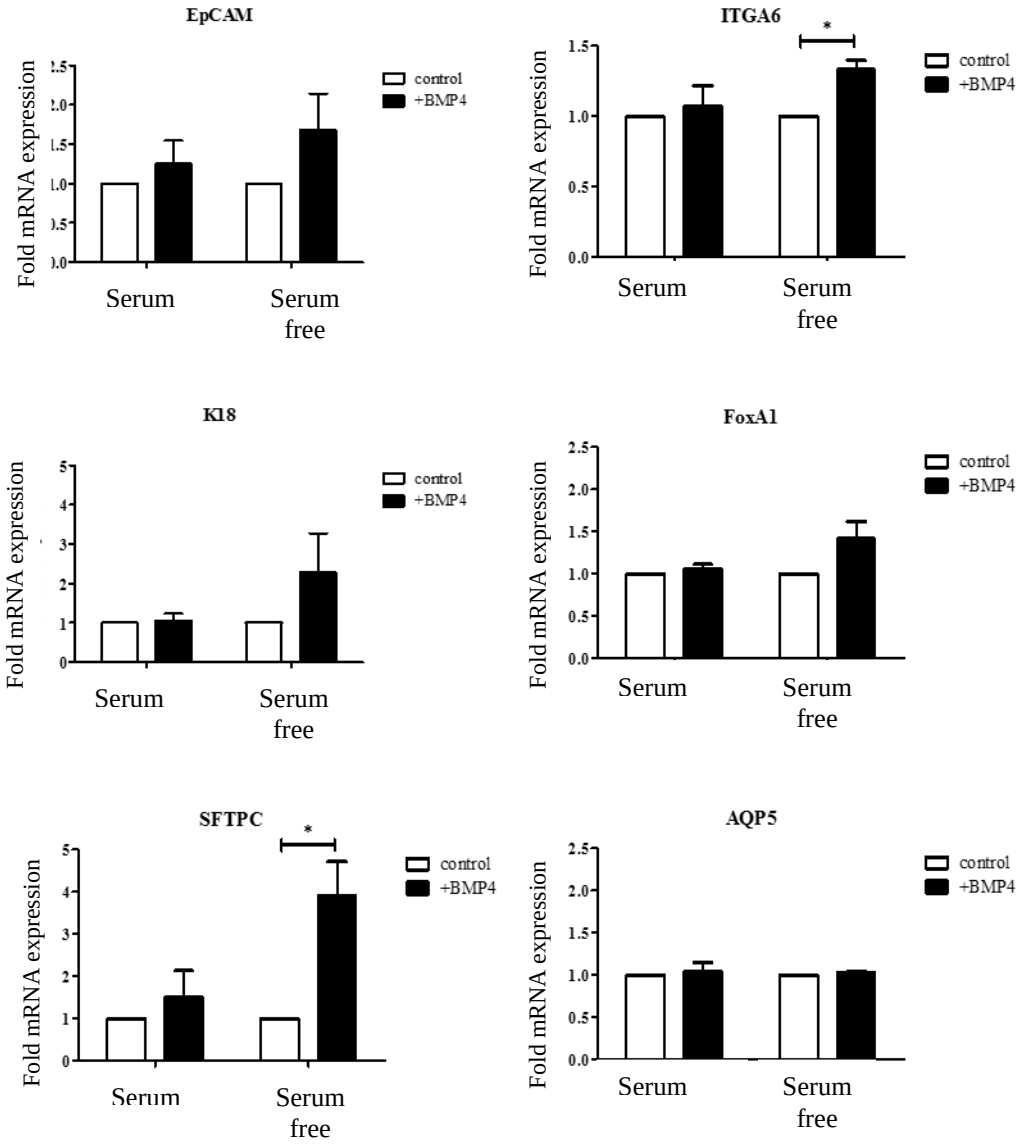

Figure 5.0.15 Expression of epithelial cell markers in porcine tracheal explants following BMP-4 stimulation

There was a significant increase in mRNA expression of the basal cell surface marker ITGA6 and type II alveolar cell marker SFTPC in the tracheal explants following 24 hr incubation with 100 ng/ml BMP-4. An increase in EpCAM, K18 and FoxA1 mRNA was evident, although not significant. There was no change in AQP-5 mRNA expression. n=3, * = $p < 0.05$

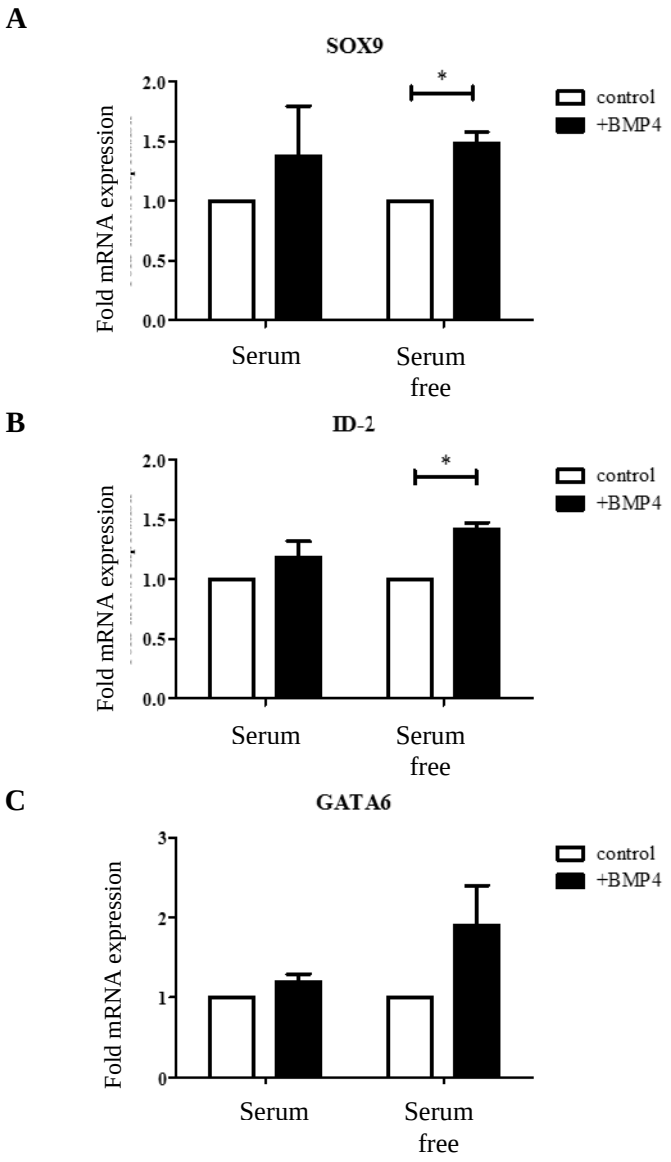

Figure 5.0.16 Expression of transcription factors of the distal epithelium in porcine tracheal explants following BMP-4 stimulation

(A)Elevated mRNA expression of SOX-9 was detected following BMP-4 treated. (B) Elevated mRNA expression of ID-2 was detected following BMP-4 treatment (C) No significant difference in GATA-6 mRNA expression was detected following BMP-4 treatment. n=3, *=$p<0.005$

5.2 Discussion

It is believed that signalling pathways involved in lung morphogenesis are reactivated in the airways during repair and recovery after injury. These signalling pathways are also activated in lung diseases, such as cancer and inflammatory lung diseases. Furthermore, gradients of morphogens, such as BMP4, are critical in forming the lung architecture as well as directing the spatial distribution of epithelial cells types throughout the airways during embryogenesis (Bellusci et al. 1996; Weaver et al. 1999). The concept of BMP signalling gradients in adult lungs remains unaddressed. Without understanding growth factor expression patterns in healthy adult airways, the framework provided by developmental and disease studies will continue to act as a weak translational model for human disease and the design of therapeutics. The map generated in this study highlights BMP signalling as an important mediator of normal epithelial homeostasis in adult airways. BMP signalling components were expressed endogeneously in the descending lung epithelium of porcine airways and a BMP ligand-antagonist gradient was detected. We have identified a potential role for BMP-4 mediated signalling in the maintenance of distal epithelial cell populations and adult airway homeostasis.

The porcine lung was chosen as the best available, clinically-relevant model of adult airways. Porcine lungs are steadily becoming a widely accepted model of adult human airways (Benahmed et al. 2014; Harrison et al. 2014; Judge et al. 2014; Rogers et al. 2008). On an economic level, no respiratory tissue is required in food production so the lungs are readily available from the local abattoir and circumvent the need for ethical approval. Large animal models are also translationally relevant. When comparing the lung anatomical features of humans and small vertebrates,

there are a large number of discrepancies. Gross differences in lung size and lobe numbers and more subtle differences such as the club cell distribution in the mouse trachea and the lack of terminal bronchioles in mice make the respiratory system of large animals such as the pig a more attractive and relevant model (Fox et al. 2006).

Initially we investigated the changing architecture of the descending porcine epithelium throughout the airways. By using a map generated previously in the O'Dea lab, we carried out an extensive histological analysis of the large porcine airways and demonstrated the gradual transition of tall pseudostratified columnar epithelium of the trachea and upper airways to the simple ciliated epithelium in the smaller bronchioles. By combining this study with histological analysis of the descending left cranial bronchus we generated an extensive map of the changing epithelium in porcine airways (Figure 5.0.2, 5.6, 5.7). The use of the PAS stain allowed for visualisation of submucosal glands and goblet cells in the descending airways. Goblet cells were more infrequent in the descending airways of porcine lungs, as expected. The presence of basal cells lining the basement membrane were evident in the E-cadherin stained sections. This data also showed that no basement membrane deposition or epithelial disruption had occurred in the porcine airways. This study allowed for the optimisation of techniques required for additional studies in the project and provided an extensive characterisation of the gross anatomy of descending porcine epithelium. To the best of our knowledge, a similar histological characterisation of the descending porcine lung epithelium has not been completed.

We hypothesised that BMP signalling was active in the healthy adult porcine airways. The existence of a BMP signalling gradient in fully developed lungs has not been explored. A previous study of porcine tissue showed that the BMP-4 gene was highly conserved between humans and pigs and that BMP-4 transcript was

present in the lung tissue of pigs at day 7, day 14, day 28 and also in a 1.5 yr old sow (Li et al. 2010). In the pig ovary it was found that a functional BMP signalling network exists (Brankin et al. 2005). These results indicate that BMP signalling does play some role in adult homeostasis in the body. Data from mouse and human asthmatic studies highlighted a tentative role for BMP signalling in adult airway homeostasis. Elevated expression of all three BMP receptors, BMPRIa, BMPRIb and BMPRII in the late stage of mouse lung development and in the post-natal epithelium further supported this hypothesis (Alejandre-Alcázar et al. 2007; Kariyawasam et al. 2008; Rosendahl et al. 2002). In this study, we demonstrated that BMPRIa and BMPRIb expression was maintained in the adult porcine epithelium (Figure 5.0.10). A reduction of BMPRIb RNA expression was detected in the distal epithelium. As BMP signalling requires a single type-1 BMP receptor to propagate the downstream SMAD signalling cascade the maintained expression of BMPRIa in the distal epithelium supported the concept of active BMP signalling in the airways, as evidenced by pSMAD 1/5/8 expression. This active signalling was further supported by the presence of BMPRIa protein throughout the airways, as detected by western blot (Figure 5.0.9). Interestingly a lower level of BMPRIa protein was detected in the distal airways compared to the trachea which could indicate that BMP signalling is more active in the proximal regions of the airways. BMPRIb and BMPRII protein expression were not examined in the distal airways due to a lack of specific antibodies. In summary the expression of BMP receptors in the adult porcine lung epithelium indicate that the airways are responsive to BMP signalling.

The lung epithelium is the first point of contact with all inhaled pathogens, toxins, allergens and noxious gases and there is a constant low level of epithelial turnover.

Damaged, aged or injured cells need to be replaced to maintain airway homeostasis, ensure epithelial integrity is maintained and lung health is not compromised. (Brune et al. 2015; Crosby and Waters 2010). Repopulation of damaged regions of the epithelial sheath occurs through activation of regional progenitor populations and proliferation of existing undamaged cells in the airways. We hypothesise that the active pSMAD 1/5/8 signalling evident in the porcine lung epithelium is involved in regulating epithelial turnover and proliferation events. There was no gradient in total pSMAD 1/5/8 expression along the proximal-distal axis (Figure 5.0.9). We hypothesise that active pSMAD 1/5/8 expression is induced by BMP ligands such as BMP-2, BMP-4 and BMP-7, which were also observed throughout the airways. We speculate that the inverse patterns of BMP-2,-4 and -7 expression in the descending lung epithelium may account for the uniform pSMAD 1/5/8 expression throughout the airways.

Non canonical BMP signalling occurs via Rho-like small GTPases, phosphatidylinositol-3-kinase/AKT and other MAP kinase pathways. These Rho-GDP induce downstream signalling cascades and induce phosphorylation of ERK/MEK. As a mediator of BMP signalling and other signalling cascades we investigated the presence of pERK-1 and pERK-2 in the descending lung epithelium. We found that phosphorylated ERK-1 and 2 (pERK1/2) were present in the descending porcine epithelium which indicated that a non-SMAD pathway was active in the airways. We hypothesise BMP ligand expression is responsible, at least in part, for this signalling however the lack of a gradient in expression is indicative of the presence of alternative growth factors.

In summary, these findings indicate that BMP signalling is active in healthy descending porcine airways. The activity of SMAD-dependent and –independent

signalling pathways highlights a role for BMP signalling in normal epithelial turnover and maintaining epithelial homeostasis.

Inhibitors of the BMP pathway are involved in controlling signalling events during lung morphogenesis. Our study found that a significant gradient in both BMP antagonists was present in the descending airways of healthy porcine lungs (Figure 5.0.8). We hypothesise that the gradient in antagonist expression could be associated with BMP regulation of normal epithelial cell turnover and the differentiation processes governing airway homeostasis. Furthermore we hypothesise that the elevated expression of BMP antagonists in the proximal airways may be linked to regulation of distal epithelial populations. Reduced expression of BMP-2,-4 ligands in the trachea supported this hypothesis. Although there was a high level of gremlin and noggin in the trachea, a basal level of pSMAD 1/5/8 expression was detected by western blot. This also supports the hypothesis that these inhibitors were regulating the BMP pathway – as opposed to preventing pathway activation completely. Furthermore, in the tracheal explant study, we speculate that the introduction of ectopic BMP-4 ligand overcame the control exerted on the pathway via endogenous gremlin and noggin expression and thus accounted for the observed increased in pSMAD 1/5/8 expression (Figure 5.0.14).

The expression of iSMADs displayed a similar pattern as the extracellular antagonists when investigated by quantitative PCR. The expression of SMAD-7 in the porcine airways may be associated with TGF- β expression. Both SMAD-6 and SMAD-7 mRNA expression was higher in the tracheal epithelium compared to distal bronchial epithelium (Figure 5.0.8). The gradient along the proximal-distal axis supports the hypothesis that elevated BMP signalling is associated with maintaining distal epithelial cell populations. The role of SMAD-6 in maintaining

correct cell phenotype and homeostasis of the heart and has previously been demonstrated in mouse. Studies mutating Madh6, the gene that codes for SMAD-6 protein, show that SMAD-6 plays an important role in adult cardiac homeostasis. The viable adult mutants displayed hyperplasia of mesenchymal cells, aortic ossification and hypertension(Galvin et al. 2000).

In summary, these results indicate the importance of regulating the BMP signalling pathway in healthy adult airways. We hypothesise that the regulation of BMP signalling in the adult lung epithelium by iSMADs and other antagonists is an important process in adult airway homeostasis and could be involved in maintaining correct distal epithelial cell distribution. Antagonising BMP signalling has been shown to be vital for muscle, bone and adipose tissue homeostasis and our results indicate that BMP signalling regulation is also involved in lung homeostasis (Krause 2014)

We identified a gradient in BMP-2 and BMP-7 ligand mRNA expression along the respiratory axis of the porcine lung (Figure 5.0.8). The presence of BMP ligand mRNA in healthy porcine epithelium is supported by evidence that BMP-2 -4 and -7 ligands are also expressed in healthy human airway epithelium (Kariyawasam et al. 2008). No distinct role for BMP-2 in lung morphogenesis or lung epithelial cell differentiation has been discovered, however BMP-2 expression is elevated during inflammation by IL-1 and TNF-a (Fukui et al. 2003). BMP-2 also possesses the ability to induce EMT in human airway epithelial cells during epithelial restitution (McCormack et al. 2013). Thus, we hypothesise that there is a basal level of BMP-2 ligand expression may be present in the airways and that following airway injury and the induction of pro-inflammatory cytokines, BMP-2 expression is elevated above a threshold and leads to the induction of EMT and the restoration of epithelial

integrity. BMP-7 is also elevated in the bronchial epithelium following the airway insult and it has been shown that BMP-7 co-localised with the Major Basic Protein subunit of infiltrating eosinophils in human asthmatic airways (Kariyawasam et al. 2008). Similar to Kariyawasam et al., 2008 we hypothesise that BMP-7 is involved in airway repair and that the expression of BMP-7 in the healthy bronchial epithelium can be activated on demand following airway damage. These ligands could also be contributing to the basal activation of pSMAD 1/5/8 in the airway epithelium and contributing to control of epithelial cell proliferation.

In summary, we speculate that BMP-2 and BMP-7 expression is involved in epithelial homeostasis and the maintenance of basal BMP signalling expression which can be elevated following epithelial injury to facilitate epithelial repair and restoration of homeostatic conditions. We propose a potential diverging role for BMP-2 and BMP-7 as outlined in previous work with the DLKP cell lines whereby BMP-7 may be involved in anti-inflammatory processes in the airways.

BMP-4 is important for determining epithelial cell fate along the proximal-distal respiratory axis during development. By generating two independent overexpression systems of Xenopus Noggin (Xnoggin) and a dominant negative BMPRIb under the control of the Sp-C promoter, inhibition of BMP signalling in mice caused expansion of proximal cells in distal regions of the transgenic lung. Distal epithelial cell populations were completely ablated (Weaver et al. 1999). Similar proximal cell expansion was seen in the distal lung epithelium of mice possessing a Sp-C/Gremlin overexpression gene (Lu et al. 2001). In summary, these results indicated that cells exposed to high levels of BMP-4 develop a distal epithelial cell fate while those exposed to little or no BMP-4 adopt a proximal epithelial phenotype. A similar BMP-4 expression gradient was detected in the

healthy porcine airways (Figure 5.0.8). We hypothesised that the BMP-4 gradient is involved in maintaining distal epithelial cell population in healthy adult airways. This hypothesis was supported by the observation of high levels of gremlin and noggin expression in the tracheal epithelium.

Following treatment of the tracheal explant with exogenous BMP-4, we found that the expression of the distal epithelial markers ITGA6 and SFTPC were increased (Figure 5.0.16). Furthermore, the expression of transcription factors ID-2 and SOX-9 was elevated. These transcription factors are involved in cell differentiation and distal epithelial bud branching during lung development (Rockich et al. 2013). Our results indicate that BMP-4 treatment of the tracheal explants induced a more distal-like epithelial cell phenotype via the induction of distal transcription factor expression.

ITGA6 is a marker for basal cells which possess stem cell qualities and SFTPC is the common marker of alveolar type II cells (Barkauskas et al. 2013; Rock et al. 2009). Lineage tracing and clonal assay experiments have previously shown that epithelial cell populations expressing either of these markers have the potential to self-renew and differentiate (Barkauskas et al. 2013; Rock et al. 2009). A mouse model of airway injury highlighted the significance of BMP signalling in epithelial cell renewal. It was found that following club cell ablation by naphthelene exposure, the expression of a GFP construct under the control of a BMP-responsive element was localised around NEBs and in the terminal bronchioles. These regions are populated by airway progenitors cells which are responsible for controlling cell proliferation and differentiation during development and airway repair (Sountoulidis et al. 2012). Both of these markers were elevated in tracheal epithelial explants following BMP-4 treatment. Taken together these results

indicate that BMP-4 induced signalling could be important for controlling epithelial cell differentiation in addition to promoting a distal epithelial cell phenotype in the tracheal epithelial cells.

Previous experiments using ID-2 luciferase reporter constructs in C2C12 cells identified a BMP-responsive region in the ID-2 promoter. The 267-bp region contained two bipartite units – one containing the canonical BMP-responsive sequence (GGCGCC and GTCT) and one containing a variant of the SMAD-responsive element (GGCGCC and GGCG/CCGC). (Nakahiro et al. 2010). Furthermore, ID-2 is expressed in the developing lung bud and is known as a marker for distal endoderm progenitors. Linage tracing experiments have also shown that ID-2 + cells in the distal tip of the lung epithelium give rise to both club cell, neuroendocrine cell and distal (alveolar type I and II) cell populations (Liu and Hogan 2002; Rawlins et al. 2009). In our experiments, BMP-4 treatment caused a significant increase in ID-2 expression in the epithelium of porcine tracheal explants (Figure 5.0.16). We hypothesise that in the porcine epithelium, this BMP-responsive element in the ID-2 promoter is activated following BMP-4 treatment. The direct cellular effect of ID-2 expression in the explant remains undefined but we speculate that it is involved in promoting a distal epithelial cell phenotype and regulating proliferation events. We speculate that the expression of the transcription factor ID-2 could be responsible for the induction of SFTPC expression in the porcine tracheal explants. SFTPC-expressing cells are present in the distal epithelium and are capable of self-renewal and differentiation as previously mentioned (Figure 5.0.15).

ID-1 genes are involved in regulating cell cycle progression and inhibiting cell proliferation via upregulation of p16, a cyclin-dependent kinase inhibitor, and E2A

transcription factors E12/47 also known as TCF3. For cell cycle progression, the E2F and pRB protein complex is phosphorylated by cyclin-D. This phosphorylation event facilitates cell cycle progression from G-phase to the S-phase (Giacinti and Giordano 2006). p16, as a cyclin dependent kinase inhibitor can block the phosphorylation event of pRB by Cyclin-D and inhibit cell cycle progression (Ruzinova and Benezra 2003; Sikder et al. 2003; Stone et al. 1995). Suppression of cell proliferation by ID-1 has been documented in human fibroblasts and mammary epithelial cells. This group used mouse-mammary-viral transfection of sense and anti-sense ID-1 vector systems in SPc2 cells (Desprez et al. 1995). Conversely, ID-2 has been found to stimulate cell cycle progression by inhibiting the anti-proliferative effects of pRB in human osteosarcoma and glioma cell lines (Iavarone et al. 1994; Lasorella, Iavarone, and Israel 1996; Lasorella, Uo, and Iavarone 2001; Sikder et al. 2003). In our porcine tracheal explant model, an increase in ID-1 expression was detected following BMP-4 treatment. Our experiments showed that ID-2 was also elevated in our study of porcine tracheal explants. The confounds the hypothesis that ID-1 could be causing decreased cell proliferation in the porcine tissue. While the relationship between ID proteins and cell cycle progression remains undefined in our culture model, we hypothesise that BMP induces ID expression in an attempt to regulate epithelial cell proliferation during adult airway homeostasis.

SOX-9 is a transcription factor expressed at the distal bronchial epithelium and is involved in regulating branching morphogenesis and proliferation profiles of distal cell progenitors in the developing airways. Both SOX-9 ectopic expression in proximal airways and in distal epithelium inhibited cell proliferation highlighting that a finely tuned balance of SOX-9 signalling is required for correct control of

cell proliferation. In our experiments, BMP-4 treatment of porcine tracheal explants caused an increase in SOX-9 mRNA expression in the tracheal explants. We speculate that SOX-9 could be involved in controlling cell proliferation in the BMP-4 treated tracheal explants, perhaps antagonising the pro-proliferative effect of ID-2 signalling (Kowanetz et al. 2004).

Gain- and loss- of function studies found that SOX-9 is involved in regulating the organisation of cytoskeletal proteins and extracellular matrix proteins of mouse epithelial cells such as F-actin and acetylate tubulin, COL2A1 and laminin respectively (Rockich et al. 2013). Rockisch et al., highlighted the role of SOX-9 in epithelial movement in the mouse lung and demonstrated reduced cell migration and wound closure following abrogation of SOX-9. During embryogeneis, SOX-9 is also involved in EMT during neural crest delamination and interacts with BMP to orchestrate correct gut-tube morphogenesis (Liu et al. 2013). The process of EMT is also an important phenomenon for correct lung formation, airway repair and disease (Shannon and Hyatt 2004). BMP-4 induces epithelial cell movement in human bronchial epithelial cells and also during epithelial restitution following injury (McCormack et al. 2013; Molloy et al. 2008). We have also highlighted the role of BMP-4 in EMT in DLKP cell lines in this study. It is possible that EMT is induced in these tracheal explant cells following exogenous BMP-4 treatment and that SOX-9 expression is subsequently elevated and contributes to altered epithelial cell phenotype. A similar link between SOX-9 and the EMT process exists in endocardial endothelial cells whereby SOX-9 promotes EMT after delamination (Akiyama et al. 2004). The essential role of SOX-9 and the organisation of extracellular matrix proteins is also seen in an embryonic-lethal model of cardial-SOX-9 knockdown (Lincoln et al. 2007).

In summary, the induction of elevated SFTPC, ITGA-6, ID-2, ID-1 and SOX-9 expression in the porcine tracheal explants following BMP-4 treatment indicated that BMP-4 mediated signalling is important for determining distal epithelial cell fate. Furthermore, the results highlight the potential role of BMP signalling in regulating cell proliferation.

While porcine explants allowed further investigation of the role of BMP signalling the airways, future experiments should utilise primary culture of airway epithelial cells. Development of air-liquid interface cultures would provide a robust platform for studying the role of BMP signalling during airway homeostasis. Using targeted inhibition of BMP signalling by siRNA, the role of BMP pathway activation in epithelial cell proliferation and differentiation could be elucidated. Furthermore, determination of the expression of pro-inflammatory cytokines following targeted injury of the epithelium and the effect of BMP ligands/inhibitors on cytokine release would provide further insight into the role of BMP signalling in airway repair and inflammation.

Our work focused primarily on characterising canonical BMP signalling in the descending airways. The presence of pERK 1/2 in the descending airways highlighted that non-canonical BMP pathways were active in the airways. Future experiments should characterise non-canonical BMP signalling and other growth factor signalling in the descending airways. This could highlight different signalling gradients responsible for maintaining homeostasis in the lung epithelium.

It is important for future work investigating the BMP pathway in the airways to identify the specific cell populations involved in BMP signalling and to investigate if there is any modulation in BMP signal expression following damage and during

repair of the airways. For example, double immunostaining of histological sections with epithelial cell markers would allow characterisation of the cells responsible for BMP pathway activation.

Our study has shown that the BMP signalling pathway is active during adult lung homeostasis in a large animal model. We have mapped the expression of BMP ligands, SMAD signalling molecules and antagonists of the BMP pathway throughout the descending lung epithelium of a large animal model. By demonstrating the existence of BMP signalling gradients in the healthy epithelium we can speculate about the function of BMP pathway activation in healthy adult airways. In addition, we developed an *ex vivo* porcine tracheal explant model to further investigate the function of the ligand-antagonist axis which was evident in the descending lung epithelium. Following BMP-4 stimulation, tracheal explant upregulated various transcription factors involved in the control of epithelial cell proliferation and distal epithelial cell phenotype. While BMP signalling is now widely recognised as an important mediator of lung morphogenesis and epithelial repair following injury, our results indicate that basal BMP signalling is involved in maintaining epithelial homeostasis in adult airways.

Chapter 6

Mapping the BMP signalling pathway in healthy, asthmatic and recovering rhesus macaques airways

6.1 Introduction

Both the architecture of the lungs and the epithelial cells types that line the airways change throughout the descending respiratory tract to reflect specialised functions therein. The trachea and bronchi are lined with ciliated and secretory cells in the form of a pseudostratified epithelium in order to facilitate the mucociliary escalator and the clearance of inhaled pathogens. At the terminal end of the bronchioles, a single layer of airway epithelial cells (AEC) type I and II line the alveolar sacs. These cells facilitate the bi-directional movement of gases between the airways and the blood (Chang et al. 2008). The establishment of these distinct niches during lung morphogenesis is tightly controlled by signalling molecules, growth factors and morphogens such as FGF, Wnt and BMP. These signalling factors communicate across the Epithelial-Mesenchymal-Trophic Unit (EMTU) which is made up of opposing layers of epithelial and mesenchymal cells encompassing a

network of basement membrane, fibroblasts, nerves and endothelial cells (Evans et al. 1999).

In adult lungs, the EMTU is constantly challenged by irritants, pathogens and disease-causing agents. It is believed that the signalling factors governing lung morphogenesis are re-activated following an injury. This causes the lung epithelium to initiate proliferation and differentiation pathways to correctly restore epithelial integrity. However, in situations of chronic injury or prolonged inflammation, the epithelium will likely undergo incorrect repair such as abnormal epithelial cell differentiation and remodelling events. While lung morphogenesis, normal repair and abnormal disease processes have been extensively studied, the underlying signalling processes governing lung phenotypic changes, remodelling, inflammation and restitution of epithelial homeostasis remain unclear (Beers and Morrisey 2011; Warburton 2012).

We have established that BMP pathway is active in porcine lungs and that a BMP signalling gradient exists in healthy porcine airways. In addition, we have provided evidence that BMP-4 can induce tracheal epithelial cells to adopt a distal epithelial cell phenotype. The aim of this work was to investigate the role of BMP signalling in the healthy airways of non-human primates. In addition, BMP signalling in airways undergoing inflammatory lung disease and airways provided with a recovery period following inflammatory disease would be examined. We hypothesise that a BMP signalling gradient exists in healthy adult airways similar to that present during lung development and homeostatic porcine airways, and that this gradient may be altered during inflammatory airway disease and regeneration. In order to address these aims, we used an established model of allergic airway disease in rhesus macaques. As outlined previously these monkeys displayed

increased levels of HDMA-specific IgE in the serum, elevated numbers of eosinophils in the BAL and higher CD25 expression on circulating T lymphocytes (Schelegle et al. 2001). In addition, monkeys exposed to HDMA and O_3 displayed rapid shallow breathing and a cough during aerosol challenge. Following necropsy, these monkeys displayed thickened basement membrane zone in the airways in addition to increased eosinophil accumulation in the conducting airways and mucus cell hyperplasia (Schelegle, Miller, et al. 2003; Van Winkle et al. 2004). We examined BMP signalling in the left cranial bronchus of the monkeys, similar to our study of healthy porcine airways.

6.1.1 The rhesus macaque model of allergic airway disease and recovery

Rhesus macaque models of asthma and recovery were developed previously (Figure 6.0.1 A). All monkeys in the study were male. Group 1 monkeys were exposed to filtered air for six months and served as healthy controls. Group 2 monkeys were sensitised to the HDMA *Dermatophagoides farniae* and housed in specialised air chambers supplied with cyclic doses of aerosolised *Der f.* HDMA and O_3 for five months (Figure 6.0.1 B). These monkeys developed asthma and were sent to necropsy at six months old. A recovery model, Group 4, was also established whereby monkeys were exposed to cyclic doses of *Der f.* HDMA and O_3 for five months followed by six months of filtered air, including one dose of aerosolised *Der f.* HDMA per month. These monkeys were sacrificed at twelve months old. Control animals, Group 3, were housed in filtered air for twelve months.

Sequential airway generations of the left cranial lobe were dissected and characterised as trachea, conducting airways and distal bronchioles for the purpose of this study (Figure 6.0.1 C). Tissue from the trachea of 6 month old monkeys was no longer available and so could not be included in this study. We chose to examine expression of the BMP receptor, BMPRIa, as an indicator of potential cell responsiveness to BMP ligands. We used an antibody that recognises phosphorylated SMADs 1, 5 and 8 to detect nuclear localised SMADs as an indicator of active BMP signalling. We also examined expression of proliferating cell nuclear antigen (PCNA) as an indicator of regeneration in the airway epithelium. Immunofluorescence was carried out and stereologic quantification was performed using a Morphometrix software platform developed in UC Davis.

A

	Asthma model		Recovery model	
Age	**Group 1: Control**	**Group 2: Treatment**	**Group 3: Control**	**Group4: Treatment**
2 days	Selected for the study based on weight & negative HDM skin prick test	Selected for the study based on weight & negative HDM skin prick test	Selected for the study based on weight & negative HDM skin prick test	Selected for the study based on weight & negative HDM skin prick test
↓				
14 days	FA	sensitised to *D. farniae* in alum + heat killed *B. pertussis*	FA	sensitised to *D. farniae* in alum + heat-killed *B. pertussis*
↓				
28 days	FA	sensitised to *D. farniae* in alum + heat-killed *B. pertussis*	FA	sensitised to *D. farniae* in alum + heat-killed *B. pertussis*
↓				
30 days	FA	11 cycle regimen (see B)	FA	11 cycle regimen (see B)
↓				
6 months	Necropsy	Necropsy	FA	FA*
↓				
7-11 months			FA	FA*
↓				
12 months			Necropsy	Necropsy

B

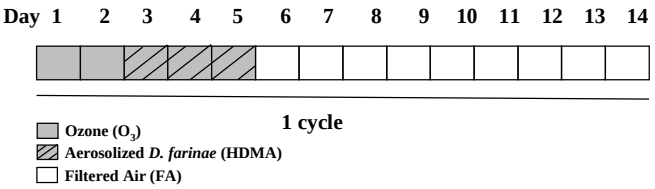

C

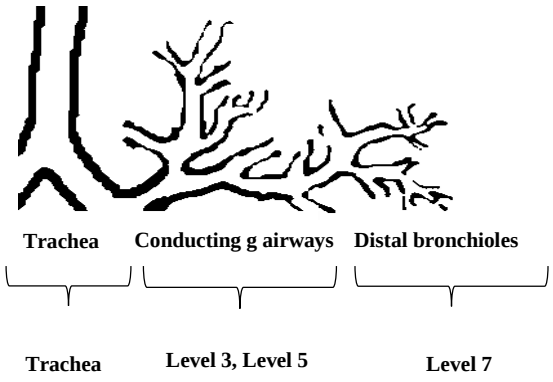

Figure 6.0.1 Experimental outline

(A) Animals were chosen for the study based on a negative intradermal skin sensitivity test to *Dermatophaoides farinae,* a common house dust mite allergen (HDMA). Male rhesus macaques were included in the study. At 14 days old *D. farinae* in alum was injected subcutaneously in addition to an intramuscular injection of heat-killed *Bortetella pertussis*. At 28 days old, a repeated dose of *D. farniae* was given in alum. When the rhesus macaques were 30 days old they were moved to specially regulated air chambers. The asthma model cohort received 11 repeated doses of ozone and aerosolized HDMA and were sent to necropsy at 6 months old, as outlined in B. In the recovery model, the monkeys received the same cyclic exposure. After the 11^{th} cycle, filtered air (FA) was supplied to the chambers for an additional 6 months. These monkeys underwent necropsy when they were twelve months old. *HDMA + O_3 was given for 2 hours on a monthly basis to maintain sensitivity. (B) Aerosolized ozone was supplied for five days (grey fill), with aerosolized HMDA (strike-through) on days three to five. Filtered air was subsequently supplied for nine days. This regimen was repeated 11 times. Treatment lasted for 5 months. (C) The left cranial lobe was harvested and the main stem bronchus was dissected into consecutive sections for paraffin wax embedding. For the purpose of this study, airway levels 3 and 5 are classified as the conducting airways with a ciliated pseudostratified columnar epithelium. Airway level 7 sections are classified as distal bronchioles. The epithelial wall is made of simple ciliated columnar epithelium.

6.1.2 Expression of PCNA. BMPRIa and pSMAD 1/5/8 expression in healthy six month old rhesus macaques

Immunofluorescence was carried out to examine PCNA, BMPRIa and pSMAD 1/5/8 expression in lung tissue sections from airway epithelium of healthy six month old (Figure 6.0.1). The volume of positively labelled epithelial cells per unit basal lamina was counted following randomised sampling of airway sections. Expression of PCNA was observed in the nuclei of epithelial cells throughout the airways of these animals. Following quantification, no significant difference in the level of PCNA expression was detected throughout the airways (Figure 6.0.2). This demonstrated that a low level of proliferation was present in the healthy descending airways, as expected. The expression of BMPRIa was observed in all epithelial regions examined and no significant difference in the level of membrane-bound BMPRIa expression was evident in the conducting airways and distal bronchioles in six month old rhesus macaques (Figure 6.0.3)

Finally, the expression of nuclear-localised pSMAD 1/5/8 was investigated in healthy juvenile monkey airways and no significant difference was present between conducting airways and distal bronchioles (Figure 6.0.4). Nuclear pSMAD 1/5/8 indicated that active BMP signalling was present in these healthy airways.

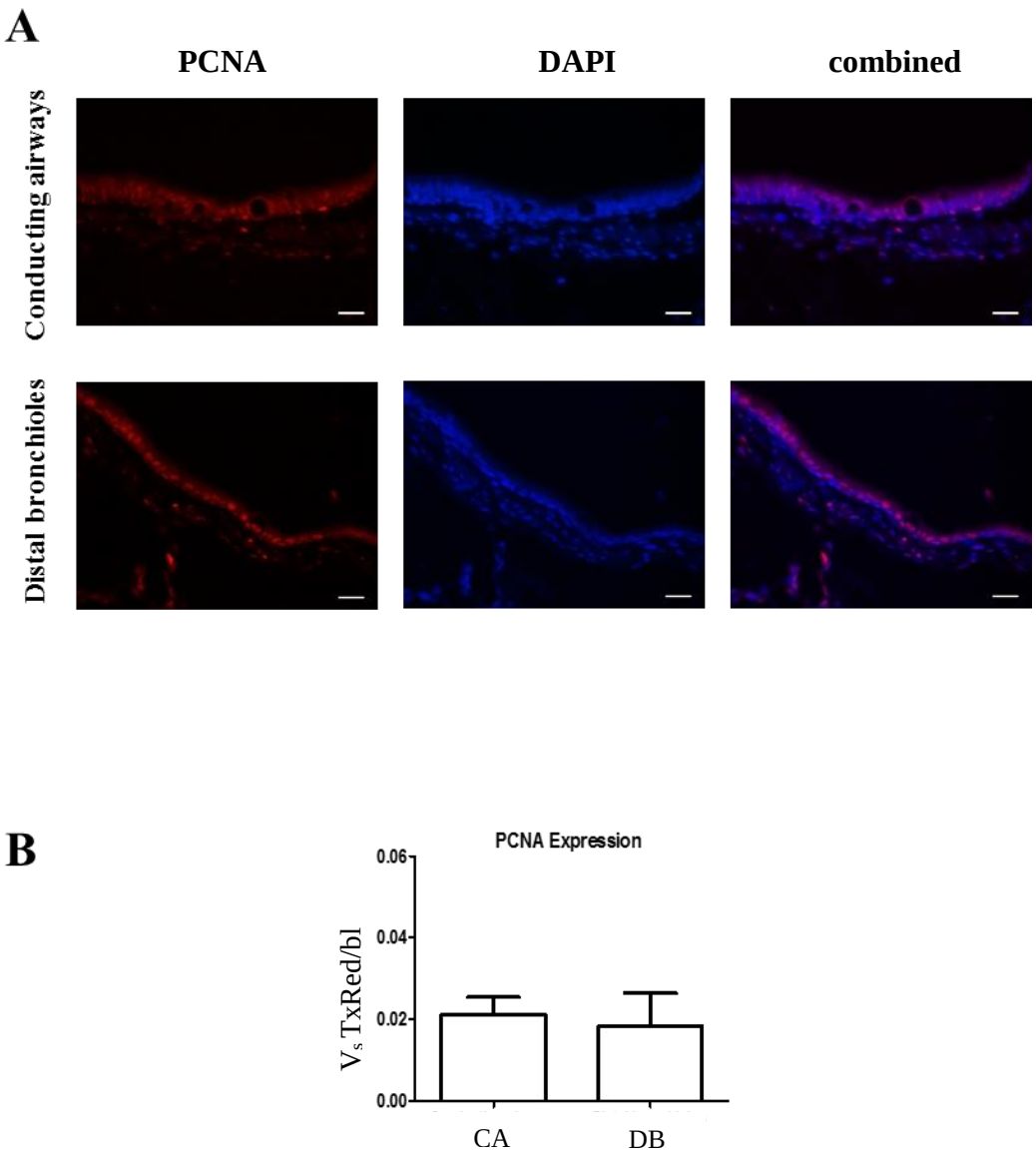

Figure 6.0.2 PCNA expression in healthy six month old rhesus macaque airways

Representative micrographs of PCNA immunofluorescence in healthy rhesus macaque airways. (A) Immunofluorescence of the descending airways showed that PCNA expression was present in the nuclei of epithelial cells in the conducting airways and distal bronchioles (B) Stereologic quantification of immunofluorescent images stained for PCNA did not reveal a significant difference in PCNA expression throughout the airways. CA, conducting airways, DB, distal bronchioles, V_s TxRed/bl = volume of positively stained epithelial cells per unit of basal lamina. Scale bars represent 50uM, n=3.

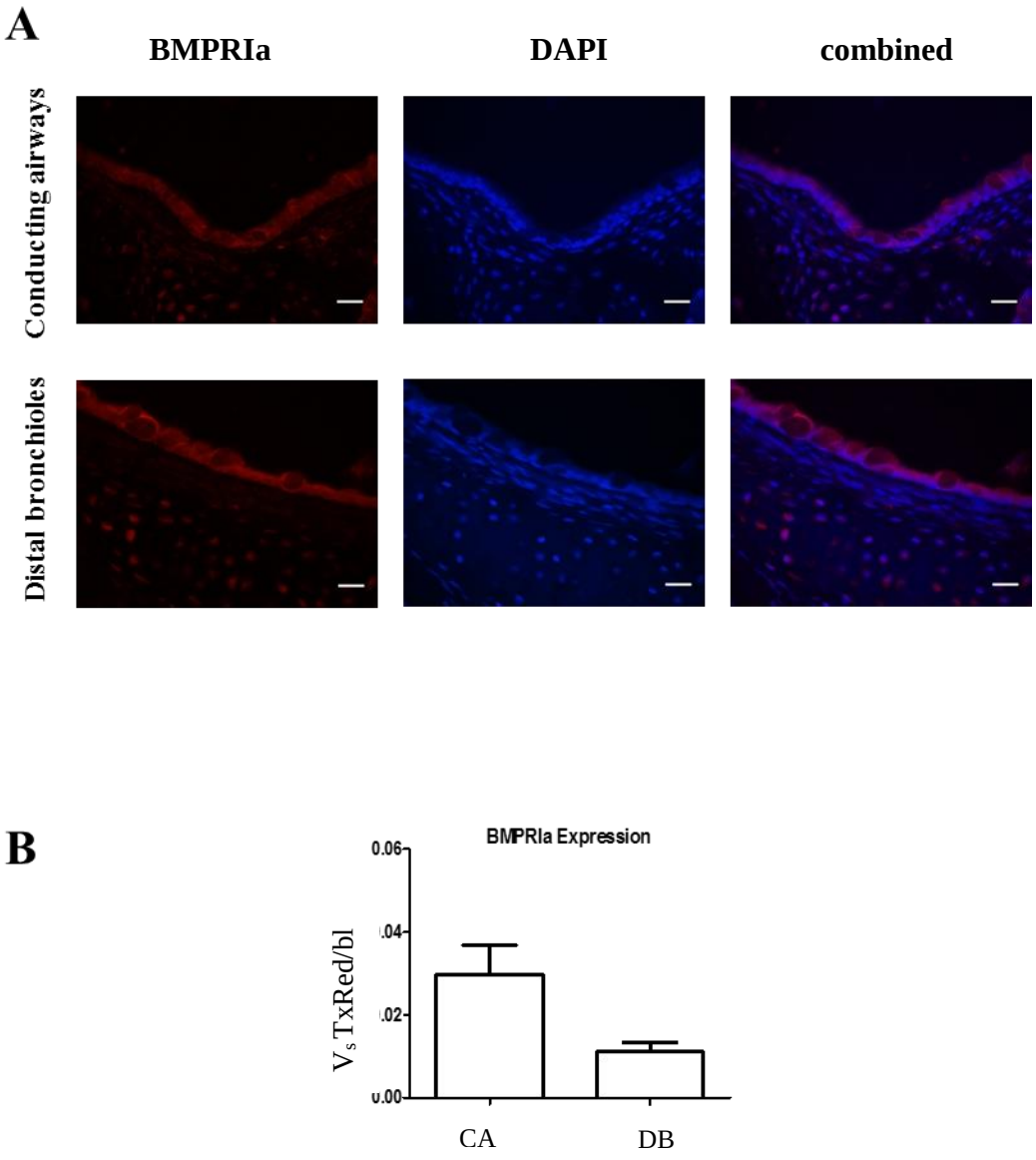

Figure 6.0.3 BMRPIa expression in healthy six month old rhesus macaque airways

Representative micrographs of BMPRIa immunofluorescence in healthy rhesus macaque airways. (A) Immunofluorescence of the descending airways showed that BMPRIa expression was present in the cytoplasm and at the membrane of epithelial cells in the conducting airways and distal bronchioles (B) Stereologic quantification of immunofluorescent images stained for BMPRIa did not reveal a significant difference in BMPRIa expression throughout the airways. CA, conducting airways, DB, distal bronchioles, V_s TxRed/bl = volume of positively stained epithelial cells per unit of basal lamina Scale bars represent 50uM, n=3.

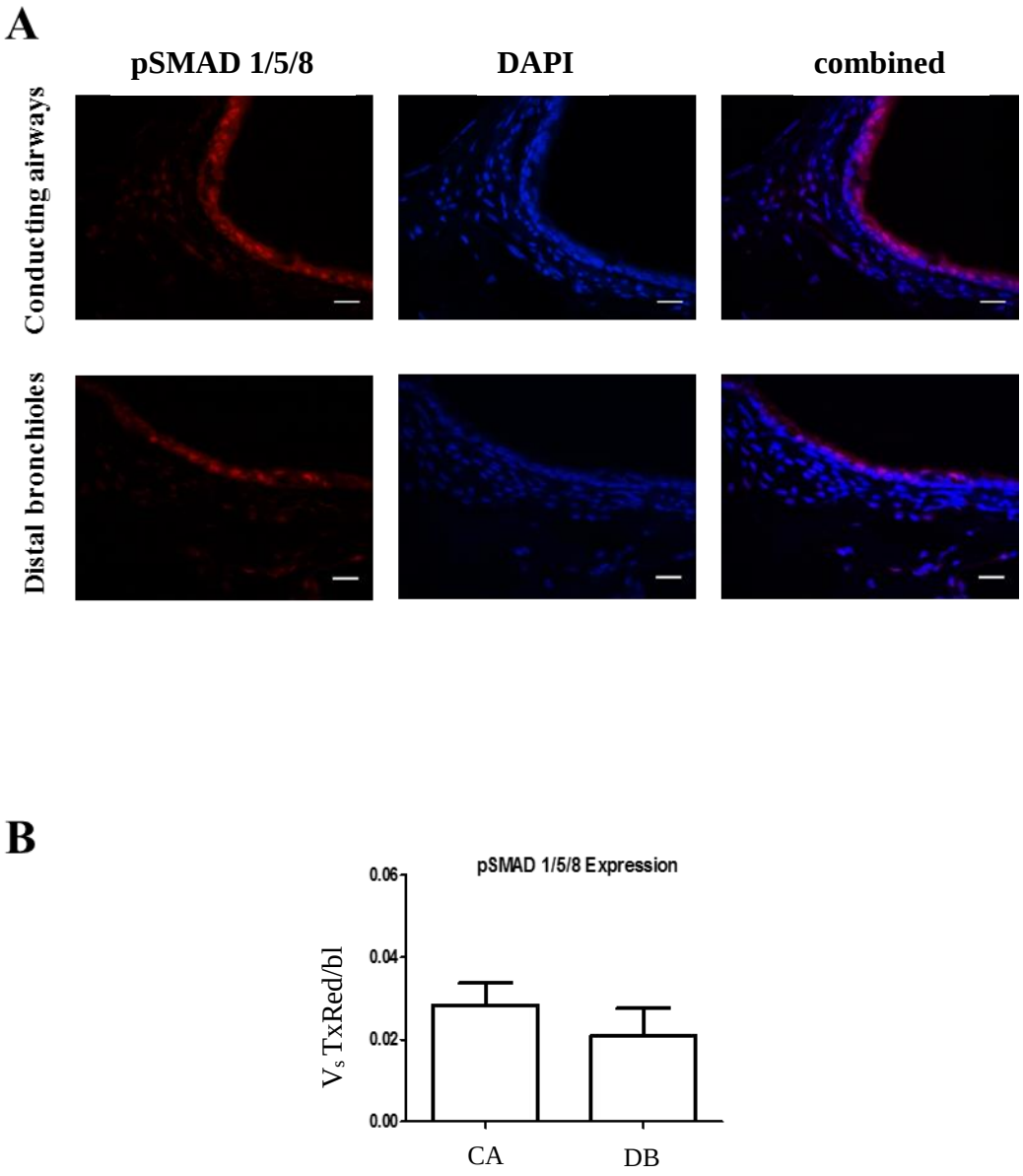

Figure 6.0.4 pSMAD 1/5/8 expression in healthy six month old rhesus macaque airways

Representative micrographs of pSMAD 1/5/8 immunofluorescence in healthy rhesus macaque airways. (A) Immunofluorescence of the descending airways showed that pSMAD 1/5/8 expression was present in the nuclei of epithelial cells in the conducting airways and distal bronchioles (B) Stereologic quantification of immunofluorescent images stained for pSMAD 1/5/8 did not reveal a significant difference in expression throughout the airways. CA, conducting airways, DB, distal bronchioles, V_s TxRed/bl = volume of positively stained epithelial cells per unit of basal lamina. Scale bars represent 50uM, n=3.

6.1.3 Expression of PCNA, BMPRIa and pSMAD 1/5/8 expression in healthy twelve month old rhesus macaques

The expression of PCNA, BMPRIa and pSMAD 1/5/8 were also examined in healthy twelve month old rhesus macaques. These monkeys had been housed in filtered air chambers for twelve months (Figure 6.0.1). Tracheal tissue was available for these monkeys which allowed for increased investigation of signalling gradients throughout the airways.

PCNA expression was examined throughout the airways and similar to six month old rhesus macaques, a low level of nuclear expression was evident in the descending epithelium (Figure 6.0.5). Following quantification of the positively labelled epithelial cells, no significant difference in expression was present between trachea, conducting airways and distal bronchioles. BMPRIa expression levels were examined in the descending airways by immunofluorescence. Membrane localised BMPRIa staining was present throughout the airways (Figure 6.0.6). This indicates that the descending epithelium is responsive to BMP ligands. Stereology did not reveal any difference in BMPRIa expression throughout the airways.

pSMAD 1/5/8 expression was examined in the twelve month old healthy monkey airways. Similar to six month old monkeys, nuclear pSMAD 1/5/8 expression was present in the descending epithelium, indicating active BMP signalling (Figure 6.0.7). pSMAD 1/5/8 expression was significantly higher in the tracheal epithelium compared to both conducting airways and distal bronchioles.

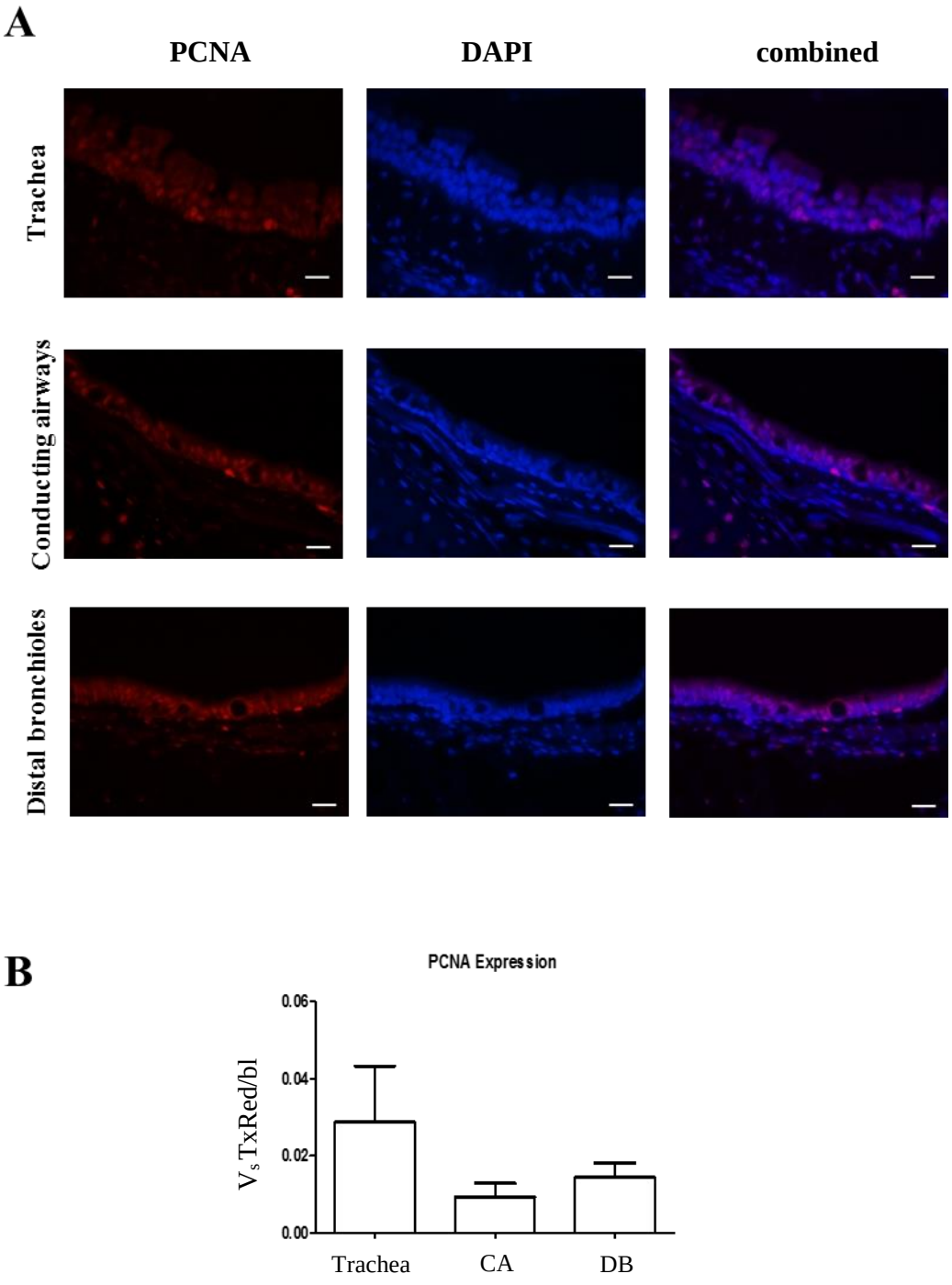

Figure 6.0.5 PCNA expression in healthy twelve month old rhesus macaque airways

Representative micrographs of PCNA immunofluorescence in healthy rhesus macaque airways. (A) Immunofluorescence of the descending airways showed that PCNA expression is present in the nuclei of epithelial cells of the trachea, conducting airways and distal bronchioles (B) Stereologic quantification of immunofluorescent images stained for PCNA did not reveal a significant difference in PCNA expression throughout the airways. CA, conducting airways, DB, distal bronchioles, V_s TxRed/bl = volume of positively stained epithelial cells per unit of basal lamina Scale bars represent 50uM, n=3

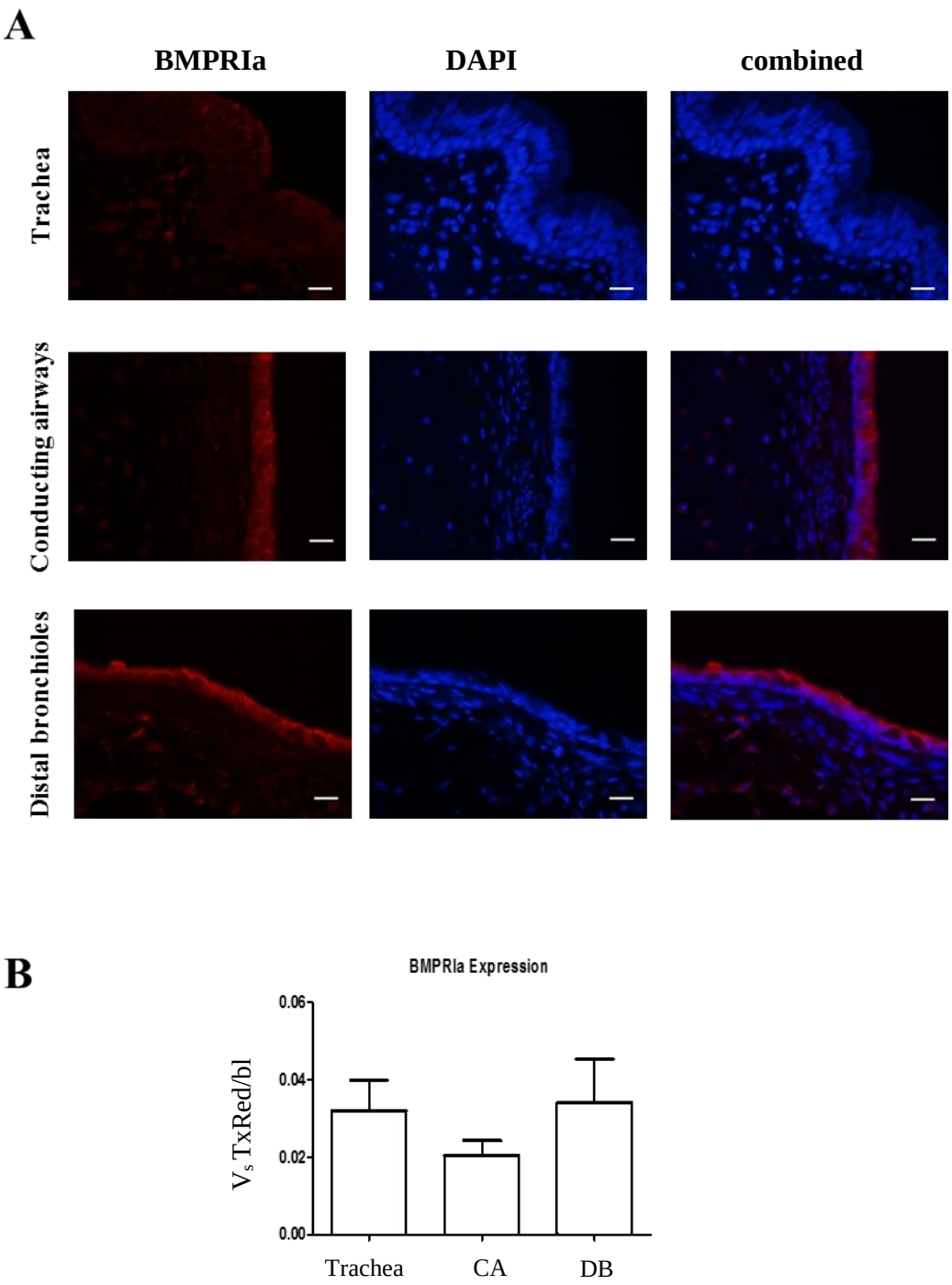

Figure 6.0.6 BMPRIa expression in healthy twelve month old rhesus macaque airways

Representative micrographs of BMPRIa immunofluorescence in healthy rhesus macaque airways. (A) Immunofluorescence of the descending airways showed that BMPRIa expression is present in the cytoplasm and at the membrane of epithelial cells in the trachea, conducting airways and distal bronchioles (B) Stereologic quantification of immunofluorescent images stained for BMPRIa did not reveal a significant difference in protein expression throughout the airways. CA, conducting airways, DB, distal bronchioles, V_s TxRed/bl = volume of positively stained epithelial cells per unit of basal lamina Scale bars represent 50uM, n=3.

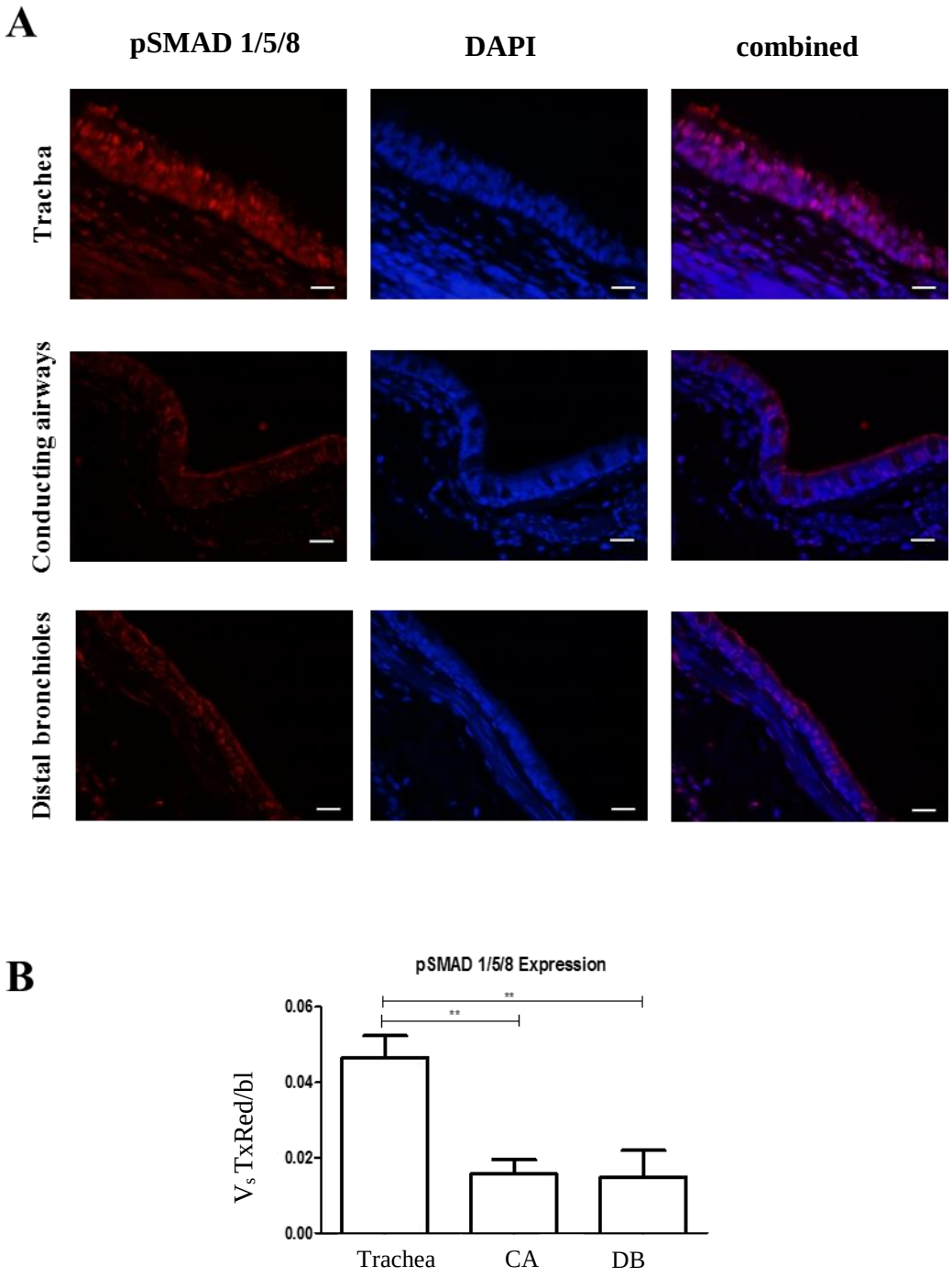

Figure 6.0.7 pSMAD 1/5/8 expression in healthy twelve month old rhesus macaque airways

Representative micrographs of pSMAD 1/5/8 immunofluorescence in healthy rhesus macaque airways. (A) Immunofluorescence of the descending airways showed that pSMAD 1/5/8 expression is present in the nuclei of epithelial cells in the trachea, conducting airways and distal bronchioles (B) Stereologic quantification of immunofluorescent images stained for pSMAD 1/5/8 reveals a significant decrease in protein expression between trachea and conducting airways and distal bronchioles. CA, conducting airways, DB, distal bronchioles, V_s TxRed/bl = volume of positively stained epithelial cells per unit of basal lamina Scale bars represent 50uM, **p<0.005, n=3

6.1.4 Expression of PCNA, BMPRIa and pSMAD 1/5/8 expression in asthmatic rhesus macaques

Following the induction of allergic airway disease in the rhesus macaques as previously described (Schelegle, Walby, et al. 2003), we investigated changes in the expression of BMP signalling components in the descending airways. We hypothesised that BMP pathway expression would be altered in asthmatic monkey airways, compared to healthy controls.

No significant difference in PCNA expression was found throughout the descending airways of asthmatic monkey airways compared to healthy monkeys (Figure 6.0.8). Similarly, no significant difference in BMPRIa expression was found by stereologic quantification (Figure 6.0.9). Interestingly, some evidence of nuclear BMPRIa expression was present in asthmatic monkey airways. This result is explored further in section 6.1.6 . When pSMAD 1/5/8 immunofluorescence was carried out and quantified, a significant decrease in nuclear expression was found in the epithelium of asthmatic conducting airways compared to healthy controls (Figure 6.0.10).

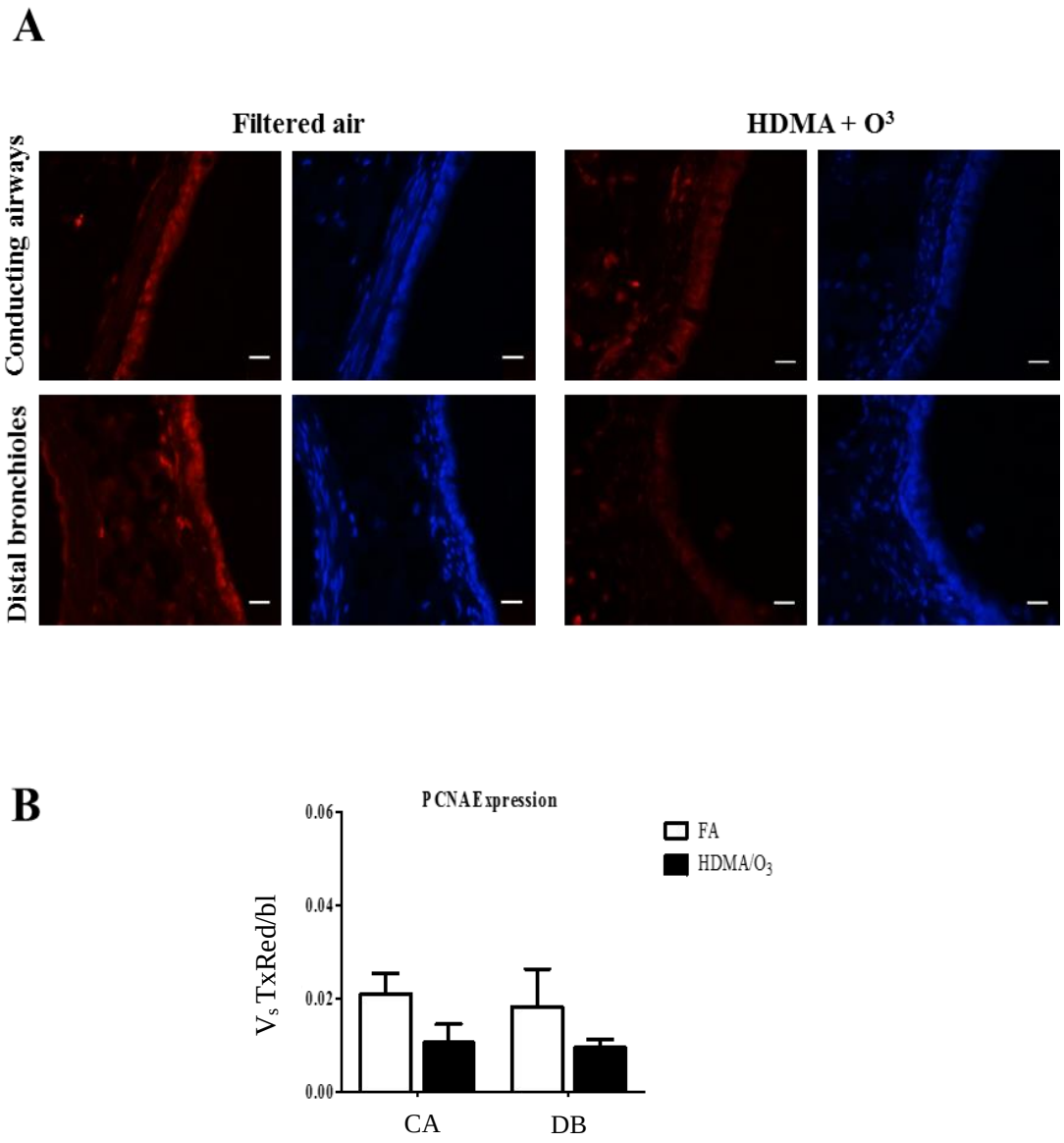

Figure 6.0.8 PCNA expression in healthy and asthmatic rhesus macaques

Representative micrographs of PCNA immunofluorescence in healthy and asthmatic rhesus macaque airways. (A) Immunofluorescence of the descending airways showed that PCNA expression was present in the nuclei of healthy epithelial cells in the conducting airways and distal bronchioles. There appeared to be a reduction in PCNA protein expression in asthmatic airways (B) Stereologic quantification of immunofluorescent images stained for PCNA did not reveal a significant difference in protein expression throughout the airways between healthy and asthmatic monkeys. CA, conducting airways, DB, distal bronchioles, V_s TxRed/bl = volume of positively stained epithelial cells per unit of basal lamina. Scale bars represent 50uM, n=3.

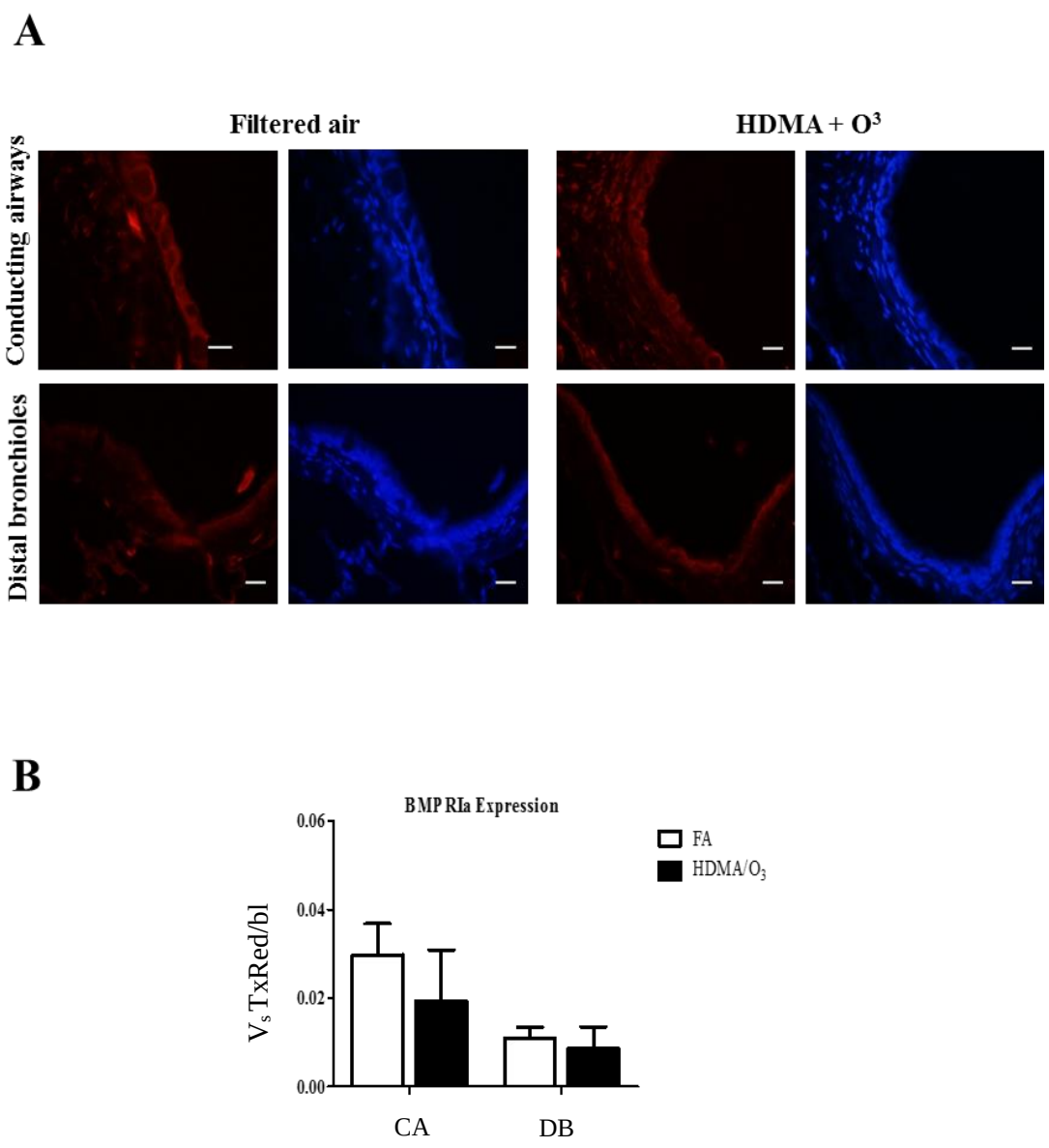

Figure 6.0.9 BMRPIa expression in healthy and asthmatic rhesus macaques

Representative micrographs of BMPRIa immunofluorescence in healthy and asthmatic rhesus macaque airways. (A) Immunofluorescence of the descending airways showed that BMPRIa was expressed in the cytoplasm and at the cell membrane of epithelial cells in the conducting airways and distal bronchioles. There appeared to be a reduction in BMPRIa protein expression in asthmatic airways (B) Stereologic quantification of immunofluorescent images stained for BMPRIa did not reveal a significant difference in protein expression throughout the airways between healthy and asthmatic monkeys. CA, conducting airways, DB, distal bronchioles, V_s TxRed/bl = volume of positively stained epithelial cells per unit of basal lamina Scale bars represent 50uM, n=3.

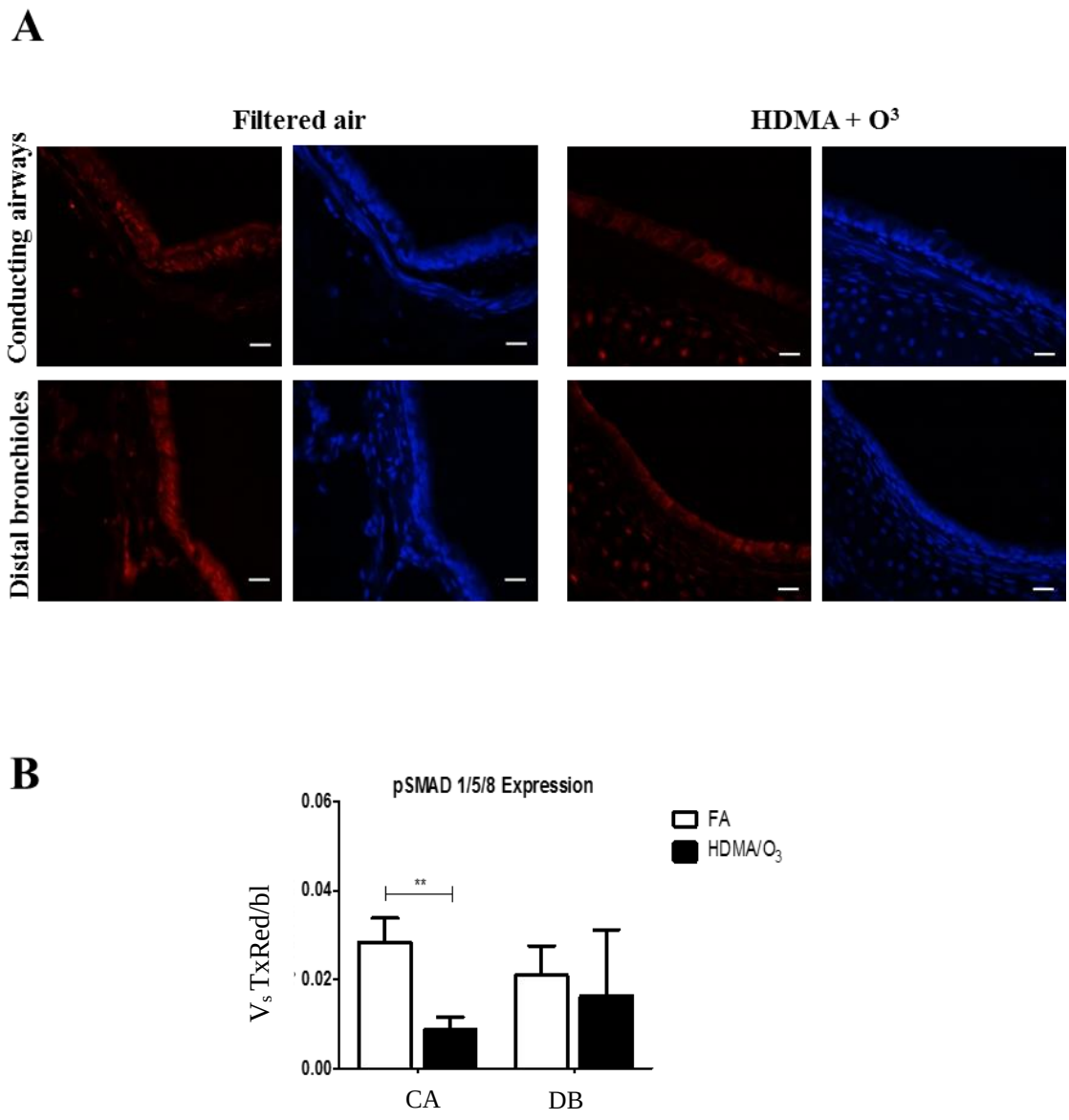

Figure 6.0.10 pSMAD 1/5/8 expression in healthy and asthmatic rhesus macaques

Representative micrographs of pSMAD 1/5/8 immunofluorescence in healthy and asthmatic rhesus macaque airways. (A) Immunofluorescence of the descending airways showed that pSMAD 1/5/8 was expressed in the nuclei of epithelial cells in the conducting airways and distal bronchioles. There appeared to be a reduction in pSMAD 1/5/8 protein expression in asthmatic airways (B) Stereologic quantification of immunofluorescent images stained for pSMAD 1/5/8 revealed a significant decrease in protein expression between healthy and asthmatic monkeys in the conducting airways. CA, conducting airways, DB, distal bronchioles, V_s TxRed/bl = volume of positively stained epithelial cells per unit of basal lamina Scale bars represent 50uM, **p<0.005, n=3.

6.1.5 Immunofluorescence and stereological analysis of PCNA, BMPRIa and pSMAD 1/5/8 expression in recovering rhesus macaques

Following cyclic exposure to HDMA/O_3 over a six month period, a group of animals were subsequently housed in chambers supplied with filtered air for an additional six months in order to investigate the extent to which recovery, if any, could occur following a chronic lung injury, as previously reported (Evans et al. 2004). Immunofluorescence showed a significant increase in nuclear PCNA expression ($p=0.0013$) in the conducting airways of recovering monkeys compared to healthy twelve month old controls (Figure 6.0.11). Similarly, an increase in membrane bound BMPRIa and nuclear pSMAD 1/5/8 expression was evident in the epithelium of conducting airway in recovering monkeys (Figure 6.0.12 - .13) ($p=0.0037$ and 0.045 respectively).

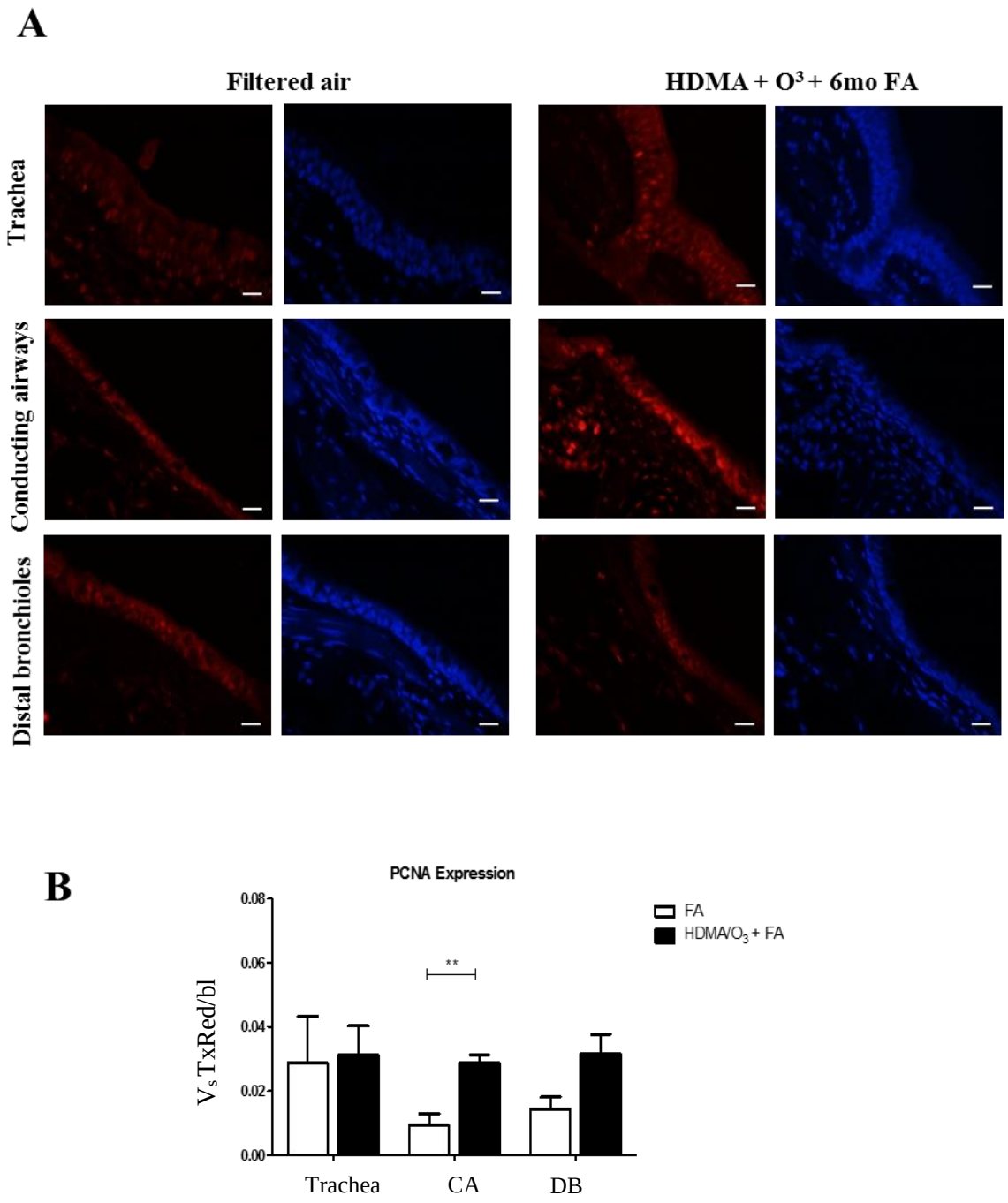

Figure 6.0.11 PCNA expression in healthy and recovering rhesus macaque airways

Representative micrographs of PCNA immunofluorescence in healthy and recovering rhesus macaque airways. (A) Immunofluorescence of the descending airways showed that nuclear PCNA expression was present in the epithelium of both healthy and recovering airways (B) Stereologic quantification of immunofluorescent images stained for PCNA showed that there was a significant increase in PCNA expression in the conducting airways between healthy and recovering monkeys. CA, conducting airways, DB, distal bronchioles, V_s TxRed/bl = volume of positively stained epithelial cells per unit of basal lamina. Scale bars represent 50uM, **p<0.005, n=3.

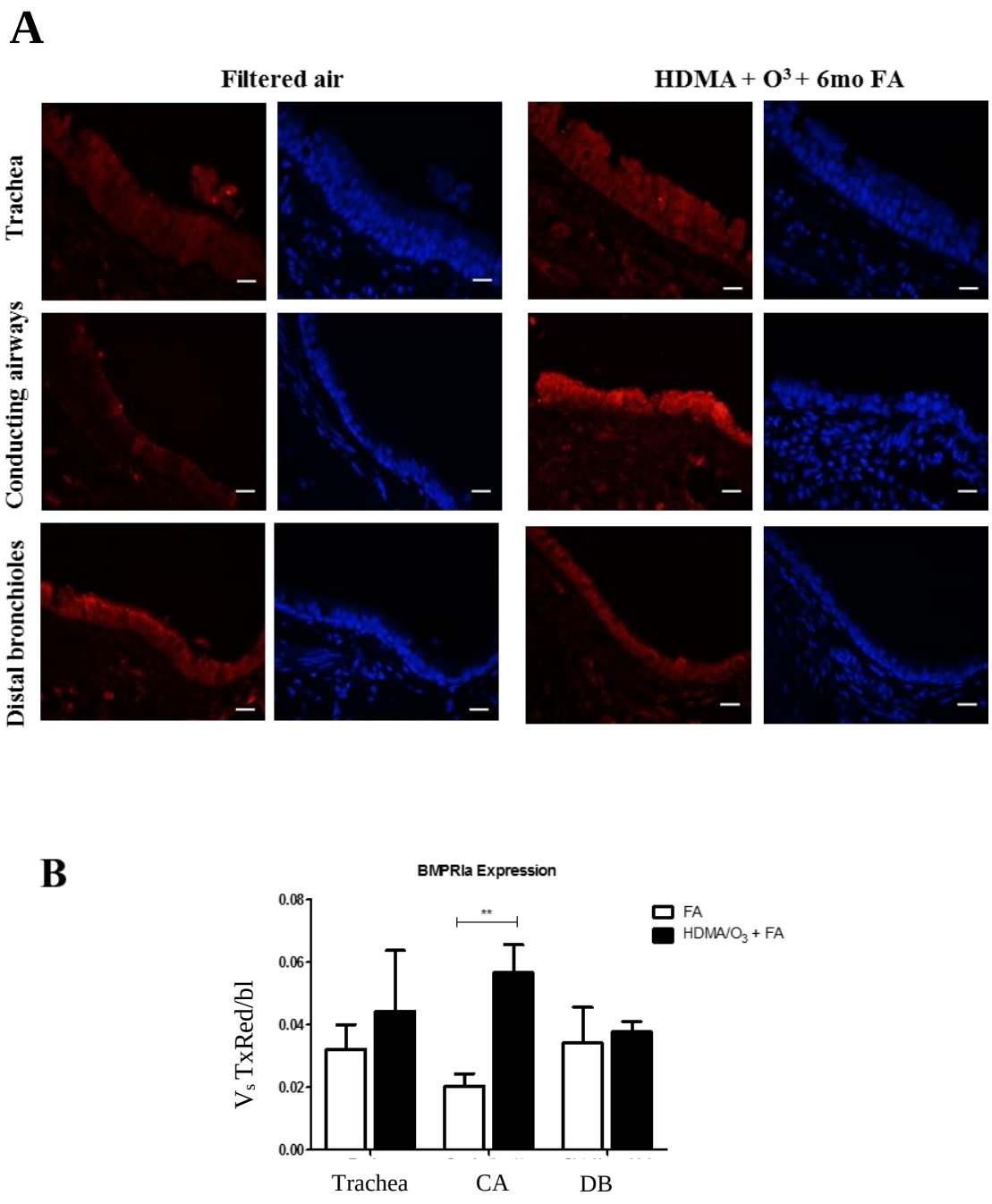

Figure 6.0.12 BMPRIa expression in healthy and recovering rhesus macaque airways

Representative micrographs of BMPRIa immunofluorescence in healthy and recovering rhesus macaque airways. (A) Immunofluorescence showed that BMPRIa was expressed in the cytoplasm and at the cell membrane of epithelial cells in both healthy and recovering airways (B) Stereologic quantification of immunofluorescent images stained for BMPRIa showed that there was a significant increase in BMPRIa expression in the conducting airways between healthy and recovering monkeys. CA, conducting airways, DB, distal bronchioles, V_s TxRed/bl = volume of positively stained epithelial cells per unit of basal lamina. Scale bars represent 50uM, **p<0.005, n=3.

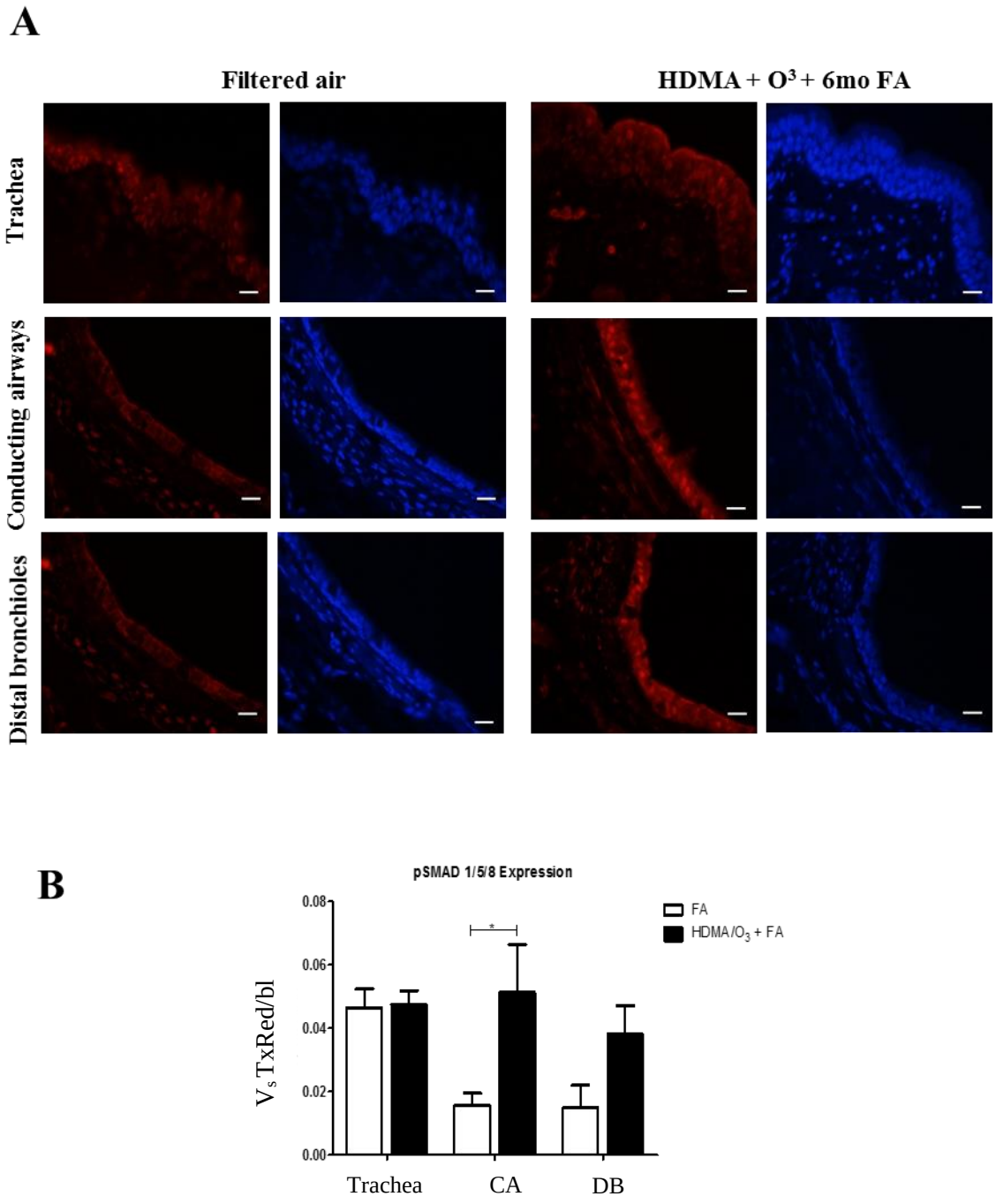

Figure 6.0.13 pSMAD 1/5/8 expression in healthy and recovering rhesus macaque airways

Representative micrographs of pSMAD 1/5/8 immunofluorescence in healthy and recovering rhesus macaque airways. (A) Immunofluorescence of the descending airways showed that nuclear pSMAD 1/5/8 expression was present in the epithelium of both healthy and recovering airways (B) Stereologic quantification of immunofluorescent images stained for pSMAD 1/5/8 showed that there was a significant increase in nuclear protein expression in the conducting airways between healthy and recovering monkeys. . CA, conducting airways, DB, distal bronchioles, V_s TxRed/bl = volume of positively stained epithelial cells per unit of basal lamina. Scale bars represent 50uM, **p<0.005, n=3.

6.1.6 Immunofluorescence analysis of nuclear translocation of BMPRIa in the epithelium of asthmatic monkeys

The epithelium of asthmatic monkeys displayed increased expression of nuclear BMPRIa. Healthy monkey airways expressed membrane bound BMPRIa. Nuclear BMPRIa expression was present in asthmatic airways (Figure 6.0.14 A).

To investigate this expression further, pixel density analysis was carried out using Olympus cellSens Dimension 1.9 software. Analysis of nuclear staining patterns in control and asthmatic epithelial sections highlight elevated nuclear BMPRIa expression in asthmatic airways, as evidence by the overlapping DAPI and TxRed expression patterns (Figure 6.0.14 B**)**. In the control airways, it was clear that BMPRIa/TxRed staining is excluded from the nucleus.

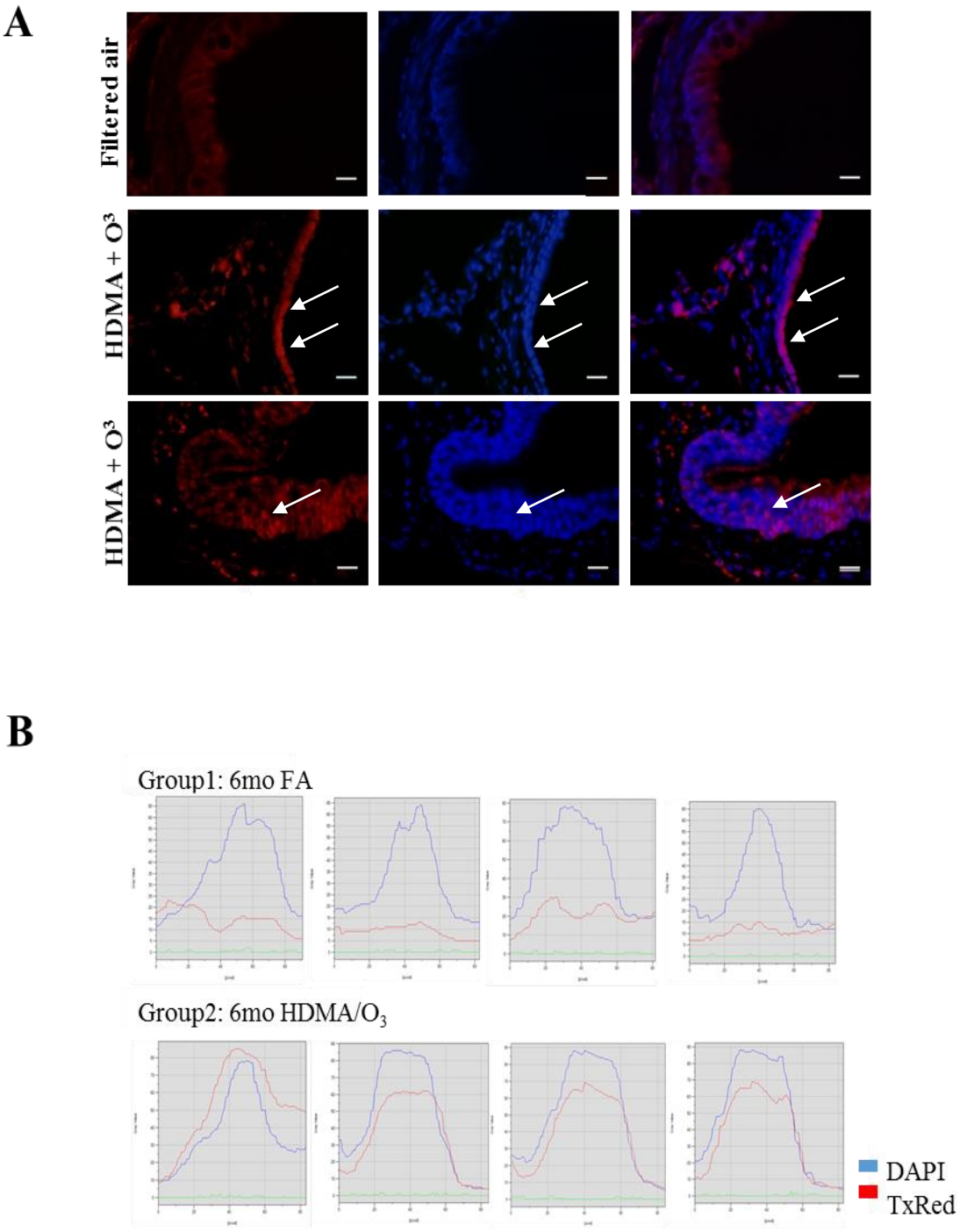

Figure 6.0.14 BMPRIa nuclear translocation in six month old asthmatic monkey airways

Representative micrographs of BMPRIa immunofluorescence of six month old healthy and asthmatic monkeys. (A) Immunostaining showed membrane localised BMPRIa staining in the epithelium of healthy six month old rhesus macaque airways. Following six months exposure to HDMA + O_3 there was evidence of nuclear translocation of BMPRIa, as indicated by the white arrows. (B) Image analysis using Olympus cellSens Dimension 1.9 software illustrated the pixel density of BMPRIa labelled with Alexa568 TxRed and DAPI staining. There was BMPRIa protein expression in the nuclei of epithelial cells in the asthmatic monkeys as evidenced by overlapping DAPI and TxRed staining.

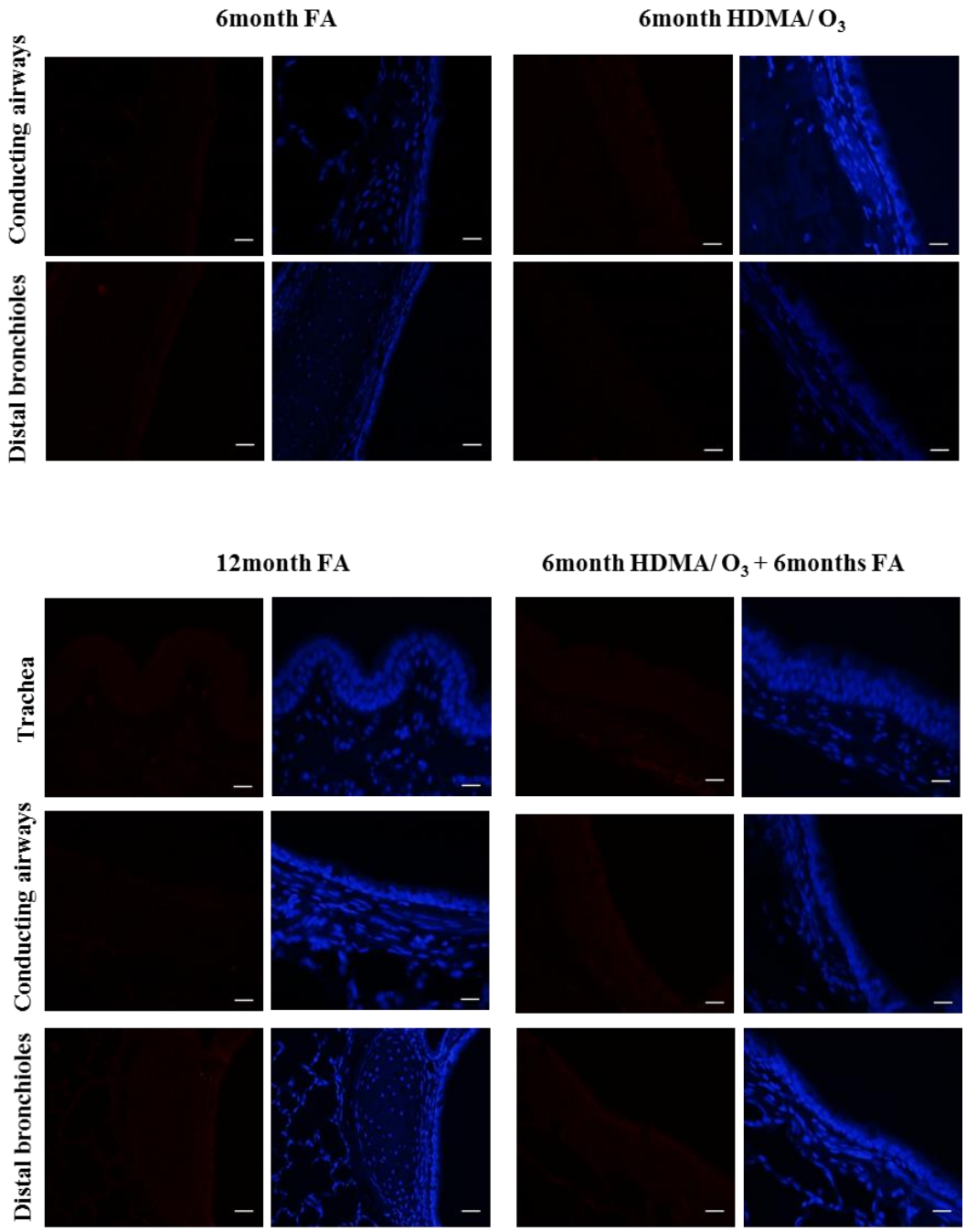

Figure 6.0.15 Secondary antibody controls

Representative immunofluorescence images of antibody controls on the descending airways of rhesus macaques. Secondary antibody controls were incubated with TBS in place of the omitted primary antibody. The anti-rabbit Alexa568-conjugated secondary antibody was then added. (A) Immunofluorescent images of controls in six month healthy and asthmatic rhesus macaques. (B) Immunofluorescent images from 12 month old healthy and recovering rhesus macaques. All scale bars represent 50uM.

6.2 Discussion

Lung development relies on a complex interplay between different signalling pathways. It is understood that growth factor gradients, such as BMP4, are critical in forming the lung architecture as well as directing the spatial distribution of epithelial cells types throughout the airways (Bellusci et al. 1996; Weaver et al. 1999). These pathways are believed to be reactivated in injured and diseased adult lungs to orchestrate epithelial repair and to restore healthy airway homeostasis. Our group and others have shown that BMP signalling is activated during repair in rodent models of airway injury using ovalbumin, nitronaphthalene and bleomycin exposure (Masterson et al. 2011; Rosendahl et al. 2002). Furthermore, BMP signalling is activated in lung stem cell niches following injury, highlighting the importance of the BMP pathway in epithelial cell differentiation and proliferation (Sountoulidis et al. 2012). However, to date, the concept of signalling gradients along the respiratory axis has not been investigated in healthy adult lungs. We have identified a BMP signalling gradient in rhesus macaque airways and demonstrated a reduction in BMP pathway activation in asthma. In addition, we showed that BMP pathway activity was elevated during active recovery in the airways and highlighted a potential mechanistic relationship between inflammation and BMP signalling.

In our study, the presence of nuclear pSMAD 1/5/8 in the conducting airways and distal bronchioles of healthy six and twelve month old monkeys demonstrated constitutive activation of BMP signalling in these regions. Similar results have been reported by us and others in rat and human airway epithelium, although pSMAD 1/5/8 was reported absent from the bronchial epithelium of PBS-treated mouse lungs (Rosendahl et al. 2002; Sountoulidis et al. 2012). In the present study, we also

detected a significant gradient in nuclear pSMAD 1/5/8 expression in the distal airways of healthy twelve month old non-human primates. This suggests that BMP signalling could be involved in the maintenance of homeostasis throughout the airways, but plays a more active role in the trachea compared with lower airways. Interestingly, membrane bound BMPRIa expression did not vary significantly throughout the airway epithelium. This indicates that positive regulators of BMP signalling, such as BMP ligands themselves, may be more active in the tracheal epithelium, or that negative regulators, such as noggin and gremlin, may be more active in the lower airways. The levels of nuclear PCNA in the healthy airways did not vary significantly, consistent with health and homeostasis.

As presented earlier in this thesis, we found that BMPRIa and pSMAD 1/5/8 were also expressed in the lung epithelium of healthy porcine airways but no expression gradients were detected. In porcine airways we analysed total pSMAD 1/5/8 expression in the lung epithelium whereas in primate airways we examined the level of nuclear pSMAD 1/5/8 expression specifically. This could account for the lack of a pSMAD 1/5/8 gradient in the pig lungs. We speculate that pSMAD 1/5/8 expression is linked to epithelial turnover and proliferation events in the porcine airways as the induction of pSMAD 1/5/8 expression by BMP-4 treatment caused upregulation of ID-1 and ID-2 in tracheal explants, known regulators of cell cycle progression. In the primate airways, elevated levels of pSMAD 1/5/8 in the trachea could also be linked to epithelial cell proliferation and differentiation. We have shown that BMP-4 can induce a distal epithelial cell phenotype in porcine tracheal cells thus, we hypothesise that the elevated pSMAD 1/5/8 in the healthy primate tracheal epithelium may be induced by different BMP ligands, namely BMP-2 or BMP-7.

In summary, our results indicate a role for BMP signalling in airway homeostasis. Given that BMP signalling governs cell cycle progression *in vitro* and orchestrates correct epithelial cell differentiation during lung morphogenesis, we speculate that BMP signalling is involved in epithelial cell turnover in healthy airways and mediating epithelial homeostasis (Masterson et al. 2011; Molloy et al. 2008; Weaver et al. 1999).

Repeat exposure to HDMA/O_3 was used to induce allergic airway disease in the 6 month treatment group of rhesus macaques. Previous studies of these monkeys demonstrated both immune and structural responses in the airways (Schelegle, Miller, et al. 2003). The animals displayed elevated eosinophil accumulation in both proximal and distal airways and increased eosinophil presence in bronchoalveolar fluid. Furthermore, the lungs displayed extensive remodelling which directly affected the functionality of the airways. Conducting airways and terminal bronchioles exhibited elevated mucous cell mass and a negative correlation between baseline airway resistance and the ratio of conducting airways to lung parenchyma was evident (Schelegle, Miller, et al. 2003). This suggested that the cyclic exposure model causing allergic airway disease potentially alters the rudimental growth factor and morphogen patterns that orchestrate correct respiratory tract repair and epithelial cell distribution. By examining the expression profile of BMP components along the airways, we have shown that the normal BMP pathway signals are indeed perturbed as a result of HDMA/O_3 exposure. A significant decrease in nuclear pSMAD 1/5/8 in the lung epithelium of conducting airways was evident. Furthermore, although the results proved not to be statistically significant, a decreasing trend of BMPRIa expression could be seen in epithelium of the both the conducting airways and distal bronchioles.

Interestingly, in addition to reduced pSMAD 1/5/8 expression, nuclear localisation of BMPRIa was evident in the conducting airway epithelium of the six month asthma group (Figure 6.0.16). Infiltrating eosinophils were previously shown to be significantly elevated in the conducting airways and distal bronchioles of these monkeys and we hypothesised a link between these inflammatory cells and the BMP pathway. Many studies have shown that eosinophils and specifically their secondary derived proteins play a central role in airway remodelling, perpetuating airway hyper-responsiveness in asthma and inflammatory airway diseases but the signalling pathways governing these events remain poorly understood (Costello et al. 2009; Gleich and Adolphson 1993a, 1993b; Humbles et al. 2004). Previous results in our lab carried out by Dr. Emer Molloy, have shown that transient BMPRIa trafficking can be induced by eosinophil derived cationic proteins. When MAECs were treated with eosinophil derived cationic proteins BMPRIa was transiently trafficked from the membrane to the nucleus. This indicates a potential mechanism whereby the eosinophil-derived proteins may influence BMP signalling by altering the localisation of BMPRIa. Moreover, if reduced pSMAD 1/5/8 signalling is a consequence of this modulation, this could explain the significant reduction in levels of nuclear pSMAD 1/5/8 in the conducting airways in the six month asthma group. This possibility is further supported by Kariyawasam et al., who demonstrated that eosinophils are the predominate producer of BMP-7 in the lung epithelium of asthmatic airways (Kariyawasam et al. 2008). Co-localisation of BMP-7 with MBP-positive eosinophils was observed in these asthmatic airways. As BMP-7 is known to act as an anti-inflammatory ligand in other organs, the authors speculated that the increase in ligand expression could be an attempt to regulate inflammation as part of the reparative processes in the airways

(Kariyawasam et al. 2008; Maric et al. 2003). Previous work presented here indicated that BMP-7 could also be linked to inducing MET to control fibrosis, as shown in the DLKP cell line. In addition, an *in vitro* study using the neuroblast IMR32 cell line reported a similar down-regulation of BMPRIa RNA expression following a 4hr exposure to eosinophil-derived MBP. Co-incubation of the cells with BMP-7 and MBP decreased the induction of ID-1, an established downstream target of the BMP pathway (Costello et al. 2009).

Taken together with our results, we hypothesise that the attenuated expression levels of BMP signalling present in this non-human primate model of asthma are due to eosinophil-induced nuclear translocation of membrane-bound BMPRIa. Subsequent inhibition of downstream BMP signalling pathways interferes with appropriate epithelial repair processes mediated by BMP and its signalling partners such as FGF-7 (Desai and Cardoso 2002). This could contribute to a chronic disease state promoting incorrect epithelial turnover, an inflammatory phenotype and epithelial remodelling, all of which are well-established hallmarks of asthma.

While BMP receptor processing and trafficking between the nucleus and the membrane are common in receptor synthesis and normal signal transduction, incorrect receptor trafficking can contribute to disease as evidenced by BMPRII mutations in pulmonary hypertension (Lane et al. 2000). Trafficking of receptors from the membrane and nuclear accumulation of FGF, EGF, NGF, IL-5 and Notch receptors have all been previously described (Di Guglielmo et al. 2003; Jans et al. 1997; Lo and Hung 2006; Stachowiak et al. 1996; Struhl and Adachi 1998; Zwaagstra, Guimond, and O'Connor-McCourt 2000). As reviewed by Carpenter (2003) there are a number of possible routes into the nucleus. Following ligand binding at the membrane, receptors enter the endosome where some are degraded

and others are re-cycled to the membrane or into the nucleus. Using a putative Golgi-ER pathway and the NLS to facilitate traversing across the nuclear envelope, the receptors can be translocated to the nucleus (Jans and Hassan 1998). Ligand-independent nuclear accumulation has also been documented for TGF-β and EGFR (Carpenter 2003; Dittmann, Mayer, and Rodemann 2005; Lo and Hung 2006; Zwaagstra et al. 2000).

The mechanism through which eosinophil cationic protein induce BMPRIa trafficking has not yet been elucidated. Despite multiple studies examining receptor trafficking and endosomal translocation in TGF- β and other TRK signal transduction pathways, BMP signalling trafficking remains largely enigmatic. Ligand-mediated BMPRIa trafficking has been previously reported in primary human lymphoblastoid cell lines (de la Peña et al. 2005). Differential receptor internalisation pathways were explored in HEK and C2C12 cells and results showed that the activation of SMAD-dependent and –independent pathways by BMP ligands could be attributed to specific routes of endocytosis (Hartung et al. 2006). Furthermore, nuclear BMPRIa expression has also been reported when it co-localised with the splicing factor SAP49 in the inner leaflet of the nuclear membrane (Nishanian and Waldman 2004). We hypothesise that BMPRIa receptor translocation in that primate epithelial cells could be caused by eosinophil-induced ligand production by the epithelial cells or underlying fibroblasts to internalise the receptor. This could occur by the induction of BMP-2 which possesses a potential NLS and has been shown to bind directly to BMPRIa ((Nickel et al. 2001, E.L Molloy, PhD). Alternatively, a ligand independent pathway could be occurring which is mediated through the kinase activity of BMPRIa. Our results demonstrate that reduced membrane receptor expression could lead to reduced downstream

BMP signalling by preventing phosphorylation of the R-SMAD receptor complex and subsequent translocation of pSMAD 1/5/8 into the nucleus. However, a specific role for BMPRIa in the nucleus has yet to be shown.

The regenerating airway model used here provided further evidence for the involvement of BMP signalling in inflammatory airway disease and repair processes. The increased incidence of nuclear PCNA is consistent with repair processes in the conducting airways following a period of chronic injury and inflammation. Increased expression of membrane-localised BMPRIa in these regions indicates a role for BMP signalling in the repair/regeneration processes. In other mouse and human asthma models, similar increases in BMP signalling evidenced by nuclear pSMAD1/5/8 were observed in bronchial epithelium challenged with OVA or an aeroallergen, respectively (Kariyawasam et al. 2008; Rosendahl et al. 2002). Previous studies of this rhesus macaque model showed that these monkeys displayed modest signs of repair and airway regeneration. Perlecan was re-introduced at the basement membrane and there was evidence for the re-establishment of correct mucous cell expression in the proximal airways (Evans et al. 2010). We speculate that this recovering phenotype of the airways is further promoted by increased BMPRIa expression at the membrane, promoting elevated ligand-induced nuclear translocation of pSMAD 1/5/8 protein. This causes the epithelial cells to enter a state of active repair and proliferation in an attempt to restore an appropriate homeostatic environment in the airways. This occurs perhaps through the expression of ID genes and elevated production of BMP-7 ligand in an attempt to counteract the anti-mitogenic properties of TGF-β to regulate cell proliferation, remodelling and epithelial differentiation (Moses, Yang, and Pietenpol 1991; Tirado-rodriguez et al. 2014).

We speculate that the higher BMPRIa membrane staining present in the recovery monkeys is a result of reduced eosinophil infiltration in the airways. This is supported by the reduced eosinophil presence in the BAL fluid of the recovery monkeys compared to the asthmatic monkey and previous human asthmatic airway studies that show attenuated cellular inflammation following the removal of airway insult (Kariyawasam et al. 2007). Lowered levels of eosinophilic granule proteins could decrease the nuclear translocation of BMPRIa and thus account for the elevated membrane--localised BMPRIa expression and nuclear pSMAD 1/5/8 signalling present in the cells. As a result, an important feedback mechanism in the lung epithelium may exist whereby the removal of airway insult reduces eosinophil infiltration and eosinophil-induced downregulation of BMP signalling. This mechanistic hypothesis is supported by recent studies showing for the first time a definitive anti-inflammatory function of BMP signalling in the stomach and airway epithelium (Li et al. 2014; Takabayashi et al. 2014). The enhanced BMP pathway activity could induce the putative anti-inflammatory function of BMPs, preventing further inflammation and damage to the epithelium and facilitating the restoration of correct epithelial cell turnover and repair (Figure 6.0.16).

We have shown that BMPRIa localisation is altered in asthmatic airways. We speculate that eosinophils – and particularly the cationic effector proteins of eosinophils - could be responsible for the altered receptor expression. The mechanisms involved in BMP receptor trafficking, the effect of nuclear localised BMPRIa and the definitive role of eosinophilic effector proteins in this process remain poorly understood. Future experiments should address this potential mechanistic relationship between eosinophils and BMP signalling.

To conclude, this study using this non-human primate model of allergic airway disease indicate that not only are developmental pathways re-activated during inflammatory airway disease involving epithelial injury, but that basal expression of the BMP signalling pathway is important for maintaining healthy airways.

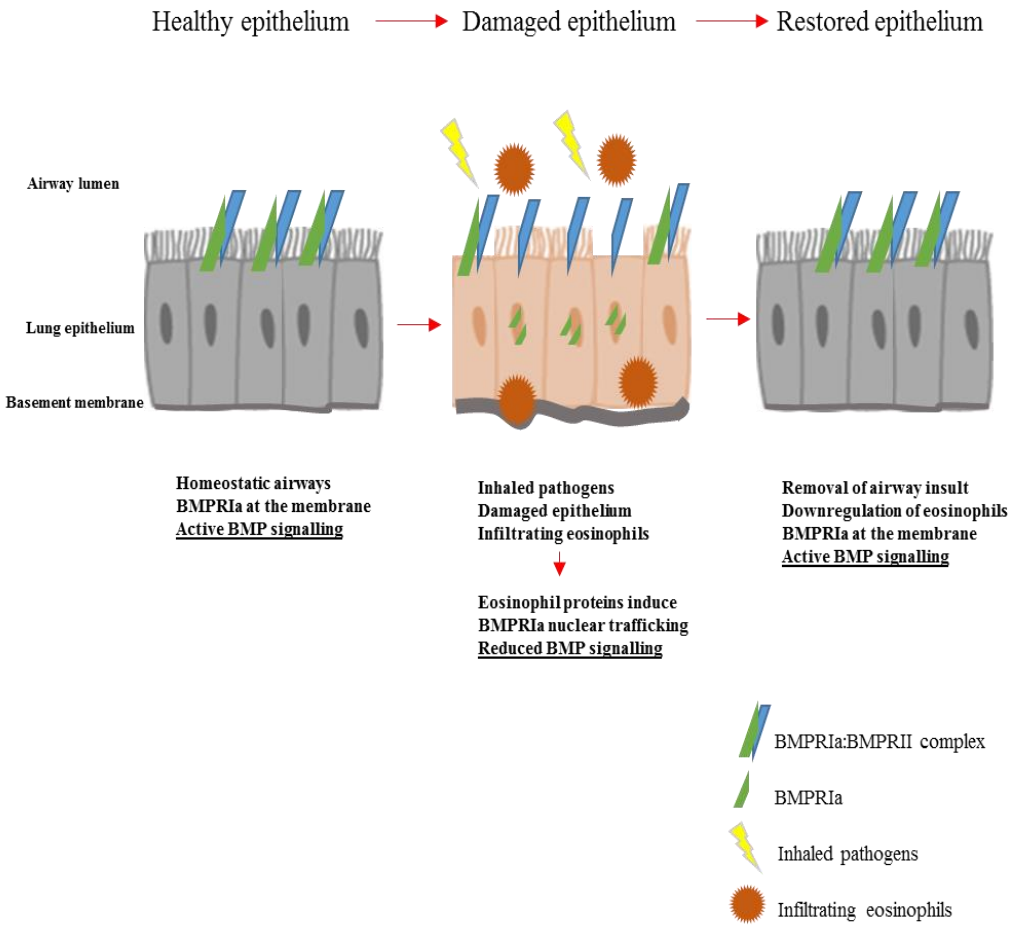

Figure 6.0.16 Hypothesis of eosinophil-induced transient trafficking of BMPRIa

Healthy airway epithelial cells express BMPRIa at the membrane and normal homeostatic BMP signalling occurs via downstream activation of pSMAD 1/5/8. Following airway insult and the induction of an inflammatory response in the airway epithelium, infiltrating eosinophils are recruited to the site which illicit their response by releasing cationic proteins. Either by binding BMPRIa directly or inducing BMP ligands, eosinophilic cationic proteins potentially induce BMPRIa nuclear-translocation and the BMP signalling pathway is disrupted. Reduced BMP signalling occurs which in turn affects cell proliferation and epithelium remodelling events. Removal of the pathogen facilitates the restoration of membrane bound BMPRIa signalling and activation of normal BMP signalling events. This encourages active epithelial repair and restoration of epithelial integrity.

Chapter 7

Final Conclusions

7.1 Conclusion

Bone morphogenetic signalling is involved in correct lung morphogenesis and establishing correct epithelial cell distribution along the developing airways. We have shown that BMP signalling remains active in healthy adult airways. Using porcine bronchial tissue, we demonstrated that BMP ligands, BMP antagonists and intracellular SMAD molecules are expressed in homeostatic lung epithelium. We detected a BMP signalling gradient in the airways and illustrated that this BMP-4 expression gradient may be responsible for maintaining distal epithelial cell distribution in the airways. In addition, we have demonstrated active BMP signalling is present in healthy rhesus monkey airways. These results provide evidence that basal BMP pathway signalling is maintained in healthy adult airways. The work also highlights a potential role for active BMP signalling in homeostatic airways.

In order to investigate BMP signalling in adult lung diseases we used an established model of allergic airway disease in rhesus macaques. BMP signalling was reduced in asthma and subsequently elevated during active recovery of the lung epithelium. We highlighted a potential mechanistic relationship between inflammation and BMP in the airways. Using a lung cancer cell model, we investigated the role of BMP signalling in EMT-mediated phenotypic switching. Firstly, by stimulating subpopulations of a heterogeneous lung cancer cell line with BMP-4 or gremlin, we

showed that BMP signalling was capable of inducing phenotypic switching between the clones. Moreover, using an E-cadherin reporter plasmid we demonstrated the differences in phenotype along the cadherin axis and highlighted that differences in E-cadherin gene processing between the clones result in a more invasive and mesenchymal cell phenotype. This work implicates BMP signalling with increased tumour invasiveness and the induction of EMT in cancer cells.

Overall these data highlight the presence and importance of BMP signalling gradients in healthy adult airways and further implicate BMP signalling in the pathogenesis of inflammatory and malignant airway diseases.

7.2 Future directions

We have shown that BMP signalling is active in the descending lung epithelium of both porcine and non-human primate airways. While porcine explants allowed further investigation of the role of BMP signalling the airways, future experiments should utilise primary culture of airway epithelial cells. Development of air-liquid interface cultures would provide a robust platform for studying the role of BMP signalling during airway homeostasis. Using targeted inhibition of BMP signalling by siRNA, the role of BMP pathway activation in epithelial cell proliferation and differentiation could be elucidated. Furthermore, determination of the expression of pro-inflammatory cytokines following targeted injury of the epithelium and the effect of BMP ligands/inhibitors on cytokine release would provide further insight into the role of BMP signalling in airway repair and inflammation.

Our work focused primarily on characterising canonical BMP signalling in the descending airways. The presence of pERK 1/2 in the descending airways highlighted that non-canonical BMP pathways were active in the airways. Future experiments should characterise non-canonical BMP signalling and other growth factor signalling in the descending airways. This could highlight different signalling gradients responsible for maintaining homeostasis in the lung epithelium.

It is important for future work investigating the BMP pathway in the airways to identify the specific cell populations involved in BMP signalling and to investigate if there is any modulation in BMP signal expression following damage and during repair of the airways. For example, double immunostaining of histological sections with epithelial cell markers would allow characterisation of the cells responsible for BMP pathway activation.

We have shown that BMPRIa localisation is altered in asthmatic airways. We speculate that eosinophils – and particularly the cationic effector proteins of eosinophils - could be responsible for the altered receptor expression. The mechanisms involved in BMP receptor trafficking, the effect of nuclear localised BMPRIa and the definitive role of eosinophilic effector proteins in this process remain poorly understood. Future experiments should address this potential mechanistic relationship between eosinophils and BMP signalling.

We have shown that the DLKP cell lines are a dynamic model for studying tumour heterogeneity and phenotypic switching. Our results demonstrated the differences in E-cadherin gene processing, growth patterns and expression of cell adhesion proteins between the DLKP clones. Further characterisation of these clones would be beneficial and provide further insights into the re-programming events that have occurred to give rise to the different cell phenotypes. This would provide important information regarding potential therapeutic targets for cancer treatments.

Investigating the effect of the E-cadherin reporter plasmids in DLKP-I clones would be very useful. These cells express N-cadherin, similar to DLKP-M but lack E-cadherin. They represent an EMP population between DLKP-SQ and DLKP-M on the EMT axis. Transfection of DLKP-I cells would further elucidate where on the cadherin axis this "intermediate" population exists. Future experiments should address the potential cleavage events and downregulation of the E-cadherin protein which occurs in DLKP-M cells following E-cadherin overexpression.

In this study, we investigated the effect of BMP-4 and gremlin on DLKP cell populations. Further experiments should utilise BMP-2 and BMP-7 to investigate the effect of these ligands on motility and EMT. In addition the role of TGF-β has

not been explore in DLKP cells lines. Firstly, the level of expression of endogenous TGF-β ligands and receptors would be investigated in DLKP cell lines. In addition, targeted inhibition of TGF-β / BMP signalling using siRNA or neutralising antibodies would provide a greater insight into the role of BMP and TGF-β signalling in EMT. By silencing BMP signalling in DLKP-M cells, their mesenchymal metastatic properties may be reversed. These experiments could also elucidate the role of BMP signalling with proliferation in DLKP cell populations.

Future experiments investigating BMP signalling and EMT should be carried out. Treatment experiments involving DLKP-M clones and BMP-4 could lead to important findings regarding growth factor induced EMT and fibrosis. The role of BMP signalling *in vivo* during tissue fibrosis would be of particular interest and could highlight BMP as a potential therapeutic target.

Chapter 8

Appendix

A

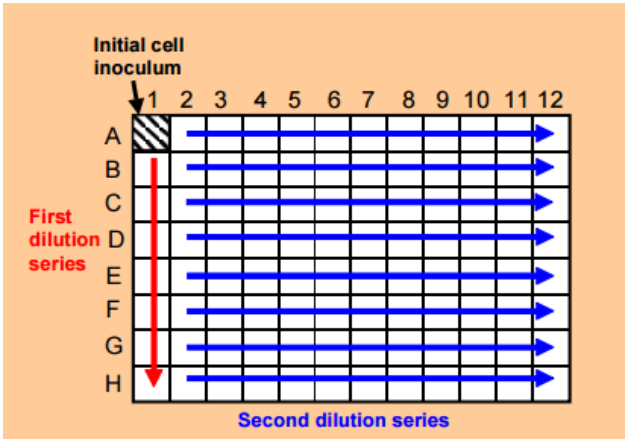

B

DLKP-SQ Em^2 purified population

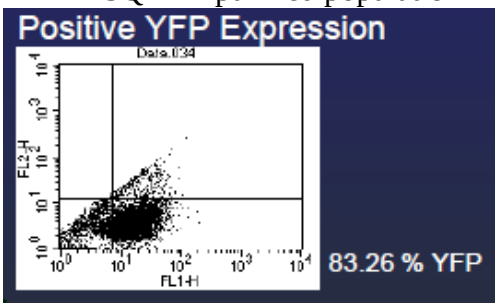

DLKP-M Em^2 purified population

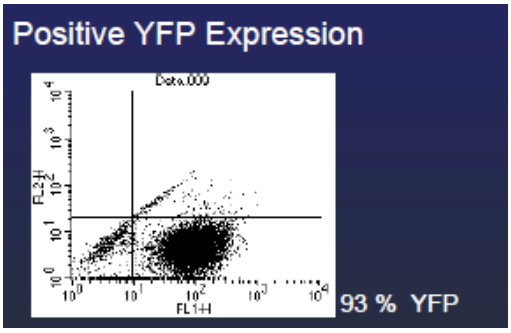

Figure 8.0.1. Generation of fluorescent DLKP-SQ and DLKP-M clones by Dr. Emer Molloy. (A) Expansion of the fluorescent clones was carried out by serial dilution for clonal expansion was carried out using the Corning ® Serial dilution protocol. Single Fluorescence cells were selected based on FACS fluorescence. (B) FACS analysis of purified DLKP-SQ Em^2 and DLKP-M Em^2 populations displayed 83.26% and 93% YFP expression, respectively. This work was carried out by Dr. Emer Molloy (O'Dea lab).

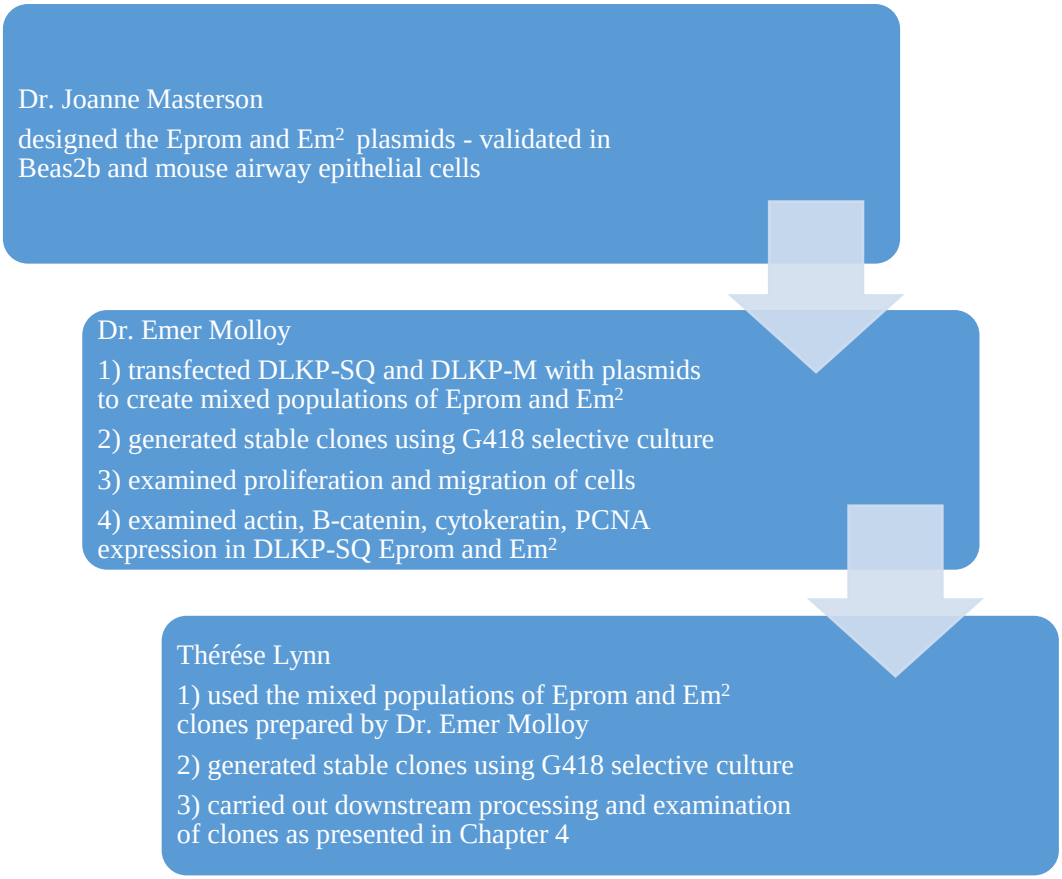

Figure 8.0.2 Flow chart of DLKP work carried out in the O'Dea lab

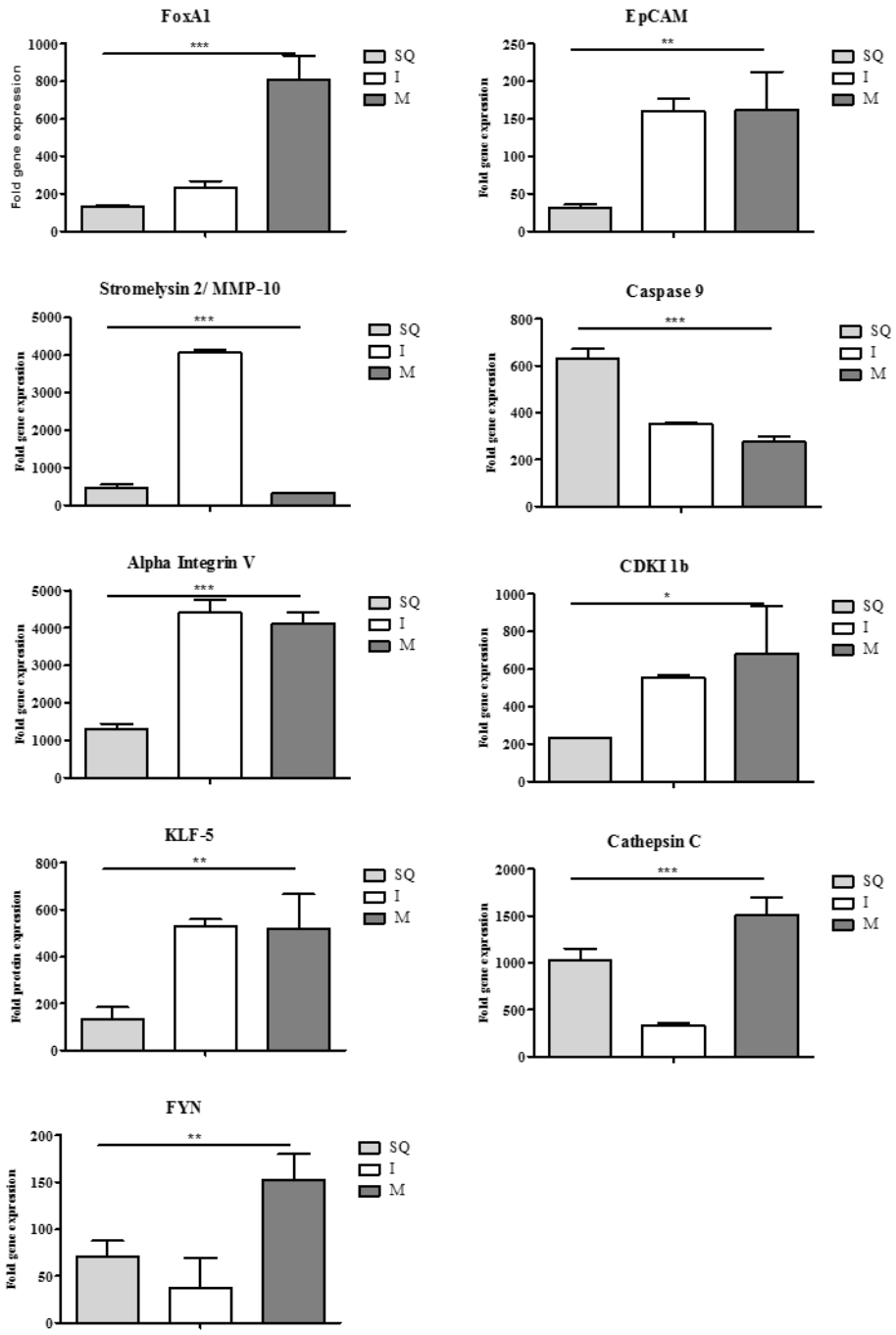

Figure 8.0.3 Gene expression analysis in DLKP clones

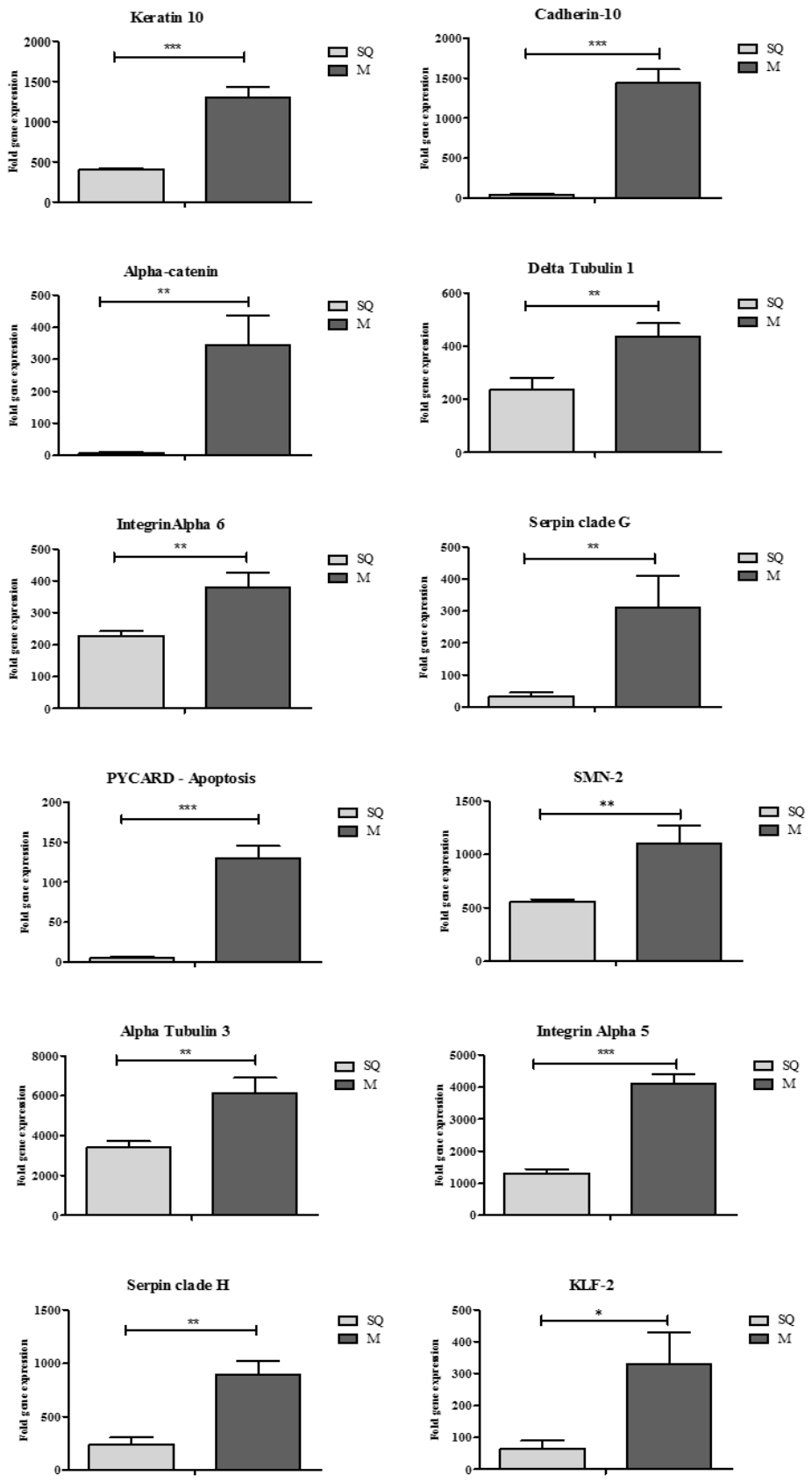

Figure 8..0.4 Gene expression analysis in DLKP-SQ and DLKP-M clones

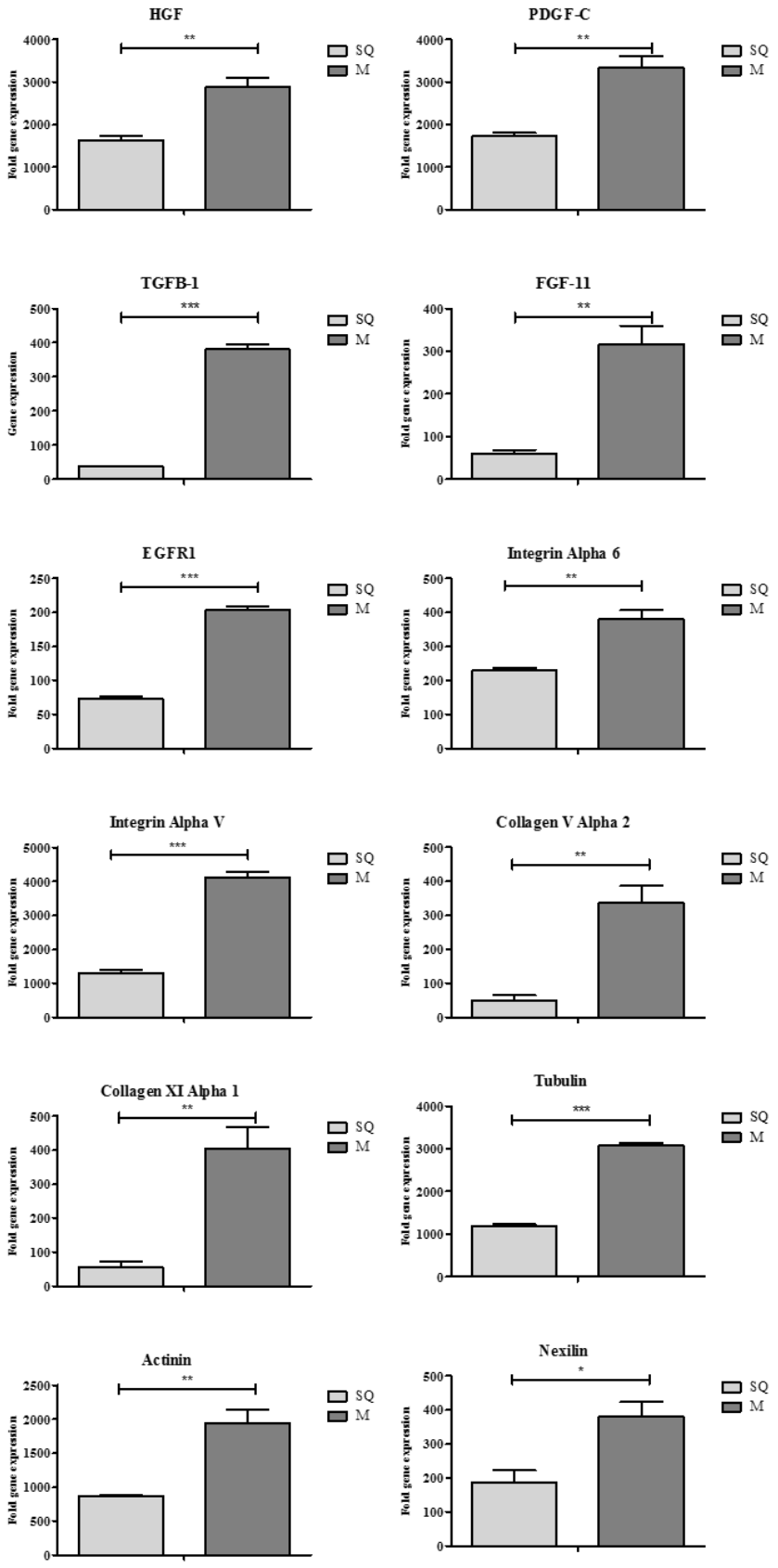

Figure 8.0.5 Genes expressed higher in DLKP-M compared to DLKP-SQ

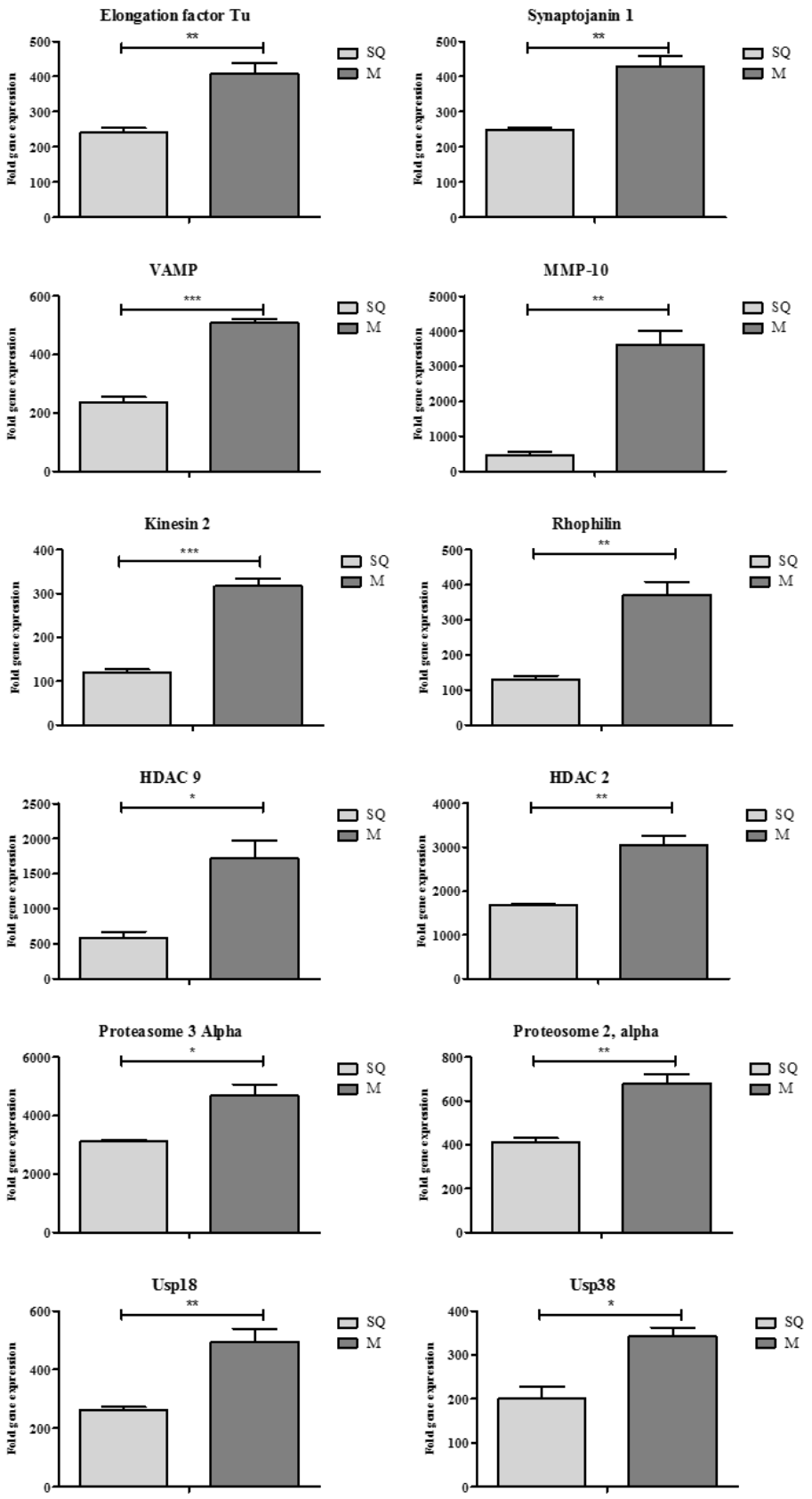

Figure 8.0.6 Genes expressed higher in DLKP-M compared to DLKP-SQ

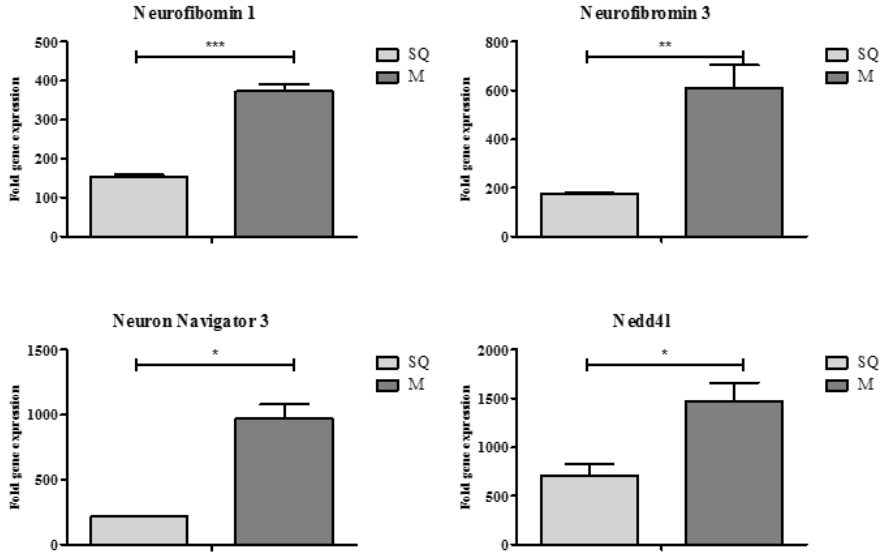

Figure 8.0.7 Genes expressed higher in DLKP-M compared to DLKP-SQ

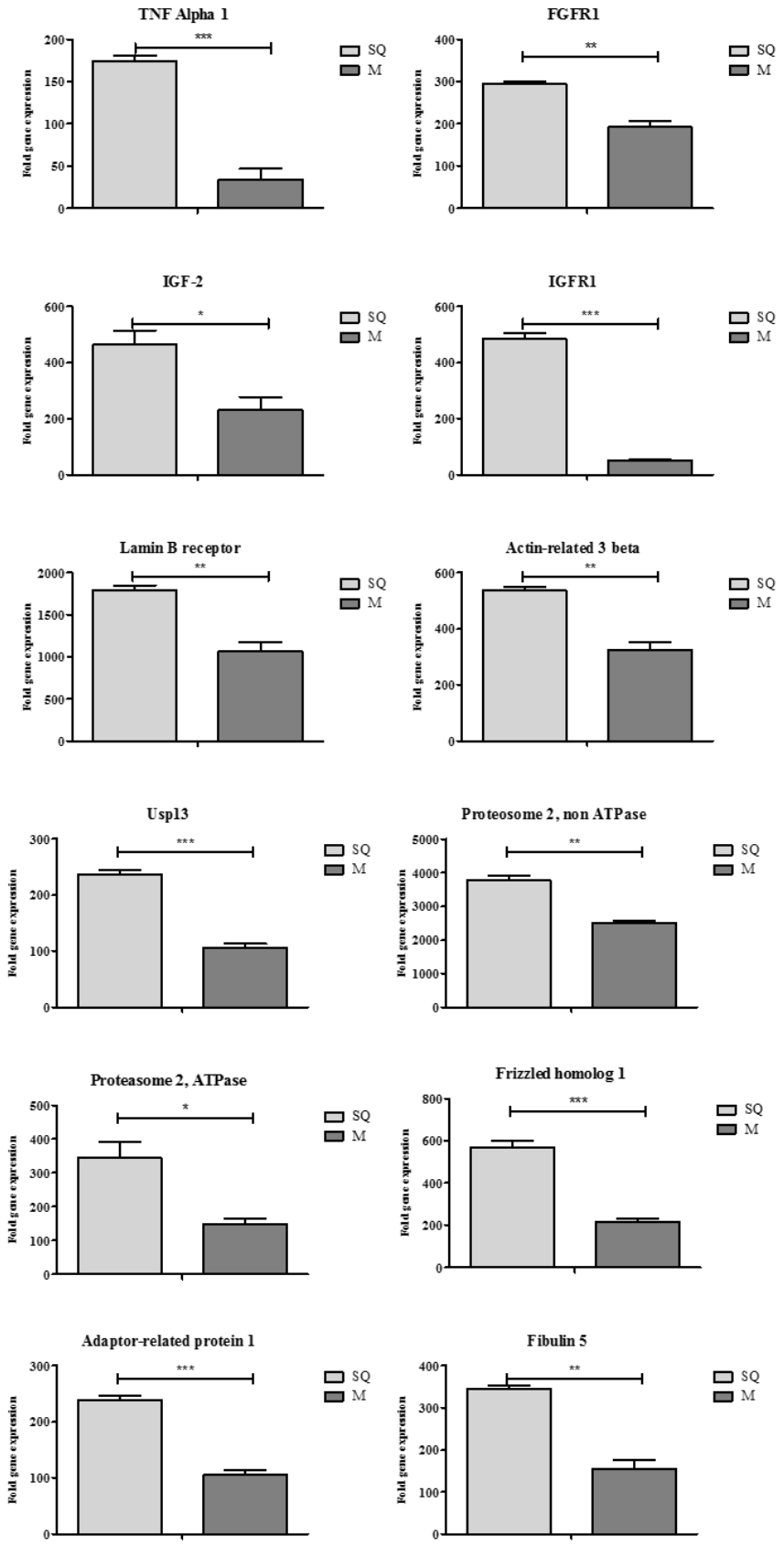

Figure 8.0.8 Genes expressed higher in DLKP-SQ compared to DLKP-M

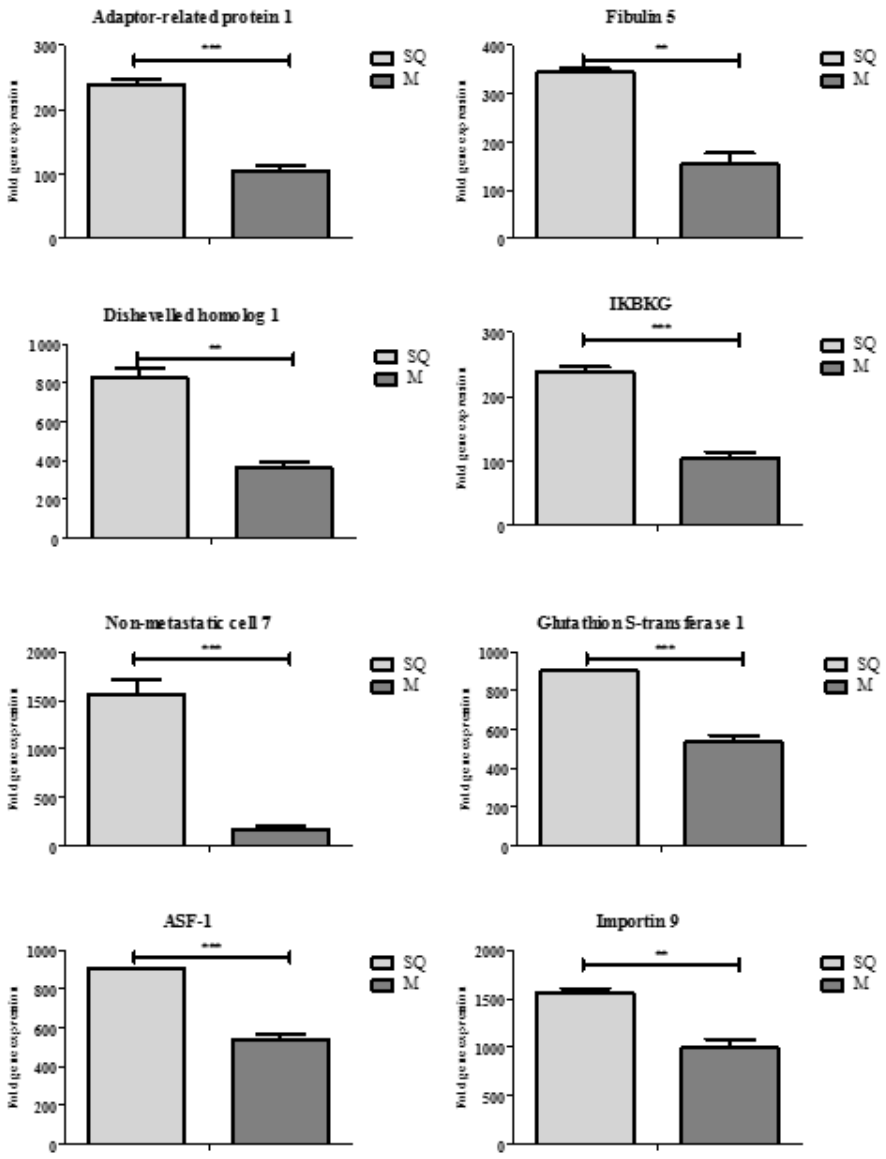

Figure 8.0.9 Genes expressed higher in DLKP-SQ compared to DLKP-M

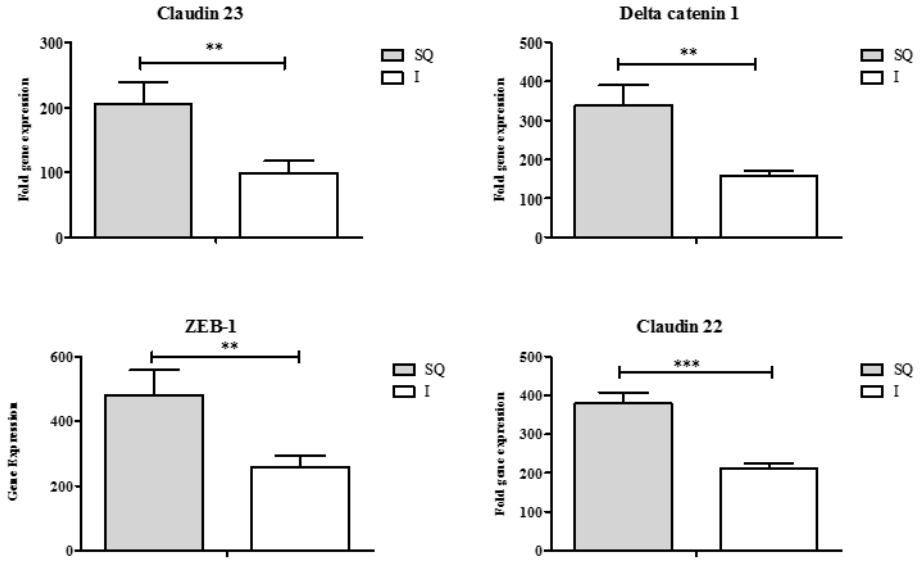

Figure 8.0.10 Genes expressed higher in DLKP-SQ compared to DLKP-SQ

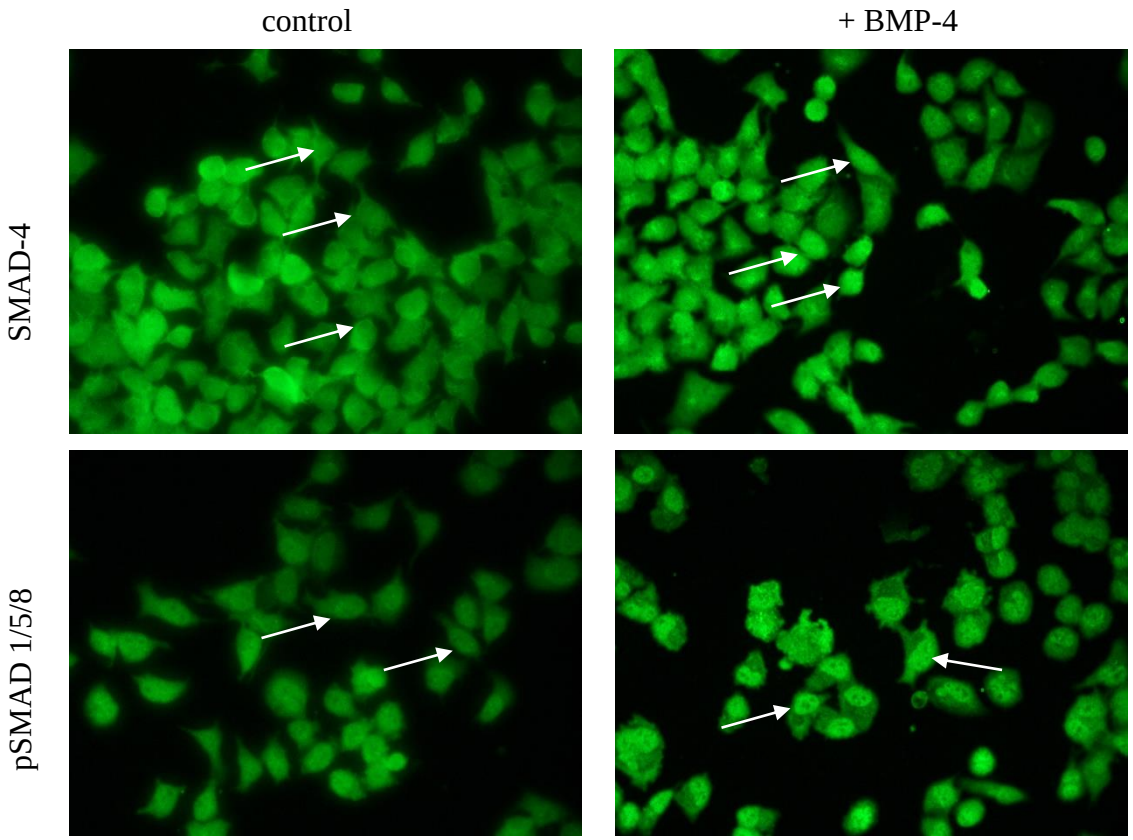

Figure 8.0.11 Larger images of DLKP-SQ cells treated with BMP-4
Continued from figure 3.0.4. At the same microscope exposure, increased nuclear localisation of SMAD-4 and pSMAD 1/5/8 was evident in DLKPSQ cells treated with 100 ng/ml BMP-4 for 24 hrs, as indicated by the white arrows.

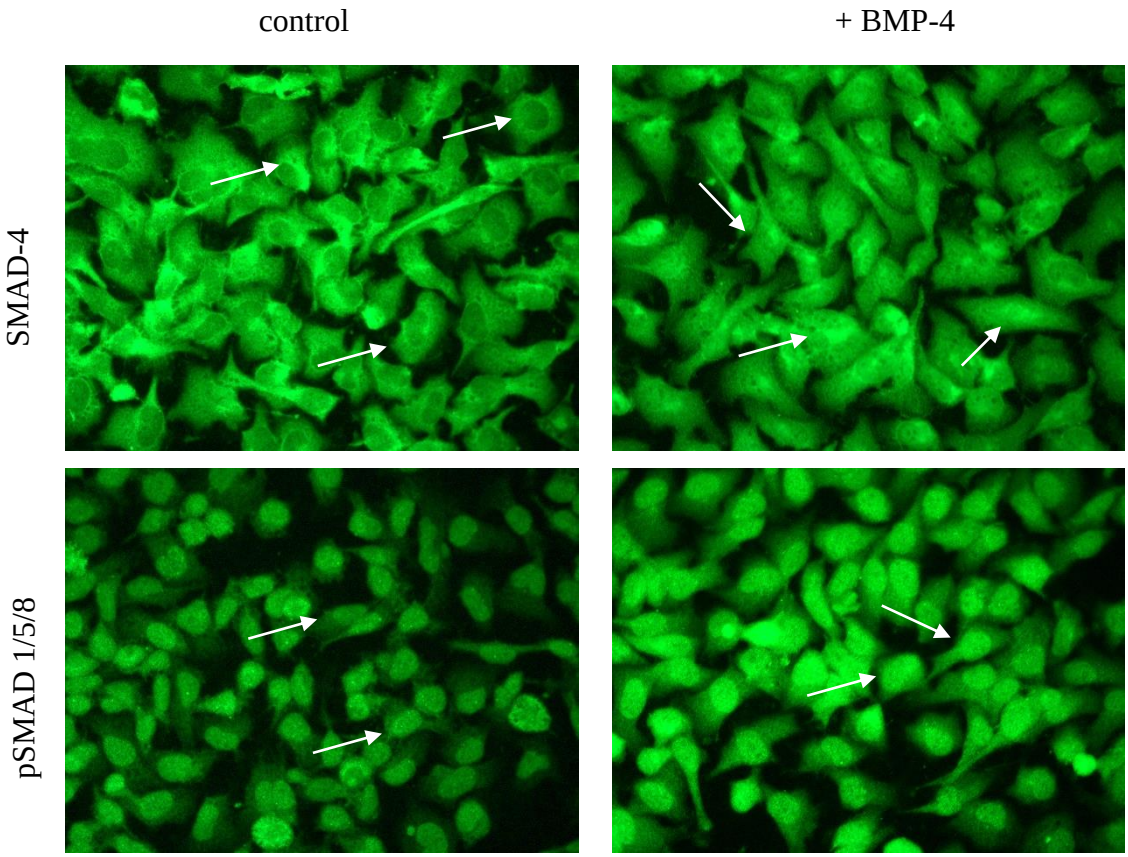

Figure 8.0.12 Larger images of DLKP-M cells treated with BMP-4
Continued from figure 3.0.6. At the same microscope exposure, increased nuclear localisation of SMAD-4 and pSMAD 1/5/8 was evident in DLKP-M cells treated with 100 ng/ml BMP-4 for 24 hrs, as indicated by the white arrows.

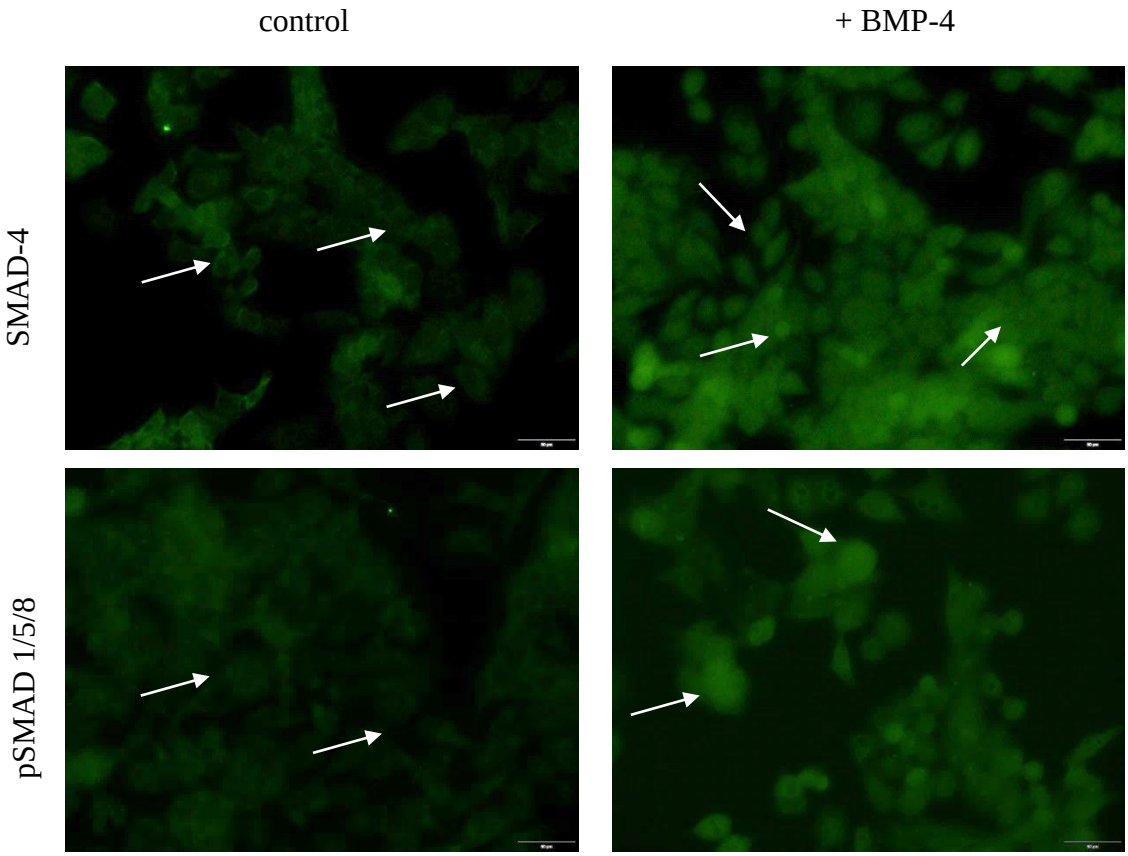

Figure 8.0.13 Larger images of DLKP-I cells treated with BMP-4
Continued from figure 3.0.8. At the same microscope exposure, increased nuclear localisation of SMAD-4 and pSMAD 1/5/8 was evident in DLKP-I cells treated with 100 ng/ml BMP-4 for 24 hrs, as indicated by the white arrows.

Chapter 9

Publications and presentations

Therese M. Lynn, Emer L. Molloy, Joanne C. Masterson, Senan F. Glynn, Richard W. Costello, Mark V. Avdalovic, Edward S. Schelegle, Lisa A. Miller, Dallas M. Hyde, Shirley O'Dea. **SMAD signaling in the airways of healthy versus asthmatic rhesus macaques highlights a relationship between inflammation and BMPs.** Am J Respir Cell Mol Biol. First published online 28 Sep 2015 as DOI: 10.1165/rcmb.2015-0210OC

Poster title	**Conference**	**Location**	**Date**
Examining BMP signalling in healthy and asthmatic rhesus macaques airways	Human Disease Mapping, RCSI	RCSI, Dublin, Ireland	16-17th Dec 2013
The BMP pathway in the lung epithelium of healthy and diseased primate and porcine airways.	10th International BMP conference	FreieUniversitat, Berlin, Germany	16-20th Sept 2014
Mapping the expression of Bone Morphogenetic Proteins in healthy and diseased airways	Young Life Scientists Symposium, Biochemical society	UCDConway Dublin, Ireland	12th Nov, 2014
BMP signalling in the airway epithelium	The Lung epithelium in health and disease, Keystone	Keystone Conference Centre, Colorado USA	16-20th Feb 2015
SMAD signaling in descending airways of healthy versus asthmatic rhesus macaques highlights a relationship between inflammation and BMPs	British Association of Lung Research	Bath Assembly, Bath, UK	2-4th Sept 2015

Chapter 10

Bibliography

Acharya, Prasad, Jonathan Beckel, Wily G. Ruiz, Edward Wang, Raul Rojas, Lori Birder, Gerard Apodaca, and Gerard Apodaca Distribution. 2004. "Distribution of the Tight Junction Proteins ZO-1 , Occludin , and Claudin-4 , -8 , and -12 in Bladder Epithelium." *Am J Physiol Lung Cell Mol Physiol* 287:305–18.

Acloque, Hervé, Meghan S. Adams, Katherine Fishwick, Marianne Bronner-Fraser, and M. Angela Nieto. 2009. "Epithelial-Mesenchymal Transitions: The Importance of Changing Cell State in Development and Disease." *Journal of Clinical Investigation* 119(6):1438–49.

Ahdieh, M., T. Vandenbos, and A. Youakim. 2001. "Lung Epithelial Barrier Function and Wound Healing Are Decreased by IL-4 and IL-13 and Enhanced by IFN-Gamma." *American journal of physiology. Cell physiology* 281(6):C2029–38. Retrieved September 11, 2015 (http://www.ncbi.nlm.nih.gov/pubmed/11698262).

Akiyama, Haruhiko, Marie-Christine Chaboissier, Richard R. Behringer, David H. Rowitch, Andreas Schedl, Jonathan A. Epstein, and Benoit de Crombrugghe. 2004. "Essential Role of Sox9 in the Pathway That Controls Formation of Cardiac Valves and Septa." *Proceedings of the National Academy of Sciences of the United States of America* 101(17):6502–7. Retrieved August 18, 2015 (http://www.pubmedcentral.nih.gov/articlerender.fcgi?artid=404074&tool=pmcentrez&rendertype=abstract).

Alejandre-Alcázar, Miguel a, Petar D. Shalamanov, Oana V Amarie, Julia Sevilla-Pérez, Werner Seeger, Oliver Eickelberg, and Rory E. Morty. 2007. "Temporal and Spatial Regulation of Bone Morphogenetic Protein Signaling in Late Lung Development." *Developmental dynamics : an official publication of the American Association of Anatomists* 236(10):2825–35. Retrieved November 9, 2013 (http://www.ncbi.nlm.nih.gov/pubmed/17823941).

Angst, B. D., C. Marcozzi, and a I. Magee. 2001. "The Cadherin Superfamily: Diversity in Form and Function." *Journal of cell science* 114(Pt 4):629–41. Retrieved (http://www.ncbi.nlm.nih.gov/pubmed/11171368).

Aplin, John D., Teresa Haigh, Ljilyana Vicovac, Heather J. Church, and Carolyn J. P. Jones. 1998. "Anchorage in the Developing Placenta: An Overlooked Determinant of Pregnancy Outcome?" *Human fertility (Cambridge, England)* 1(1):75–79. Retrieved September 14, 2015 (http://www.ncbi.nlm.nih.gov/pubmed/11844314).

Arndt, Stephanie, Ina Poser, Markus Moser, and Anja-Katrin Bosserhoff. 2007.

"Fussel-15, a Novel Ski/Sno Homolog Protein, Antagonizes BMP Signaling." *Molecular and cellular neurosciences* 34(4):603–11. Retrieved September 9, 2015 (http://www.sciencedirect.com/science/article/pii/S1044743107000036).

Azarschab, Pia, Agnieszka Stembalska, Mirela Baus Loncar, Markus Pfister, Maria M. Sasiadek, and Nikolaus Blin. 2003. "Epigenetic Control of E-Cadherin (CDH1) by CpG Methylation in Metastasising Laryngeal Cancer." *Oncology reports* 10(2):501–3. Retrieved September 15, 2015 (http://www.ncbi.nlm.nih.gov/pubmed/12579297).

Babitt, Jodie L., Franklin W. Huang, Diedra M. Wrighting, Yin Xia, Yisrael Sidis, Tarek A. Samad, Jason A. Campagna, Raymond T. Chung, Alan L. Schneyer, Clifford J. Woolf, Nancy C. Andrews, and Herbert Y. Lin. 2006. "Bone Morphogenetic Protein Signaling by Hemojuvelin Regulates Hepcidin Expression." *Nature genetics* 38(5):531–39.

Bai, Tony R. and Darryl a Knight. 2005. "Structural Changes in the Airways in Asthma: Observations and Consequences." *Clinical science (London, England : 1979)* 108(6):463–77. Retrieved (http://www.ncbi.nlm.nih.gov/pubmed/15896192).

Balda, M. S. and K. Matter. 2000. "Transmembrane Proteins of Tight Junctions." *Seminars in cell & developmental biology* 11(4):281–89. Retrieved December 4, 2014 (http://www.ncbi.nlm.nih.gov/pubmed/10966862).

Barkauskas, Christina E., Michael J. Cronce, Craig R. Rackley, Emily J. Bowie, Douglas R. Keene, Barry R. Stripp, Scott H. Randell, Paul W. Noble, and Brigid L. M. Hogan. 2013. "Type 2 Alveolar Cells Are Stem Cells in Adult Lung." *Journal of Clinical Investigation* 123(7):3025–36. Retrieved August 19, 2015 (http://www.jci.org/articles/view/68782).

Baron, J., J. P. Burke, F. P. Guengerich, W. B. Jakoby, and J. M. Voigt. 1988. "Sites for Xenobiotic Activation and Detoxication within the Respiratory Tract: Implications for Chemically Induced Toxicity." *Toxicology and applied pharmacology* 93(3):493–505. Retrieved September 10, 2015 (http://www.ncbi.nlm.nih.gov/pubmed/3285523).

Beers, Michael F. and Edward E. Morrisey. 2011. "Science in Medicine The Three R ' S of Lung Health and Disease : Repair , Remodeling , and Regeneration." *The Journal of clinical investigation* 121(6):2065–73.

Behrens, J., O. Löwrick, L. Klein-Hitpass, and W. Birchmeier. 1991. "The E-Cadherin Promoter: Functional Analysis of a G.C-Rich Region and an Epithelial Cell-Specific Palindromic Regulatory Element." *Proceedings of the National Academy of Sciences of the United States of America* 88(24):11495–99. Retrieved (http://www.pubmedcentral.nih.gov/articlerender.fcgi?artid=53162&tool=pmcentrez&rendertype=abstract).

Bellusci, S., R. Henderson, G. Winnier, T. Oikawa, and B. L. Hogan. 1996. "Evidence from Normal Expression and Targeted Misexpression That Bone Morphogenetic Protein (Bmp-4) Plays a Role in Mouse Embryonic Lung Morphogenesis." *Development (Cambridge, England)* 122(6):1693–1702. Retrieved (http://www.ncbi.nlm.nih.gov/pubmed/8674409).

Benahmed, Malika A., Karim Elbayed, François Daubeuf, Nicola Santelmo, Nelly Frossard, and Izzie J. Namer. 2014. "NMR HRMAS Spectroscopy of Lung Biopsy Samples: Comparison Study between Human, Pig, Rat, and Mouse Metabolomics." *Magnetic resonance in medicine* 71(1):35–43. Retrieved August 18, 2015 (http://www.ncbi.nlm.nih.gov/pubmed/23412987).

Bilek, Anastacia M., Kay C. Dee, and Donald P. Gaver. 2003. "Mechanisms of Surface-Tension-Induced Epithelial Cell Damage in a Model of Pulmonary Airway Reopening." *Journal of applied physiology (Bethesda, Md. : 1985)* 94(2):770–83. Retrieved September 11, 2015 (http://jap.physiology.org/content/94/2/770).

Boers, J;, A. Q; Ambergen, and F. B. J. M; Thunnissen. 1998. "Number and Proliferation of Basal and Parabasal Cells in Normal Human Airway Epithelium." *American journal of respiratory and critical care medicine* 157:2000–2006.

Borradori, L. and A. Sonnenberg. 1999. "Structure and Function of Hemidesmosomes: More than Simple Adhesion Complexes." *The Journal of investigative dermatology* 112(4):411–18. Retrieved September 10, 2015 (http://dx.doi.org/10.1046/j.1523-1747.1999.00546.x).

Borthwick, Duncan W., Mariam Shahbazian, Q. Todd Krantz, Julia R. Dorin, and Scott H. Randell. 2001. "Evidence for Stem-Cell Niches in the Tracheal Epithelium." *American Journal of Respiratory Cell and Molecular Biology* 24(6):662–70. Retrieved September 10, 2015 (http://www.ncbi.nlm.nih.gov/pubmed/11415930).

Brankin, Victoria, Ruth L. Quinn, Robert Webb, and Morag G. Hunter. 2005. "Evidence for a Functional Bone Morphogenetic Protein (BMP) System in the Porcine Ovary." *Domestic animal endocrinology* 28(4):367–79. Retrieved December 4, 2014 (http://www.ncbi.nlm.nih.gov/pubmed/15826772).

Breeze, Roger G. and Eric B. Wheeldon. 1977. "The Cells of the Pulmonary Airways." *American Review of Respiratory Disease* 116(4):705–77. Retrieved September 10, 2015 (http://www.atsjournals.org/doi/abs/10.1164/arrd.1977.116.4.705#.VfGa6xFViko).

Bremnes, Roy M., Robert Veve, Fred R. Hirsch, and Wilbur a. Franklin. 2002. "The E-Cadherin Cell–cell Adhesion Complex and Lung Cancer Invasion, Metastasis, and Prognosis." *Lung Cancer* 36(2):115–24. Retrieved (http://linkinghub.elsevier.com/retrieve/pii/S0169500201004718).

Brune, Kieran, James Andrew Frank, Andreas Schwingshackl, James H. Finigan, and Venkataramana K. Sidhaye. 2015. "Pulmonary Epithelial Barrier Function- Some New Players and Mechanisms." *American Journal of Physiology - Lung Cellular and Molecular Physiology* 308(8). Retrieved August 19, 2015 (http://www.scopus.com/inward/record.url?eid=2-s2.0-84927740385&partnerID=tZOtx3y1).

Bryant, David M. and Jennifer L. Stow. 2004. "The Ins and Outs of E-Cadherin Trafficking." *Trends in Cell Biology* 14(8):427–34.

Burrell, R., N. McGranahan, J. Bartek, and C. Swanton. 2013. "The Causes and

Consequences of Genetic Heterogeneity in Cancer Evolution." *Nature* 501(7467):338–45. Retrieved July 9, 2014 (http://dx.doi.org/10.1038/nature12625).

Cardoso, Wellington V. 2001. "Molecular Regulation of Lung Development." *Annual review of physiology* 63:471–94.

Carpenter, Graham. 2003. "Nuclear Localization and Possible Functions of Receptor Tyrosine Kinases." *Current Opinion in Cell Biology* 15(2):143–48. Retrieved September 9, 2015 (http://www.sciencedirect.com/science/article/pii/S0955067403000152).

Carroll, N., C. Cooke, and A. James. 1997. "The Distribution of Eosinophils and Lymphocytes in the Large and Small Airways of Asthmatics." *The European respiratory journal* 10(2):292–300. Retrieved September 12, 2015 (http://www.ncbi.nlm.nih.gov/pubmed/9042623).

Cavallaro, Ugo and Gerhard Christofori. 2004. "Cell Adhesion and Signalling by Cadherins and Ig-CAMs in Cancer." *Nature reviews. Cancer* 4(2):118–32.

Center for Disease Control and Prevention. 2011. "CDC Vital Signs: Asthma in the US." *Center for Disease Control and Prevention* (May):4. Retrieved (http://www.cdc.gov/VitalSigns/Asthma/index.html).

Challem, J. J. 1997. "Risk Factors for Lung Cancer and for Intervention Effects in CARET, the Beta-Carotene and Retinol Efficacy Trial." *Journal of the National Cancer Institute* 89(4):325–26.

Chang, Mary Mann-jong, Laura Shih, and Reen Wu. 2008. *Pulmonary Epithelium : Cell Types*.

Chao, Yvonne L., Christopher R. Shepard, and Alan Wells. 2010. "Breast Carcinoma Cells Re-Express E-Cadherin during Mesenchymal to Epithelial Reverting Transition." *Molecular Cancer* 9(1):179. Retrieved September 21, 2015 (http://www.molecular-cancer.com/content/9/1/179).

Chapman, Anna, Laura Fernandez del Ama, Jennifer Ferguson, Jivko Kamarashev, Claudia Wellbrock, and Adam Hurlstone. 2014. "Heterogeneous Tumor Subpopulations Cooperate to Drive Invasion." *Cell reports* 8(3):688–95. Retrieved April 25, 2015 (http://www.sciencedirect.com/science/article/pii/S2211124714005294).

Chapman, Harold A., Xiaopeng Li, Jonathan P. Alexander, Alexis Brumwell, Walter Lorizio, Kevin Tan, Arnoud Sonnenberg, Ying Wei, and Thiennu H. Vu. 2011. "Integrin α6β4 Identifies an Adult Distal Lung Epithelial Population with Regenerative Potential in Mice." *The Journal of clinical investigation* 121(7):2855–62. Retrieved August 21, 2015 (http://www.jci.org/articles/view/57673).

Chidgey, M. and C. Dawson. 2007. "Desmosomes: A Role in Cancer?" *British journal of cancer* 96(12):1783–87. Retrieved September 15, 2015 (http://www.pubmedcentral.nih.gov/articlerender.fcgi?artid=2359958&tool=pmcentrez&rendertype=abstract).

Chu, Yeh-Shiu, William A. Thomas, Olivier Eder, Frederic Pincet, Eric Perez, Jean Paul Thiery, and Sylvie Dufour. 2004. "Force Measurements in E-Cadherin-Mediated Cell Doublets Reveal Rapid Adhesion Strengthened by Actin Cytoskeleton Remodeling through Rac and Cdc42." *The Journal of*

cell biology 167(6):1183–94. Retrieved September 15, 2015 (http://www.pubmedcentral.nih.gov/articlerender.fcgi?artid=2172605&tool=pmcentrez&rendertype=abstract).

Church, Rachel H., Arjun Krishnakumar, Annika Urbanek, Stefan Geschwindner, Julie Meneely, Alessandro Bianchi, Barbro Basta, Sean Monaghan, Christopher Elliot, Maria Strömstedt, Neil Ferguson, Finian Martin, and Derek P. Brazil. 2015. "Gremlin1 Preferentially Binds to Bone Morphogenetic Protein-2 (BMP-2) and BMP-4 over BMP-7." *The Biochemical journal* 466(1):55–68. Retrieved September 25, 2015 (http://www.ncbi.nlm.nih.gov/pubmed/25378054).

Ciruna, B. and J. Rossant. 2001. "FGF Signaling Regulates Mesoderm Cell Fate Specification and Morphogenetic Movement at the Primitive Streak." *Developmental cell* 1(1):37–49. Retrieved September 15, 2015 (http://www.ncbi.nlm.nih.gov/pubmed/11703922).

Cohen, Ethan David, Zhishan Wang, John J. Lepore, Min Min Lu, Makoto M. Taketo, Douglas J. Epstein, and Edward E. Morrisey. 2007. "Wnt / β - Catenin Signaling Promotes Expansion of Isl-1 – Positive Cardiac Progenitor Cells through Regulation of FGF Signaling." *The Journal of clinical investigation* 117(7).

Coppens, John T., Charles G. Plopper, Shannon R. Murphy, and Laura S. Van Winkle. 2009. "Postnatal Lung Development of Rhesus Monkey Airways: Cellular Expression of Clara Cell Secretory Protein." *Developmental dynamics : an official publication of the American Association of Anatomists* 238(12):3016–24. Retrieved October 16, 2014 (http://www.ncbi.nlm.nih.gov/pubmed/19877270).

Costello, Christine M., Edwina Cahill, Finian Martin, Sean Gaine, and Paul McLoughlin. 2010. "Role of Gremlin in the Lung: Development and Disease." *American journal of respiratory cell and molecular biology* 42(5):517–23. Retrieved November 19, 2013 (http://www.ncbi.nlm.nih.gov/pubmed/19574532).

Costello, SF Glynn, MT Walsh, and RW. 2009. "Eosinophil Mediated Airway Remodelling and the Bone Morphogenetic Protein (BMP) Pathway in Asthma." *American Thoracic Society International Conference Meetings Abstracts*. Retrieved May 23, 2015 (http://www.atsjournals.org/doi/abs/10.1164/ajrccm-conference.2009.179.1_MeetingAbstracts.A6325).

Crosby, Lynn M. and Christopher M. Waters. 2010. "Epithelial Repair Mechanisms in the Lung." *Am J Physiol Lung Cell Mol Physiol* 298:715–31.

D'Addario, G., M. Früh, M. Reck, P. Baumann, W. Klepetko, and E. Felip. 2010. "Metastatic Non-Small-Cell Lung Cancer: ESMO Clinical Practice Guidelines for Diagnosis, Treatment and Follow-Up." *Annals of Oncology* 116–19. Retrieved September 12, 2015 (http://annonc.oxfordjournals.org/content/21/suppl_5/v116.full).

Davies, Donna E. 2009. "The Role of the Epithelium in Airway Remodeling in Asthma." *Proceedings of the American Thoracic Society* 6(8):678–82. Retrieved November 19, 2013 (http://www.pubmedcentral.nih.gov/articlerender.fcgi?artid=2797070&tool=

pmcentrez&rendertype=abstract).

Van Denderen, Bryce J. M. and Erik W. Thompson. 2013. “The to and Fro of Tumour Spread.” *Nature* 498:487–88.

Derynck, R., R. J. Akhurst, and A. Balmain. 2001. “TGF-Beta Signaling in Tumor Suppression and Cancer Progression.” *Nature genetics* 29(2):117–29. Retrieved May 25, 2015 (http://www.ncbi.nlm.nih.gov/pubmed/11586292).

Desai, Tushar J. and Wellington V Cardoso. 2002. “Growth Factors in Lung Development and Disease: Friends or Foe?” *Respiratory research* 3:2. Retrieved (http://www.pubmedcentral.nih.gov/articlerender.fcgi?artid=64813&tool=pmcentrez&rendertype=abstract).

Desprez, P. Y., E. Hara, M. J. Bissell, and J. Campisi. 1995. “Suppression of Mammary Epithelial Cell Differentiation by the Helix-Loop-Helix Protein Id-1.” *Molecular and cellular biology* 15(6):3398–3404. Retrieved August 19, 2015 (http://www.pubmedcentral.nih.gov/articlerender.fcgi?artid=230574&tool=pmcentrez&rendertype=abstract).

ten Dijke, P., H. Yamashita, TK. Sampath, A. Reddi, M. Estevez, D. Riddle, H. Ichijo, C. Heldin, and K. Miyazono. 1994. “Identification of Type I Receptors for Osteogenic Protein-1 and Bone Morphpgenetic Protein 4.” *The Journal of Biological Chemistry* 269(24):16985–88.

Dittmann, Klaus, Claus Mayer, and Hans-Peter Rodemann. 2005. “Inhibition of Radiation-Induced EGFR Nuclear Import by C225 (Cetuximab) Suppresses DNA-PK Activity.” *Radiotherapy and oncology : journal of the European Society for Therapeutic Radiology and Oncology* 76(2):157–61. Retrieved September 9, 2015 (http://www.ncbi.nlm.nih.gov/pubmed/16024112).

Dondelinger, R. F., M. P. Ghysels, D. Brisbois, E. Donkers, F. R. Snaps, J. Saunders, and J. Devière. 1998. “Relevant Radiological Anatomy of the Pig as a Training Model in Interventional Radiology.” *European radiology* 8(7):1254–73. Retrieved August 17, 2015 (http://www.ncbi.nlm.nih.gov/pubmed/9724449).

Dupuit, F., D. Gaillard, J. Hinnrasky, E. Mongodin, S. de Bentzmann, E. Copreni, and E. Puchelle. 2000. “Differentiated and Functional Human Airway Epithelium Regeneration in Tracheal Xenografts.” *American journal of physiology. Lung cellular and molecular physiology* 278(1):L165–76. Retrieved September 11, 2015 (http://www.ncbi.nlm.nih.gov/pubmed/10645904).

Eblaghie, Maxwell C., Mary Reedy, Tim Oliver, Yuji Mishina, and Brigid L. M. Hogan. 2006. “Evidence That Autocrine Signaling through Bmpr1a Regulates the Proliferation, Survival and Morphogenetic Behavior of Distal Lung Epithelial Cells.” *Developmental biology* 291(1):67–82. Retrieved November 19, 2013 (http://www.ncbi.nlm.nih.gov/pubmed/16414041).

Erjefalt, J. S., M. Korsgren, M. C. Nilsson, F. Sundler, and C. G. A. Persson. 1997a. “Association between Inflammation and Epithelial Damage-Restitution Processes in Allergic Airways in Vivo.” *Clinical & Experimental Allergy* 27(11):1344–55. Retrieved September 11, 2015

(http://doi.wiley.com/10.1111/j.1365-2222.1997.tb01181.x).

Erjefalt, J. S., M. Korsgren, M. C. Nilsson, F. Sundler, and C. G. A. Persson. 1997b. "Prompt Epithelial Damage and Restitution Processes in Allergen Challenged Guinea-Pig Trachea in Vivo." *Clinical & Experimental Allergy* 27(12):1458–70. Retrieved September 11, 2015 (http://doi.wiley.com/10.1046/j.1365-2222.1997.1200932.x).

Evans, M. J., M. V Fanucchi, G. L. Baker, L. S. Van Winkle, L. M. Pantle, S. J. Nishio, E. S. Schelegle, Laurel J. Gershwin, Lisa A. Miller, Dallas M. Hyde, and Charles G. Plopper. 2004. "The Remodelled Tracheal Basement Membrane Zone of Infant Rhesus Monkeys after 6 Months of Recovery." *Clinical & Experimental Allergy* 34(11):1131–36.

Evans, M. J., L. S. Van Winkle, M. V Fanucchi, and C. G. Plopper. 1999. "The Attenuated Fibroblast Sheath of the Respiratory Tract Epithelial-Mesenchymal Trophic Unit." *American journal of respiratory cell and molecular biology* 21(6):655–57. Retrieved (http://www.ncbi.nlm.nih.gov/pubmed/10572061).

Evans, Michael J., Michelle V Fanucchi, Charles G. Plopper, and Dallas M. Hyde. 2010. "Postnatal Development of the Lamina Reticularis in Primate Airways." *Anatomical record (Hoboken, N.J. : 2007)* 293(6):947–54. Retrieved November 21, 2013 (http://www.ncbi.nlm.nih.gov/pubmed/20503389).

Fanning, A. S., B. J. Jameson, L. A. Jesaitis, and J. M. Anderson. 1998. "The Tight Junction Protein ZO-1 Establishes a Link between the Transmembrane Protein Occludin and the Actin Cytoskeleton." *Journal of Biological Chemistry* 273(45):29745–53. Retrieved July 5, 2015 (http://www.jbc.org/content/273/45/29745.short).

Feeley, Brian T., Seth C. Gamradt, Wellington K. Hsu, Nancy Liu, Lucie Krenek, Paul Robbins, Johnny Huard, and Jay R. Lieberman. 2005. "Influence of BMPs on the Formation of Osteoblastic Lesions in Metastatic Prostate Cancer." *Journal of bone and mineral research : the official journal of the American Society for Bone and Mineral Research* 20(12):2189–99. Retrieved December 17, 2013 (http://www.ncbi.nlm.nih.gov/pubmed/16294272).

Fei, Zheng-Hua, Cheng-Yun Yao, Xiao-Lei Yang, Xin-En Huang, and Sheng-Lin Ma. 2013. "Serum BMP-2 up-Regulation as an Indicator of Poor Survival in Advanced Non-Small Cell Lung Cancer Patients." *Asian Pacific journal of cancer prevention : APJCP* 14(9):5293–99. Retrieved September 5, 2014 (http://www.ncbi.nlm.nih.gov/pubmed/24175816).

Ferguson, Edwin L. and Kathryn V. Anderson. 1992. "Decapentaplegic Acts as a Morphogen to Organize Dorsal-Ventral Pattern in the Drosophila Embryo." *Cell* 71(3):451–61. Retrieved November 28, 2013 (http://www.sciencedirect.com/science/article/pii/009286749290514D).

Ferrao, Petranel T., Andreas Behren, Robin L. Anderson, and Erik W. Thompson. 2015. "Cellular and Phenotypic Plasticity in Cancer." *Frontiers in Oncology* 5(171). Retrieved August 21, 2015 (http://journal.frontiersin.org/article/10.3389/fonc.2015.00171/abstract).

Ferrer-Vaquer, Anna, Manuel Viotti, and Anna-Katerina Hadjantonakis. 2010.

"Transitions between Epithelial and Mesenchymal States and the Morphogenesis of the Early Mouse Embryo." *Cell adhesion & migration* 4(3):447–57. Retrieved August 19, 2015 (http://www.pubmedcentral.nih.gov/articlerender.fcgi?artid=2958623&tool=pmcentrez&rendertype=abstract).

Fidler, Isaiah J. 2003. "The Pathogenesis of Cancer Metastasis: The 'Seed and Soil' Hypothesis Revisited." *Nature reviews. Cancer* 3(6):453–58.

Fischer, Susanne, Florian Bayersdorfer, Eva Harant, Renate Reng, Stephanie Arndt, Anja-Katrin Bosserhoff, and Stephan Schneuwly. 2012. "Fussel (fuss)--A Negative Regulator of BMP Signaling in Drosophila Melanogaster." *PloS one* 7(8):e42349. Retrieved September 9, 2015 (http://journals.plos.org/plosone/article?id=10.1371/journal.pone.0042349).

Fox, James G., Stephen W. Barthold, Muriel T. Davisson, Christian E. Newcomer, Fred W. Quimby, and Abigail L. Smith. 2006. *The Mouse in Biomedical Research: Normative Biology, Husbandry, and Models*. Academic Press. Retrieved August 18, 2015 (https://books.google.com/books?id=Gi6rIvx7Ni4C&pgis=1).

Fukui, Naoshi, Yong Zhu, William J. Maloney, John Clohisy, and Linda J. Sandell. 2003. "Stimulation of BMP-2 Expression by pro-Inflammatory Cytokines IL-1 and TNF-Alpha in Normal and Osteoarthritic Chondrocytes." *The Journal of bone and joint surgery. American volume* 85-A Suppl:59–66. Retrieved July 6, 2015 (http://www.ncbi.nlm.nih.gov/pubmed/12925611).

Galichon, Pierre and Alexandre Hertig. 2011. "Epithelial to Mesenchymal Transition as a Biomarker in Renal Fibrosis: Are We Ready for the Bedside?" *Fibrogenesis & tissue repair* 4(11):1–7. Retrieved September 15, 2015 (http://www.pubmedcentral.nih.gov/articlerender.fcgi?artid=3079627&tool=pmcentrez&rendertype=abstract).

Gallea, S., F. Lallemand, a Atfi, G. Rawadi, V. Ramez, S. Spinella-Jaegle, S. Kawai, C. Faucheu, L. Huet, R. Baron, and S. Roman-Roman. 2001. "Activation of Mitogen-Activated Protein Kinase Cascades Is Involved in Regulation of Bone Morphogenetic Protein-2-Induced Osteoblast Differentiation in Pluripotent C2C12 Cells." *Bone* 28(5):491–98. Retrieved (http://www.ncbi.nlm.nih.gov/pubmed/11344048).

Galvin, K. M., M. J. Donovan, C. a Lynch, R. I. Meyer, R. J. Paul, J. N. Lorenz, V. Fairchild-Huntress, K. L. Dixon, J. H. Dunmore, M. a Gimbrone, D. Falb, and D. Huszar. 2000. "A Role for smad6 in Development and Homeostasis of the Cardiovascular System." *Nature genetics* 24(2):171–74.

Gamell, Cristina, Nelson Osses, Ramon Bartrons, Thomas Rückle, Montserrat Camps, José Luis Rosa, and Francesc Ventura. 2008. "BMP2 Induction of Actin Cytoskeleton Reorganization and Cell Migration Requires PI3-Kinase and Cdc42 Activity." *Journal of cell science* 121(Pt 23):3960–70. Retrieved November 14, 2013 (http://www.ncbi.nlm.nih.gov/pubmed/19001503).

Gay, Olivia, Benoît Gilquin, Amandine Pitaval, and Jacques Baudier. 2011. "Refilins: A Link between Perinuclear Actin Bundle Dynamics and Mechanosensing Signaling." *Bioarchitecture* 1(5):245–49. Retrieved August 27, 2015

(http://www.pubmedcentral.nih.gov/articlerender.fcgi?artid=3384578&tool=pmcentrez&rendertype=abstract).

Ger, L. P., S. H. Liou, C. Y. Shen, S. J. Kao, and K. T. Chen. 1992. "Risk factors of lung cancer." *Journal of the Formosan Medical Association = Taiwan yi zhi* 91 Suppl 3:S222–31. Retrieved September 11, 2015 (http://europepmc.org/abstract/med/1362909).

Ghadiali, Samir N. and Donald P. Gaver. 2008. "Biomechanics of Liquid-Epithelium Interactions in Pulmonary Airways." *Respiratory physiology & neurobiology* 163(1-3):232–43. Retrieved September 11, 2015 (http://www.pubmedcentral.nih.gov/articlerender.fcgi?artid=2652855&tool=pmcentrez&rendertype=abstract).

Giacinti, C. and A. Giordano. 2006. "RB and Cell Cycle Progression." *Oncogene* 25(38):5220–27. Retrieved April 19, 2015 (http://dx.doi.org/10.1038/sj.onc.1209615).

Gleich, G. J. and C. Adolphson. 1993a. "Bronchial Hyperreactivity and Eosinophil Granule Proteins." *Agents and actions. Supplements* 43(1):223–30. Retrieved (http://dx.doi.org/10.2332/allergolint.45.35).

Gleich, G. J. and C. Adolphson. 1993b. "Bronchial Hyperreactivity and Eosinophil Granule Proteins." *Agents and actions. Supplements* 43:223–30. Retrieved July 28, 2015 (http://www.ncbi.nlm.nih.gov/pubmed/8368165).

Gontan, Cristina, Anne de Munck, Marcel Vermeij, Frank Grosveld, Dick Tibboel, and Robbert Rottier. 2008. "Sox2 Is Important for Two Crucial Processes in Lung Development: Branching Morphogenesis and Epithelial Cell Differentiation." *Developmental biology* 317(1):296–309. Retrieved December 4, 2014 (http://www.ncbi.nlm.nih.gov/pubmed/18374910).

Goodenough, Daniel A. and David L. Paul. 2009. "Gap Junctions." *Cold Spring Harbor perspectives in biology* 1(1):a002576. Retrieved June 4, 2015 (http://www.pubmedcentral.nih.gov/articlerender.fcgi?artid=2742079&tool=pmcentrez&rendertype=abstract).

Görlich, D. and U. Kutay. 1999. "Transport between the Cell Nucleus and the Cytoplasm." *Annual review of cell and developmental biology* 15:607–60. Retrieved August 3, 2015 (http://www.ncbi.nlm.nih.gov/pubmed/10611974).

Gould, Stephen E., Maria Day, Simon S. Jones, and Haimanti Dorai. 2002. "BMP-7 Regulates Chemokine, Cytokine, and Hemodynamic Gene Expression in Proximal Tubule cells1." *Kidney International* 61(1):51–60. Retrieved September 14, 2015 (http://www.ncbi.nlm.nih.gov/pubmed/11786084).

Gravdal, Karsten, Ole J. Halvorsen, Svein a Haukaas, and Lars a Akslen. 2007. "A Switch from E-Cadherin to N-Cadherin Expression Indicates Epithelial to Mesenchymal Transition and Is of Strong and Independent Importance for the Progress of Prostate Cancer." *Clinical cancer research : an official journal of the American Association for Cancer Research* 13(23):7003–11. Retrieved December 4, 2014 (http://www.ncbi.nlm.nih.gov/pubmed/18056176).

Di Guglielmo, Gianni M., Christine Le Roy, Anne F. Goodfellow, and Jeffrey L. Wrana. 2003. "Distinct Endocytic Pathways Regulate TGF-Beta Receptor

Signalling and Turnover." *Nature cell biology* 5(5):410–21. Retrieved September 9, 2015 (http://www.scopus.com/inward/record.url?eid=2-s2.0-0037598870&partnerID=tZOtx3y1).

Gundel, Robert H., L. Gordon Letts, and Gerald J. Gleich. 1991. "Human Eosinophile Major Basic Protein Induces Airway Constriction and Airway Hyperresponsiveness in Primates." *Journal of Clinical Investigation* 87(April):1470–73.

Gundersen, H. J. G., T. F. Bendtsen, L. Korbo, N. Marcussen, K. Nielsen, J. R. Nyengaard, B. Pakkenberg, A. Vesterby, M. J. West, and Hvidovre Hospital. 1988. "Some New , Simple and Efficient Stereological Methods and Their Use in Pathological Research and Diagnosis." *APMIS* 96:379–94.

Gupta, Reshu, Chandramu Chetty, Praveen Bhoopathi, Sajani Lakka, Sanjeeva Mohanam, Jasti S. Rao, and Dzung Eta Dinh. 2011. "Downregulation of uPA/uPAR Inhibits Intermittent Hypoxia-Induced Epithelial-Mesenchymal Transition (EMT) in DAOY and D283 Medulloblastoma Cells." *International journal of oncology* 38(3):733–44. Retrieved September 15, 2015 (http://www.ncbi.nlm.nih.gov/pubmed/21181094).

Hanahan, Douglas and Robert a. Weinberg. 2000. "The Hallmarks of Cancer." *Cell* 100:57–70.

Hardwick, James C., Liudmila L. Kodach, G. Johan Offerhaus, and Gijs R. van den Brink. 2008. "Bone Morphogenetic Protein Signalling in Colorectal Cancer." *Nature reviews. Cancer* 8(10):806–12.

Harrison, Freya, Aneesha Muruli, Steven Higgins, and Stephen P. Diggle. 2014. "Development of an Ex Vivo Porcine Lung Model for Studying Growth, Virulence, and Signaling of Pseudomonas Aeruginosa." *Infection and immunity* 82(8):3312–23. Retrieved August 18, 2015 (http://iai.asm.org/content/82/8/3312.full).

Hartung, Anke, Keren Bitton-Worms, Maya Mouler Rechtman, Valeska Wenzel, Jan H. Boergermann, Sylke Hassel, Yoav I. Henis, and Petra Knaus. 2006. "Different Routes of Bone Morphogenic Protein (BMP) Receptor Endocytosis Influence BMP Signaling." *Molecular and cellular biology* 26(20):7791–7805.

Ten Have-Opbroek, A. A. 1991. "Lung Development in the Mouse Embryo." *Experimental lung research* 17(2):111–30. Retrieved November 28, 2013 (http://www.ncbi.nlm.nih.gov/pubmed/2050021).

Hay, Elizabeth D. 2005. "The Mesenchymal Cell, Its Role in the Embryo, and the Remarkable Signaling Mechanisms That Create It." *Developmental dynamics : an official publication of the American Association of Anatomists* 233(3):706–20. Retrieved September 15, 2015 (http://www.ncbi.nlm.nih.gov/pubmed/15937929).

Hayashi, Masanori, Keisuke Nimura, Katsunobu Kashiwagi, Taku Harada, Kunio Takaoka, Hiroyuki Kato, Katsuto Tamai, and Yasufumi Kaneda. 2007. "Comparative Roles of Twist-1 and Id1 in Transcriptional Regulation by BMP Signaling." *Journal of cell science* 120(Pt 8):1350–57. Retrieved November 14, 2013 (http://www.ncbi.nlm.nih.gov/pubmed/17374642).

Haynes, Jennifer, Jyoti Srivastava, Nikki Madson, Torsten Wittmann, and Diane

L. Barber. 2011. “Dynamic Actin Remodeling during Epithelial-Mesenchymal Transition Depends on Increased Moesin Expression.” *Molecular biology of the cell* 22(24):4750–64. Retrieved July 19, 2015 (http://www.pubmedcentral.nih.gov/articlerender.fcgi?artid=3237619&tool=pmcentrez&rendertype=abstract).

Hazan, Rachel B., Rui Qiao, Rinat Keren, Ines Badano, and Kimita Suyama. 2004. “Cadherin Switch in Tumor Progression.” *Annals of the New York Academy of Sciences* 1014(1):155–63. Retrieved December 4, 2014 (http://doi.wiley.com/10.1196/annals.1294.016).

Helbing, Thomas, Eva-Maria Herold, Alexandra Hornstein, Stefanie Wintrich, Jennifer Heinke, Sebastian Grundmann, Cam Patterson, Christoph Bode, and Martin Moser. 2013. “Inhibition of BMP Activity Protects Epithelial Barrier Function in Lung Injury.” *The Journal of pathology* 231(1):105–16. Retrieved November 19, 2013 (http://www.ncbi.nlm.nih.gov/pubmed/23716395).

Heldin, C. H., K. Miyazono, and P. ten Dijke. 1997. “TGF-Beta Signalling from Cell Membrane to Nucleus through SMAD Proteins.” *Nature* 390(6659):465–71. Retrieved (http://www.ncbi.nlm.nih.gov/pubmed/9393997).

Helms, Mike W., Jens Packeisen, Christian August, Birgit Schittek, Werner Boecker, Burkhard H. Brandt, and Horst Buerger. 2005. “First Evidence Supporting a Potential Role for the BMP/SMAD Pathway in the Progression of Oestrogen Receptor-Positive Breast Cancer.” *The Journal of pathology* 206(3):366–76. Retrieved September 13, 2015 (http://www.ncbi.nlm.nih.gov/pubmed/15892165).

Hervé, Jean-Claude. 2008. “Preface: The Apical Junctional Complexes, Composition, Structure, and Characteristics.” *Biochimica et biophysica acta* 1778(3):559–61. Retrieved December 4, 2014 (http://www.ncbi.nlm.nih.gov/pubmed/18325352).

Hirohashi, Setsuo. 1998. “Inactivation of the E-Cadherin-Mediated Cell.” *American Journal of Pathology* 153(2):333–39.

Hogan, B. L. 1996. “Bone Morphogenetic Proteins: Multifunctional Regulators of Vertebrate Development.” *Genes & Development* 10(13):1580–94. Retrieved November 22, 2013 (http://www.genesdev.org/cgi/doi/10.1101/gad.10.13.1580).

Hong, K. U., S. D. Reynolds, A. Giangreco, C. M. Hurley, and B. R. Stripp. 2001. “Clara Cell Secretory Protein-Expressing Cells of the Airway Neuroepithelial Body Microenvironment Include a Label-Retaining Subset and Are Critical for Epithelial Renewal after Progenitor Cell Depletion.” *American journal of respiratory cell and molecular biology* 24(6):671–81. Retrieved September 10, 2015 (http://www.ncbi.nlm.nih.gov/pubmed/11415931).

Hong, Kyung U., Susan D. Reynolds, Simon Watkins, Elaine Fuchs, and Barry R. Stripp. 2004. “In Vivo Differentiation Potential of Tracheal Basal Cells: Evidence for Multipotent and Unipotent Subpopulations.” *American journal of physiology. Lung cellular and molecular physiology* 286(4):L643–49. Retrieved August 31, 2015

(http://www.ncbi.nlm.nih.gov/pubmed/12871857).

Hoodless, P. A., T. Tsukazaki, S. Nishimatsu, L. Attisano, J. L. Wrana, and G. H. Thomsen. 1999. "Dominant-Negative Smad2 Mutants Inhibit activin/Vg1 Signaling and Disrupt Axis Formation in Xenopus." *Developmental biology* 207(2):364–79. Retrieved August 29, 2015 (http://www.ncbi.nlm.nih.gov/pubmed/10068469).

Howe, J. R., M. G. Sayed, A. F. Ahmed, J. Ringold, J. Larsen-Haidle, A. Merg, F. A. Mitros, C. A. Vaccaro, G. M. Petersen, F. M. Giardiello, S. T. Tinley, L. A. Aaltonen, and H. T. Lynch. 2004. "The Prevalence of MADH4 and BMPR1A Mutations in Juvenile Polyposis and Absence of BMPR2, BMPR1B, and ACVR1 Mutations." *Journal of medical genetics* 41(7):484–91. Retrieved September 13, 2015 (http://www.pubmedcentral.nih.gov/articlerender.fcgi?artid=1735829&tool=pmcentrez&rendertype=abstract).

Huang, Sarah X. L., Mohammad Naimul Islam, John O'Neill, Zheng Hu, Yong-Guang Yang, Ya-Wen Chen, Melanie Mumau, Michael D. Green, Gordana Vunjak-Novakovic, Jahar Bhattacharya, and Hans-Willem Snoeck. 2014. "Efficient Generation of Lung and Airway Epithelial Cells from Human Pluripotent Stem Cells." *Nature biotechnology* 32(1):84–91. Retrieved May 28, 2014 (http://www.ncbi.nlm.nih.gov/pubmed/24291815).

Huguenin, Maya, Eliane J. Müller, Sandra Trachsel-Rösmann, Beatrice Oneda, Daniel Ambort, Erwin E. Sterchi, and Daniel Lottaz. 2008. "The Metalloprotease Meprinbeta Processes E-Cadherin and Weakens Intercellular Adhesion." *PloS one* 3(5):e2153. Retrieved June 13, 2014 (http://www.pubmedcentral.nih.gov/articlerender.fcgi?artid=2359857&tool=pmcentrez&rendertype=abstract).

Humbles, Alison A., Clare M. Lloyd, Sarah J. McMillan, Daniel S. Friend, Georgina Xanthou, Erin E. McKenna, Sorina Ghiran, Norma P. Gerard, Channing Yu, Stuart H. Orkin, and Craig Gerard. 2004. "A Critical Role for Eosinophils in Allergic Airways Remodeling." *Science (New York, N.Y.)* 305(5691):1776–79. Retrieved May 24, 2015 (http://www.ncbi.nlm.nih.gov/pubmed/15375268).

Huse, Morgan and Ye-guang Chen. 1999. "Crystal Structure of the Cytoplasmic Domain of the Type I TGF ᴺʟ Receptor in Complex with FKBP12 * Laboratories of Molecular Biophysics." *Cell* 96:425–36.

Hyatt, B. .., X. .. Shangguan, and JM. .. Shannon. 2002. "BMP4 Modulates Fibroblast Growth Factor-Mediated Induction of Proximal and Distal Lung Differentiation in Mouse Embryonic Tracheal Epithelium in Mesenchyme-Free Culture." *Developmental dynamics : an official publication of the American Association of Anatomists* 225(2):153–65. Retrieved November 19, 2013 (http://www.ncbi.nlm.nih.gov/pubmed/12242715).

Iavarone, a., P. Garg, a. Lasorella, J. Hsu, and M. a. Israel. 1994. "The Helix-Loop-Helix Protein Id-2 Enhances Cell Proliferation and Binds to the Retinoblastoma Protein." *Genes and Development* 8(11):1270–84.

Ikenouchi, Junichi, Miho Matsuda, Mikio Furuse, and Shoichiro Tsukita. 2003. "Regulation of Tight Junctions during the Epithelium-Mesenchyme

Transition: Direct Repression of the Gene Expression of Claudins/occludin by Snail." *Journal of cell science* 116(Pt 10):1959–67. Retrieved July 28, 2015 (http://www.ncbi.nlm.nih.gov/pubmed/12668723).

Ino, Yoshinori, Masahiro Gotoh, Michiie Sakamoto, Kiyomi Tsukagoshi, and Setsuo Hirohashi. 2002. "Dysadherin, a Cancer-Associated Cell Membrane Glycoprotein, down-Regulates E-Cadherin and Promotes Metastasis." *Proceedings of the National Academy of Sciences of the United States of America* 99(1):365–70. Retrieved September 15, 2015 (http://www.pnas.org/content/99/1/365.abstract).

Jacinto, A., A. Martinez-Arias, and P. Martin. 2001. "Mechanisms of Epithelial Fusion and Repair." *Nature cell biology* 3(5):E117–23. Retrieved September 11, 2015 (http://dx.doi.org/10.1038/35074643).

Jackman, David M. and Bruce E. Johnson. 2005. "Small-Cell Lung Cancer." *Lancet (London, England)* 366(9494):1385–96. Retrieved September 11, 2015 (http://www.sciencedirect.com/science/article/pii/S0140673605675691).

Jans, D. A. and G. Hassan. 1998. "Nuclear Targeting by Growth Factors, Cytokines, and Their Receptors: A Role in Signaling?" *BioEssays : news and reviews in molecular, cellular and developmental biology* 20(5):400–411. Retrieved September 9, 2015 (http://www.ncbi.nlm.nih.gov/pubmed/9670813).

Jans, David A., Lyndall J. Briggs, Sonja E. Gustin, Patricia Jans, Sally Ford, and Ian G. Young. 1997. "A Functional Bipartite Nuclear Localisation Signal in the Cytokine Interleukin-5." *FEBS Letters* 406(3):315–20. Retrieved September 9, 2015 (http://www.researchgate.net/publication/14081267_A_functional_bipartite_nuclear_localization_signal_in_the_cytokine_IL-5).

Jefferson, Julius J., Conrad L. Leung, and Ronald K. H. Liem. 2004. "Plakins: Goliaths That Link Cell Junctions and the Cytoskeleton." *Nature reviews. Molecular cell biology* 5(7):542–53. Retrieved September 10, 2015 (http://dx.doi.org/10.1038/nrm1425).

Jiang, Y. S., T. Jiang, B. Huang, P. S. Chen, and J. Ouyang. 2013. "Epithelial-Mesenchymal Transition of Renal Tubules: Divergent Processes of Repairing in Acute or Chronic Injury?" *Medical hypotheses* 81(1):73–75. Retrieved September 15, 2015 (http://www.ncbi.nlm.nih.gov/pubmed/23601763).

Judge, Eoin P., J. M. Lynne Hughes, Jim J. Egan, Michael Maguire, Emer L. Molloy, and Shirley O'Dea. 2014. "Anatomy and Bronchoscopy of the Porcine Lung. A Model for Translational Respiratory Medicine." *American journal of respiratory cell and molecular biology* 51(3):334–43. Retrieved August 17, 2015 (http://www.atsjournals.org/doi/abs/10.1165/rcmb.2013-0453TR#.VdHWhPlViko).

Kaiser, S., P. Schirmacher, A. Philipp, M. Protschka, I. Moll, K. Nicol, and M. Blessing. 1998. "Induction of Bone Morphogenetic Protein-6 in Skin Wounds. Delayed Reepitheliazation and Scar Formation in BMP-6 Overexpressing Transgenic Mice." *The Journal of investigative dermatology* 111(6):1145–52. Retrieved September 14, 2015 (http://www.ncbi.nlm.nih.gov/pubmed/9856831).

Kajekar, Radhika. 2007. “Environmental Factors and Developmental Outcomes in the Lung.” *Pharmacology & therapeutics* 114(2):129–45. Retrieved September 9, 2015 (http://www.ncbi.nlm.nih.gov/pubmed/17408750).

Kalluri, Raghu; and Robert A; Weinberg. 2009. “The Basics of Epithelial-Mesenchymal Transition.” *The Journal of clinical investigation* 119(6):1420–28. Retrieved (http://www.pubmedcentral.nih.gov/articlerender.fcgi?artid=2689101&tool=pmcentrez&rendertype=abstract).

Kanazawa, Takamitsu, Toshiaki Watanabe, Shinsuke Kazama, Toshihiro Tada, Shinichiro Koketsu, and Hirokazu Nagawa. 2002. “Poorly Differentiated Adenocarcinoma and Mucinous Carcinoma of the Colon and Rectum Show Higher Rates of Loss of Heterozygosity and Loss of E-Cadherin Expression due to Methylation of Promoter Region.” *International journal of cancer. Journal international du cancer* 102(3):225–29. Retrieved September 15, 2015 (http://www.ncbi.nlm.nih.gov/pubmed/12397640).

Kang, Myoung Hee, Sang Cheul Oh, Hyun Joo Lee, Han Na Kang, Jung Lim Kim, Jun Suk Kim, and Young A. Yoo. 2011. “Metastatic Function of BMP-2 in Gastric Cancer Cells: The Role of PI3K/AKT, MAPK, the NF-κB Pathway, and MMP-9 Expression.” *Experimental cell research* 317(12):1746–62. Retrieved September 13, 2015 (http://www.sciencedirect.com/science/article/pii/S0014482711001418).

Karhu, Ritva and Tuula Kuukasja. 2006. “Bone Morphogenetic Protein 7 Is Widely Overexpressed in Primary Breast Cancer.” *Genes, chromosomes and cancer* 419(January):411–19.

Kariyawasam, Harsha H., Maxine Aizen, Julia Barkans, Douglas S. Robinson, and a Barry Kay. 2007. “Remodeling and Airway Hyperresponsiveness but Not Cellular Inflammation Persist after Allergen Challenge in Asthma.” *American journal of respiratory and critical care medicine* 175(9):896–904. Retrieved November 19, 2013 (http://www.ncbi.nlm.nih.gov/pubmed/17272787).

Kariyawasam, Harsha H., Georgina Xanthou, Julia Barkans, Maxine Aizen, a Barry Kay, and Douglas S. Robinson. 2008. “Basal Expression of Bone Morphogenetic Protein Receptor Is Reduced in Mild Asthma.” *American journal of respiratory and critical care medicine* 177(10):1074–81. Retrieved November 19, 2013 (http://www.ncbi.nlm.nih.gov/pubmed/18292470).

Kavsak, Peter, Richele K. Rasmussen, Carrie G. Causing, Shirin Bonni, Haitao Zhu, Gerald H. Thomsen, Jeffrey L. Wrana, Stony Brook, New York, and Smad Smad. 2000. “Smad7 Binds to Smurf2 to Form an E3 Ubiquitin Ligase That Targets the TGF Receptor for Degradation State University of New York at Stony Brook.” *Molecular cell* 6:1365–75.

Kemper, Kristel, Pauline L. de Goeje, Daniel S. Peeper, and Renée van Amerongen. 2014. “Phenotype Switching: Tumor Cell Plasticity as a Resistance Mechanism and Target for Therapy.” *Cancer research* 74(21):5937–41. Retrieved August 26, 2015 (http://cancerres.aacrjournals.org/content/74/21/5937.figures-only).

Kim, Carla F. Bender, Erica L. Jackson, Amber E. Woolfenden, Sharon Lawrence, Imran Babar, Sinae Vogel, Denise Crowley, Roderick T. Bronson, and Tyler Jacks. 2005. "Identification of Bronchioalveolar Stem Cells in Normal Lung and Lung Cancer." *Cell* 121(6):823–35. Retrieved March 3, 2015 (http://www.sciencedirect.com/science/article/pii/S0092867405003429).

Kingsley, D. M. 1994. "The TGF-Beta Superfamily: New Members, New Receptors, and New Genetic Tests of Function in Different Organisms." *Genes & Development* 8(2):133–46. Retrieved November 10, 2013 (http://www.genesdev.org/cgi/doi/10.1101/gad.8.2.133).

Knight, Darryl a and Stephen T. Holgate. 2003. "The Airway Epithelium: Structural and Functional Properties in Health and Disease." *Respirology (Carlton, Vic.)* 8(4):432–46.

Kodach, Liudmila L., Sylvia A. Bleuming, Alex R. Musler, Maikel P. Peppelenbosch, Daniel W. Hommes, Gijs R. van den Brink, Carel J. M. van Noesel, G. Johan A. Offerhaus, and James C. H. Hardwick. 2008. "The Bone Morphogenetic Protein Pathway Is Active in Human Colon Adenomas and Inactivated in Colorectal Cancer." *Cancer* 112(2):300–306. Retrieved September 13, 2015 (http://www.scopus.com/inward/record.url?eid=2-s2.0-38049029612&partnerID=tZOtx3y1).

Koenig, B. B., J. S. Cook, D. H. Wolsing, J. Ting, J. P. Tiesman, P. E. Correa, C. a Olson, a L. Pecquet, F. Ventura, and R. a Grant. 1994. "Characterization and Cloning of a Receptor for BMP-2 and BMP-4 from NIH 3T3 Cells." *Molecular and cellular biology* 14(9):5961–74. Retrieved (http://www.pubmedcentral.nih.gov/articlerender.fcgi?artid=359122&tool=pmcentrez&rendertype=abstract).

Koli, Katri, Marjukka Myllärniemi, Kirsi Vuorinen, Kaisa Salmenkivi, Merja J. Ryynänen, Vuokko L. Kinnula, and Jorma Keski-Oja. 2006. "Bone Morphogenetic Protein-4 Inhibitor Gremlin Is Overexpressed in Idiopathic Pulmonary Fibrosis." *The American journal of pathology* 169(1):61–71. Retrieved November 19, 2013 (http://www.pubmedcentral.nih.gov/articlerender.fcgi?artid=1698771&tool=pmcentrez&rendertype=abstract).

Komiya, Yuko and Raymond Habas. 2008. "Wnt Signal Transduction Pathways." *Organogenesis* 4(2):68–75. Retrieved January 12, 2015 (http://www.pubmedcentral.nih.gov/articlerender.fcgi?artid=2634250&tool=pmcentrez&rendertype=abstract).

Kowanetz, Marcin, Ulrich Valcourt, Rosita Bergström, Carl-Henrik Heldin, and Aristidis Moustakas. 2004. "Id2 and Id3 Define the Potency of Cell Proliferation and Differentiation Responses to Transforming Growth Factor Beta and Bone Morphogenetic Protein." *Molecular and cellular biology* 24(10):4241–54.

Krampert, Monika, Wilhelm Bloch, Takako Sasaki, Philippe Bugnon, Thomas Ru, Eckhard Wolf, Monique Aumailley, William C. Parks, and Sabine Werner. 2004. "Activities of the Matrix Metalloproteinase Stromelysin-2 (MMP-10) in Matrix Degradation and Keratinocyte Organization in Wounded Skin." *Molecular biology of the cell* 15(December):5242–54.

Krause, Carola. 2014. “The Imperative Balance of Agonist and Antagonist for BMP Signalling Driven Adult Tissue Homeostasis.” *Austin Biomarkers and Diagnosis* 1(2):1–2.

Krieken, J. Han J. M. Van and Sergey V Litvinov. 2003. “The Epithelial Cell Adhesion Molecule (Ep-CAM) as Pathology.” *American Journal of Pathology* 163(6):2139–48.

Kyuno, Daisuke, Hiroshi Yamaguchi, Tatsuya Ito, Tsuyoshi Kono, Yasutoshi Kimura, Masafumi Imamura, Takumi Konno, Koichi Hirata, Norimasa Sawada, and Takashi Kojima. 2014. “Targeting Tight Junctions during Epithelial to Mesenchymal Transition in Human Pancreatic Cancer.” *World journal of gastroenterology : WJG* 20(31):10813–24. Retrieved September 15, 2015 (http://www.pubmedcentral.nih.gov/articlerender.fcgi?artid=4138461&tool=pmcentrez&rendertype=abstract).

de la Peña, Lourdes Serrano, Paul C. Billings, Jennifer L. Fiori, Jaimo Ahn, Frederick S. Kaplan, and Eileen M. Shore. 2005. “Fibrodysplasia Ossificans Progressiva (FOP), a Disorder of Ectopic Osteogenesis, Misregulates Cell Surface Expression and Trafficking of BMPRIA.” *Journal of bone and mineral research : the official journal of the American Society for Bone and Mineral Research* 20(7):1168–76. Retrieved September 9, 2015 (http://www.ncbi.nlm.nih.gov/pubmed/15940369).

Lamouille, Samy, Jian Xu, and Rik Derynck. 2014. “Molecular Mechanisms of Epithelial-Mesenchymal Transition.” *Nature reviews. Molecular cell biology* 15(3):178–96. Retrieved July 10, 2014 (http://dx.doi.org/10.1038/nrm3758).

Lane, K. B., R. D. Machado, M. W. Pauciulo, J. R. Thomson, J. A. Phillips, J. E. Loyd, W. C. Nichols, and R. C. Trembath. 2000. “Heterozygous Germline Mutations in BMPR2, Encoding a TGF-Beta Receptor, Cause Familial Primary Pulmonary Hypertension.” *Nature genetics* 26(1):81–84. Retrieved May 23, 2015 (http://dx.doi.org/10.1038/79226).

Langenfeld, Elaine M., John Bojnowski, John Perone, and John Langenfeld. 2005. “Expression of Bone Morphogenetic Proteins in Human Lung Carcinomas.” *The Annals of thoracic surgery* 80(3):1028–32. Retrieved November 19, 2013 (http://www.ncbi.nlm.nih.gov/pubmed/16122479).

Langenfeld, Elaine M., Steve E. Calvano, Fadi Abou-Nukta, Stephen F. Lowry, Peter Amenta, and John Langenfeld. 2003. “The Mature Bone Morphogenetic Protein-2 Is Aberrantly Expressed in Non-Small Cell Lung Carcinomas and Stimulates Tumor Growth of A549 Cells.” *Carcinogenesis* 24(9):1445–54. Retrieved November 19, 2013 (http://www.ncbi.nlm.nih.gov/pubmed/12819188).

Lasorella, A., A. Iavarone, and M. A. Israel. 1996. “Id2 Specifically Alters Regulation of the Cell Cycle by Tumor Suppressor Proteins.” *Molecular and cellular biology* 16(6):2570–78. Retrieved August 19, 2015 (http://www.pubmedcentral.nih.gov/articlerender.fcgi?artid=231247&tool=pmcentrez&rendertype=abstract).

Lasorella, A., T. Uo, and A. Iavarone. 2001. “Id Proteins at the Cross-Road of Development and Cancer.” *Oncogene* 20(58):8326–33. Retrieved August 19, 2015 (http://www.ncbi.nlm.nih.gov/pubmed/11840325).

Law, Elizabeth, Una Gilvarry, Vincent Lynch, Bernard Gregory, Geraldine Grant, and Martin Clynes. 1992. "Cytogenetic Comparison of Two Poorly Differentiated Human Lung Squamous Cell Carcinoma Lines." *Cancer Genetics and Cytogenetics* 59(2):111–18. Retrieved June 18, 2015 (http://www.sciencedirect.com/science/article/pii/016546089290204L).

Lee, Jonathan M., Shoukat Dedhar, Raghu Kalluri, and Erik W. Thompson. 2006. "The Epithelial-Mesenchymal Transition: New Insights in Signaling, Development, and Disease." *Journal of Cell Biology* 172(7):973–81.

Lee, Jonathan M., Shoukat Dedhar, Raghu Kalluri, and Erik W. Thompson. 2006. "The Epithelial-Mesenchymal Transition: New Insights in Signaling, Development, and Disease." *The Journal of cell biology* 172(7):973–81. Retrieved November 9, 2013 (http://www.pubmedcentral.nih.gov/articlerender.fcgi?artid=2063755&tool=pmcentrez&rendertype=abstract).

Leonardi, Salvatore, Alfina Coco, Michele Miraglia Del Giudice, Gianluigi L. Marseglia, and Mario La Rosa. 2013. "The Airway Epithelium Dysfunction in the Pathogenesis of Asthma: The Evidence." *Health* 05(02):331–38. Retrieved September 13, 2015 (http://www.scirp.org/journal/PaperInformation.aspx?PaperID=28371).

Li, Frederic Zhentao., Amardeep Singh. Dhillon, Robin L. Anderson, Grant. McArthur, and Petranel T. Ferrao. 2015. "Phenotype Switching in Melanoma: Implications for Progression and Therapy." *Frontiers in Oncology* 5(February):1–7. Retrieved (http://journal.frontiersin.org/Article/10.3389/fonc.2015.00031/abstract).

Li, Ming, Qixin Chen, Guirong Sun, Xiaowei Shi, Qiaohui Zhao, Chi Zhang, Jianshe Zhou, and Nan Qin. 2010. "Characterization and Expression of Bone Morphogenetic Protein 4 Gene in Postnatal Pigs." *Molecular biology reports* 37(5):2369–77. Retrieved December 4, 2014 (http://www.ncbi.nlm.nih.gov/pubmed/19688269).

Li, Zhengtu, Jian Wang, Yan Wang, Hua Jiang, Xiaoming Xu, Chenting Zhang, Defu Li, Chuyi Xu, Kedong Zhang, Yafei Qi, Xuefang Gong, Chun Tang, Nanshan Zhong, and Wenju Lu. 2014. "Bone Morphogenetic Protein 4 Inhibits Liposaccharide-Induced Inflammation in the Airway." *European journal of immunology* 44(11):3283–94. Retrieved May 24, 2015 (http://www.ncbi.nlm.nih.gov/pubmed/25142202).

Lincoln, Joy, Ralf Kist, Gerd Scherer, and Katherine E. Yutzey. 2007. "Sox9 Is Required for Precursor Cell Expansion and Extracellular Matrix Organization during Mouse Heart Valve Development." *Developmental biology* 305(1):120–32. Retrieved August 18, 2015 (http://www.sciencedirect.com/science/article/pii/S0012160607000942).

Lipschutz, J. H. 1998. "Molecular Development of the Kidney: A Review of the Results of Gene Disruption Studies." *American journal of kidney diseases : the official journal of the National Kidney Foundation* 31(3):383–97. Retrieved September 22, 2015 (http://www.ncbi.nlm.nih.gov/pubmed/9506676).

Liu, F., C. Pouponnot, and J. Massagué. 1997. "Dual Role of the Smad4/DPC4 Tumor Suppressor in TGFbeta-Inducible Transcriptional Complexes." *Genes*

& development 11(23):3157–67. Retrieved August 5, 2015 (http://www.pubmedcentral.nih.gov/articlerender.fcgi?artid=316747&tool=pmcentrez&rendertype=abstract).

Liu, Jessica A. J., Ming-Hoi Wu, Carol H. Yan, Bolton K. H. Chau, Henry So, Alvis Ng, Alan Chan, Kathryn S. E. Cheah, James Briscoe, and Martin Cheung. 2013. "Phosphorylation of Sox9 Is Required for Neural Crest Delamination and Is Regulated Downstream of BMP and Canonical Wnt Signaling." *Proceedings of the National Academy of Sciences of the United States of America* 110(8):2882–87. Retrieved August 18, 2015 (http://www.pnas.org/content/110/8/2882).

Liu, P., M. Wakamiya, M. J. Shea, U. Albrecht, R. R. Behringer, and A. Bradley. 1999. "Requirement for Wnt3 in Vertebrate Axis Formation." *Nature genetics* 22(4):361–65. Retrieved July 13, 2015 (http://www.ncbi.nlm.nih.gov/pubmed/10431240).

Liu, Yuru and Brigid L. M. Hogan. 2002. "Differential Gene Expression in the Distal Tip Endoderm of the Embryonic Mouse Lung." *Gene expression patterns : GEP* 2(3-4):229–33. Retrieved August 18, 2015 (http://www.ncbi.nlm.nih.gov/pubmed/12617806).

Lo, H. W. and M. C. Hung. 2006. "Nuclear EGFR Signalling Network in Cancers: Linking EGFR Pathway to Cell Cycle Progression, Nitric Oxide Pathway and Patient Survival." *British journal of cancer* 94(2):184–88. Retrieved September 9, 2015 (http://dx.doi.org/10.1038/sj.bjc.6602941).

Lories, Rik J. U. and Frank P. Luyten. 2009. "Bone Morphogenetic Protein Signaling and Arthritis." *Cytokine & growth factor reviews* 20(5-6):467–73. Retrieved September 14, 2015 (http://www.sciencedirect.com/science/article/pii/S1359610109000847).

Lötvall, Jan, Cezmi A. Akdis, Leonard B. Bacharier, Leif Bjermer, Thomas B. Casale, Adnan Custovic, Robert F. Lemanske, Andrew J. Wardlaw, Sally E. Wenzel, and Paul A. Greenberger. 2011. "Asthma Endotypes: A New Approach to Classification of Disease Entities within the Asthma Syndrome." *The Journal of allergy and clinical immunology* 127(2):355–60. Retrieved June 23, 2015 (http://www.ncbi.nlm.nih.gov/pubmed/21281866).

Lu, M. M., H. Yang, L. Zhang, W. Shu, D. G. Blair, and E. E. Morrisey. 2001. "The Bone Morphogenic Protein Antagonist Gremlin Regulates Proximal-Distal Patterning of the Lung." *Developmental dynamics : an official publication of the American Association of Anatomists* 222(4):667–80. Retrieved November 28, 2013 (http://www.ncbi.nlm.nih.gov/pubmed/11748835).

Luo, Kunxin, Shannon L. Stroschein, Wei Wang, Dan Chen, Eric Martens, Sharleen Zhou, and Qiang Zhou. 1999. "The Ski Oncoprotein Interacts with the Smad Proteins to Repress TGF?? Signaling." *Genes and Development* 13(17):2196–2206.

Lynn, Therese M., Emer L. Molloy, Joanne C. Masterson, Senan F. Glynn, Richard W. Costello, Mark V Avdalovic, Edward S. Schelegle, Lisa A. Miller, Dallas M. Hyde, and Shirley O'Dea. 2015. "SMAD Signaling in the Airways of Healthy Versus Asthmatic Rhesus Macaques Highlights a Relationship Between Inflammation and BMPs." *American journal of*

respiratory cell and molecular biology. Retrieved September 30, 2015 (http://www.ncbi.nlm.nih.gov/pubmed/26414797).

Maina, John N. and Peter van Gils. 2001. "Morphometric Characterization of the Airway and Vascular Systems of the Lung of the Domestic Pig, Sus Scrofa: Comparison of the Airway, Arterial and Venous Systems." *Comparative Biochemistry and Physiology Part A: Molecular & Integrative Physiology* 130(4):781–98. Retrieved July 22, 2015 (http://www.sciencedirect.com/science/article/pii/S1095643301004111).

Mamuya, Fahmy A. and Melinda K. Duncan. 2012. "aV Integrins and TGF-β-Induced EMT: A Circle of Regulation." *Journal of cellular and molecular medicine* 16(3):445–55. Retrieved September 15, 2015 (http://www.pubmedcentral.nih.gov/articlerender.fcgi?artid=3290750&tool=pmcentrez&rendertype=abstract).

Mao, Qiqi, Yubing Li, Xiangyi Zheng, Kai Yang, Huafeng Shen, Jie Qin, Yu Bai, Debo Kong, Xiaolong Jia, and Liping Xie. 2008. "Up-Regulation of E-Cadherin by Small Activating RNA Inhibits Cell Invasion and Migration in 5637 Human Bladder Cancer Cells." *Biochemical and biophysical research communications* 375(4):566–70. Retrieved December 4, 2014 (http://www.ncbi.nlm.nih.gov/pubmed/18725195).

Maretzky, Thorsten, Karina Reiss, Andreas Ludwig, Julian Buchholz, Felix Scholz, Erhardt Proksch, Bart de Strooper, Dieter Hartmann, and Paul Saftig. 2005. "ADAM10 Mediates E-Cadherin Shedding and Regulates Epithelial Cell-Cell Adhesion, Migration, and Beta-Catenin Translocation." *Proceedings of the National Academy of Sciences of the United States of America* 102(26):9182–87. Retrieved (http://www.pubmedcentral.nih.gov/articlerender.fcgi?artid=1166595&tool=pmcentrez&rendertype=abstract).

Maric, Ivana, Natalia Kucic, Tamara Turk Wensveen, Ivana Smoljan, Blazenka Grahovac, Sanja Zoricic Cvek, Tanja Celic, Dragica Bobinac, and Slobodan Vukicevic. 2012. "BMP Signaling in Rats with TNBS-Induced Colitis Following BMP7 Therapy." *American journal of physiology. Gastrointestinal and liver physiology* 302(10):G1151–62. Retrieved September 14, 2015 (http://ajpgi.physiology.org/content/302/10/G1151.abstract).

Maric, Ivana, Ljiljana Poljak, Sanja Zoricic, Dragica Bobinac, Dattatreyamurty Bosukonda, Kuber T. Sampath, and Slobodan Vukicevic. 2003. "Bone Morphogenetic Protein-7 Reduces the Severity of Colon Tissue Damage and Accelerates the Healing of Inflammatory Bowel Disease in Rats." *Journal of cellular physiology* 196(2):258–64. Retrieved December 16, 2013 (http://www.ncbi.nlm.nih.gov/pubmed/12811818).

Martin, P. and J. Lewis. 1992. "Actin Cables and Epidermal Movement in Embryonic Wound Healing." *Nature* 360(6400):179–83. Retrieved September 11, 2015 (http://dx.doi.org/10.1038/360179a0).

Marudamuthu, Amarnath Satheesh, Yashodhar Prabhakar Bhandary, Shwetha Kumari Shetty, Jian Fu, Venkatachalem Sathish, Ys Prakash, and Sreerama Shetty. 2015. "Role of the Urokinase-Fibrinolytic System in Epithelial-Mesenchymal Transition during Lung Injury." *The American journal of*

pathology 185(1):55–68. Retrieved September 15, 2015 (http://www.ncbi.nlm.nih.gov/pubmed/25447049).

Marusyk, Andriy, Vanessa Almendro, and Kornelia Polyak. 2012. "Intra-Tumour Heterogeneity: A Looking Glass for Cancer?" *Nature Reviews Cancer* 12(5):323–34. Retrieved (http://dx.doi.org/10.1038/nrc3261).

Maschler, Sabine, Gerhard Wirl, Herbert Spring, Dorothea V Bredow, Isabelle Sordat, Hartmut Beug, and Ernst Reichmann. 2005. "Tumor Cell Invasiveness Correlates with Changes in Integrin Expression and Localization." *Oncogene* 24(12):2032–41. Retrieved September 15, 2015 (http://www.ncbi.nlm.nih.gov/pubmed/15688013).

Massague, Joan. 2003. "Integration of Smad and MAPK Pathways: A Link and a Linker Revisited." *Genes & development* 17(24):2993–97. Retrieved May 6, 2015 (http://genesdev.cshlp.org/content/17/24/2993.full).

Masterson, Joanne C. 2008. "E-Cadherin." *e-thesis* 1–309.

Masterson, Joanne C., Emer L. Molloy, Jennifer L. Gilbert, Natasha McCormack, Aine Adams, and Shirley O'Dea. 2011. "Bone Morphogenetic Protein Signalling in Airway Epithelial Cells during Regeneration." *Cellular Signalling* 23(2):398–406. Retrieved (http://dx.doi.org/10.1016/j.cellsig.2010.10.010).

Masterson, Joanne C., Emer L. Molloy, Jennifer L. Gilbert, Natasha McCormack, Aine Adams, and Shirley O'Dea. 2011. "Bone Morphogenetic Protein Signalling in Airway Epithelial Cells during Regeneration." *Cellular signalling* 23(2):398–406. Retrieved November 19, 2013 (http://www.ncbi.nlm.nih.gov/pubmed/20959141).

Masterson, Joanne and Shirley O. Dea. 2007. "Posttranslational Truncation of E-Cadherin and Significance for Tumour Progression." *Cells, tissues, organs* 958:1–5.

Matter, Karl and Maria S. Balda. 2003. "Signalling to and from Tight Junctions." *Nature reviews. Molecular cell biology* 4(3):225–36. Retrieved November 17, 2014 (http://www.ncbi.nlm.nih.gov/pubmed/12612641).

Mcbride, Shirley., Paula. Meleady, Alan. Baird, David. Dinsdale, and Martin. Clynes. 1998. "Human Lung Carcinoma Cell Line DLKP Contains 3 Distinct Subpopulations with Different Growth and Attachement Properties." *Tumor Biology* 19:88–103.

McCormack, N., E. L. Molloy, and S. ODea. 2013. "Bone Morphogenetic Proteins Enhance an Epithelial-Mesenchymal Transition in Normal Airway Epithelial Cells during Restitution of a Disrupted Epithelium." *Respiratory Research* 14(1):1. Retrieved (Respiratory Research).

McCormack, N. and S. O'Dea. 2013. "Regulation of Epithelial to Mesenchymal Transition by Bone Morphogenetic Proteins." *Cellular Signalling* 25(12):2856–62. Retrieved (http://dx.doi.org/10.1016/j.cellsig.2013.09.012).

McLean, Karen and Ronald J. Buckanovich. 2013. "Cell Cycle News and Views BMPs Morph into New Roles in Ovarian Cancer." *Cell Cycle* 12(3):389–90.

McMorrow, L. E., S. R. Wolman, S. Bornstein, and J. E. Talmadge. 1988. "Irradiation-Induced Marker Chromosomes in a Metastasizing Murine

Tumor." *Cancer research* 48(4):999–1003. Retrieved September 12, 2015 (http://www.ncbi.nlm.nih.gov/pubmed/3338091).

Minoo, P., G. Su, H. Drum, P. Bringas, and S. Kimura. 1999. "Defects in Tracheoesophageal and Lung Morphogenesis in Nkx2.1(-/-) Mouse Embryos." *Developmental biology* 209(1):60–71. Retrieved September 10, 2015 (http://www.sciencedirect.com/science/article/pii/S0012160699992345).

Mitu, Grace and Raimund Hirschberg. 2008. "Bone Morphogenetic Protein-7 (BMP7) in Chronic Kidney Disease." *Frontiers in bioscience : a journal and virtual library* 13:4726–39. Retrieved September 14, 2015 (http://www.ncbi.nlm.nih.gov/pubmed/18508541).

Miyazono, Kohei, Shingo Maeda, and Takeshi Imamura. 2005. "BMP Receptor Signaling: Transcriptional Targets, Regulation of Signals, and Signaling Cross-Talk." *Cytokine & growth factor reviews* 16(3):251–63. Retrieved November 8, 2013 (http://www.ncbi.nlm.nih.gov/pubmed/15871923).

Miyazono, Kohei., Yuto. Kamiya, and Masato Morikawa. 2010. "Bone Morphogenetic Protein Receptors and Signal Transduction." *Journal of biochemistry* 147(1):35–51. Retrieved November 11, 2013 (http://www.ncbi.nlm.nih.gov/pubmed/19762341).

Molloy, Emer L., Aine Adams, J. Bernadette Moore, Joanne C. Masterson, Laura Madrigal-Estebas, Bernard P. Mahon, and Shirley O'Dea. 2008. "BMP4 Induces an Epithelial-Mesenchymal Transition-like Response in Adult Airway Epithelial Cells." *Growth factors (Chur, Switzerland)* 26(1):12–22. Retrieved November 19, 2013 (http://www.ncbi.nlm.nih.gov/pubmed/18365875).

Monteiro, Rui M., Susana M. Chuva de Sousa Lopes, Monika Bialecka, Sophie de Boer, An Zwijsen, and Christine L. Mummery. 2008. "Real Time Monitoring of BMP Smads Transcriptional Activity during Mouse Development." *Genesis (New York, N.Y. : 2000)* 46(7):335–46. Retrieved November 19, 2013 (http://www.ncbi.nlm.nih.gov/pubmed/18615729).

Moon, Randall T., Aimee D. Kohn, Giancarlo V De Ferrari, and Ajamete Kaykas. 2004. "WNT and Beta-Catenin Signalling: Diseases and Therapies." *Nature reviews. Genetics* 5(9):691–701. Retrieved November 8, 2013 (http://www.ncbi.nlm.nih.gov/pubmed/15372092).

Morrisey, Edward E., Wellington V. Cardoso, Robert H. Lane, Marlene Rabinovitch, Steven H. Abman, Xingbin Ai, Kurt H. Albertine, Richard D. Bland, Harold a. Chapman, William Checkley, Jonathan a. Epstein, Christopher R. Kintner, Maya Kumar, Parviz Minoo, Thomas J. Mariani, Donald M. McDonald, Yoh-suke Mukouyama, Lawrence S. Prince, Jeff Reese, Janet Rossant, Wei Shi, Xin Sun, Zena Werb, Jeffrey a. Whitsett, Dorothy Gail, Carol J. Blaisdell, and Qing S. Lin. 2013. "Molecular Determinants of Lung Development." *Annals of the American Thoracic Society* 10(2):S12–16. Retrieved November 19, 2014 (http://www.atsjournals.org/doi/abs/10.1513/AnnalsATS.201207-036OT).

Morrisey, E., Hogan, BL. 2010. "Preparing for the First Breath: Genetic and Cellular Mechanisms in Lung Development." *Developmental Cell* 18(1):8–23.

Moser, Martin, Olav Binder, Yaxu Wu, Julius Aitsebaomo, Rongqin Ren, Christoph Bode, Victoria L. Bautch, and L. Frank. 2003. "BMPER , a Novel Endothelial Cell Precursor-Derived Protein , Antagonizes Bone Morphogenetic Protein Signaling and Endothelial Cell Differentiation BMPER , a Novel Endothelial Cell Precursor-Derived Protein , Antagonizes Bone Morphogenetic Protein Signalin." *Molecular and cellular biology* 23(16):5664–79.

Moses, H. L., E. Y. Yang, and J. A. Pietenpol. 1991. "Regulation of Epithelial Proliferation by TGF-Beta." *Ciba Foundation symposium* 157:66–74; discussion 75–80. Retrieved July 28, 2015 (http://www.ncbi.nlm.nih.gov/pubmed/2070684).

Moustakas, a, S. Souchelnytskyi, and C. H. Heldin. 2001. "Smad Regulation in TGF-Beta Signal Transduction." *Journal of cell science* 114(Pt 24):4359–69.

Murakami, Gyo, Tetsuro Watabe, Kunio Takaoka, Kohei Miyazono, and Takeshi Imamura. 2003. "Cooperative Inhibition of Bone Morphogenetic Protein Signaling by Smurf1 and Inhibitory Smads." *Molecular biology of the cell* 14:2809–17.

Murakami, Koko, Rajamma Mathew, Jing Huang, Reza Farahani, Hong Peng, Susan C. Olson, and Joseph D. Etlinger. 2010. "Smurf1 Ubiquitin Ligase Causes Downregulation of BMP Receptors and Is Induced in Monocrotaline and Hypoxia Models of Pulmonary Arterial Hypertension." *Experimental biology and medicine (Maywood, N.J.)* 235(7):805–13. Retrieved September 22, 2015 (http://www.ncbi.nlm.nih.gov/pubmed/20558834).

Naclerio, Robert M. 2012. "Introduction: Insights into the Upper Airway for Pulmonologists and Allergists." *Proceedings of the American Thoracic Society*. Retrieved September 9, 2015 (http://www.atsjournals.org/doi/full/10.1513/pats.8.1.30#.VfCJPBFViko).

Nakahiro, Takeshi, Hisanori Kurooka, Kentaro Mori, Kazuo Sano, and Yoshifumi Yokota. 2010. "Identification of BMP-Responsive Elements in the Mouse Id2 Gene." *Biochemical and Biophysical Research Communications* 399(3):416–21. Retrieved (http://dx.doi.org/10.1016/j.bbrc.2010.07.090).

Nam, Jeong-Seok, Setsuo Hirohashi, and Lalage M. Wakefield. 2007. "Dysadherin: A New Player in Cancer Progression." *Cancer letters* 255(2):161–69. Retrieved September 15, 2015 (http://www.pubmedcentral.nih.gov/articlerender.fcgi?artid=2094007&tool=pmcentrez&rendertype=abstract).

Natsume, Tohru, Shuichiro Tomita, Naoto Ueno, and J. Biol Chem. 1997. "Protein Chemistry and Structure : Interaction between Soluble Type I Receptor for Bone Morphogenetic Protein Interaction between Soluble Type I Receptor for Bone Morphogenetic Protein and Bone Morphogenetic Protein-4 *." *The Journal of biological chemistry* 1–7.

Nickel, J., M. K. Dreyer, T. Kirsch, and W. Sebald. 2001. "The Crystal Structure of the BMP-2:BMPR-IA Complex and the Generation of BMP-2 Antagonists." *The Journal of bone and joint surgery. American volume* 83-A Suppl(Pt 1):S7–14. Retrieved September 9, 2015 (http://www.ncbi.nlm.nih.gov/pubmed/11263668).

Nishanian, Tagvor G. and Todd Waldman. 2004. “Interaction of the BMPR-IA Tumor Suppressor with a Developmentally Relevant Splicing Factor.” *Biochemical and biophysical research communications* 323(1):91–97. Retrieved September 9, 2015 (http://www.ncbi.nlm.nih.gov/pubmed/15351706).

Nishita, M., N. Ueno, and H. Shibuya. 1999. “Smad8B, a Smad8 Splice Variant Lacking the SSXS Site That Inhibits Smad8-Mediated Signalling.” *Genes to cells : devoted to molecular & cellular mechanisms* 4(10):583–91. Retrieved September 22, 2015 (http://www.ncbi.nlm.nih.gov/pubmed/10583507).

Nohe, Anja, Sylke Hassel, Marcelo Ehrlich, Florian Neubauer, Walter Sebald, Yoav I. Henis, and Petra Knaus. 2002. “The Mode of Bone Morphogenetic Protein (BMP) Receptor Oligomerization Determines Different BMP-2 Signaling Pathways.” *The Journal of biological chemistry* 277(7):5330–38. Retrieved November 14, 2013 (http://www.ncbi.nlm.nih.gov/pubmed/11714695).

Nojima, D., K. Nakajima, L. C. Li, J. Franks, L. Ribeiro-Filho, N. Ishii, and R. Dahiya. 2001. “CpG Methylation of Promoter Region Inactivates E-Cadherin Gene in Renal Cell Carcinoma.” *Molecular carcinogenesis* 32(1):19–27. Retrieved September 15, 2015 (http://www.ncbi.nlm.nih.gov/pubmed/11568972).

Nose, A., A. Nagafuchi, and M. Takeichi. 1988. “Expressed Recombinant Cadherins Mediate Cell Sorting in Model Systems.” *Cell* 54(7):993–1001.

O’Connor, Michael B., David Umulis, Hans G. Othmer, and Seth S. Blair. 2006. “Shaping BMP Morphogen Gradients in the Drosophila Embryo and Pupal Wing.” *Development (Cambridge, England)* 133(2):183–93. Retrieved September 13, 2015 (http://www.ncbi.nlm.nih.gov/pubmed/16368928).

Ogata, T., J. M. Wozney, R. Benezra, and M. Noda. 1993. “Bone Morphogenetic Protein 2 Transiently Enhances Expression of a Gene, Id (inhibitor of Differentiation), Encoding a Helix-Loop-Helix Molecule in Osteoblast-like Cells.” *Proceedings of the National Academy of Sciences of the United States of America* 90(19):9219–22. Retrieved (http://www.pubmedcentral.nih.gov/articlerender.fcgi?artid=47534&tool=pmcentrez&rendertype=abstract).

Onichtchouk, D., Y. G. Chen, R. Dosch, V. Gawantka, H. Delius, J. Massagué, and C. Niehrs. 1999. “Silencing of TGF-Beta Signalling by the Pseudoreceptor BAMBI.” *Nature* 401(6752):480–85. Retrieved (http://www.ncbi.nlm.nih.gov/pubmed/10519551).

Park, Jin-Ah, Jae Hun Kim, Dapeng Bi, Jennifer A. Mitchel, Nader Taheri Qazvini, Kelan Tantisira, Chan Young Park, Maureen McGill, Sae-Hoon Kim, Bomi Gweon, Jacob Notbohm, Robert Steward, Stephanie Burger, Scott H. Randell, Alvin T. Kho, Dhananjay T. Tambe, Corey Hardin, Stephanie A. Shore, Elliot Israel, David A. Weitz, Daniel J. Tschumperlin, Elizabeth P. Henske, Scott T. Weiss, M. Lisa Manning, James P. Butler, Jeffrey M. Drazen, and Jeffrey J. Fredberg. 2015. “Unjamming and Cell Shape in the Asthmatic Airway Epithelium.” *Nature materials* advance on. Retrieved August 5, 2015 (http://dx.doi.org/10.1038/nmat4357).

Park, W. Y., B. Miranda, D. Lebeche, G. Hashimoto, and W. V Cardoso. 1998.

"FGF-10 Is a Chemotactic Factor for Distal Epithelial Buds during Lung Development." *Developmental biology* 201(2):125–34. Retrieved (http://www.ncbi.nlm.nih.gov/pubmed/9740653).

Perl, A. K., P. Wilgenbus, U. Dahl, H. Semb, and G. Christofori. 1998. "A Causal Role for E-Cadherin in the Transition from Adenoma to Carcinoma." *Nature* 392(6672):190–93. Retrieved August 26, 2015 (http://www.ncbi.nlm.nih.gov/pubmed/9515965).

Peters, Kevin, Sabine Werner, Xiang Liao, Susan Wert, Jeffrey Whitsett, and Lewis Williams. 1994. "Targeted Expression of a Moninant Negative FGF Receptor Blocks Branching Morphogenesis and Epithelial Differentiation of the Mouse Lung." 13(14):3296–3301.

Phimphilai, Mattabhorn, Zhouran Zhao, Heidi Boules, Hernan Roca, and Renny T. Franceschi. 2006. "BMP Signaling Is Required for RUNX2-Dependent Induction of the Osteoblast Phenotype." *Journal of bone and mineral research : the official journal of the American Society for Bone and Mineral Research* 21(4):637–46. Retrieved September 13, 2015 (http://www.pubmedcentral.nih.gov/articlerender.fcgi?artid=2435171&tool=pmcentrez&rendertype=abstract).

Pinto, Cletus A., Edwin Widodo, Mark Waltham, and Erik W. Thompson. 2013. "Breast Cancer Stem Cells and Epithelial Mesenchymal Plasticity - Implications for Chemoresistance." *Cancer letters* 341(1):56–62. Retrieved September 22, 2015 (http://www.ncbi.nlm.nih.gov/pubmed/23830804).

Plisov, S. Y., S. V Ivanov, K. Yoshino, L. F. Dove, T. M. Plisova, K. G. Higinbotham, I. Karavanova, M. Lerman, and A. O. Perantoni. 2000. "Mesenchymal-Epithelial Transition in the Developing Metanephric Kidney: Gene Expression Study by Differential Display." *Genesis (New York, N.Y. : 2000)* 27(1):22–31. Retrieved September 22, 2015 (http://www.ncbi.nlm.nih.gov/pubmed/10862152).

Plopper, C. G., J. E. Halsebo, W. J. Berger, K. S. Sonstegard, and P. Nettesheim. 1983. "Distribution of Nonciliated Bronchiolar Epithelial (Clara) Cells in Intra- and Extrapulmonary Airways of the Rabbit." *Experimental lung research* 5(2):79–98. Retrieved September 10, 2015 (http://www.ncbi.nlm.nih.gov/pubmed/6628348).

Plopper, C. G., S. J. Nishio, J. L. Alley, P. Kass, and D. M. Hyde. 1992. "The Role of the Nonciliated Bronchiolar Epithelial (Clara) Cell as the Progenitor Cell during Bronchiolar Epithelial Differentiation in the Perinatal Rabbit Lung." *American journal of respiratory cell and molecular biology* 7(6):606–13. Retrieved September 10, 2015 (http://www.atsjournals.org/doi/abs/10.1165/ajrcmb/7.6.606?url_ver=Z39.88-2003&rfr_id=ori:rid:crossref.org&rfr_dat=cr_pub%3dpubmed#.VfF_MRFViko).

Pöpperl, H., C. Schmidt, V. Wilson, C. R. Hume, J. Dodd, R. Krumlauf, and R. S. Beddington. 1997. "Misexpression of Cwnt8C in the Mouse Induces an Ectopic Embryonic Axis and Causes a Truncation of the Anterior Neuroectoderm." *Development (Cambridge, England)* 124(15):2997–3005. Retrieved September 15, 2015

(http://www.ncbi.nlm.nih.gov/pubmed/9247341).

Puchelle, E. 2000. "Airway Epithelium Wound Repair and Regeneration after Injury." *Acta oto-rhino-laryngologica Belgica* 54(3):263–70. Retrieved September 11, 2015 (http://europepmc.org/abstract/med/11082761).

Puchelle, Edith, Jean-Marie Zahm, Jean-Marie Tournier, and Christelle Coraux. 2006. "Airway Epithelial Repair, Regeneration, and Remodeling after Injury in Chronic Obstructive Pulmonary Disease." *Proceedings of the American Thoracic Society* 3(8):726–33. Retrieved November 10, 2014 (http://www.ncbi.nlm.nih.gov/pubmed/17065381).

Que, Jianwen, Xiaoyan Luo, Robert J. Schwartz, and Brigid L. M. Hogan. 2009. "Multiple Roles for Sox2 in the Developing and Adult Mouse Trachea." *Development (Cambridge, England)* 136(11):1899–1907. Retrieved December 4, 2014 (http://www.pubmedcentral.nih.gov/articlerender.fcgi?artid=2680112&tool=pmcentrez&rendertype=abstract).

Rawlins, Emma L., Cheryl P. Clark, Yan Xue, and Brigid L. M. Hogan. 2009. "The Id2+ Distal Tip Lung Epithelium Contains Individual Multipotent Embryonic Progenitor Cells." *Development (Cambridge, England)* 136(22):3741–45. Retrieved November 18, 2013 (http://www.pubmedcentral.nih.gov/articlerender.fcgi?artid=2766341&tool=pmcentrez&rendertype=abstract).

Reynolds, S. D., a Giangreco, J. H. Power, and B. R. Stripp. 2000. "Neuroepithelial Bodies of Pulmonary Airways Serve as a Reservoir of Progenitor Cells Capable of Epithelial Regeneration." *The American journal of pathology* 156(1):269–78. Retrieved (http://www.pubmedcentral.nih.gov/articlerender.fcgi?artid=1868636&tool=pmcentrez&rendertype=abstract).

Rios-Doria, Jonathan, Kathleen C. Day, Rainer Kuefer, Michael G. Rashid, Arul M. Chinnaiyan, Mark a Rubin, and Mark L. Day. 2003. "The Role of Calpain in the Proteolytic Cleavage of E-Cadherin in Prostate and Mammary Epithelial Cells." *The Journal of biological chemistry* 278(2):1372–79. Retrieved June 13, 2014 (http://www.ncbi.nlm.nih.gov/pubmed/12393869).

Rittenberg, B., E. Partridge, G. Baker, C. Clokie, R. Zohar, J. W. Dennis, and H. C. Tenenbaum. 2005. "Regulation of BMP-Induced Ectopic Bone Formation by Ahsg." *Journal of orthopaedic research : official publication of the Orthopaedic Research Society* 23(3):653–62. Retrieved (http://www.ncbi.nlm.nih.gov/pubmed/15885488).

Rock, Jason, Xia; Gao, Scott H; Randell, Young-Yun; Kong, and Brigid LM; Hogan. 2013. "Notch-Dependent Differentiation of Adult Airway Basal Stem Cells." *Cell Stem cell* 8(6):639–48.

Rock, Jason R., Mark W. Onaitis, Emma L. Rawlins, Yun Lu, Cheryl P. Clark, Yan Xue, Scott H. Randell, and Brigid L. M. Hogan. 2009. "Basal Cells as Stem Cells of the Mouse Trachea and Human Airway Epithelium." *Proceedings of the National Academy of Sciences of the United States of America* 106(31):12771–75. Retrieved April 18, 2015 (http://www.pnas.org/content/106/31/12771.long).

Rockich, Briana E., Steven M. Hrycaj, Hung Ping Shih, Melinda S. Nagy, Michael a H. Ferguson, Janel L. Kopp, Maike Sander, Deneen M. Wellik, and Jason R. Spence. 2013. "Sox9 Plays Multiple Roles in the Lung Epithelium during Branching Morphogenesis." *Proceedings of the National Academy of Sciences of the United States of America* 110(47):E4456–64. Retrieved (http://www.pubmedcentral.nih.gov/articlerender.fcgi?artid=3839746&tool=pmcentrez&rendertype=abstract).

Rogers, Christopher S., William M. Abraham, Kim A. Brogden, John F. Engelhardt, John T. Fisher, Paul B. Mccray, Geoffrey Mclennan, David K. Meyerholz, Eman Namati, Lynda S. Ostedgaard, Randall S. Prather, Juan R. Sabater, David Anthony Stoltz, Joseph Zabner, and Michael J. Welsh. 2008. "The Porcine Lung as a Potential Model for Cystic Fibrosis." *Am J Physiol Lung Cell Mol Physiol* 295:240–63.

Rosendahl, Alexander, Evangelia Pardali, Matthaios Speletas, Peter Ten Dijke, Carl-Henrik Heldin, and Paschalis Sideras. 2002. "Activation of Bone Morphogenetic protein/Smad Signaling in Bronchial Epithelial Cells during Airway Inflammation." *American journal of respiratory cell and molecular biology* 27(2):160–69. Retrieved (http://www.ncbi.nlm.nih.gov/pubmed/12151307).

Rosenzweig, B. L., T. Imamura, T. Okadome, G. N. Cox, H. Yamashita, P. ten Dijke, C. H. Heldin, and K. Miyazono. 1995. "Cloning and Characterization of a Human Type II Receptor for Bone Morphogenetic Proteins." *Proceedings of the National Academy of Sciences of the United States of America* 92(17):7632–36. Retrieved (http://www.pubmedcentral.nih.gov/articlerender.fcgi?artid=41199&tool=pmcentrez&rendertype=abstract).

Ruzinova, Marianna B. and Robert Benezra. 2003. "Id Proteins in Development, Cell Cycle and Cancer." *Trends in Cell Biology* 13(8):410–18. Retrieved August 19, 2015 (http://www.sciencedirect.com/science/article/pii/S0962892403001478).

Saetta, M. and G. Turato. 2001. "Airway Pathology in Asthma." *European Respiratory Journal* 18(1):18–23. Retrieved November 19, 2013 (http://erj.ersjournals.com/cgi/doi/10.1183/09031936.01.00229501).

Saitoh, Masao, Takuya Shirakihara, Akira Fukasawa, Kana Horiguchi, Kei Sakamoto, Hiroshi Sugiya, Hideyuki Beppu, Yasuyuki Fujita, Ikuo Morita, Kohei Miyazono, and Keiji Miyazawa. 2013. "Basolateral BMP Signaling in Polarized Epithelial Cells." *PloS one* 8(5):e62659. Retrieved November 19, 2013 (http://www.pubmedcentral.nih.gov/articlerender.fcgi?artid=3652834&tool=pmcentrez&rendertype=abstract).

Samad, Tarek A., Anuradha Rebbapragada, Esther Bell, Ying Zhang, Yisrael Sidis, Sung-jin Jeong, Jason A. Campagna, David A. Fabrizio, L. Alan, Herbert Y. Lin, Ali H. Brivanlou, Liliana Attisano, Clifford J. Woolf, Stephen Perusini, and Alan L. Schneyer. 2005. "Mechanisms of Signal Transduction : DRAGON , a Bone Morphogenetic Protein DRAGON , a Bone Morphogenetic Protein Co-Receptor *." *The Journal of biological*

chemistry 280:14122–29.

Savagner, P. 2010. "The Epithelial-Mesenchymal Transition (EMT) Phenomenon." *Annals of Oncology* 21(SUPPL. 7):89–92.

Savagner, Pierre. 2007. *Rise and Fall of Epithelial Phenotype: Concepts of Epithelial-Mesenchymal Transition*. Springer Science & Business Media. Retrieved August 21, 2015 (https://books.google.com/books?id=DHmA12sU4n0C&pgis=1).

Scagliotti, Giorgio Vittorio, Vera Hirsh, Salvatore Siena, David H. Henry, Penella J. Woll, Christian Manegold, Philippe Solal-Celigny, Gladys Rodriguez, Maciej Krzakowski, Nilesh D. Mehta, Lara Lipton, José Angel García-Sáenz, José Rodrigues Pereira, Kumar Prabhash, Tudor-Eliade Ciuleanu, Vladimir Kanarev, Huei Wang, Arun Balakumaran, and Ira Jacobs. 2012. "Overall Survival Improvement in Patients with Lung Cancer and Bone Metastases Treated with Denosumab versus Zoledronic Acid: Subgroup Analysis from a Randomized Phase 3 Study." *Journal of thoracic oncology : official publication of the International Association for the Study of Lung Cancer* 7(12):1823–29. Retrieved September 12, 2015 (http://www.ncbi.nlm.nih.gov/pubmed/23154554).

Scheel, Christina and Robert a. Weinberg. 2011. "Phenotypic Plasticity and Epithelial-Mesenchymal Transitions in Cancer - and Normal Stem Cells?" *Int J Cancer* 129(10):2310–14.

Schelegle, E. S., L. J. Gershwin, L. a Miller, M. V Fanucchi, L. S. Van Winkle, J. P. Gerriets, W. F. Walby, a M. Omlor, a R. Buckpitt, B. K. Tarkington, V. J. Wong, J. P. Joad, K. B. Pinkerton, R. Wu, M. J. Evans, D. M. Hyde, and C. G. Plopper. 2001. "Allergic Asthma Induced in Rhesus Monkeys by House Dust Mite (Dermatophagoides Farinae)." *The American journal of pathology* 158(1):333–41. Retrieved (http://www.pubmedcentral.nih.gov/articlerender.fcgi?artid=1850255&tool=pmcentrez&rendertype=abstract).

Schelegle, Edward S., Lisa a Miller, Laurel J. Gershwin, Michelle V Fanucchi, Laura S. Van Winkle, Joan E. Gerriets, William F. Walby, Valerie Mitchell, Brian K. Tarkington, Viviana J. Wong, Gregory L. Baker, Lorraine M. Pantle, Jesse P. Joad, Kent E. Pinkerton, Reen Wu, Michael J. Evans, Dallas M. Hyde, and Charles G. Plopper. 2003. "Repeated Episodes of Ozone Inhalation Amplifies the Effects of Allergen Sensitization and Inhalation on Airway Immune and Structural Development in Rhesus Monkeys." *Toxicology and Applied Pharmacology* 191(1):74–85. Retrieved November 21, 2013 (http://linkinghub.elsevier.com/retrieve/pii/S0041008X03002187).

Schelegle, Edward S., William F. Walby, Mario F. Alfaro, Viviana J. Wong, Lei Putney, Mary Y. Stovall, Anja Sterner-Kock, Dallas M. Hyde, and Charles G. Plopper. 2003. "Repeated Episodes of Ozone Inhalation Attenuates Airway Injury/repair and Release of Substance P, but Not Adaptation." *Toxicology and Applied Pharmacology* 186(3):127–42. Retrieved January 6, 2015 (http://linkinghub.elsevier.com/retrieve/pii/S0041008X02000261).

Shannon, John M. and Brian a Hyatt. 2004. "Epithelial-Mesenchymal Interactions in the Developing Lung." *Annual review of physiology* 66(2):625–45. Retrieved November 18, 2013

(http://www.ncbi.nlm.nih.gov/pubmed/14977416).

Sharma, Sreenath V, Diana Y. Lee, Bihua Li, Margaret P. Quinlan, Fumiyuki Takahashi, Shyamala Maheswaran, Ultan McDermott, Nancy Azizian, Lee Zou, Michael A. Fischbach, Kwok-Kin Wong, Kathleyn Brandstetter, Ben Wittner, Sridhar Ramaswamy, Marie Classon, and Jeff Settleman. 2010. "A Chromatin-Mediated Reversible Drug-Tolerant State in Cancer Cell Subpopulations." *Cell* 141(1):69–80. Retrieved February 3, 2015 (http://www.pubmedcentral.nih.gov/articlerender.fcgi?artid=2851638&tool=pmcentrez&rendertype=abstract).

Shi, Yigong and Joan Massagué. 2003. "Mechanisms of TGF-Beta Signaling from Cell Membrane to the Nucleus." *Cell* 113(6):685–700. Retrieved (http://www.ncbi.nlm.nih.gov/pubmed/12809600).

Shi, Yigong, Yan-Fei Wang, Lata Jayaraman, Haijuan Yang, Joan Massagué, and Nikola P. Pavletich. 1998. "Crystal Structure of a Smad MH1 Domain Bound to DNA." *Cell* 94(5):585–94. Retrieved September 13, 2015 (http://www.sciencedirect.com/science/article/pii/S0092867400816001).

Shiozaki, H., T. Kadowaki, Y. Doki, M. Inoue, S. Tamura, H. Oka, K. Shimaya, M. Takeichi, and T. Mon. 1995. "Effect of Epidermal Growth Factor on Cadherin-Mediated Adhesion in." *British Journal of Cancer* (71):250–58.

Shu, Weiguo, Susan Guttentag, Zhishan Wang, Thomas Andl, Philip Ballard, Min Min Lu, Stefano Piccolo, Walter Birchmeier, Jeffrey a Whitsett, Sarah E. Millar, and Edward E. Morrisey. 2005. "Wnt/beta-Catenin Signaling Acts Upstream of N-Myc, BMP4, and FGF Signaling to Regulate Proximal-Distal Patterning in the Lung." *Developmental biology* 283(1):226–39. Retrieved November 14, 2013 (http://www.ncbi.nlm.nih.gov/pubmed/15907834).

Sikder, Hashmat a, Meghann K. Devlin, Shariff Dunlap, Byungwoo Ryu, and Rhoda M. Alani. 2003. "Id Proteins in Cell Growth and Tumorigenesis." *Cancer cell* 3(6):525–30. Retrieved (http://www.ncbi.nlm.nih.gov/pubmed/12842081).

Sillat, Tarvo, Riste Saat, Raimo Pöllänen, Mika Hukkanen, Michiaki Takagi, and Yrjö T. Konttinen. 2012. "Basement Membrane Collagen Type IV Expression by Human Mesenchymal Stem Cells during Adipogenic Differentiation." *Journal of cellular and molecular medicine* 16(7):1485–95. Retrieved August 12, 2015 (http://www.pubmedcentral.nih.gov/articlerender.fcgi?artid=3823217&tool=pmcentrez&rendertype=abstract).

Simon, Matthias, John G. Maresh, Stephen E. Harris, James D. Hernandez, Mazen Arar, Merle S. Olson, and Hanna E. Abboud. 2013. "Expression of Bone Morphogenetic Protein-7 mRNA in Normal and Ischemic Adult Rat Kidney Expression of Bone Morphogenetic Protein-7 mRNA in Normal and Ischemic Adult Rat Kidney."

Skromne, I. and C. D. Stern. 2001. "Interactions between Wnt and Vg1 Signalling Pathways Initiate Primitive Streak Formation in the Chick Embryo." *Development (Cambridge, England)* 128(15):2915–27. Retrieved September 15, 2015 (http://www.ncbi.nlm.nih.gov/pubmed/11532915).

Somasiri, A., C. Wu, T. Ellchuk, S. Turley, and C. D. Roskelley. 2000.

"Phosphatidylinositol 3-Kinase Is Required for Adherens Junction-Dependent Mammary Epithelial Cell Spheroid Formation." *Differentiation; research in biological diversity* 66(2-3):116–25. Retrieved August 26, 2015 (http://www.ncbi.nlm.nih.gov/pubmed/11100902).

Sountoulidis, Alexandros, Athanasios Stavropoulos, Stavros Giaglis, Eirini Apostolou, Rui Monteiro, Susana M. Chuva de Sousa Lopes, Huaiyong Chen, Barry R. Stripp, Christine Mummery, Evangelos Andreakos, and Paschalis Sideras. 2012. "Activation of the Canonical Bone Morphogenetic Protein (BMP) Pathway during Lung Morphogenesis and Adult Lung Tissue Repair." *PloS one* 7(8):e41460. Retrieved November 11, 2013 (http://www.pubmedcentral.nih.gov/articlerender.fcgi?artid=3423416&tool=pmcentrez&rendertype=abstract).

Spooner, B. S. and N. K. Wessells. 1970. "Mammalian Lung Development: Interactions in Primordium Formation and Bronchial Morphogenesis." *The Journal of experimental zoology* 175(4):445–54. Retrieved November 22, 2013 (http://www.ncbi.nlm.nih.gov/pubmed/5501462).

Stachowiak, M. K., P. A. Maher, A. Joy, E. Mordechai, and E. K. Stachowiak. 1996. "Nuclear Localization of Functional FGF Receptor 1 in Human Astrocytes Suggests a Novel Mechanism for Growth Factor Action." *Molecular Brain Research* 38(1):161–65. Retrieved July 14, 2015 (http://www.sciencedirect.com/science/article/pii/0169328X96000101).

Steinhusen, U., J. Weiske, V. Badock, R. Tauber, K. Bommert, and O. Huber. 2001. "Cleavage and Shedding of E-Cadherin after Induction of Apoptosis." *The Journal of biological chemistry* 276(7):4972–80. Retrieved November 7, 2013 (http://www.ncbi.nlm.nih.gov/pubmed/11076937).

Stelnicki, E. J., M. T. Longaker, D. Holmes, K. Vanderwall, M. R. Harrison, C. Largman, and W. Y. Hoffman. 1998. "Bone Morphogenetic Protein-2 Induces Scar Formation and Skin Maturation in the Second Trimester Fetus." *Plastic and reconstructive surgery* 101(1):12–19. Retrieved September 14, 2015 (http://www.ncbi.nlm.nih.gov/pubmed/9427911).

Stone, S., P. Jiang, P. Dayananth, S. V Tavtigian, H. Katcher, D. Parry, G. Peters, and A. Kamb. 1995. "Complex Structure and Regulation of the P16 (MTS1) Locus." *Cancer research* 55(14):2988–94. Retrieved August 19, 2015 (http://www.ncbi.nlm.nih.gov/pubmed/7606716).

Stovold, R., S. L. Meredith, J. L. Bryant, M. Babur, K. J. Williams, E. J. Dean, C. Dive, F. H. Blackhall, and A. White. 2013. "Neuroendocrine and Epithelial Phenotypes in Small-Cell Lung Cancer: Implications for Metastasis and Survival in Patients." *British journal of cancer* 108(8):1704–11. Retrieved August 31, 2015 (http://www.pubmedcentral.nih.gov/articlerender.fcgi?artid=3668479&tool=pmcentrez&rendertype=abstract).

Stovold, Rachel, Fiona Blackhall, Suzanne Meredith, JianMei Hou, Caroline Dive, and Anne White. 2012. "Biomarkers for Small Cell Lung Cancer: Neuroendocrine, Epithelial and Circulating Tumour Cells." *Lung cancer (Amsterdam, Netherlands)* 76(3):263–68. Retrieved September 12, 2015 (http://www.ncbi.nlm.nih.gov/pubmed/22177533).

Struhl, Gary and Atsuko Adachi. 1998. "Nuclear Access and Action of Notch In

Vivo." *Cell* 93(4):649–60. Retrieved September 9, 2015 (http://www.sciencedirect.com/science/article/pii/S0092867400811939).

Sun, Jianping, Hui Chen, Cheng Chen, Jeffrey a Whitsett, Yuji Mishina, Pablo Bringas, Jeffrey C. Ma, David Warburton, and Wei Shi. 2008. "Prenatal Lung Epithelial Cell-Specific Abrogation of Alk3-Bone Morphogenetic Protein Signaling Causes Neonatal Respiratory Distress by Disrupting Distal Airway Formation." *The American journal of pathology* 172(3):571–82. Retrieved November 13, 2013 (http://www.pubmedcentral.nih.gov/articlerender.fcgi?artid=2258256&tool=pmcentrez&rendertype=abstract).

Suyama, Kimita, Irina Shapiro, Mitchell Guttman, and Rachel B. Hazan. 2002. "A Signaling Pathway Leading to Metastasis Is Controlled by N-Cadherin and the FGF Receptor." *Cancer Cell* 2(4):301–14. Retrieved September 15, 2015 (http://www.sciencedirect.com/science/article/pii/S1535610802001502).

Tajima, Yoshitaka, Kouichiro Goto, Minoru Yoshida, Kenichi Shinomiya, Toshihiro Sekimoto, Yoshihiro Yoneda, Kohei Miyazono, and Takeshi Imamura. 2003. "Chromosomal Region Maintenance 1 (CRM1)-Dependent Nuclear Export of Smad Ubiquitin Regulatory Factor 1 (Smurf1) Is Essential for Negative Regulation of Transforming Growth Factor-Beta Signaling by Smad7." *The Journal of biological chemistry* 278(12):10716–21. Retrieved November 14, 2013 (http://www.ncbi.nlm.nih.gov/pubmed/12519765).

Takabayashi, Hidehiko, Masahiko Shinohara, Maria Mao, Piangwarin Phaosawasdi, Mohamad El-Zaatari, Min Zhang, Tuo Ji, Kathryn A. Eaton, Duyen Dang, John Kao, and Andrea Todisco. 2014. "Anti-Inflammatory Activity of Bone Morphogenetic Protein Signaling Pathways in Stomachs of Mice." *Gastroenterology* 147(2):396–406.e7. Retrieved May 24, 2015 (http://www.gastrojournal.org/article/S0016508514005411/fulltext).

Talmadge, J. E., K. Benedict, J. Madsen, and I. J. Fidler. 1984. "Development of Biological Diversity and Susceptibility to Chemotherapy in Murine Cancer Metastases." *Cancer research* 44(9):3801–5. Retrieved September 12, 2015 (http://www.ncbi.nlm.nih.gov/pubmed/6744297).

Talmadge, James E. 2007. "Clonal Selection of Metastasis within the Life History of a Tumor." *Cancer Research* 67(24):11471–75.

Van Tam, Janice Kal, Koichiro Uto, Mitsuhiro Ebara, Stefania Pagliari, Giancarlo Forte, and Takao Aoyagi. 2012. "Mesenchymal Stem Cell Adhesion but Not Plasticity Is Affected by High Substrate Stiffness." *Science and Technology of Advanced Materials* 13(6):064205. Retrieved September 10, 2015 (http://iopscience.iop.org/article/10.1088/1468-6996/13/6/064205).

Tang, Vivian W. and William M. Brieher. 2013. "FSGS3/CD2AP Is a Barbed-End Capping Protein That Stabilizes Actin and Strengthens Adherens Junctions." *The Journal of cell biology* 203(5):815–33. Retrieved August 26, 2015 (http://www.pubmedcentral.nih.gov/articlerender.fcgi?artid=3857477&tool=pmcentrez&rendertype=abstract).

Tata, Purushothama Rao, Hongmei Mou, Ana Pardo-Saganta, Rui Zhao, Mythili Prabhu, Brandon M. Law, Vladimir Vinarsky, Josalyn L. Cho, Sylvie Breton, Amar Sahay, Benjamin D. Medoff, and Jayaraj Rajagopal. 2013.

"Dedifferentiation of Committed Epithelial Cells into Stem Cells in Vivo." *Nature* 503(7475):218–23. Retrieved May 27, 2014 (http://www.ncbi.nlm.nih.gov/pubmed/24196716).

Thawani, Jayesh P., Anthony C. Wang, Khoi D. Than, Chia-Ying Lin, Frank La Marca, and Paul Park. 2010. "Bone Morphogenetic Proteins and Cancer: Review of the Literature." *Neurosurgery* 66(2):233–46; discussion 246. Retrieved September 13, 2015 (http://www.ncbi.nlm.nih.gov/pubmed/20042986).

Thiery, Jean Paul. 2002. "Epithelial-Mesenchymal Transitions in Tumour Progression." *Nature reviews. Cancer* 2(6):442–54. Retrieved November 7, 2013 (http://www.ncbi.nlm.nih.gov/pubmed/12189386).

Thiery, Jean Paul, Hervé Acloque, Ruby Y. J. Huang, and M. Angela Nieto. 2009. "Epithelial-Mesenchymal Transitions in Development and Disease." *Cell* 139(5):871–90. Retrieved November 8, 2013 (http://www.ncbi.nlm.nih.gov/pubmed/19945376).

Thompson, E. W. and I. Haviv. 2011. "The Social Aspects of EMT-MET Plasticity." *Nature medicine* 17(9):1048–49. Retrieved (http://dx.doi.org/10.1038/nm.2437).

Timm, Andrew and Jill M. Kolesar. 2013. "Crizotinib for the Treatment of Non-Small-Cell Lung Cancer." *American journal of health-system pharmacy : AJHP : official journal of the American Society of Health-System Pharmacists* 70(11):943–47. Retrieved August 3, 2015 (http://www.ncbi.nlm.nih.gov/pubmed/23686600).

Tirado-rodriguez, Belen, Enrique Ortega, Patricia Segura-medina, and Sara Huerta-yepez. 2014. "TGF-β : An Important Mediator of Allergic Disease and a Molecule with Dual Activity in Cancer Development." 2014.

Tsai, Jeff H., Joana Liu Donaher, Danielle A. Murphy, Sandra Chau, and Jing Yang. 2012. "Spatiotemporal Regulation of Epithelial-Mesenchymal Transition Is Essential for Squamous Cell Carcinoma Metastasis." *Cancer cell* 22(6):725–36. Retrieved July 1, 2015 (http://www.pubmedcentral.nih.gov/articlerender.fcgi?artid=3522773&tool=pmcentrez&rendertype=abstract).

Tsai, Jeff H. and Jing Yang. 2013. "Epithelial-Mesenchymal Plasticity in Carcinoma Metastasis." *Genes & development* 27(20):2192–2206. Retrieved September 2, 2015 (http://genesdev.cshlp.org/content/27/20/2192.abstract).

Tsao, Po-Nien, Michelle Vasconcelos, Konstantin I. Izvolsky, Jun Qian, Jining Lu, and Wellington V Cardoso. 2009. "Notch Signaling Controls the Balance of Ciliated and Secretory Cell Fates in Developing Airways." *Development (Cambridge, England)* 136(13):2297–2307. Retrieved November 12, 2013 (http://www.pubmedcentral.nih.gov/articlerender.fcgi?artid=2729343&tool=pmcentrez&rendertype=abstract).

Ulloa, L. and S. Tabibzadeh. 2001. "Lefty Inhibits Receptor-Regulated Smad Phosphorylation Induced by the Activated Transforming Growth Factor-Beta Receptor." *The Journal of biological chemistry* 276(24):21397–404. Retrieved November 19, 2013 (http://www.ncbi.nlm.nih.gov/pubmed/11278746).

Urist, Marshall R. 1965. “Bone: Formation by Autoinduction.” *Clinical orthopaedics and related research* 150(395):4–10. Retrieved (http://www.ncbi.nlm.nih.gov/pubmed/11937861).

Valcourt, Ulrich, Marcin Kowanetz, Hideki Niimi, Carl-Henrik Heldin, and Aristidis Moustakas. 2005. “TGF-Beta and the Smad Signaling Pathway Support Transcriptomic Reprogramming during Epithelial-Mesenchymal Cell Transition.” *Molecular biology of the cell* 16(4):1987–2002. Retrieved September 15, 2015 (http://www.pubmedcentral.nih.gov/articlerender.fcgi?artid=1073677&tool=pmcentrez&rendertype=abstract).

Vallenius, Tea. 2013. “Actin Stress Fibre Subtypes in Mesenchymal-Migrating Cells.” *Open biology* 3(6):130001. Retrieved August 26, 2015 (http://www.pubmedcentral.nih.gov/articlerender.fcgi?artid=3718327&tool=pmcentrez&rendertype=abstract).

Varlet, I., J. Collignon, and E. J. Robertson. 1997. “Nodal Expression in the Primitive Endoderm Is Required for Specification of the Anterior Axis during Mouse Gastrulation.” *Development (Cambridge, England)* 124(5):1033–44. Retrieved September 15, 2015 (http://www.ncbi.nlm.nih.gov/pubmed/9056778).

Wagner, Darja Obradovic, Christina Sieber, Raghu Bhushan, Jan H. Börgermann, Daniel Graf, and Petra Knaus. 2010. “BMPs: From Bone to Body Morphogenetic Proteins.” *Science signaling* 3(107):mr1. Retrieved September 14, 2015 (http://www.ncbi.nlm.nih.gov/pubmed/20124549).

Wagner, Patrick L., Naoki Kitabayashi, Yao-Tseng Chen, and Anjali Saqi. 2009. “Combined Small Cell Lung Carcinomas: Genotypic and Immunophenotypic Analysis of the Separate Morphologic Components.” *American journal of clinical pathology* 131(3):376–82. Retrieved September 12, 2015 (http://ajcp.ascpjournals.org/content/131/3/376.abstract).

Walford, Hannah H. and Taylor a Doherty. 2014. “Diagnosis and Management of Eosinophilic Asthma: A US Perspective.” *Journal of asthma and allergy* 7:53–65. Retrieved (http://www.pubmedcentral.nih.gov/articlerender.fcgi?artid=3990389&tool=pmcentrez&rendertype=abstract).

Wang, Dongsheng, Ling Su, Donghai Huang, Hongzheng Zhang, Dong M. Shin, and Zhuo G. Chen. 2011. “Downregulation of E-Cadherin Enhances Proliferation of Head and Neck Cancer through Transcriptional Regulation of EGFR.” *Molecular cancer* 10(1):116. Retrieved December 4, 2014 (http://www.pubmedcentral.nih.gov/articlerender.fcgi?artid=3192774&tool=pmcentrez&rendertype=abstract).

Wang, Elizabeth A., Vicki Rosen, Josephine S. D. Alessandro, Marc Bauduy, Paul Cordes, Tomoko Harada, David Israel, Rodney M. Hewick, Kelvin M. Kerns, Peter Lapan, Deborah P. Luxenberg, David Mcquaid, Ioannis K. Moutsatsos, John Nove, and John M. Wozney. 1990. “Recombinant Human Bone Morphogenetic Protein Induces Bone Formation.” 87(March):2220–24.

Wang, Richard N., Jordan Green, Zhongliang Wang, Youlin Deng, Min Qiao, Michael Peabody, Qian Zhang, Jixing Ye, Zhengjian Yan, Sahitya Denduluri, Olumuyiwa Idowu, Melissa Li, Christine Shen, Alan Hu, Rex C.

Haydon, Richard Kang, James Mok, Michael J. Lee, Hue L. Luu, and Lewis L. Shi. 2014. "Bone Morphogenetic Protein (BMP) Signaling in Development and Human Diseases." *Genes & Diseases* 1(1):87–105. Retrieved March 1, 2015 (http://www.sciencedirect.com/science/article/pii/S2352304214000105).

Warburton, D., M. Schwarz, D. Tefft, G. Flores-Delgado, K. D. Anderson, and W. V Cardoso. 2000. "The Molecular Basis of Lung Morphogenesis." *Mechanisms of development* 92(1):55–81. Retrieved (http://www.ncbi.nlm.nih.gov/pubmed/10704888).

Warburton, David. 2012. "Developmental Responses to Lung Injury: Repair or Fibrosis." *Fibrogenesis & tissue repair* 5 Suppl 1(Suppl 1):S2. Retrieved (http://www.pubmedcentral.nih.gov/articlerender.fcgi?artid=3368777&tool=pmcentrez&rendertype=abstract).

Warburton, David, Laura Perin, Roger Defilippo, Saverio Bellusci, Wei Shi, and Barbara Driscoll. 2008. "Stem/progenitor Cells in Lung Development, Injury Repair, and Regeneration." *Proceedings of the American Thoracic Society* 5(6):703–6. Retrieved November 18, 2013 (http://www.pubmedcentral.nih.gov/articlerender.fcgi?artid=2645263&tool=pmcentrez&rendertype=abstract).

Weaver, M., N. R. Dunn, and B. L. Hogan. 2000. "Bmp4 and Fgf10 Play Opposing Roles during Lung Bud Morphogenesis." *Development (Cambridge, England)* 127(12):2695–2704. Retrieved (http://www.ncbi.nlm.nih.gov/pubmed/10821767).

Weaver, M., J. M. Yingling, N. R. Dunn, S. Bellusci, and B. L. Hogan. 1999. "Bmp Signaling Regulates Proximal-Distal Differentiation of Endoderm in Mouse Lung Development." *Development (Cambridge, England)* 126(18):4005–15. Retrieved (http://www.ncbi.nlm.nih.gov/pubmed/10457010).

Wilson, P. A., G. Lagna, A. Suzuki, and A. Hemmati-Brivanlou. 1997. "Concentration-Dependent Patterning of the Xenopus Ectoderm by BMP4 and Its Signal Transducer Smad1." *Development (Cambridge, England)* 124(16):3177–84. Retrieved September 13, 2015 (http://www.ncbi.nlm.nih.gov/pubmed/9272958).

Van Winkle, Laura S., Michelle V Fanucchi, Lisa a Miller, Gregory L. Baker, Laurel J. Gershwin, Edward S. Schelegle, Dallas M. Hyde, Michael J. Evans, and Charles G. Plopper. 2004. "Epithelial Cell Distribution and Abundance in Rhesus Monkey Airways during Postnatal Lung Growth and Development." *Journal of applied physiology (Bethesda, Md. : 1985)* 97(6):2355–63; discussion 2354. Retrieved November 19, 2013 (http://www.ncbi.nlm.nih.gov/pubmed/15298983).

Winnier, G., M. Blessing, P. a Labosky, and B. L. Hogan. 1995. "Bone Morphogenetic Protein-4 Is Required for Mesoderm Formation and Patterning in the Mouse." *Genes & Development* 9(17):2105–16. Retrieved November 26, 2013 (http://www.genesdev.org/cgi/doi/10.1101/gad.9.17.2105).

Woolley, K. and P. Martin. 2000. "Conserved Mechanisms of Repair: From Damaged Single Cells to Wounds in Multicellular Tissues." *BioEssays :*

news and reviews in molecular, cellular and developmental biology 22(10):911–19. Retrieved September 11, 2015 (http://www.ncbi.nlm.nih.gov/pubmed/10984717).

Wozney, J. M. 1989. "Bone Morphogenetic Proteins." *Progress in growth factor research* 1(4):267–80. Retrieved November 19, 2013 (http://www.ncbi.nlm.nih.gov/pubmed/2491264).

Wozniak, Michele A., Katarzyna Modzelewska, Lina Kwong, and Patricia J. Keely. 2004. "Focal Adhesion Regulation of Cell Behavior." *Biochimica et biophysica acta* 1692(2-3):103–19. Retrieved February 19, 2015 (http://www.sciencedirect.com/science/article/pii/S0167488904000990).

Xia, Yin, Jodie L. Babitt, Richard Bouley, Ying Zhang, Nicolas Da Silva, Shanzhuo Chen, Zhenjie Zhuang, Tarek a Samad, Gary J. Brenner, Jennifer L. Anderson, Charles C. Hong, Alan L. Schneyer, Dennis Brown, and Herbert Y. Lin. 2010. "Dragon Enhances BMP Signaling and Increases Transepithelial Resistance in Kidney Epithelial Cells." *Journal of the American Society of Nephrology : JASN* 21(4):666–77. Retrieved November 19, 2013 (http://www.pubmedcentral.nih.gov/articlerender.fcgi?artid=2844302&tool=pmcentrez&rendertype=abstract).

Xiao, Z., N. Watson, C. Rodriguez, and H. F. Lodish. 2001. "Nucleocytoplasmic Shuttling of Smad1 Conferred by Its Nuclear Localization and Nuclear Export Signals." *The Journal of biological chemistry* 276(42):39404–10. Retrieved August 29, 2015 (http://www.ncbi.nlm.nih.gov/pubmed/11509558).

Xiao, Zhan, Robert Latek, and Harvey F. Lodish. 2003. "An Extended Bipartite Nuclear Localization Signal in Smad4 Is Required for Its Nuclear Import and Transcriptional Activity." *Oncogene* 22(7):1057–69. Retrieved August 18, 2015 (http://dx.doi.org/10.1038/sj.onc.1206212).

Xiao, Zhan., Robert. Latek, and Harvey F. Lodish. 2003. "An Extended Bipartite Nuclear Localization Signal in Smad4 Is Required for Its Nuclear Import and Transcriptional Activity." *Oncogene* 22(7):1057–69. Retrieved August 18, 2015 (http://www.ncbi.nlm.nih.gov/pubmed/12592392).

Xu, Lan, Claudio Alarcón, Seda Cöl, and Joan Massagué. 2003. "Distinct Domain Utilization by Smad3 and Smad4 for Nucleoporin Interaction and Nuclear Import." *The Journal of biological chemistry* 278(43):42569–77. Retrieved August 18, 2015 (http://www.jbc.org/content/278/43/42569.abstract?ijkey=a00a083b8f4279e02886268d8705db1eba28693f&keytype2=tf_ipsecsha).

Yamashita, H;, P; ten Dijke, Carl-Henrik; Heldin, and Kohei. .. Miyazono. 1996. "Bone Morphogenetic Protein Receptors." *Bone* 19(6):569–74.

Yang, Gengxia, Zhonghui Zhu, Yan Wang, Ai Gao, Piye Niu, and Lin Tian. 2013. "Bone Morphogenetic Protein-7 Inhibits Silica-Induced Pulmonary Fibrosis in Rats." *Toxicology letters* 220(2):103–8. Retrieved September 15, 2015 (http://www.ncbi.nlm.nih.gov/pubmed/23639248).

Yang, Honghua, Min Min Lu, Lili Zhang, Jeffrey a Whitsett, and Edward E. Morrisey. 2002. "GATA6 Regulates Differentiation of Distal Lung

Epithelium." *Development (Cambridge, England)* 129(9):2233–46.

Yang, Jibing., Miranda. Velikoff, Kleaveland. Kathryn, Manisha. Agarwal, and K. Kim. Kevin. 2014. "Overexpression Of Id2 Transcription Factor Promotes Alveolar Epithelial Cell Proliferation And Attenuates Bleomycin-Induced Pulmonary Fibrosis." *ATS Journals*. Retrieved June 30, 2015 (http://www.atsjournals.org/doi/pdf/10.1164/ajrccm-conference.2014.189.1_MeetingAbstracts.A2372).

Yang, Jun, Xiaohui Li, Ying Li, Mark Southwood, Lingying Ye, Lu Long, Rafia S. Al-Lamki, and Nicholas W. Morrell. 2013. "Id Proteins Are Critical Downstream Effectors of BMP Signaling in Human Pulmonary Arterial Smooth Muscle Cells." *American journal of physiology. Lung cellular and molecular physiology* 305(4):L312–21. Retrieved December 16, 2013 (http://ajplung.physiology.org/content/305/4/L312.full-text.pdf+html).

Yang, Junwei and Youhua Liu. 2002. "Blockage of Tubular Epithelial to Myofibroblast Transition by Hepatocyte Growth Factor Prevents Renal Interstitial Fibrosis." *Journal of the American Society of Nephrology : JASN* 13(1):96–107. Retrieved September 15, 2015 (http://www.ncbi.nlm.nih.gov/pubmed/11752026).

Ye, Lin and Heath Park. 2009. "Bone Morphogenetic Proteins in Cancer : Clinical and Therapeutic Considerations." 4(3):75–77.

Ying, Qi Long, Jennifer Nichols, Ian Chambers, and Austin Smith. 2003. "BMP Induction of Id Proteins Suppresses Differentiation and Sustains Embryonic Stem Cell Self-Renewal in Collaboration with STAT3." *Cell* 115(3):281–92. Retrieved (http://www.ncbi.nlm.nih.gov/pubmed/14636556).

Yuen, Hiu-Fung, Yuen-Piu Chan, Wai-Lok Cheung, Yong-Chuan Wong, Xianghong Wang, and Kwok-Wah Chan. 2008. "The Prognostic Significance of BMP-6 Signaling in Prostate Cancer." *Modern pathology : an official journal of the United States and Canadian Academy of Pathology, Inc* 21(12):1436–43. Retrieved November 19, 2013 (http://www.ncbi.nlm.nih.gov/pubmed/18931653).

Zahm, J. M., M. Chevillard, and E. Puchelle. 1991. "Wound Repair of Human Surface Respiratory Epithelium." *American journal of respiratory cell and molecular biology* 5(3):242–48. Retrieved August 13, 2015 (http://www.ncbi.nlm.nih.gov/pubmed/1910810).

Zahm, J. M., H. Kaplan, A. L. Hérard, F. Doriot, D. Pierrot, P. Somelette, and E. Puchelle. 1997. "Cell Migration and Proliferation during the in Vitro Wound Repair of the Respiratory Epithelium." *Cell motility and the cytoskeleton* 37(1):33–43. Retrieved September 11, 2015 (http://www.ncbi.nlm.nih.gov/pubmed/9142437).

Zaidi, Sayyed K., Andrew J. Sullivan, Andre J. van Wijnen, Janet L. Stein, Gary S. Stein, and Jane B. Lian. 2002. "Integration of Runx and Smad Regulatory Signals at Transcriptionally Active Subnuclear Sites." *Proceedings of the National Academy of Sciences of the United States of America* 99(12):8048–53.

Zeisberg, Michael, Jun-ichi Hanai, Hikaru Sugimoto, Tadanori Mammoto, David Charytan, Frank Strutz, and Raghu Kalluri. 2003. "BMP-7 Counteracts TGF-

beta1-Induced Epithelial-to-Mesenchymal Transition and Reverses Chronic Renal Injury." *Nature medicine* 9(7):964–68. Retrieved (http://www.ncbi.nlm.nih.gov/pubmed/12808448).

Zeisberg, Michael, Amish A. Shah, and Raghu Kalluri. 2005. "Bone Morphogenic Protein-7 Induces Mesenchymal to Epithelial Transition in Adult Renal Fibroblasts and Facilitates Regeneration of Injured Kidney." *The Journal of biological chemistry* 280(9):8094–8100. Retrieved September 22, 2015 (http://www.ncbi.nlm.nih.gov/pubmed/15591043).

Zhang, Ying E. 2009. "Non-Smad Pathways in TGF-Beta Signaling." *Cell research* 19(1):128–39. Retrieved January 13, 2015 (http://www.pubmedcentral.nih.gov/articlerender.fcgi?artid=2635127&tool=pmcentrez&rendertype=abstract).

Zhang, Yong-Tao, Arthur D. Lander, and Qing Nie. 2007. "Computational Analysis of BMP Gradients in Dorsal-Ventral Patterning of the Zebrafish Embryo." *Journal of theoretical biology* 248(4):579–89. Retrieved September 13, 2015 (http://www.pubmedcentral.nih.gov/articlerender.fcgi?artid=4151269&tool=pmcentrez&rendertype=abstract).

Zhou, Qian, Jennifer Heinke, Alberto Vargas, Stephan Winnik, Tobias Krauss, Christoph Bode, Cam Patterson, and Martin Moser. 2007. "ERK Signaling Is a Central Regulator for BMP-4 Dependent Capillary Sprouting." *Cardiovascular research* 76(3):390–99. Retrieved August 19, 2015 (http://cardiovascres.oxfordjournals.org/content/76/3/390).

Zwaagstra, J. C., a Guimond, and M. D. O'Connor-McCourt. 2000. "Predominant Intracellular Localization of the Type I Transforming Growth Factor-Beta Receptor and Increased Nuclear Accumulation after Growth Arrest." *Experimental cell research* 258(1):121–34. Retrieved November 19, 2013 (http://www.ncbi.nlm.nih.gov/pubmed/10912794).